Biochemical effects of organophosphorous compounds on cultured rat and human cardiomyocyte-like cells

Shatha G. Felemban

A thesis submitted in partial fulfilment of the requirements of Nottingham Trent University for the degree of

Doctor of Philosophy

September 2016

ABSTRACT

At present, little is known about the effect(s) of organophosphorous compounds (OPs) on cardiomyocytes. The present study aimed to investigate the effects of phenyl saligenin phosphate (PSP), two organophosphorothioate insecticides (diazinon and chlorpyrifos), and their acutely toxic metabolites (diazoxon and chlorpyrifos oxon) on rat H9c2 and human cardiomyocyte-like cells. The rat embryonic H9c2 myoblast cell line, which has the ability to differentiate into a cardiac muscle phenotype, can be instrumental in understanding OP cytotoxicity at different differentiation stages. Human induced pluripotent stem cell derived cardiomyocytes (hiPSC-CMs) were used for the validation of selected OP effects in a more human relevant system. The differentiation of both H9c2 and human cardiomyocytes resulted in increased expression of differentiated muscle markers such as troponin 1, tropomyosin and α-actin.

OP-induced cytotoxicity was assessed by monitoring MTT reduction, LDH release, and caspase-3 activity. Cell death was not observed in mitotic or differentiated H9c2 cells with diazinon, diazoxon, or chlorpyrifos oxon (48 h exposure; 200 μM). Chlorpyrifos-induced cell death was only evident at concentrations >100 μM. In marked contrast, PSP displayed pronounced cytotoxicity towards both mitotic and differentiated H9c2 cells. PSP triggered the activation of JNK1/2, suggesting a role for this pro-apoptotic protein kinase in PSP-induced cell death, which was attenuated by the JNK1/2 inhibitor SP 600125, confirming the role of JNK1/2 activation in PSP-induced cytotoxicity. Dansylated PSP was used to identify novel PSP binding proteins. 2D-gel electrophoresis profiles of cells treated with dansylated PSP (25 μM) were used to identify proteins fluorescently labeled with dansylated PSP. Proteomic analysis identified tropomyosin, heat shock protein β-1 and nucleolar protein 58 as novel protein targets for PSP.

The present study also examined the effect of sublethal concentrations of OP on differentiating H9c2 cells. This was assessed by monitoring morphological changes, levels of cardiac cytoskeleton protein expression and AChE activity in cells induced to differentiate in the presence and absence of OPs. Results showed that exposure to diazinon and chlorpyrifos induced morphological changes, AChE inhibition and decreases in troponin 1 expression. Morphological changes were observed with PSP treated cells concomitant with altered expression of cardiac cytoskeleton proteins, troponin 1, tropomyosin, α-actin and other novel proteins. When hiPSC-CMs were employed to validate differences in cardiac toxicity induced by OPs, a similar cardiotoxic pattern when compared to differentiated H9c2 cells. In summary, PSP induced cytotoxicity was associated with JNK activation and apoptrosis whereas little cytotoxicity was observed with the other OPs. However PSP, chlorpyrifos and diazinon induced sub-lethal effects in cultured H9c2 and hiPSC-CMs were associated with decrease levels of cardiac cytoskeleton protein expression.

DECLARATION

It is hereby certified that the experimental work and analysis embodied in this thesis is the original research carried out by the author, unless otherwise stated at the School of Science and Technology, Nottingham Trent University, UK. This work is the intellectual property of the author. You may copy up to 5% of this work for the private study or personal, non-commercial research. Any information used from this thesis should be fully cited.

Shatha Felemban

ACKNOWLEDGEMENTS

I would first like to thank my project supervisor Dr. John Dickenson for his support, guide and continuous monitoring. His office door was always open for me when I ever had a problem or a question about my research or writing. He steered me in the right direction whenever I was out of the track all this 4 years period. I am so grateful for his exceptional supervision and help particularly during the thesis evaluation.

I would also like to thank the expert who was involved in this project, my second supervisor Dr. Alan Hargreaves. His enthusiasm, support and professional help accompanied all the period of preparing and finishing this work. Without his participate input this project haven't been successfully conducted.

I would also like to acknowledge Nottingham Trent University, in particular the Biomedical Department for accepting me and involved me in this part of research.

I would also like to acknowledge my sponsor scholarship provided by King Abdullah Bin-Abdulaziz Al-saud (may he rest in peace) and Ministry of Higher Education of Saudi Arabia. Thank you for giving me this opportunity to expand my knowledge in science.

Special thanks to who this work is dedicated for, the most two important persons in my life, my mother Amal and father Ghazi providing me with unfailing support, continuous encouragements and prayers all my way. I will never forget their word "you will make it", without their love and wonderful spirit I wouldn't be able to make it to this stage.

I would also like to thank my brothers and sisters, Alaa, Mohammed, Abdulrahman, Dania, Abdulaziz, Sondos and Reem for their support.

I would gratefully like to thank my lab mates and colleague in the Biomedical Department Dr. James Daubney, Dr. Maha Aldobian and Dr. Ibtisam Almami. Our wonderful teamwork made my experience during my PhDs journey pleasant and comfortable with them.

Finally I would also like take this opportunity to thank my friends and sisters Marwah Maashi Reham Balahmar, Hayat Alzhrani, Huda Rayani, Mashail Masshi, Najla Alharbi, Alanod Algarni, Hiba Almasmoum, Nada Binzagr and Raja Alahmadi. Thank you for being part of my life along this way, thank you for sharing my happiness and sadness moments and being my second family in Nottingham.

Table of Contents

LIST OF FIGURES

LIST OF TABLES

PUBLICATIONS

Felemban, S. G., Garner, A. C., Smida, F. A., Boocock, D. J., Hargreaves, A. J., & Dickenson, J. M. (2015). Phenyl saligenin phosphate induced caspase-3 and c-Jun N-terminal kinase activation in cardiomyocyte-like cells. *Chemical research in toxicology*, *28*(11), pp.2179-2191.

CONFERENCE (POSTER)

Felemban, S. G., Hargreaves, A. J., & Dickenson, J. M. (2016). New binding protein targets for Phenyl saligenin phosphate in differentiated H9c2 cells. Proceedings of the 9th Saudi Scientific International Conference, Birmingham University, United kingdom, Poster presentation, abstract no: 515, pp.221.

Felemban, S. G., Hargreaves, A. J., & Dickenson, J. M. (2014). Organophosphate induced cardiomyocyte toxicity. *The 18th Intentional Congress on In Vitro Toxicology*, Egmond aan Zee, Netherland, June 2014, Poster presentation, abstract no: 7.18, pp.220.

Felemban, S. G., Hargreaves, A. J., & Dickenson, J. M. (2014). The Effects of Organophosphates on Cardiomyocytes. Proceedings of the 7th Saudi Scientific International Conference, Edinburgh University, United Kingdom, Poster presentation, abstract no: 303, pp.223.

Felemban, S.G., Hargreaves, A. J., & Dickenson, J. M. (2013). The acute effects of organophosphate on H9c2 cardiomyocytes Proceedings of the 7th annual School of Science and Technology Research Conference, Nottingham Trent university, Nottingham, the United Kingdom, Poster and oral presentation, abstract no: 10,pp.23.

Abbreviations

ACh: Acetylcholine

AChE: Acetylcholinesterase

AP-1: Transcription factor activator protein 1

Apaf-1: Apoptotic protease activating factor-1

APH: Acyl peptide hydrolase

ASCs: Adult stem cells

ATP: Adenosine triphosphate

Bak : BCL2 antagonist/killer 1

Bax: Bcl-2-associated X protein

Bcl-X_L: B-cell lymphoma-extra large

Bid: BH3-interacting domain death agonist

BuChE: Butyrylcholinesterase

c-FLIP: cellular FLICE-like inhibitory protein)

CRABP: Cellular retinoic acid-binding protein

CREB: cAMP response element-binding protein

CYP : Cytochrome P450

DEP: Diethylphosphate

DETP: Diethylthiophosphate

DISC: Death-inducing signalling complex

DMEM: Dulbecco's Modified Eagle's Medium

ECG: Electrocardiogram

EGF: Epidermal growth factor

ERK1/2: Extracellular signal-regulated kinases

ESCs: Embryonic stem cells

FADD: Fas associated death domain

Fas-L: Fas ligand

FBS: Foetal bovine serum

FGF: Fibroblast growth factor

Fos: FBJ osteosarcoma oncogene

GPCR: G-protein-coupled receptors

Grb2: Growth factor receptor bound protein 2

hiPSCs-CMs: mature human-induced pluripotent stem cell-derived cardiomyocytes

ICAD: Inhibitor of caspase activated DNase

Ier2: Immediate early response 2

IL-1β: Cytokine Interleukin-1 beta

iPSCs: Induced pluripotent stem cells

JNK: c-Jun N-terminal kinases

LDH: Lactate dehydrogenase

MALDI-TOF MS: Matrix-assisted laser desorption/ionization

MAPK: Mitogen-activated protein kinase

MAP 1B: Microtubule associated protein 1B

MDA: Malondialdehyde

MS: Mass spectrometry

MSC: Mesenchymal stem cells

mTORC2: Mammalian target of rapamycin Complex 2

NFAT: Nuclear factor of activated T cells

NTE: Neuropathy target esterase

OPIDN: Organophosphate-induced delayed neuropathy

OPs :Organophosphorous compounds

Oxt: Oxytocin/neurophysin I prepropeptide

PDGF: Platelet-derived growth factor

PDK1: Pyruvate dehydrogenase kinase 1

PI-3K/PKB: Phosphoinositol-3 kinase/ protein kinase B

PIP_2: Phosphorylates phosphatidylinositol 4,5-bisphosphate

PIP_3: Phosphatidylinositol (3,4,5)-trisphosphate

PKB/Akt: Protein kinase B/Akt

PKCδ: Protein kinase Cδ

PMF: Peptide mass fingerprinting

PSCs: Pluripotent stem cells

PSP: Phenyl saligenin phosphate

PTEN: Phosphatase and tensin homolog

RA: Retinoic acid

RAR: Retinoic acid receptor

RARE: RA response element

RXR: Retinoid X receptor

SCOTP: Saligenin cyclic-o-tolyl phosphate

Smac/DIABLO proteins: Second mitochondria-derived activator of caspases /direct IAP binding proteins

Sos: Son of sevenless

SERCA2a: sarcoplasmic Ca^{2+} ATPase

TCPy: 3,5,6- Trichloro-2-pyridinol

TNF-α: Tumor necrosis factors-α

TOCP: Tri-ortho-cresyl phosphate

TRAIL: TNF-related apoptosis-inducing ligand

VEGF: Vascular endothelial growth factor

Chapter 1:

Introduction

1.1 Background

Organophosphorous (OP) compounds were first synthesised in the 1800s by French chemists Jean Louis Lassaigne and Philip de Clermoun (Gallo & Lawryk, 1991). These chemical compounds were deployed as nerve agents in World War II (Chambers & Levi, 1992) and as chemical gas warfare weapons in the 1995 Tokyo subway terrorist attack (Suzuki *et al*., 1995). In the latter case, OPs were developed as pesticides by the German chemist Gerhard Schrader (Gallo & Lawryk, 1991). Since then, numerous OPs have been synthesised and commercialised worldwide.

Nowadays, OP pesticides are widely used for a variety of purposes due to their wide ranging chemical and physical properties. For example, in developing countries they are used against microbial agents, plant pathogens and insects (Lotti, 2000). Some OPs are also used in jet engine lubricants as anti-wear additives, due to their fire-resistant properties (Solbu *et al*., 2007). However in the last 25 years, numerous publications have reported passengers suffering from chronic symptoms such as cognitive problems and even paralysis (Montgomery *et al*., 1977; Winder *et al*., 2002). Moreover, neurotoxicity was reported in approximately 10–50,000 Americans who suffered from Tri-ortho-cresyl phosphate (TOCP) adulterant poisoning, an ethanolic organophosphate compound was first extracted from Jamaica ginger known as “Ginger Jake paralysis” (Smith & Lillie, 1931).

The increase in the global use of OPs has heightened concerns regarding their associated health problems. More than three million cases of OP pesticide poisoning have been reported and over 250,000 cases of mortality per year have occurred world wide (Carey *et al*., 2013). As a consequence, there is now considerable interest in determining the molecular mechanisms of OP-induced toxicity. This study will investigate the effects of phenyl saligenin phosphate (PSP), the organophosphorothioate insecticides diazinon and chlorpyrifos and their acutely toxic metabolites diazoxon and chlorpyrifos oxon on mitotic and differentiated H9c2 cardiomyoblasts.

1.2 Mechanism of Organophosphate Toxicity

The most well-known effect of organophosphate acute toxicity is due to the significant inhibition of acetylcholinesterase (AChE). AChE enzymes belong to the serine hydrolase family and mainly found at the neuromuscular junction, where it is responsible for acetylcholine (ACh) hydrolysis in the preganglionic and postganglionic neurons of the nervous system. Thus AChE terminates the transfer of signals to skeletal muscles, cardiac system and secretory glands (Ray & Richards, 2001). In recent years researchers have also shown that AChE activity may play a regulatory role in cell differentiation and cell-to-cell interactions; thus, blocking AChE activity may result in obstructed cellular dynamics (Jordaan *et al.*, 2013), as shown in Figure 1.1.

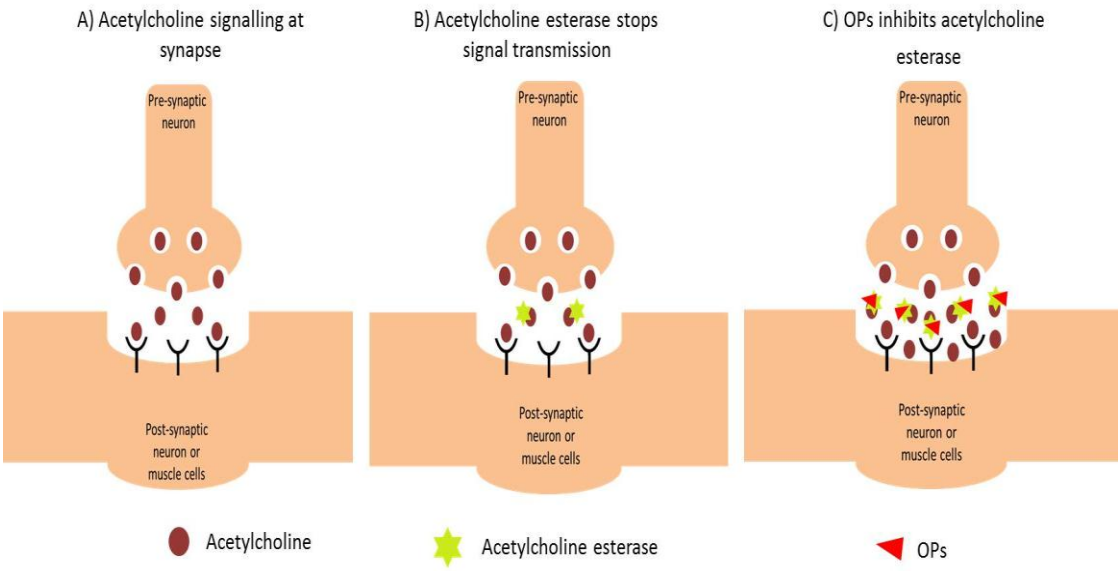

Figure 1. 1 Common neurotoxicity mechanism of OPs

(A) Release of neurotransmitter acetylcholine from pre-synaptic neuron and subsequent binding to receptors on the post-synaptic neuron or muscle cells. (B) Termination of ACh function by AChE at cholinergic synapses. (C) Organophosphates bind to AChE and inhibit enzyme action, causing accumulation of free ACh at the synapse.

The primary biological targets of OPs are serine esterases. Once the OPs have bound to the active site of AChE, this leads to enzyme organophosphorylation and the accumulation of ACh at the nerve cholingenic synapse, resulting in the hyper-stimulation of muscarinic and nicotinic receptors (Hasan *et al*., 1979, Costa, 2006). The hydrolysis of OPs can either be *via* A-esterases e.g. PON1 or B-esterases e.g. AChE, butyrylcholinesterase (BuChE), and neuropathy target esterase (NTE). Catalytic hydrolysis by A-esterases is known to break down OP compounds to their major metabolites (detoxification) without affecting esterase activity (Costa *et al*., 2003). Conversely, non-catalytic hydrolysis of OPs by B-esterases causes significant inhibition of esterase activity and leads to the adverse effect of toxicity (Costa, 2006). Poisoning with OPs may occur through inhalation, ingestion or exposure of the skin (Karki *et al.,* 2004). The severity of the symptoms depends on the extent of the OP-AChE binding. The inhibition of acetylcholinesterase by OPs through a stoichiometric reaction may last from a few hours to several days and may be reversible or irreversible, depending on the chemical nature of the OP (Chambers, 2004). Irreversible reaction is that the OP-AChE complex can undergo non-enzymatic dealkylation. This is known as an aging reaction, resulting in deactivation of phosphorylated esterase *via* the loss of one or two R groups (Costa, 2006) as shown in Figure 1.2.

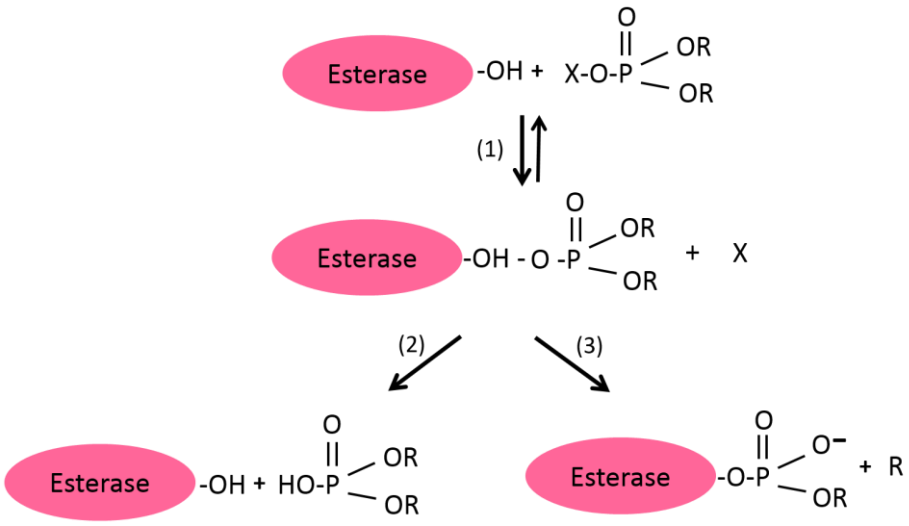

Figure 1. 2 A simplified representation of interaction mechanism between OPs and esterases.

Reaction (1) leads to reversibly organophosphorylated AChE. Reaction (2) leads to the spontaneous reactivation of AChE and hydrolysed OP. Reaction (3) leads to the stable inactive (aged) negatively charged organophosphorylated AChE.

1.3 Clinical Presentation and Possible Treatments

Clinical signs may include skeletal muscle fasciculation, respiratory failure, muscle weakness and ultimately death (Kose *et al*., 2009). Organophosphate poisoning has therefore become a major research area and a complete understanding of toxicity mechanism(s) is essential to identify novel OP protein targets. Exposure to OPs can be evaluated by measuring the activity of AChE in the blood or by the detection of OP metabolites in the urine (Atala & Lanza, 2001; Eskenazi *et al.,* 2004). However, given the varying nature of AChE inhibition, this is dependent upon the specific OP involved (Atala & Lanza, 2001; Quistad, 2005). Protection from OP intoxication is suggested for military personnel (Chambers, 2004). This can be achieved through the neutralization of OPs by providing exogenous (non-target) esterases, such as oximes. This allows the phosphorylation of these non-target esterases prior to the phosphorylation of the target esterases. This retains the availability of active AChE and prevents undesirable toxic effects (Chambers, 2004). Also, in case of OPs poisoning, atropine can be provided for patients to reactivate unaged acetylcholinesterase (Worek & Eyer,

2006). However, their use were controversial and treatment depends on the type of OPs and the severity of poisoning (Cherian *et al.*, 2005).

1.4 Chemical Structure of Organophosphorous Compounds

Organophosphates are esters derived from phosphoric acid (Figure 1.3), which inhibit AChE (Eddleston *et al.,* 2008). Organophosphate molecules contain two lipophilic groups R1 and R2, and an X group which is the "leaving group" more liable to be displaced when an OP binds to the active site serine on AChE, through an organophosphorylation reaction forming a stable bond (Costa, 2006). Figure 1.4 illustrates the structures of several common OP compounds. Some OPs, such as, chlorpyrifos, diazinon and PSP, which will be focused on in this study.

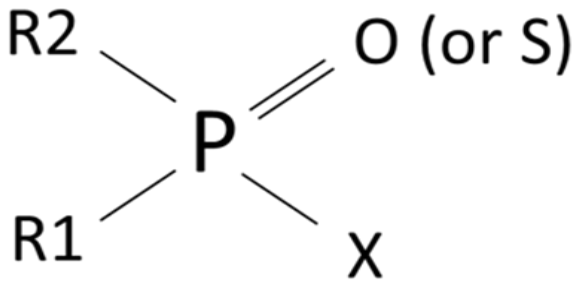

Figure 1.3 General chemical formula of organophosphorous esters.

Oxygen or sulphur are attached to the phosphorus. The leaving group detaches when OPs interact covalently at the active site of AChE. R1 and R2 are commonly alkoxy, amino, thio alkyl and phenyl groups, which can be the same or vary. X can be a halogen or alkyl, alkoxy group.

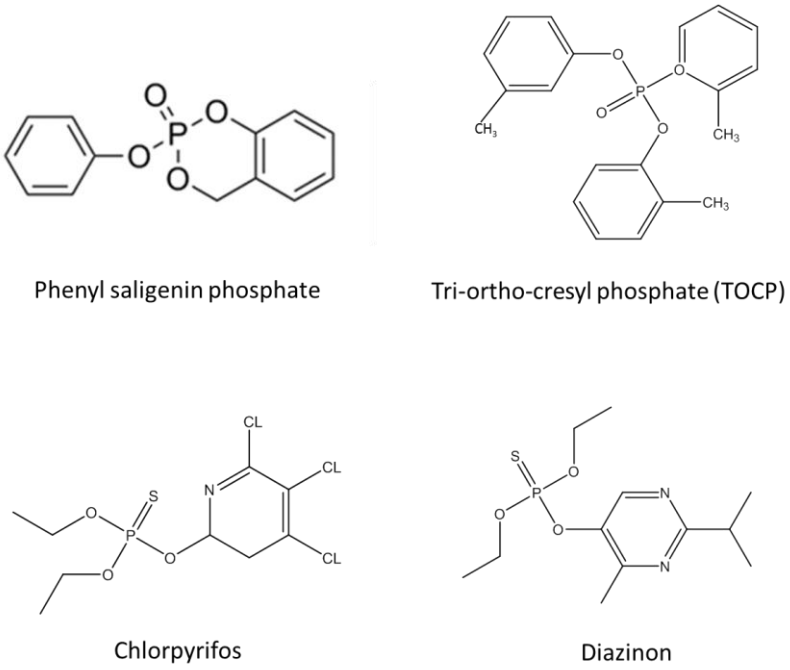

Figure 1.4 The chemical structures of several common OP compounds.

1.5 OPs of Relevance to this Study

This study investigated the effects of PSP, two organophosphorothioate insecticides (diazinon and chlorpyrifos) and their acutely toxic metabolites (diazoxon and chlorpyrifos-oxon) on mitotic and differentiated H9c2 cardiomyoblasts, the chemical structures of which are shown in Figure 1.4. These OPs exhibit differential binding affinity either to AChE or to NTE from human tissue to exert their toxicity as shown in Table 1.1. Their bioactivation and mechanism to induce toxicity will be briefly discussed in the following sections.

Table 1. 1 Sensitivity of different inhibitors of OPs toward human AChE and NTE.

OPs	AChE I_{50} (μM)	NTE I_{50} (μM)
Chlorpyrifos oxon	0.01	0.2 (Lotti, 2000)
Diazoxon	0.0068 (Colović, 2010)	no data presented
Phenyl saligenin phosphate	0.12	0.003 (Lotti, 2000)

I_{50}: half maximal inhibitory concentration.

1.5.1 Chlorpyrifos

Chlorpyrifos (O, O-diethyl O-3,5,6-trichloropyridin-2-yl phosphorothioate, chlorpyrifos-ethyl) was the first OP to be released onto the market. It has been used globally as an active pesticide in the agricultural sector (Fenske *et al*.,2002) and is also used widely in the non-agricultural sector. For example, in professional golf lawn care, retail lawn care and in termite liquid barriers (Eaton *et al*., 2008; Rush *et al.,* 2010). However, exposure to trace amounts of more than 0.001–0.01 µg/kg/day of these toxic pesticides poses a health risk for farm workers (Eaton *et al.*, 2008).

Chlorpyrifos is well absorbed by the intestines and lungs and rapidly metabolized. The toxicity of chlorpyrifos is dependent on its biotransformation via oxidation reactions to form the active metabolites TCPy (3,5,6- trichloro-2-pyridinol), diethylthiophosphate (DETP) and diethylphosphate (DEP), or via desulphuration to form chlorpyrifos oxon (Chambers, 1992) as shown in Figure 1.5. These metabolites are mainly formed in the liver and brain (Chambers & Chambers, 1989).

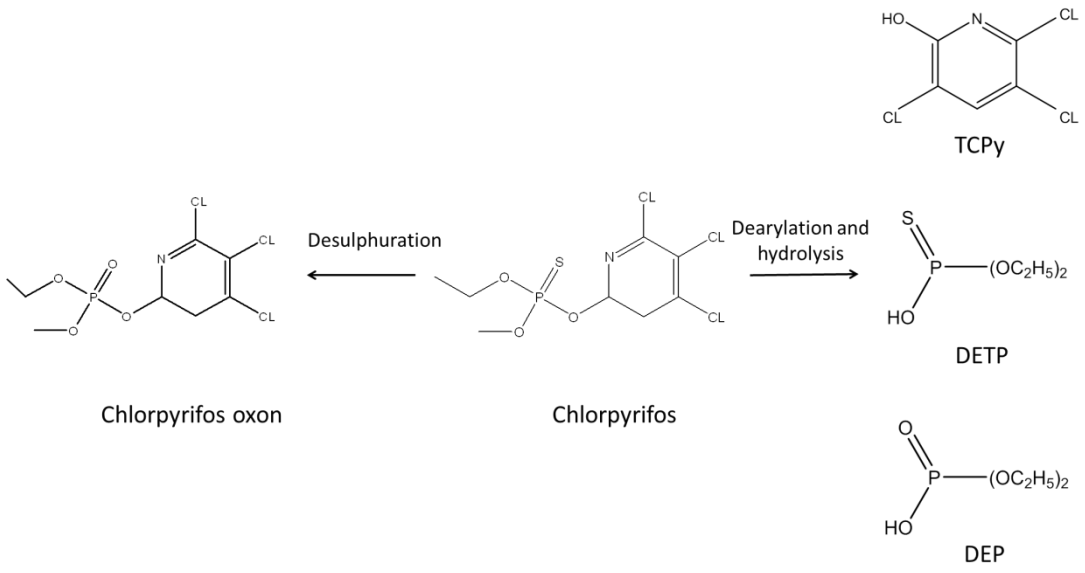

Figure 1.5 Metabolic pathway of chlorpyrifos.

Desulphuration reaction lead to bioactivation of chlorpyrifos to a more potent cholinesterase inhibitor chlorpyrifos oxon, or dearylation reaction lead to the degradation of chlorpyrifos to TCPy , DETP and DEP. Taken from (Eaton *et al.,* 2008).

Bioactivation of chlorpyrifos is mainly induced by various cytochrome P450 (CYP) isoforms to produce chlorpyrifos oxon. Cytochrome P450 enzymes are present in the liver and the activity of specific isoforms varies between individuals (Demorais *et al*., 1994) CYP isoforms such as CYP2B6, CYP1A1, CYP3A4 and are responsible for OP biotransformation and CYP2C19 and paraoxonase is important for OP detoxification processes (Sams *et al*., 2004; Rose & Hodgson, 2005). However, the balance between the formation of oxon and its detoxification is dependent upon the expression/activity of the various CYP isoforms (Rose & Hodgson, 2005). For example, CYP2B6 is mostly responsible for the formation of chlorpyrifos oxon, whilst CYP2C19 seems to have the highest deactivation activity. Furthermore, the expression levels of these isoforms varies between individuals (Sams *et al*., 2000). Thus, individuals with high CYP2B6 and low CYP2C19 are highly susceptible to chlorpyrifos toxicity (Sams *et al*., 2004; Mutch & Williams, 2006). Therefore, the profile of CYP isoforms may be an important contributor to differences between individuals in their susceptibility to the adverse effects of chlorpyrifos (Stevens *et al*., 2003).

Several studies have assessed the direct effects of exposure to chlorpyrifos oxon, which is known to be more potent inhibitor to AChE than its parent compound chlorpyrifos (Das & Barone, 1999; Zhao *et al.*, 2006; Eaton *et al*., 2008). The influence of chlorpyrifos oxon were reported to cause cholingenic hyper-stimulation, which evokes neurobehavioral changes and induces alterations in gene expression (Slotkin *et al*., 2007). Chlorpyrifos toxicity has also been reported. For example, chlorpyrifos (60 µM) reduced pro-apoptotic gene expression (e.g. Bcl-2 (B-cell lymphoma 2), CDKN2A (cyclin-dependent kinase inhibitor 2A) and MTA2 (metastasis associated 1 family member 2) in JAR cells (Saulsbury *et al*., 2008). It has also been reported that chlorpyrifos not only causes the inhibition of AChE activity but may also affect other organs. For example, Haas *et al*. (1983) reported gastrointestinal effects in piglets when exposed to chlorpyrifos and necropsy examination showed an increased level of intestinal fluid associated with severe diarrhoea and ending in mortality resulted from chlorpyrifos poisoning. Finally, chlorpyrifos can be detected in blood immediately after exposure. Its clearance from blood can occur rapidly, whereas its clearance from the whole body appears to be slow, and higher concentrations of chlorpyrifos are found in lipid adipose tissue in its steady state (Eaton *et al*., 2008).

1.5.2 Diazinon

Diazinon (O,O-diethyl-O-(2-isopropyl-4-methyl-6-pyrimidinyl phosphorothionate) is one of the most common and widely used pesticides. However, it has a potential toxic effect on water and food resources and therefore its use is highly restricted. Diazinon evaporates easily and its half-life varies depending on sunlight, pH, microorganisms present and the temperature of the environment (Zhang *et al.,* 2011). Diazinon undergoes degradation through direct oxidation degradation hydrolysis, producing the metabolites 2-isopropyl-6-methyl-pyrimidin-4-ol and diazoxon (Kouloumbos *et al.,* 2003). Diazinon undergoes a sulphoxidation reaction to form the toxic metabolite diazoxon (Vittozzi *et al.,* 2001). The structures of these metabolites are shown in Figure 1.6.

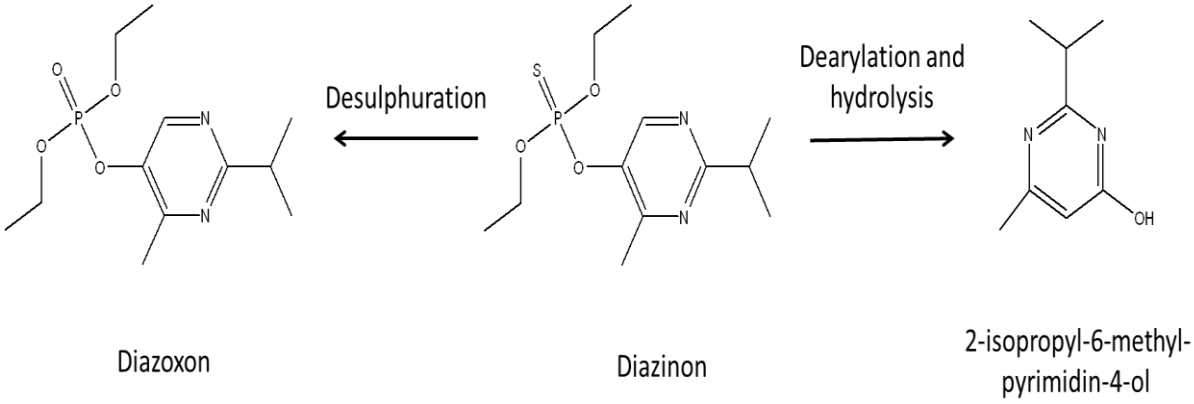

Figure 1.6 Metabolic pathway of diazinon.

The metabolite from the hydrolysis reaction is 2-isopropyl-6-methyl-pyrimidin-4-ol, while metabolite from the desulphuration pathway is diazoxon, which exhibits more potency in inhibiting AChE. Taken from (Kappers *et al.,* 2001).

Diazoxon is produced by oxidative desulphuration (P=S), which involves the substitution of sulphur with oxygen (P=O; Zhang *et al.,* 2011). Moreover, diazoxon shows a high reactivity, which gives it a greater potency to inhibit AChE. It also exhibits more polarity than the parent compound and possesses a greater stability in aquatic environments (Kouloumbos *et al.,* 2003). *In vivo,* diazinon metabolism is mediated by several cytochrome P450 isoforms

that include CYP2C19, CYP1A2, CYP3A4 and CYP2C19 (Kappers *et al*., 2001). Several enzymes e.g. CYP450, PON1 (paraoxonase 1), and B-esterase present in the intestines and liver are responsible for diazinon detoxification. Therefore, resistance to toxicity relies on the balance between bioactivation and detoxification following exposure to diazinon (Poet *et al*., 2003).

Acute exposure to diazinon has been associated with long-term health problems (Barrett & Jaward, 2012). For example, it has been reported that diazinon can cause mutagenicity resulting in chromosome abnormalities and sister chromatid exchange (Cox, 2000). Other studies have reported renal toxicity following exposure to diazinon (Jha *et al*., 2013). For example, diazinon decreases the activity of metabolizing enzymes such as glutathione-S-transferase and quinine reductase, leading to increased levels of blood urea nitrogen and serum creatinine (Shah & Iqbal, 2010).

1.5.3 Phenyl saligenin phosphate

PSP is an analogue of saligenin cyclic-o-tolyl phosphate (SCOTP), the active metabolite of tri-ortho cresyl phosphate (TOCP), produced in hepatic cells (Fowler *et al*., 2008). Since TOCP is mainly used in aircraft engines. This may lead to an occupational exposure from toxic aerosols, potentially resulting in memory loss and cognitive dysfunction (Winder & Balouet, 2001, Michaelis, 2011). Extensive studies revealed that some OPs, including PSP and TOCP, neither of which is a pesticide, exert their toxicity by organophosphorylation and inhibition of NTE which results in organophosphate-induced delayed neuropathy (OPIDN) *in vivo* (Nomeir & Abou-Donia, 1986; Zhao *et al*., 2006). Both PSP and TOCP act similarly to produce neurodegenerative poisoning (Hargreaves, 2012). However, to date, human exposure to TOCP is poorly documented; this therefore represents a wide area for research which needs to be undertaken (Baker *et al*., 2013).

1.6 *Molecular Targets of PSP*

PSP has been found to interfere with other cellular targets such as cytoskeletal proteins, neurotrophin receptors and transglutaminase enzyme activity (Carlson & Ehrich, 2001; Harris *et al.,* 2009; Pomeroy-Black & Ehrich, 2012). Therefore, it is worthwhile to discuss other targets involved after PSP exposure, in order to understand the potential molecular basis of PSP toxicity more fully.

1.6.1 Effect of PSP on neuropathy target esterase

PSP has been shown to be a classical inhibitor of the NTE enzyme (Baker *et al.,* 2013). NTEs are anchored in the endoplasmic reticulum and are essential for lipid metabolism (Forshaw *et al.,* 2001; Van Teinhoven *et al*., 2002). Moreover, NTEs display high catalytic activity in neuronal cells, although NTE activity has been demonstrated in non-neuronal tissue and cells such as testicles, kidney, and lymphocytes. Increased expression of NTE occurs in the early stages of embryo development and is thought to play an important role in signal transduction and nervous system development (Lotti & Moretto, 1993; Moser *et al*., 2000; Road, 2010). Thus any alteration in neuronal NTE activity may cause disruption of the endoplasmic reticulum, followed by vacuolation in cell bodies leading to defects in cellular function (Van Teinhoven *et al*., 2002; Akassoglou *et al.,* 2004).

Organophosphorylation of NTE by OPs is necessary for the development of OPIDN (Costa, 2006). OPIDN occurs when OPs interact with NTE and the latter undergoes an "aging" reaction, forming a terminal group with a negative charge linked to the active site of esterase, preventing enzyme to reactivate, as shown previously in Figure 1.2 (Williams, 1983). Complete organophosphorylation of NTE prevents the outgrowth of axon-like processes in differentiating N2a cells, following exposure to PSP (Flaskos *et al.,* 1994). Moreover, the inhibition of NTE may lead to neuronal degeneration and to modification of axonal morphology, both of which are early events of OPIDN in response to OP exposure (Ehrich & Jortner, 2001).

1.6.2 Effect of PSP on mitogen-activated protein kinase

To further characterize PSP-induced toxicity, the effects of PSP on mitogen-activated protein kinase (MAPK) and phosphoinositide-3-kinase/protein kinase B (PI-3K/PKB) signalling pathways has been investigated (Hargreaves *et al.,* 2006; Pomeroy-Black & Ehrich, 2012). For a detailed description of MAPK and PI-3K/PKB signalling pathways, see section 1.9. These signalling pathways play a vital role in the neuronal response to OP exposure, as they are responsible for regulating neurite outgrowth and cell survival (Kaplan, 1995). An increase in both phosphorylated PKB and MEK1/2 protein kinases was observed in human SH-SY5Y neuroblastoma cells after PSP exposure (Pomeroy-Black & Ehrich, 2012). Interestingly this

study explored OP-induced activation of neurotrophin receptors by very low concentrations of PSP (e.g. 0.01-1.0 µM). Thereby any disruption in these cascades may promote morphological changes and/or neuronal cell death (Nostrandt *et al.,* 1992, Carlson *et al.,* 2000). The effect of other neuropathic OP compounds on MAPK pathway-signalling proteins has been demonstrated in differentiating mouse N2a neuroblastoma cells (Hargreaves *et al*., 2006). For example, PSP (2.5 µM; 4 h) triggered transient activation of extracellular-signal-regulated kinases 1/2 (ERK1/2) which is associated with inhibition of NTE activity in mouse N2a neuroblastoma cells (Hargreaves *et al*., 2006).

1.6.3 Effect of PSP on cytoskeleton proteins

Further studies have assessed the disruption of cytoskeleton proteins during the induction of OPDIN by PSP. For example, in white Leghorn hens, PSP (2.5 mg/kg) promoted an increase of serum autoantibodies toward cytoskeleton protein neurofilament (NF) subunits (El-Fawal & McCain, 2008). NF subunits are proteins that play a vital role in the regulation of axonal diameter and regulation of the dynamics of cytoskeletal proteins such as microtubules and actin filaments (Perrone Capano *et al.,* 2001). If this regulation fails, cells will produce unstable microtubules with consequent disruption of axonal transport. Massicotte *et al.* (2003) also showed that PSP (1 µM) induces microtubule and neurofilament degradation associated with marked masses of cytoplasmic debris and neurite swelling in chick embryo dorsal root ganglia cultures. Hargreaves *et al.* (2006) also observed an increase in the phosphorylation of NF heavy chain in differentiating mouse N2a neuroblastoma cells when exposed to a sub-lethal neurite outgrowth inhibitory concentration of PSP (2.5 µM). Therefore, changes in these proteins can be considered as biomarkers for the progression of neuronal injury and neurotoxicity and a key event of the development of OPDIN following extensive PSP exposure (McConnell *et al.*, 1999; Yang *et al.*, 1999; Lalonde & Strazielle, 2003).

Previous studies have also shown that neuronal protein myelin-basic protein (MBP) is also phosphorylated by PSP (El-Fawal & McCain, 2008). This protein is a key component of myelin and is involved in its formation and maintenance (Boggs, 2006). It is also required for neuronal cell migration, survival and neurite outgrowth (Maness & Schachner, 2007). It is possible that phosphorylation of NF heavy chain and MBP might indicate myelin

degeneration and axonal damage, which was also seen in brain and spinal cord of chickens exposed to TOCP (Abou-Donia & Lapadula, 1990). Supporting evidence has come from an in vivo study by Ehrich & Jortner (2001), which reported that a toxic dose of PSP (10 mg/kg) resulting in the appearance of abnormal neurite growth and axonal damage in large myelinated fibres. All together, these studies support the claim that chronic exposure to PSP induces cytoskeletal disruption as well as NTE inhibition, which are all characteristic of an early event of OPIDN.

1.7 *Effect of Organophosphorous Compounds on The Cardiovascular System*

A number of studies have drawn attention to the cardiac effects associated with occupational exposure to OPs (Zoltani *et al.*, 2006). Evidence suggests that cardiac complications may occur after exposure to OPs (Roth *et al*., 1993; Karalliedde, 1999); however, the pathophysiology of cardiotoxicity following exposure to OPs is still not known. Multiple studies have, however, reported that sudden death may take place after exposure to OPs, with patients showing myocardial necrosis and toxic myocarditis (Anand *et al.,* 2009). This is due to the accumulation of ACh at ganglionic and cardiac centres leading to hypoxia and disruption of ion transportation (Karki *et al*., 2004).

Growing evidence also suggests that OPs (e.g. methamidophos) may trigger cardiac hypertrophy (Calore *et al*., 2007). These authors suggest that the main cause of hypertrophy is a persistent systemic arterial hypertension following exposure to the toxin (Saadeh *et al*., 1997). Hypertrophy is caused by the modulation of several complex biochemical pathways, such as calcineurin signalling. Calcineurin is a serine/threonine phosphatase, whose activation leads to the dephosphorylation and activation of transcription factors such as the nuclear factor of activated T cells (NFAT). The NFAT transcription factor family is involved in the regulation and development of the cardiac system (Shiojima, 2005). These studies have increased the interest in the study of cardiac abnormalities associated with OP toxicity and how they may modulate cardiac specific signalling pathways.

The various alterations seen in cardiac cells reveal a clinical picture of severe poisoning, with observed symptoms such as ventricular tachycardia, prolonged QT interval (the heart rhythm condition; measurement between Q wave and T wave in the heart's electrical cycle) and atrioventricular block (Kiss & Fazekas, 1979). Some authors believe that significant

cholinesterase inhibition in the plasma may produce changes in the electrocardiogram (ECG) leading to prolonged QT and ultimately cell death (Lotti, 2000). Pimentel & Carrington da Costa (1992) also reported that cholinergic overstimulation of cardiomyocytes is associated with lysis of myofibrils, micro-necrosis and an abnormal Z band. However, at present there are no current data concerning the cardiac biochemical markers associated with cardiac damage due to OP exposure. For this reason it is important to understand the molecular mechanisms associated with OP-induced cardiotoxicity. This project will investigate the effects of OPs on rat H9c2 cells and human stem cell derived cardiomyocytes.

1.8 *Alternative Molecular Targets of Organophosphates*

Emerging evidence suggests that not all of their toxicological actions involve the inhibition of the AChE, since other proteins and enzyme targets of OPs are involved (Casida & Quistad, 2005; Lopachin & Decaprio, 2005). Investigations of other markers beyond AChE were essential to detect post-OP exposure. Interestingly, the hypothesis that OPs may affect targets other than AChE is supported by numerous studies and will be discussed in the following sections.

1.8.1 Cytoskeleton proteins

A number of studies have observed significant effects of OPs on motor proteins such as kinesin, which can result in the disruption in axonal transport (Massicotte *et al*., 2003). Thus kinesin mediates the transport of vesicles and organelles and other cellular proteins along the microtubules through the axon and it is essential for a number of cellular functions (Pernigo *et al*., 2013). Gearhart *et al*. (2007) have clearly shown that administration of 0.59 nM diisopropylfluorophosphate and 10 µM chlorpyrifos affected kinesin function leading to impairment of axonal transport and axonal swelling of bovine brain cortex cells. This is further supported by Inui *et al.* (1993) who correlated axonal swelling with the development of organophosphate induced delayed neurotoxicity in male Wistar rats exposed to TOCP. According to Abou-Donia (1993) axonal swelling is mediated through the hyper-phosphorylation of cytoskeletal proteins following TOCP exposure, leading to a decrease in transportation and an aggregation of proteins along the axon (Abou-Donia, 1993).

Organophosphorus compounds were found to target cytoskeleton proteins such as tubulin, and thus they interfere with their assembly leading to impairment in microtubule function

(Prendergast *et al.,* 2007). For example, low concentrations (0.005 and 0.01 mM) of chlorpyrifos oxon were found to bind to tubulin and prevent its polymerization (Grigoryan & Lockridge, 2009). Tubulin polymerization is implicated in the formation of microtubules which are essential components of the cytoskeletal system, which is disrupted in neurodegenerative diseases (Gendron & Petrucelli, 2009). It has also been shown that dichlorvos exposure results in increased phosphorylation of tubulin affecting its assembly, resulting in axon dissociation and synaptic dysfunction (Choudhary *et al*., 2006). Moreover, the effect of individual OPs on actin cytoskeleton filaments in human neuroblastoma cells varies and relies on their distinct potency and structural activity (Carlson & Ehrich, 2001). Future studies should focus on the identification of possible non-cholinergic targets of OP compounds, which will help to increase understanding of the molecular mechanisms of OP-induced toxicity.

1.8.2 Albumin adducts

In 2005, Peeples *et al.* investigated novel protein targets for OPs used as pesticides. Initially, their research started by incubating mice with OP-labelled with FB-biotin (10-(fluoroethoxyphosphinyl)-N-(biotinamidopentyl) decanamide). Labeled FP-biotin can be used to identify proteins that bind to OPs (Schopfer *et al*., 2005). Organophosphates including chlorpyrifos oxon, dichlorvos, diisopropylfluorophosphate and sarin were incubated with human serum albumin, after which albumin peptide sequences were compared with and without OP treatment by mass spectrometry (MS; Peeples *et al.,* 2005). These compounds were found to bind covalently to Tyr411 and residue in albumin (Li *et al*., 2007). Thus, this OP-albumin binding shows more stability than OPs binding to the serine active site of cholinesterase (Read *et al*., 2010). These findings support the claim that albumin is one of the biological markers that could act as a detoxifying protein in cases of OPs endogenous intoxication, however this also depend on the type of OPs (Xu *et al*., 2007; Lockridge & Schopfer, 2010).

1.8.3 Acyl peptide hydrolase

APH is a serine acyl peptide hydrolase primarily present in red blood cells which is responsible for cleaving N-acetylated peptides for detoxification (Shimizu *et al*., 2004). The

detection of such enzyme activity may show more sensitivity than other OP targets due to its life-span, which is approximately 120 days, thus lasting long after OP *in vivo* exposures (Umlas *et al*., 1991; Quistad *et al*., 2005). *In vivo* study with mice have demonstrated that OP exposure can inhibit the activity of APH in brain (Cardona *et al*., 2013). Three types of insecticides (dichlorvos, naled, and trichlorfon) showed sensitivity to the APH enzyme (Quistad *et al* ,2005). Other study documented how other serine proteases (dipeptidyl peptidase IV and t-PA (tissue plasminogen activator) that belong to the APH subfamily may react with distinct types of OPs (Rosenblum & Kozarich, 2003). In comparison to AChE, different oxons (toxic metabolites of parent OP) showed ability to inhibit APH at lower concentrations than those required for AChE inhibition during *in vivo* exposure (Richards *et al.*, 2000). APH has been shown to be a potentially sensitive biomarker for identifying OP-delayed neurotoxicity with respect to AChE (Olmos *et al*., 2009).Based on these facts, inhibition of APH activity may be used as a biomarker for monitoring OP toxicity.

Numerous non-cholinesterase targets of OPs were discussed in the previous section. However, it needs to be emphasized that other non-cholinesterase targets may be implicated in OP toxicity. An experimental design needs to be developed to study the association of all types of OPs with their specific targets. As the current study has focused on the effects of OPs on mechanisms of cell death and signaling pathways a detailed discussion of such events would be worthwhile.

1.9 Cell Signalling

Organophosphate exposure may modulate cell signalling pathways which are critically important in the development of differentiated cells and numerous other cellular processes including cell survival and cell death (Slotkin, 2005). Cell signalling is a response that occurs within the cytoplasm when a cell receives an external signal leading to the activation of a cascade to transfer internal signals to the desired place in order to achieve the appropriate intracellular action. Moreover, this control mechanism involves regulatory proteins communicating with each other through signal transduction pathways to evoke a myriad of cellular functions (Weinberg, 2007).

1.9.1 MAPK signalling pathway

Mitogen-activated protein kinases (MAPKs) are a family of protein kinases that respond to stimuli and catalyse the phosphorylation of specific proteins inside the cell. They are involved in the regulation of numerous cellular functions that include cell proliferation, cell differentiation, cell survival and apoptosis (Kim & Choi, 2010). Their activation is induced by several external factors such as cytokines, growth factors and hormones *(*Stathopoulou *et al.,* 2008). The mammalian MAPK family consists of three major groups, which are the extracellular signal-regulated kinases (ERK1/2), the c-Jun N-terminal kinases (JNK1/2/3) and the p38 MAPKs (p38 MAPK-α/β/γ/δ). Activated MAPKs phosphorylate a multitude of protein substrates that include transcription factors, in order to bring about a specific cellular response (Zhang *et al.,* 2003). Each individual MAPK pathway involves the sequential activation of several different proteins kinases that are summarised in the following sections.

1.9.2 Extracellular-signal-regulated kinases 1/2

The ERK1/2 signalling pathway plays a key role cell proliferation and differentiation (Johnson & Lapadat, 2002). Activation of the ERK1/2 signalling pathway is initiated when a ligand such as epidermal growth factor (EGF), insulin, or platelet-derived growth factor (PDGF) binds to its respective tyrosine kinase receptor e.g. insulin receptor, EGFR, and PDGFR. This promotes receptor dimerization and auto-phosphorylation of tyrosine residues. After that the adaptor protein, growth factor receptor bound protein 2 (Grb2), binds to the phosphorylated receptor via its SH2 domain. Grb2 functions to link proteins to one another and contains one central SH2 and two SH3 domains which interact directly with Son of sevenless (Sos) and place Sos near the membrane. Sos functions as a ubiquitous guanine nucleotide exchanger for Ras and possesses a Ras binding site. Once Sos is recruited to the plasma membrane, it catalyses the exchange of GDP for GTP on the monomeric G-protein Ras (Pierre *et al*., 2011) as shown in Figure 1.7.

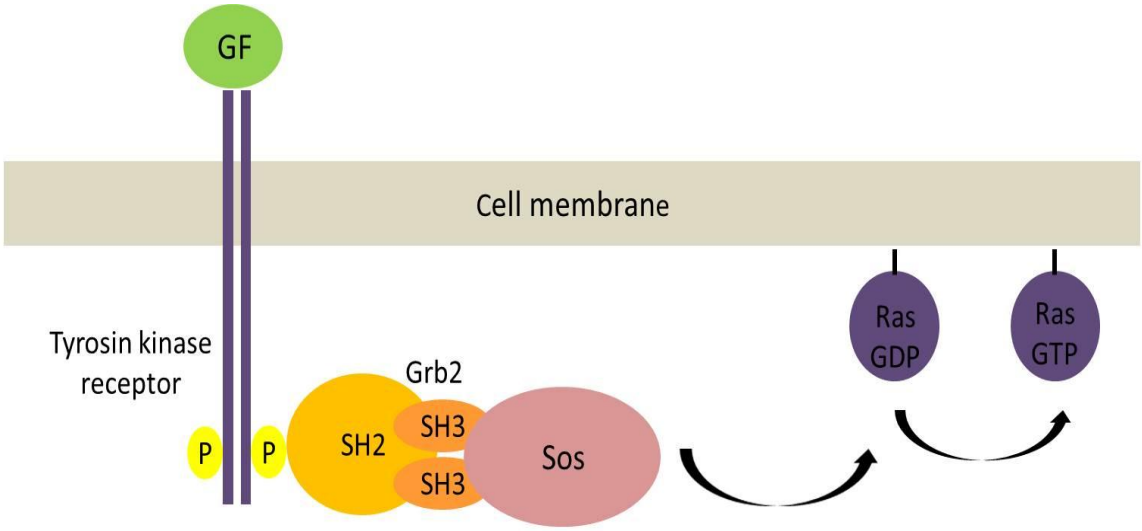

Figure 1.7 Activation of MAPK signalling transduction by RAS.

Binding of a growth factor (GF) to a tyrosine kinase linked-receptor leading to receptor dimerization. The receptor then undergoes auto-phosphorylation and binds to Grb2 (adaptor protein) via its SH2 domain. Grb2 then interacts with Sos via SH3 domains which leads to the recruitment of Sos to the plasma membrane, which stimulates the exchange of inactive Ras-GDP to its active Ras-GTP form.

Activated Ras (Ras-GTP) then promotes the activation of several members of the MAPKKK family, which in this case are Raf protein kinases (A-Raf, B-Raf, C-Raf). Activated Raf triggers the downstream phosphorylation and activation of MEK1 and MEK2 (Weinberg, 2007). After that, MEK1 and MEK2 phosphorylate and activate ERK1/2 as shown in Figure 1.8; once activated, ERK1/2 phosphorylates a number of downstream targets including transcription factors (e.g. CREB; cAMP response element-binding protein), phospholipase A_2 and ribosomal S6 protein kinase (Bornfeldt, 1996; Chen *et al*., 1998; Davies *et al.,*2000). These targets play essential roles in proliferative responses, cellular machinery and cytoskeletal reorganization (Reszka *et al.,* 1995; Roskoski, 2012). The ERK1/2 pathway plays a major role in myocardial growth in the embryonic mouse (Stathopoulou *et al.*, 2008). Similarly, reduction in phosphorylated ERK1/2 causes an alteration in the ventricular compact layer outgrowth and affects coronary vessel development (Lin *et al*., 2010). These observations support the fact that ERK1/2 is an essential regulator of myocardial growth (Kang & Sucov, 2005).

1.9.3 Jun N-terminal kinases

JNK or Jun N-terminal kinases comprise three distinct members, namely JNK1, JNK2 and JNK3 (Derijard *et al*., 1994; Kallunki, 1994; Gupta *et al*., 1996). Generally these kinases are activated in response to stress stimuli such as heat shock, UV-radiation and osmotic shock (Bogoyevitch *et al*., 1996). Initially, their activation starts with the activation of small GTPases of the Rho family (Rac, Rho, Cdc42), which promote the activation of several members of the MAPKKK family e.g. MEKK1/2/4. Activated MAPKKKs then phosphorylate and activate MAPKK family e.g. MKK4/7 which in turn phosphorylate and activate JNK1-3 (see Figure 1.8). Once JNK has been activated, it translocates to the nucleus and phosphorylates several transcription factors to induce programmed cell death or apoptosis (Weston & Davis, 2002; Dhanasekaran & Reddy, 2008).

Several studies have shown that phosphorylated JNK evokes activation of the transcription factor AP-1 (activator protein 1; Kolomeichuk *et al*., 2008). The JNK/AP-1 pathway promotes apoptotic action via the increased transcription of pro-apoptotic genes such as TNF-α (tumor necrosis factors-α), Fas-L (Fas ligand) and Bak (Bcl2 antagonist/killer 1; Dhanasekaran & Johnson, 2007; Raman *et al.,* 2007). In addition, JNK phosphorylates a number of pro-apoptotic substrates, which play a vital role in the intrinsic and extrinsic pathways involved in apoptosis (see section 1.10). For example, JNK phosphorylates pro apoptotic BAD in primary granule cells which leading to the inhibition of pro-survival proteins such as Bcl-2 (Gross *et al*., 1999). Moreover, JNK signals also induce the release of cytochrome C from mitochondria, leading to the activation of caspase-9 and ultimately apoptosis (Aoki *et al*., 2002).

There is substantial evidence derived from studies of the effect of JNK inhibition in different cell types (Chen & Tan *et al*., 1998; Maroney *et al*. 1999). For example, the inactivation of JNK prevents apoptosis in liver cells (Uehara *et al*., 2005). Similarly, Ferrandi *et al*. (2004) observed that JNK inhibitors attenuated apoptosis of rat cardiomyocytes. In addition, the knockout of JNK1 and JNK2 in mice causes a defects in T-cells and apoptosis, while JNK3 was found to be responsible for excitotoxicity of the murine hippocampus (Yang *et al*., 1997).

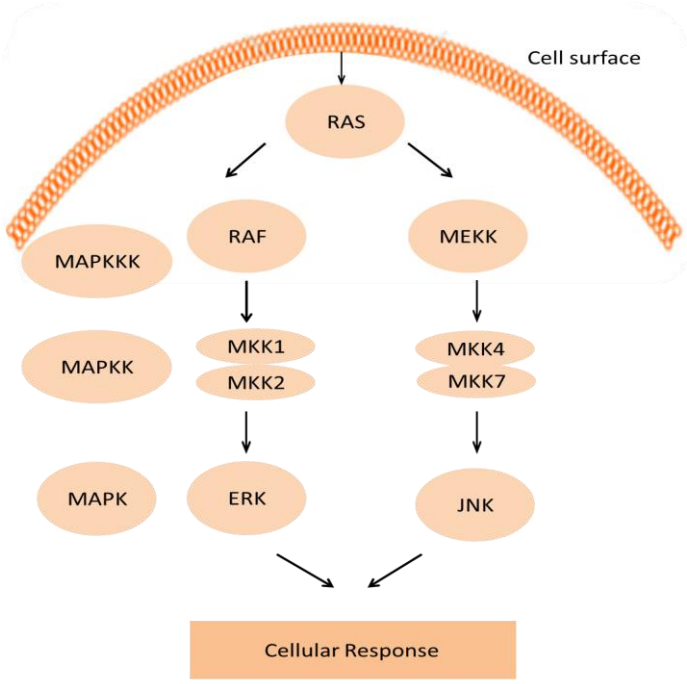

Figure 1.8 Mitogen-activated protein kinase (MAPK) signaling pathways.

ERK and JNK pathways are presented schematically. Each pathway is initiated by Ras activation, which phosphorylates serine/threonine residues of MAPKKK, which subsequently phosphorylates tyrosine/threonine residues of a MAPKK. This leads to the activation of MAPK, which in turn activates other protein kinases involved in cellular responses.

1.9.4 The Protein kinase B/Akt signalling pathway

There are three PKB/Akt isoforms in mammalian cells, namely, PKBα/Akt1, PKBβ/Akt2 and PKBγ/Akt3 (Cheng *et al*., 1992). PKB/Akt is employed in the centre of downstream signalling pathways that are activated in response to a wide variety of extracellular stimuli including GPCR (G-protein-coupled receptors) agonists and growth factors. PKB is involved in the regulation of cellular growth, metabolism and cell survival via the phosphorylation of downstream targets (Brazil & Hemmings, 2001; Song *et al*., 2005; Dillon *et al.*, 2007). PKB activation is associated with the downstream effector PI-3K. As shown in Figure 1.9, the pathway starts with the up-stream activation of PI-3K via the monomeric G-protein Ras (Wymann *et al.,* 2003). Activated PI-3K phosphorylates PIP_2 (phosphatidylinositol 4,5-bisphosphate) resulting formation of the second messenger PIP_3 (phosphatidylinositol (3,4,5)-trisphosphate). Increases in PIP_3 lead to the recruitment PDK1 (pyruvate

dehydrogenase kinase 1) to the plasma membrane and subsequent phosphorylation of PKB at Thr^{308}. PKB is then phosphorylated at Ser^{473} by mTORC2 (mammalian target of rapamycin Complex 2) leading to full activation of the enzyme (Weinberg, 2007). However, the activity of PKB can be de-regulated by PTEN (Phosphatase and tensin homolog). PTEN is a phosphatase responsible for dephosphorylating PIP_3 to PIP_2, thereby causing the inactivation of the PKB signalling pathway (Simpson & Parsons, 2001).

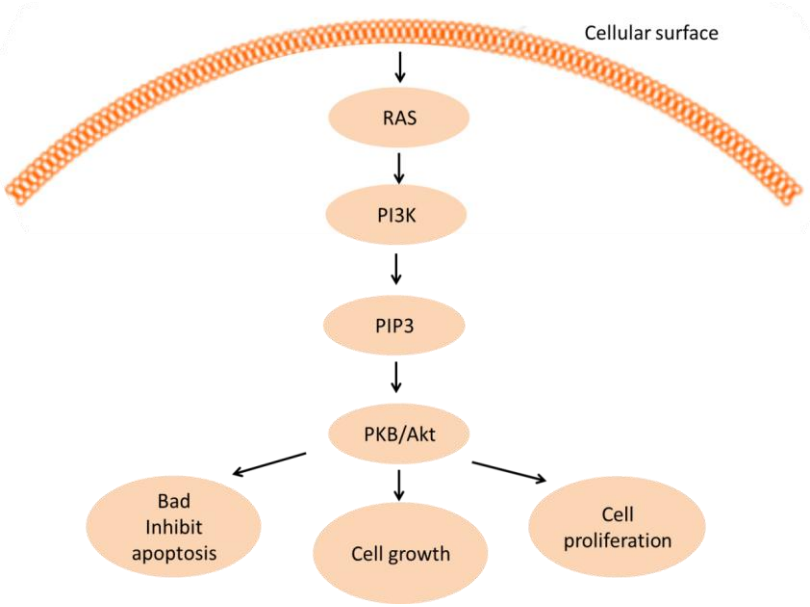

Figure 1.9 Schematic representation of PKB/Akt activation.

Activation of PKB/Akt signalling pathway is initiated by RAS activation, which in turn activates PI3K. PI3-Kinase is activated and generates the second messenger PIP3, that activates the downstream PKB/Akt. PKB/Akt is an important mediator of organismal growth.

The role of the PKB/Akt cascade in the heart is characterized as a central effector in cardiac-signalling mechanisms (Lee *et al.*, 2009). The functional description of PKB/Akt is a growth-promoting protein that stimulates myocyte growth, allowing the recruitment of angiogenic growth factors such as VEGF (Vascular endothelial growth factor) and inducing coronary angiogenesis (Shiojima & Walsh, 2006). In normal heart cells, PKB-dependent signalling pathways maintain the balance between the two mechanisms, myocyte growth and coronary angiogenesis. Activation of the PKB-mTOR pathway induces both myocyte growth and coronary angiogenesis recruitment (Takahashi *et al.,* 2002). However, prolonged

activation of PKB results in a blockage in VEGF secretion and attenuation of coronary angiogenesis, which leads to the development of cardiac pathological stimuli (Shiojima & Walsh, 2006). Thus, the PKB/Akt signalling pathway is implicated in the regulation of cardiac growth (DeBosch *et al.,* 2006).

1.10 Apoptosis and necrosis

Apoptosis is a form of programmed cell death which is energy-dependent. It plays an essential role in both physiological and pathological processes (Norbury & Hickson, 2001). It is regulated by specific receptors that activate downstream caspases, which leads to the degradation of proteins and subsequent apoptosis (Metzstein *et al.*, 1998). An alternative form of cell death is necrosis, which is considered to be an uncontrollable passive process and is known to be an energy-independent death (McLaughlin *et al*., 2001). Necrosis is characterized as the degenerative processes that can exclusively occur after cell death; it is known to be an irreversible and un-regulated process (Elmore, 2007).

Structural changes and the biochemical network of cell death have been investigated, using a number of approaches, to determine the difference between apoptosis and necrosis with regard to various extracellular stimuli. Studies found that apoptotic cells appear to be DNA-fragmented: the cells shrink and exhibit membrane blebbing, but they do not release their cellular organelles into the extracellular space; thus they are rapidly phagocytosed, preventing inflammation (Savill & Fadok, 2000; Kurosaka *et al*., 2003). In contrast, necrosis shows a swelling of the cell and a loss of membrane integrity, followed by the release of cellular constituents to the surrounding tissue, forming an inflammatory response (Kerr *et al*., 1972; Majno & Joris, 1995; Trump *et al*., 1997). However, despite the fact that each type of cell death can have different mechanisms, it can be difficult to distinguish necrosis from apoptosis using morphological analysis. In fact both forms of cell death may occur simultaneously relying on intracellular ATP (Adenosine triphosphate) and caspase activation (Zeiss, 2003). Major differences between apoptosis and necrosis are summarized in Table 1.2

Table 1.2 Apoptosis versus necrosis. Taken from (King , 2000).

	Apoptosis	Necrosis
Stimuli	Genomic damage Imbalance in signalling pathways Programmed tissue remodeling Hypoxia	Changes in pH Hypoxia Anoxia Absence of nutrients
Morphological changes	Individual cell affected Decreased cell volume Condensed chromatin Unaffected lysosome No inflammatory response Apoptotic bodies are phagocytes	Groups of cells affected Increased cell volume Fragmented chromatin Abnormal lysosome Marked inflammatory response Cell lysis
Molecular changes	Gene activity required for programmed cell death Increase in intracellular calcium Ion pumps continue to function	Don't require gene activity Unaffected intracellular calcium Impaired ion pumps

1.10.1 Two distinct signalling pathways of apoptosis

The molecular machinery of apoptosis involves two main pathways, the extrinsic and the intrinsic pathway, both of which converge on the cleavage of caspase-3 and result in a biochemical modification of the cell (Igney & Krammer, 2002). Caspase-3 is a proteolytic enzyme belonging to the cysteine protease family, playing a major role in both apoptotic pathways (Gown & Willingham, 2002). Its sequential activation occurs in the early stages of apoptosis, similar to other caspase family members, as shown in Figure 1.10 (Krysko *el al*., 2008). The extrinsic pathway is initiated by extracellular ligand binding to death receptors at the plasma membrane; such ligands are members of the TNF (tumour necrosis factor) family. Some examples of include FasL, TNF-α and TRAIL (TNF-related apoptosis-inducing ligand**.** **(**Chicheportiche *et al*., 1997). Members of their receptors possess a cytoplasmic "death domain" (Ashkenazi & Dixit, 1998). Once these receptors are activated by ligand binding, the adaptor protein FADD (Fas associated death domain) is recruited and binds to the death domains of the receptor (Wajant, 2002). The resultant DISC (death-inducing signalling complex), cleaves pro-enzyme caspase-8 into active caspase 8 (Kischkel *et al*., 1995). Caspase-8 then activates the "executioner" caspase-3, thereby converging with the intrinsic pathway (Weinberg, 2007). Following activation, caspase-3 cleaves various death substrates such as ICAD (inhibitor of caspase activated DNase) and lamin, which in turn induces the apoptotic cell phenotype (Weinberg, 2007). The extrinsic pathway can be controlled by c-

FLIP (cellular FLICE-like inhibitory protein). This protein binds to the FADD and caspase-8, thus inhibiting apoptotic signals (Kataoka *et al*., 1998).

An alternative extrinsic apoptotic pathway is triggered by cytotoxic T-cell. These cells are able to kill target cells such as tumour cells and virus-infected cells by attaching to their surface and secreting the serine protease granzyme B (Trapani & Smyth, 2002). Following secretion, granzyme B attaches and becomes internalized in the cytosol of target cells, resulting in the cleavage of pro-caspases 10 and 3. In this way, they converge with other apoptotic pathways, leading to morphological biochemical changes which characterize apoptotic cell death.

Another spectrum of apoptotic cell death is the non-receptor intrinsic pathway, since it is initiated by internal signals that originate within the cell such as excessive calcium, radiation, free radicals and hypoxia (Elmore, 2007). These signals cause the mitochondria to release cytochrome c and Smac (second mitochondria-derived activator of caspases) into the cytoplasm. Cytochrome c interacts with Apaf-1 (apoptotic protease activating factor-1) forming an apoptosome complex resulting in the activation of caspase-9, while Smac/DIABLO proteins (second mitochondria-derived activator of caspases /direct IAP binding proteins) function to inactivate anti-apoptotic proteins (Weinberg, 2007). The resultant active caspase-9 is involved in processing pro-caspase-3 into active effector caspase-3, thereby converging with the extrinsic pathway as shown in Figure 1.10 (Hill *et al.*, 2004).

The release of cytochrome c from mitochondrial channels is regulated by members of the Bcl-2 family of proteins (Cory & Adams, 2002). For example, anti-apoptotic proteins including Bcl-2 (B-cell lymphoma 2) and Bcl-X_L (B-cell lymphoma-extra-large) are involved in keeping the outer mitochondrial channel closed, thus preventing the release of cytochrome c. On the other hand, Bax (Bcl-2-associated X protein), Bad (Bcl-2-associated death promoter), Bak (BcL-2 antagonist/killer 1) and Bid (BH3-interacting domain death agonist) are pro-apoptotic proteins that function to open mitochondrial channel and induce the release of cytochrome c to stimulate the initiation of apoptosis (Weinberg, 2007). Therefore, Bcl-2 family proteins play a major role in determining whether a cell commits to apoptosis or cell survival (Elmore, 2007).

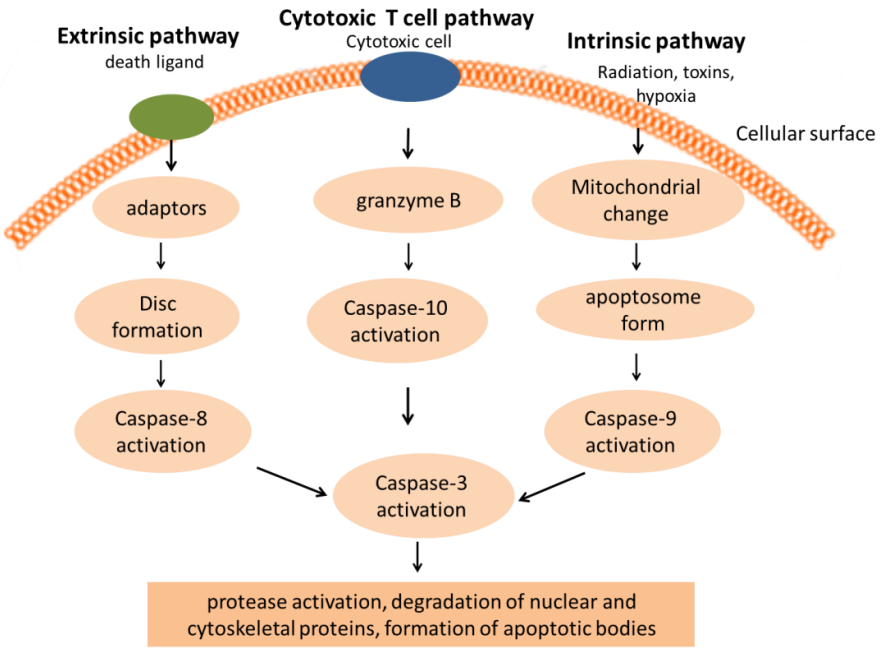

Figure 1.10 A simplified schematic representation of extrinsic and intrinsic apoptotic pathways.

Each pathway requires specific stimuli to induce molecular machinery events that promote activation of their own caspase (8,10,9). The resultant active caspase-3 induces apoptotic cell death.

1.10.2 OP-induced apoptosis

Several studies have shown that OP exposure results in the induction/modulation of apoptosis. For example, exposure to chlorpyrifos resulted in DNA double-strand breaks associated with cell apoptosis in human HeLa and HEK293 cells (Li *et al.,* 2015). A large amount of evidence has shown that OP-induced cell death involves several apoptotic markers such as cytochrome c release, caspase activation, and nuclear fragmentation (Saleh *et al*., 2003). For example, treatment of NK-92C1 cells with the OP dichlorvos triggered apoptosis via JNK activation and subsequent caspase-3 stimulation (Li *et a*l., 2007). Another study using primary cortical neuron cells reported that chlorpyrifos induced neurotoxicity, triggered apoptosis and reduced mitochondrial function via the activation of ERK1/2, JNK, and p38 MAP signalling pathways (Caughlan *et al.,* 2004). This is consistent with a recent study that found that chlorpyrifos targeted 40% of apoptotic genes in undifferentiated and differentiating PC12 cells (Slotkin & Seidler, 2012). Taken together, these findings suggest

that OPs induce cell death by apoptotic-dependent pathways both *in vivo* and *in vitro.* Studies demonstrating OP-induced apoptosis are summarized in Tables 1.3 and 1.4.

Table 1. 3 OP-induced cell death by apoptotic-dependent pathways *In vivo* studies

Organophosphate	Animal model	Dose	Incubation Time
Dichlorvos	Rat brain	6 mg/kg bw	12 weeks (Kaur *et al*., 2007)
Chlorpyrifos	Mouse retina	63 mg/kg	Single treatment- 24 h (Yu *et al*., 2008)
Diazinon	New born rats	1 or 2 mg/kg on postnatal days 1-4	4 days (Slotkin & Seidler, 2007)
Phosphamidon	Wistar strain male albino rats	35 ppm in drinking water	30 days (Akbarsha & Sivasamy, 1997)

Table 1. 4 OP-induced cell death by apoptotic-dependent pathways *in vitro* studies

Organophosphate	Cell line	Concentration	Incubation time
Chlorpyrifos	PC12 cell line	30 µM	24 and 72 h (Slotkin & Seidler, 2012)
Chlorpyrifos and dichlorvos	Human monocyte cell line U937 and NK-92MI , NK-92CI cell lines	25, 50, 100 ppm	4h (Li *et al*., 2009)
Carbofuran	Rat neuronal cortical cells	500 µM	3 days (Kim *et al*., 2003)
Endosulfan and zineb	SH-SY5Y human neuroblastoma cells	100 µM	20 h (Jia & Misra, 2007)

1.11 H9c2 cells

Of particular interest to the current study was the availability of a cardiomyocyte like rodent cell line. H9c2 cells are derived from embryonic rat heart tissue (Kimes & Brandt, 1976) and have been used widely as an *in vitro* model, since they display similar morphological, electrophysiological and biochemical properties to primary cardiac myocytes (Hescheler *et al.* 1991). A number of studies have used mitotic H9c2 cells which possess a more skeletal muscle-like phenotype and express nicotinic acetylcholine receptors (Kimes & Brandt, 1976; Zara *et al*., 2010). However, H9c2 cells in their mitotic form lack some of the properties of cardiomyocytes, such as gap junction communication and T tubules, and also show an absence of multi-nucleated cells due to cardiomyocyte de-differentiation (Hescheler *et al.*, 1991). With regard to H9c2 mitotic cells, this may actually limit the utilization of H9c2 cells and for this reason differentiated H9c2 cells represent a more physiological relevant cell model.

1.11.1 Differentiation of H9c2 cells

A number of studies have used this cell line as an *in vitro* model for cytotoxicity studies (Hosseinzadeh *et al.*, 2011). Under the right conditions, H9c2 cells are able to be differentiate into a more cardiomyocyte-like phenotype. This property enhances the use of H9c2 cells as a model cell line in which to study OP-induced toxicity. When cultured with reduced levels of foetal bovine serum (FBS) and 10 nM retinoic acid, H9c2 cells undergo morphological and physiological changes (Menard *et al*., 1999). These changes include the appearance of elongated multinucleated myotubes with recognizable actin filaments and branched fibres of differentiated cardiomyocytes (Kadivar *et al.,* 2006; Zara *et al*., 2010). Differentiation of H9c2 cells into a more cardiomyocyte-like phenotype is associated with the increased expression of cardiac specific proteins. For example, it has been shown that differentiated H9c2 cells express specific cardiac markers such as cardiac specific Ca^{2+} channels and cardiac troponin (Menard *et al*., 1999). Cardiac troponin is a specific cardiac cytoskeleton protein that is involved in muscle contraction (O'Brien *et al*., 2008). Furthermore, its expression has been shown in differentiated human embryonic stem cell-derived cardiomyocytes but not in undifferentiated human embryonic stem cells (Xu *et al.*, 2002).

At the molecular level, differentiation of H9c2 cells is regulated *via* a complex signal transduction pathway involving lipid and protein kinases. Several kinase cascades are associated with and up-regulated during cellular differentiation; the activation of such cascades may help to explain the differentiation process in cell behavior (Qiao *et al.*, 2012). For example, the PI-3K/PKB pathway promotes the differentiation of H9c2 cardiomyoblasts (Kim, 1999; Naito *et al*., 2003). In addition, PKCδ (protein kinase Cδ) has been reported to be involved in the differentiation of H9c2 cells (Zara *et al.,* 2010). The interaction of PKCδ with serine/arginine-rich splicing factor 2 (SC35) contributes to the morphological changes that are related to the cardiomyoblast phenotype (Zara *et al*., 2010). More importantly, the physiological and cellular changes associated with retinoic acid-induced differentiation is complex and involves the expression of distinct proteins (Duester, 2013). It is therefore important to identify how retinoic acid induces differentiation.

1.11.2 Cardiac excitation-contraction coupling

Excitation-contraction coupling (ECC) is the process where heart cells contact via an action potential process. Actin potential is an electrical stimulation achieved by an ion flux through a specialised channels in the cardiomyocyte membrane (sarcolemma) leading to heart contraction. Calcium ions is an important mediator for cardiac excitation-contraction process by entering in and out the heart cells during each action potential (Katz, 1992) . When calcium ions enter the cell through L-type calcium channels located on the sarcolemma. This calcium activates a calcium release from the sarcoplasmic reticulum (SR) through a specialised calcium receptors called ryanodine receptors and further induce a large release of calcium in the cell (Flucher & Franzini-Armstrong, 1996) as shown in Figure 1.11.

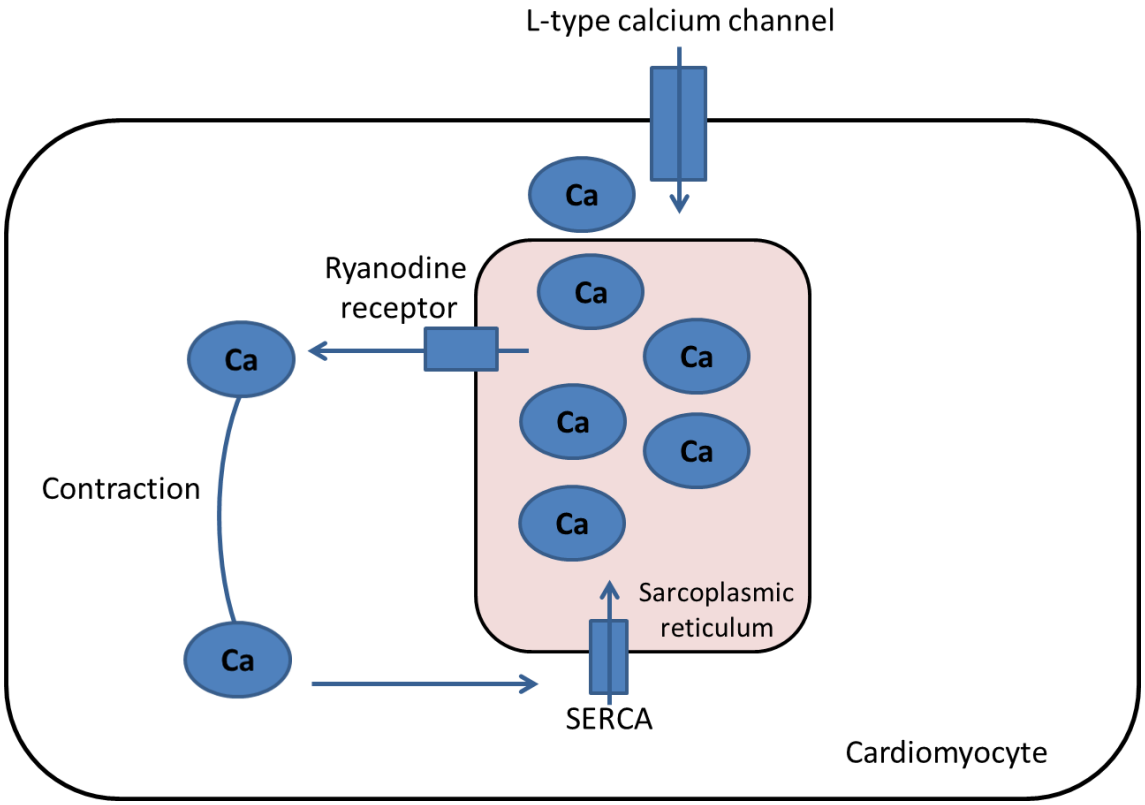

Figure 1.11 Cardiac contraction mechanism

Calcium ions inter the cardiac cell via L-type calcium channels. Calcium then activates ryanodine receptors on the sarcoplasmic reticulum. ryanodine receptors induce calcium release from the sarcoplasmic reticulum leading to increase cytosolic calcium. As the contractile cycle ends, cytosolic calcium returns to the sarcoplasmic reticulum via the sarcoplasmic reticulum calcium channel.

Cardiac contraction is regulated by binding of free calcium ions to troponin-C protein which is a part of the regulatory contract complex attached to the thin filaments (Mckillop & Geeves, 1993). Binding of calcium ions to troponin-C results in the conformational change of troponin/tropomyosin complex and exposing the actin binding site. Cross-bridge formation of myosin to actin occurs with ATP hydrolysis to ADP+P_i. A power stroke moves actin filament toward the center of the sarcomere and ADP+P_i are released from myosin heads as ATP energy is used to contract cardiac muscle (Mckillop & Geeves, 1993). At low cytosolic calcium concentration induces a conformational change in troponin complex leading troponin/tropomyosin complex binding to actin and a new ATP binds to the myosin head. Binding of ATP to myosin lowers the binding affinity of myosin to actin and allows myosin release from actin. (Balaban *et al*., 2003). Myosin then cock back to its position and ready to make cross bridge for a further contracting cycle (Balaban *et al.,* 2003).

The H9c2 cell line has been established from embryonic rat cardiac ventricle and it has properties similar to neonatal and adult cardiomyocytes (Menard *et al.,* 1999). After undergoing differentiation, these cells can functionally express L-type calcium channels ATP-sensitive potassium channels (Menard et al., 1999). Examination of the action potential and contractility of H9c2 cells cardiac cells has been well-established previously by using cell contraction assay. H9c2 cells was successfully proven to contract by measuring changes in the planar surface areas at different time point (Ku *et al*., 2011). Previous study also characterized the calcium dependent activation and ion selectivity in H9c2 cells. In H9c2 myotubes, cells were found to express L-type calcium that activates potassium channels directly or indirectly via calcium induced calcium release from sarcoplasmic reticulum. Thus, H9c2 cell line has served as a useful alternate of cardiac and skeletal muscles (Wang *et al*., 1999).

1.11.3 The role of retinoic acid in the differentiation of H9c2 cells

Retinoic acid (RA) is an active form of vitamin A (retinol). It is involved in cardiac development as well as in cellular proliferation and differentiation in the mammalian embryo (N'soukpoé-Kossi *et al.,* 2014). RA enters the cell and binds to cellular retinoic acid-binding protein (CRABP), which facilitates its transport into the nucleus. In the nucleus, RA binds to the nuclear receptor RAR/RXR (retinoic acid receptor/ retinoid X receptor) heterodimer which recognizes a specific DNA sequence within the target gene known as the

RA response element (RARE; Chambon, 1996). In response, this recruits co-activator proteins, which themselves induce transcriptional activity and trigger cardiac differentiation as shown in Figure 1.12 (Kumar & Duester, 2011).

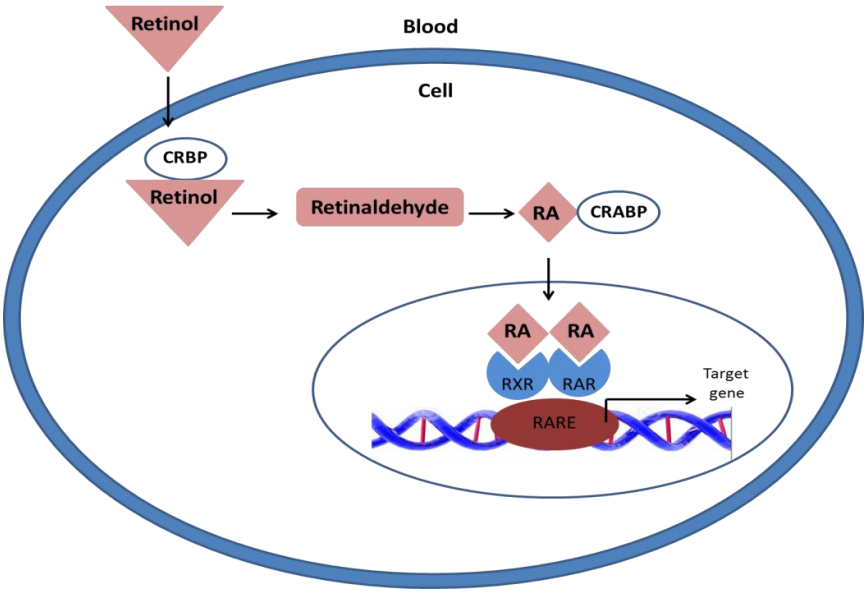

Figure 1.12 Retinoic acid signaling pathway in H9c2 cells.

Retinol enters the cell and binds to cellular retinoic acid-binding proteins (CRABPs) and is metabolized to retinaldehyde followed by metabolism of retinaldehyde to retinoic acid (RA). RA binds to CRABPs, enters the nucleus and binds to RARs and RXRs, termed heterodimer receptor (RAR/RXR). These heterodimers bind to RAREs in target genes and regulates gene expression.

Commitment to cardiac lineage is controlled by the up-regulation of specific cardiac genes such as Nkx2.5, which promotes differentiation of progenitor cells into cardiomyocytes (Martinez-Fernandez *et al*., 2014). Homeobox protein Nkx2.5 is expressed in the secondary heart field where it acts upstream of the BMP (bone morphogenic protein) and the FGF (fibroblast growth factor) pathways, both of which promote myocardial differentiation (Prall *et al*., 2007; Dyer *et al*., 2010). Nkx2.5 is also known to interact with another transcriptional factor, namely, Pitx2c, where this interaction is normally required for heart looping (Simard *et al*., 2009).

More recent studies have suggested that RA acts in parallel to EPO (erythropoietin) pathways and in this way both EPO and RA induce the release of cardiac mitogens, such as neuregulin (Chen *et al*., 2002; Kang & Sucov, 2005). RA also induces cardiomyocyte proliferation through biochemical pathways that involve the activation of PI-3K and ERK1/2 (Niederreither & Dolle, 2010). Furthermore, it has been observed in heart tissue that has a deficiency in RXR (a specific RA receptor) produces a reduction in the phosphorylation of PKB and ERK1/2, two important signalling pathways associated with cellular proliferation and differentiation (Kang & Sucov, 2005).

Another function of RA is the regulation of growth factor signalling such as FGF (fibroblast growth factor), as confirmed in a study of the developing hearts of chickens and mice (Mima *et al.*, 1995). Moreover, it was also found that FGF was responsible for controlling cardiac proliferation at early stages of development (Lavine *et al*., 2005). Potentially, the activation of FGF expression is important with regard to heart expansion, as demonstrated in Zebrafish where excess exposure to RA leading to an increased expression of fibroblast growth factor 9 in the epicardial layer (Marques *et al*., 2008).

As previously mentioned, RA-mediated pathways play a critical role in cell lineage control (Huang *et al.*, 2011). More importantly, RA induces the differentiation of cardiac myoblasts and a key to understanding this is the characterization of embryonic stem cell models that have been differentiated towards cardiac lineage. For instance, Wobus *et al. (*1997) observed that RA controls the differentiation of precursor germ cells in a concentration-dependent manner (Wobus *et al.,* 1997). Similarly, Honda *et al.* (2005) noticed that RXR directs the undifferentiating embryonic stem cell into a beating cardiomyocyte. Indeed, blocking the RA receptor prevents progenitor cells from differentiating into cardiomyocytes (Zhou *et al*., 1995; Wang *et al*., 2002). Moreover, it was also found that RA inhibited the expression of myogenin in embryonic muscle cells, leading to the inhibition of myogenic differentiation and enhancing cardiac differentiation (Xiao *et al.,* 1995). Myogenin is a transcription factor involved in the coordination of skeletal muscle development that is regarded as a specific marker for skeletal muscle (Menard *et al*., 1999).

It is also important to note that electrophysiological studies have confirmed that RA induces differentiation of cardiomyocytes (Menard *et al.*, 1999). For example, RA induces the

expression of cardiac specific ion channels e.g. L-type Ca^{2+} channels (Gassanov *et al.,* 2008) which are crucial for cardiac contractile function (Trautwein & Hescheler, 1990). Furthermore, RA is associated with an increased expression level of the pore-forming α_{1C} subunit of cardiac L-type Ca^{2+} channels, which is essential for maintaining the cardiac phenotype (Kimes & Brandt, 1976; Kolossov *et al*.,1998).

On the basis of the above it can be seen that RA is involved in the differentiation of cardiomyoblasts into cardiomyocyte-like cells. To date, very few studies have investigated the effects of organophosphates on cardiac cells. The present study will therefore investigate the effect of OPs using H9c2 cardiomyoblasts cells that have been derived from embryonic cardiac tissue and have similar features to cardiomyocytes. This will provide further valuable understanding of the cellular mechanisms involved in OP-induced cardiotoxicity.

1.12 Stem cells

Stem cells are defined by 3 fundamental properties and they the ability to self-renew and replace themselves, the ability to differentiate into 1 or more lineages or specialized cell types, and enormous proliferative potential to renew and maintain the tissues they populate (Thomson, 1998). Potency specifies the differential potential of the stem cells. Totipotent stem cell is the fertilised egg that gives rise to the first divisions of the cell. These cells can differentiate into embryonic and extraembryonic cell types; only the morula cells are totipotent which are able to become all tissue type including a placenta. Pluripotent stem cells (PSCs) are cells that originates from the inner mass cell of the blastocyst and have the ability to generate several different tissue types, excluding the placenta. Multipotent stem cells can produce only cells of a closely related family of cells e.g. cells in the brain that give rise to different neural cells and glia, but they can not produce blood cells or haematopoietic cells, which can give rise to different blood cell types, but they can't produce brain cells. Unipotent stem cells are able to develop into only one kind of cell. They normally develop into the same type of cell as those in the tissue from which they derive (Figure 1.13; Odorico *et al*.,2001). Finally, stem cells can be divided into different types, namely embryonic stem cells (ESCs), adult stem cells (ASCs) and induced PSCs (iPSCs).

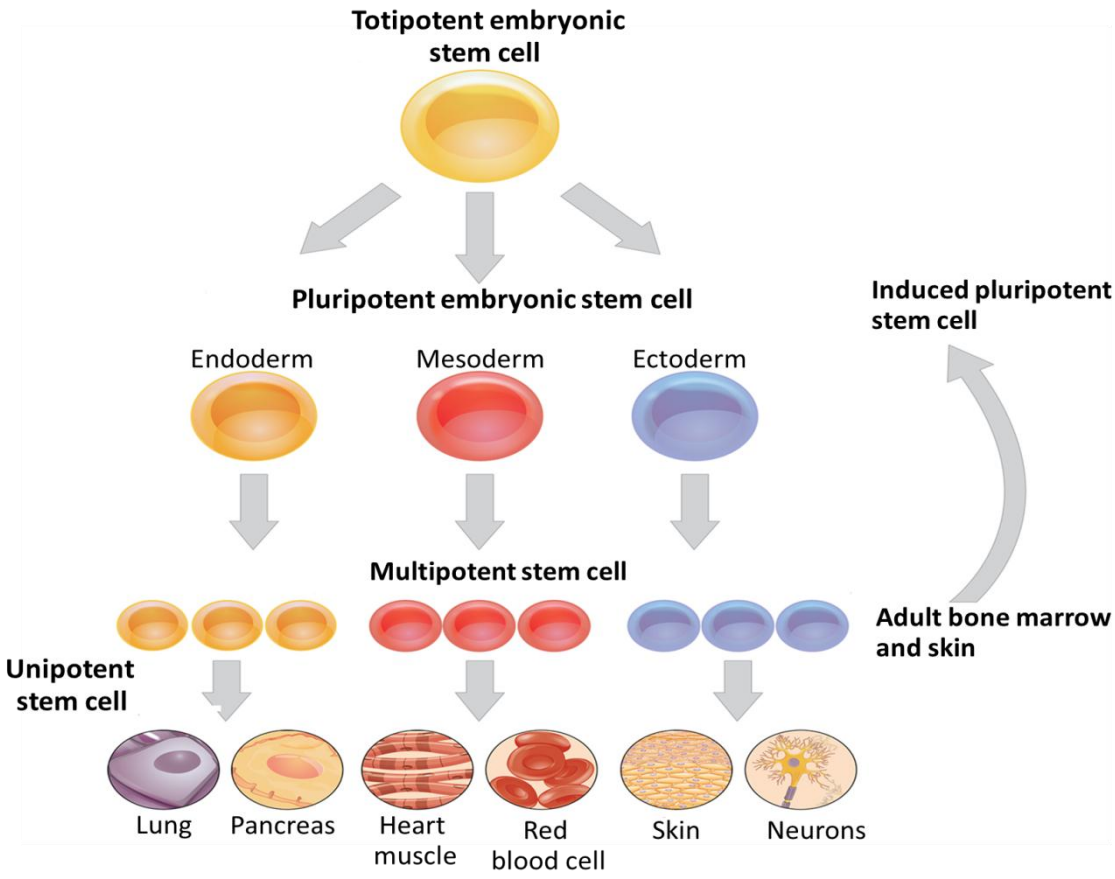

Figure 1.13 Simple diagram of stem cell potency.

Differential potential of the stem cells are totipotent embryonic stem cell that can produce any type of cells. Pluripotent stem cell that can also differentiated in to any specialized cell type, this include endoderm, mesoderm and ectoderm cell line and excluding embryonic tissue. Multipotent stem cell that can give a raise to unipotent stem cell, which can be differentiated into one specific cell type.

1.12.1 Embryonic stem cells

ESCs are PSCs that have the ability to differentiate into the three embryonic germ layers, which are the ectoderm, mesoderm, and endoderm (Shamblott *et al*., 1999). These cells can be isolated and maintained as undifferentiated cell lines or stimulated to differentiate into specific cell lineage in the body (Thompson, 1998). ESCs can be distinguished from multipotent cells present in adults according to their pluripotency, as multipotent cells are only capable to differentiate into specific tissue cells (Thompson, 1998). ESCs specific properties have attracted major research interest, particularly in cell therapy (Mitsui *et al*.,

2003). However, a number of ethical controversy have been raised in relation to the utilisation of human embryos as a cell source (McLaren, 2001).

1.12.2 Adult stem cells

ASCs are undifferentiated cells found throughout the body that divide to replace dying cells and regenerate damaged tissue. They are also known as somatic stem cells which can be found in children as well as adults (Takahashi *et al*., 2006). These cells can appear to exist in bone marrow and other tissues. However, *in vitro*, their differentiation process is challenging and poses some difficulties, as they have less possibility to differentiate in culture than ESCs. Ethically, these somatic stem cells are well accepted and they are not mired in controversy because no embryos are harmed when obtaining them (Wang *et al.*, 2009). However, most ASCs are considered unipotent, as they are destined to grow into the same cell type from which tissue they originate (Avasthi *et al*., 2008).

Certain ASC types are multipotent such as, mesenchymal stem cells (MSCs). They are highly heterogenous cells population consist of multiple cell types with different potential for proliferation and differentiations. They can be also be isolated from placenta and umbilical cord. Umbilical cord blood (UCB) makes allogeneic cell treatment possible due to the low possibility of immune rejection (Erices *et al*., 2000; Weiss & Troyer, 2006). Moreover, these cells have been shown to be useful in cellular therapy, as their healing effects have been proven in many pre-clinical and clinical studies. MSCs have been clinically tested and are associated limited ethical concerns (Hida *et al*., 2008). The possibility of healing improvement of impaired cardiac function *via* an MSC lineage derived from UCB has shown a practical recovery ability (Nishiyama *et al*., 2007). However, there is a remarkably low amount of MSCs in UCB (Kogler *et al*., 2004; Terai *et al.*, 2005). Therefore, additional experiments need to be undertaken to establish an efficient source for MSCs.

1.12.3 Induced pluripotent stem cells

Previous researchers have proposed that cardiomyocytes can be derived from various human tissues as a source of stem cells (e.g., foetal tissues, adult cardiac progenitor tissue, BM and adipose tissue). However, cardiomyocytes derived from foetal or adult tissue are controversial due to their limited plasticity, which prevents their complete differentiation into functional cardiomyocytes (Dimmeler *et al*., 2008). Cardiomyocytes derived from adult

cardiac progenitor cells were shown to possess the strong opportunity to differentiate into beating cells (Blin *et al*., 2010). Furthermore, the ability of PSCs to efficiently differentiate into contracting cardiomyocyte-like cells has been demonstrated *in vitro* (Kehat *et al*., 2001; Mummery, 2003). However, due to the difficulties to obtain cardiomyocyte from adult cardiac progenitor, there have been breakthroughs of human induced pluripotent stem cell (iPSc). New techniques have been established to provide a new source of differentiated functional cardiomyocytes *in vitro* that share similar properties of cardiomyocyte derived from hESC (Zhang *et al.,* 2009). Therefore the current study utilised cardiomyocyte iPSCs due to the difficulty of obtaining them from human PSCs.

iPSCs can be described as genetically reprogrammed somatic cells to express specific genes to transform the cells into an ESC–like state with defining properties. iPSCs possess the advantage of being similar to ESCs, as they can form different cell type (Takahashi & Yamanaka, 2006). The reprogramming of adult somatic cells (human fibroblasts) to iPSCs has been established by the transduction of transcription factors, such as Oct4 (octamer-binding transcription factor 4), Sox2 (Sex determining region Y-box 2) and Klf4 (Kruppel-like factor 4; Takahashi et al., 2007; Shi *et al.,* 2008; Huangfu *et al.,* 2008). These iPSCs are capable of indefinitely renewing themselves and differentiating into numerous cell types, including pancreatic β-cells, hepatocytes, haematopoietic cells and cardiomyocytes (Sanders, 2012). More recently, certain reprogramming factors and chemical compounds, such as 5'-azacytidine (a DNA demethylating agent) and valproic acid (a histone deacetylase inhibitor), have been demonstrated to improve the efficiency of iPSCs without causing genetic alterations (Mikkelsen *et al.,* 2008). To emphasise cardiac differentiation, iPSCs can be treated with signalling molecules, such as activin A and BMP4 (bone morphogenic protein 4; Laflamme *et al*., 2007, Yang *et al*., 2008). Remarkably, some studies have reported minimal and insignificant differences in transcriptional profiles between cardiomyocytes derived from ESCs and cardiomyocytes derived from iPSCs. Moreover, Gupta *et al.* (2010) reported that the two types of PSC-derived cardiomyocytes' transcriptional profiles were identical. It has also been demonstrated that ESC and iPSC-derived cardiomyocyte types show similar sarcomere organisation and the ability to differentiate into cardiomyocyte subtypes (eg, ventricular, atrial, and nodal); furthermore, they are both able to differentiate into cardiomyocyte subtypes like ventricular, atrial and nodal cardiomyocytes (Zhang *et al.*,

2009). This appears to indicate that it is possible for iPSCs to replace ESCs successfully for cardiac tissue engineering and cell-based treatment sources as shown in Figure 1.13 (Batalov & Feinberg, 2015).

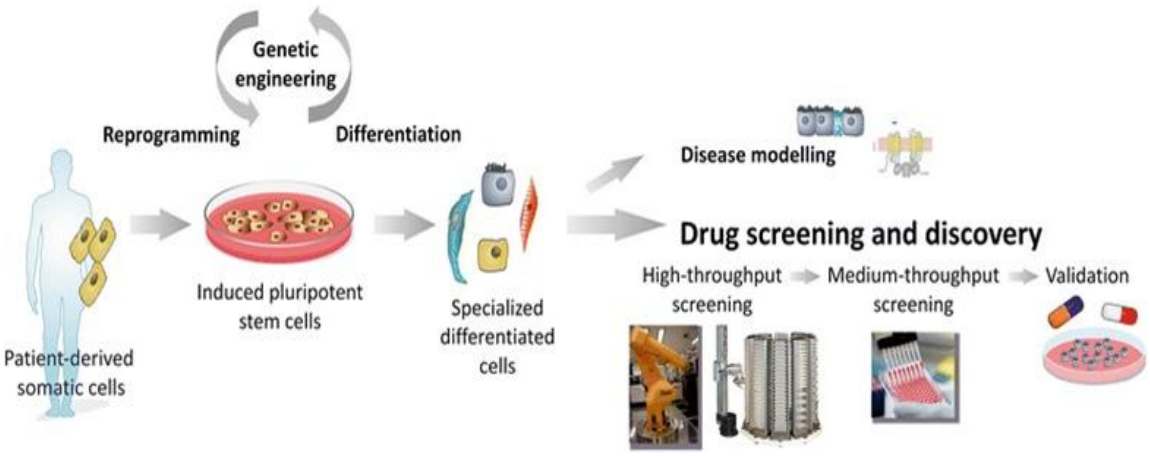

Figure 1.11 Schematic representation of iPSC generation

Patient-derived somatic cells can be reprogrammed or genetically engineered and expanded *in vitro* to produce iPSC. These cells then can differentiate into the interested specialized cell type and candidate for several use including disease modelling and drug screening. Taken from (Batalov & Feinberg, 2015).

1.15 Aims and Hypothesis

Literature review indicated that OPs can and cause human poisoning. Exposure to OPs lead to neurotoxic effects depending on the dose, frequency of exposure, and the type of OP. Toxicity of OP may also induce toxic myocarditis and a late occurrence of sudden death. At present, the majority of studies have focused on the effects of OPs on the central nervous system. There is very little information on the effect of OPs on muscle function, particularly toxic effects on cardiac muscle. There for it was important to investigate direct toxic effect of OPs on cardiomyocytes. The present study hypothesis that OPs would cause apoptotic cell death in H9c2 cardiomyocyte-like cells, and modulate cell signalling involved in cell death and cell survival. In addition OPs may target specific proteins involved in cardiac contraction leading to a serious cardiac complication. There for this study aimed :

- To study the morphological characteristics of differentiated H9c2 cardiomyocytes.
- To determine the effects of OPs on the viability of undifferentiated (mitotic) and differentiated rat H9c2 cells.
- To identify cell signalling pathways implicated in OP-induced effects.
- To detect and identify using dansylated PSP possible protein targets of PSP in differentiated H9c2 cells.
- To assess the effect of sub-lethal concentrations of OPs on the differentiation of H9c2 cells.
- To validate the cytotoxic effects of OPs in a human induced pluripotent stem cell derived cardiomyocytes

Chapter 2:

Materials and Methods

2.1 Material

2.1.1 Cell culture reagents

Dulbecco's modified Eagle's Medium (DMEM), foetal bovine serum (FBS), trypsin (10 ×), L-glutamine (200 mM), penicillin (10,000 U/ml)/streptomycin (10,000 µg/ml) were purchased from BioWhittaker Lonza Group Ltd., UK. Phosphate buffered saline (PBS) were obtained from Life Technologies (Invitrogen, UK). *All-trans*-retinoic acid was obtained from Sigma-Aldrich Co. Ltd (Gillingham, Dorset, UK). All other chemicals were purchased from Sigma-Aldrich and of analytical grade.

2.1.2 Human induced plouripotent stem cells (hiPSC-CC) cell culture

Vial of frozen hiPSC-CC, cardiomyocyte plating medium-basal, Cardiomyocyte Growth supplement were purchased from (Sciencell research laboratories, Carlsbad, USA).

2.1.3 Chemical compounds

Chlorpyrifos, chlorpyrifos oxon, diazinon, and diazoxon were purchased from Greyhound Chromatography and Allied Chemicals (Birkenhead, Merseyside, UK). Phenyl saligenin phosphate (PSP) and dansylated PSP were synthesized in house at Nottingham Trent University. Stock concentrations of 100 mM OPs were diluted in DMSO (dimethyl sulphoxide), which was present in all treatments including the control at a final concentration of 0.5 % (v/v).

2.1.4 Kinase inhibitors

LY 294002 (30 mM), PD 98059 (50 mM), SB 203580 (30 mM), SP 600 125 (20 mM) and wortmannin (10 mM) were obtained from Tocris Bioscience (Bristol, UK) were diluted in DMSO which was present in all treatments including the control at a final concentration of 0.5 % (v/v).

2.1.5 Antibodies

Table 2. 1 List if Primary antibodies for Western blotting and immunocytochemistry techniques and their working dilutions.

Antibody	Working dilution (Western blotting)	Working dilution (immuno-Cytochem.)	Company
Monoclonal phospho-specific JNK (Thr^{183}/Tyr^{185})	1:1000	NA	New England Biolab, UK, 9251
Polyclonal total unphosphorylated JNK	1:1000	NA	New England Biolab, UK, 9252
Polyclonal phospho-specific PKB (Ser^{473})	1:1000	NA	Sigma-Aldrich, UK, 9271
Polyclonal total unphosphorylated PKB	1:1000	NA	New England Biolab, UK, 9272
Monoclonal phospho-specific ERK1/2 ($Thr^{202/}Tyr^{204}$)	1:1000	NA	Sigma-Aldrich, UK, M8159
Monoclonal phospho-specific p38 MAPK (Thr^{180}/Tyr^{182})	1:1000	NA	New England Biolab, UK, 9216
Polyclonal total unphosphorylated p38 MAPK	1:1000	NA	New England Biolab, UK, 9212
Monoclonal total unphosphorylated ERK1/2 (9107)	1:1000	NA	New England Biolab, UK, 9107
Monoclonal cleaved caspase-3	1:500	1:500	New England Biolab, UK, 9661
Polyclonal Troponin 1	1:1000	1:1000	Abcam, UK, 47003
Polyclonal Tropomyosin	1:100	1:500	Abcam, UK, ab77884
Monoclonal α-actin	1:1000	1:100	Abcam, UK, ab124964
GAPDH	1:1000	NA	Abcam, Uk, ab8245

Table 2. 2 List if secondary antibodies for western blotting and immunocytochemistry techniques and their working dilutions.

Antibody	Working dilution (Western blotting)	Working dilution (immuno-cytochemistry)	Company
Anti-mouse IgG-HRP	1:5000	NA	Sigma-Aldrich,UK (A4416)
Anti-rabbit IgG-HRP	1:5000	NA	Sigma-Aldrich, UK (A0545)
Anti-mouse-Alexa 568	NA	1:200	Molecular Probes, UK, A-11031
Anti-rabbit-Alexa 568	NA	1:200	Molecular Probes Invitrogen, UK, A10042

2.2 *Methods*

2.2.1 Cell Culture

Cells (H9c2) derived from rat embryonic cardiomyoblast were purchased from the European Collection of Animal Cell Cultures in (Porton Down, UK). Mitotic H9c2 cells were cultured in T75 culture flasks in Dulbecco's Modified Eagle's Medium (DMEM), supplemented with 2 mM L-glutamine, 10% (v/v) Fetal Bovine Serum, 100 U/ml penicillin and streptomycin (100 µg/ml). Cells were grown in a humidified incubator of 5% CO_2, 95% air at 37 °C and left overnight. Cells were grown until they reached 70-80% confluence and growth monitored using a light microscope. Cells were sub-cultured by removing the medium and washing the cells with 10 ml sterile phosphate buffered saline (PBS). Cells were then detached by using trypsin (0.05 % w/v)/EDTA (0.02 % w/v) in PBS and left for 2-3 min in the humidified incubator. 10 ml of fully supplemented DMEM medium was added to the trypsinized cells and centrifuged for 5 min at 5000 xg. Supernatant was discarded and the cell pellet resuspended in 1 ml of the medium. Cells were then further sub-cultured (1:5 split ratio).

2.2.2 H9c2 cell differentiation

Differentiation of H9c2 cells were induced by culturing the myoblasts cells for 7 days with growth medium (DMEM) supplemented with 1% (v/v) FBS and 10 nM *all-trans* retinoic acid. The medium was replaced every 2 days. To confirm the effect of differentiating treatment, cells were monitored under a light microscope every 2 days. Cells showed cardiomyocyte-

like phenotype by forming multinucleated elongated myotubes. Further confirmation was performed by monitoring the expression of cardiac specific troponin 1 via immunocytochemistry and western blotting.

2.2.3 Human induced stem cell (hiPSC-CC) cell culture

Prior to HPSC-CC culture, three wells of 6-well plate were coated with 2 ml 1% (v/v) fibronectin in sterile Ca^{2+} and Mg^{2+} free Dulbecco's phosphate buffered saline, (DPBS) per well and incubated overnight in a humidified incubator at 37^{o}C. Next day Cardiomyocyte Plating Medium (CPM) was warmed at room temperature, and the coating fibronectin solution aspirated from the three wells and 1 mL of the warmed CPM was added to each well. Cryopreserved cells (hiPSC-CC), obtained from Sciencecell research laboratories, were thawed gently in a water bath (37^{o}C) for 90 seconds and transferred to a 15 mL conical tube, resuspended in 10 ml of CPM and centrifuged at 5000 xg for 5 min at room temperature. The supernatant was carefully aspirated avoiding any disturbance of the cell pellet and 6 mL of CPM add to the pellet with gentle mixing 2 - 3 times. After which 2 mL of cell suspension was added to each fibronectin coated well (3000,000 cell/well) and incubated 48 h in a humidified incubator 37^{o}C to avoid any disturbance of cultured cells. On the third day the medium was replaced by cardiomyocyte growth medium (CGM) to remove unattached cells. Cells were then detached by trypsin (0.05 % w/v)/EDTA (0.02 % w/v) in sterile phosphate buffered saline (PBS). Maturation and contraction of HPSC-CC was induced by culturing the cells for 7 days in CGM. The CGM medium was replaced every 48 h. The cells were monitored under light microscope to maturation and contraction. Further confirmation was performed by monitoring the expression of cardiac specific troponin 1, trypomyosin and α-actin via immunocytochemistry.

2.2.4 Cells count

The amount of viable cells was determined prior to any treatment. Trypan blue exclusion assay a method was used to estimate viable cell count. The H9c2 cell pellets were re-suspended in 1.0 ml of medium that was prepared during sub-culturing (section 2.2.1). A volume of 10 µl of cell re-suspension was mixed with 10 µl trypan blue dye. This mixture was pipette onto an Improved Neubauer haemocytometer (Camlab, UK) (0.1 mm depth, 400 mm^{-2}) and the cells were counted in the four (0.1 mm^{3}) corner squares via light microscope

at (100x) magnification (Olympus CK40-54-SLP, Japan). The cell density per ml was then calculated according to the following formula :

Cell density = cell number (mean from four fields) x 10^4 x dilution factor

2.2.5 Experimental procedure

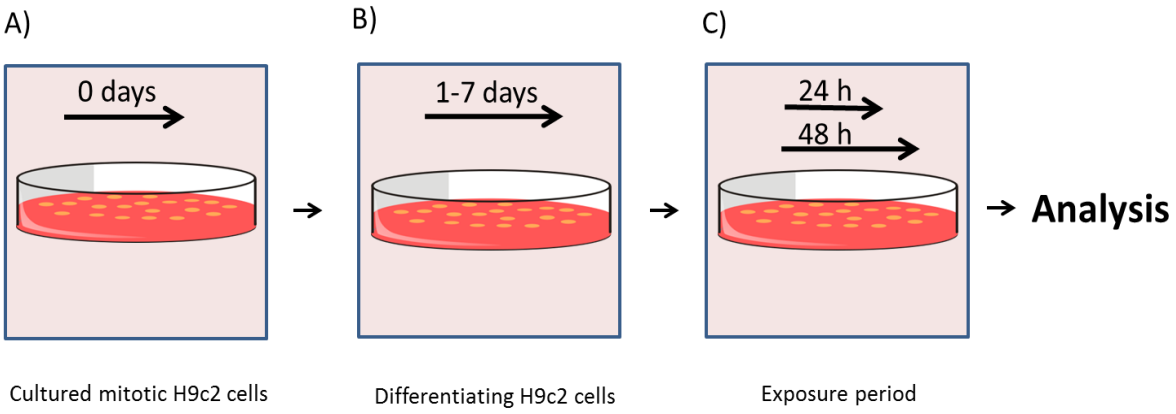

Figure 2.1 A schematic representation of the experimental procedure

A) Cultured mitotic H9c2 cells. B) Cells were induced to differentiate for 7 days. C) Differentiated H9c2 cells are incubated with the desired concentration of OPs at different time points. Different analyses were performed to study the effect of different concentrations of OPs on differentiating H9c2 cells.

2.2.6 Immunocytochemistry

Cells (H9c2) were seeded in 8-well chamber slides (BD Falcon Culture Slide) at a cell density of 15,000 cells/ chamber, for 24 hours with DMEM medium. The medium was removed and replaced with differentiation medium and incubated for a further 7 days with the differentiation medium changed every 2 days. After 7 days incubation H9c2 cells were completely differentiated. The medium was then aspirated gently from the chambers and the adherent cells were washed gently with pre-warmed PBS (37 C°) three time for 5 min. Cells were then fixed in 3.7% (w/v) paraformaldehyde (Sigma-Aldrich, UK) in PBS for 15 min at room temperature without agitation. Cells were then washed gently with pre-warmed PBS (37 °C) three times for 5 min and permeabilized with 0.1% (v/v) Triton X-100 in PBS for 15 min at room temperature without agitation. Cells were washed gently with pre-warmed PBS (37 °C) three times for 5 min. Fixed cells were then blocked by incubating the cells for 2 h with 3% (w/v) bovine serum albumin (BSA) in PBS (BSA/PBS) at room temperature without

agitation to prevent non-specific binding of antibodies. After blocking, cells were then incubated with specific primary antibody (1:1000) in 3 % (w/v) BSA in PBS (see table 2.1) and left over night at 4 °C in a humidified chamber. Cells were then washed gently with PBS three times for 5 min to remove unbound primary antibody. Cells were then then incubated for 2 h at 37 °C in a humidified chamber with the secondary antibody anti-mouse immunoglobulin G conjugated Fluorescein isothiocyanate (FITC; Abcam, UK), diluted 1:1000 in 3 % (w/v) BSA in PBS (see table 2.2). The chamber slides were then washed gently three times with PBS for 5 min. Cells were air dried and mounted with Vectashield® mounting medium (Vector laboratories Ltd, Peterborough, UK) containing DAPI (4',6-diamidino-2-phenylindole) nuclear counterstain for nuclear visualization. Slide were then cover-slipped and sealed from the edges of the cover slip by transparent nail varnish and left to dry for 5 min at room temperature. Finally, immunostained cardiomyocytes were visualized using an Olympus DP71 epifluorescence microscopic system equipped with an argon/krypton laser (FITC: EX_{493}/EM_{528}; DAPI: EX_{360}/EM_{460}).

2.3 *Cell Viability Assays*

2.3.1 MTT assay

Cell viability was determined by measuring the activity of mitochondria respiratory chain via MTT (thiazolyl blue tetrazolium bromide, Sigma-Aldrich) reduction assay. The MTT is a dye that will is converted to water-insoluble purple formazan on the reductive cleavage of its tetrazolium ring by the respiratory enzyme succinate dehydrogenase in active mitochondria. Undifferentiated H9c2 cells were seeded in 24-well plat at a density of 15,000 cells/well for 24 h (Sarstedt, Leicester, UK) in fully supplemented DMEM growth medium. Cells were then subsequently induced to differentiate for 7 days as described above in section (2.2.2). Cells were then treated with OPs at the indicated concentrations and incubation time. Following OPs exposure, cell viability was determined by incubating the cells with 0.5 mg/ml MTT solution in DMEM at 37 °C for 1 h. After that, the medium in each well was aspirated, and replaced with 500 µl of DMSO. The plate was then gently agitated to ensure sufficient dissolution of the water-insoluble purple formazan crystals. After that, 200 µl of the resulting solution was transferred into a 96-well plate (Sarstedt, Leicester, UK) and the absorbance of the solutions was read at 570 nm using a standard 96-well plate reader (Expert 96, Scientific laboratory, UK). The absorbance of the blank was subtracted from each sample absorbance

reading and the viability of the cells is directly proportional to the MTT reduction, which determined by the absorbance of the solubilized formazan product at 570 nm.

2.3.2 LDH assay

Cytotoxicity induced by OPs was assessed by lactate dehydrogenase (LDH) release into the culture medium. The LDH assay was performed according to the manufacturer's instructions (CytoTox 96® non-radioactive cytotoxic assay kit, Promega, Southampton, UK). The assay is a colorimetric assay based on the measurement of LDH release from damaged tissue that catalyze the conversion of lactate to pyruvate via reduction of NAD+ to NADH. Then, the dehydrogenase enzyme diaphorase (present in the substrate mix in the kit) coupled with NADH and the formation of red formazan product tetrazolium salt (INT). Thus, LDH release was proportional to the red formazan product. Cells (H9c2) where seeded into 96-well plates at a density of 5000 cells/well (Sarstedt, UK) and incubated overnight at 37 °C in fully supplemented DMEM growth medium to allow cell to adhere at the bottom of the plate. Cells were then differentiated for 7 days in differentiation medium as described in section (2.2.2). Following OP exposure, the plate was centrifuged (5 min, 300 g) to allow cellular debris to be compacted to the bottom of wells. A volume of 50 µl of the supernatant was then transferred to a new non-sterile 96 well plate and 50 µl of the reconstituted assay buffer (10 ml assay buffer added to one bottle of substrate mix, in kit) added to each sample well. The plate was then covered with foil and incubated at room temperature for 30 min using a mixer shaker. After that, a volume of 50 µl of assay stop solution (1 M acetic acid) was added to stop the reaction. The change in absorbance was monitored at 490 nm using a standard plate reader.

2.3.3 Acetylcholinesterase (AChE) activity assay

Cells (H9c2) were cultured in T75 culture tissue flasks and induced to differentiate for 7 days as described in section (2.2.2). Following experimentation, cells were detached using trypsin (0.05 % w/v)/EDTA (0.02 % w/v) and incubated for 2-3 min at 37 °C. Following detachment, 10 ml of fully supplemented medium was added to the flask and centrifuged for 5 min at 5000 Xg. The supernatant was then discarded and the pellet was resuspended in 1 ml ice cold PBS and transfered to an Eppendorf tube on. The cell suspension was centrifuged at 47,000 xg for 3 min. Supernatant was discarded and 1 ml of ice cold 200 mM sodium

phosphate buffer (pH 7.4) containing 0.2% (v/v) Triton X-100 was added to the pellet and mixed gently up and down using a pipette. 100 µL of the sample suspension was added to 96 well plate in four replicates, followed by 50 µL of (0.03 % w/v) 1.25 mM acetyl thiocholine iodide in PBS and 50 µL of (0.047 % w/v) 1.25 mM of 5,5-dithiobis (2-nitro-benzoic acid) DNTB in PBS with gentle mixing. Using a standard plate reader change in absorbance was monitored at 405 nm and was linear over a 10 min period. Color intensity is proportional to the enzyme activity and data were expressed as mean specific activity (absorbance change/min/mg protein) from at least three independent experiments.

2.4 *Coomassie Blue Staining*

Cells were stained with Coomassie blue for morphological change detection and visualised under light microscopy. Cells were cultured and differentiated for 7 days as mentioned previously and exposed to OPs. The growth medium was aspirated and the cells were washed with PBS three times. The cells were then fixed at -20 °C with 90 % (v/v) methanol solution for 15 min. The methanol fixing solution was then removed and Coomassie blue staining solution (0.1% (w/v) Coomassie brilliant blue G, 50 % (v/v) methanol, 10 % acetic acid) was added the cells for 10 min to stain the cells. Staining solution was aspirated and stained cells were washed three times with deionised water and left to air dry at room temperature.

2.5 *Western Blot*

2.5.1 Cell lysis

To examine the activation or the expression of cell signaling proteins, Western Blotting was employed. Cells (H9c2) were differentiated for 7 days in T25 tissue culture flasks. Following experimentation cells were rinsed twice with 2 ml of warmed PBS. A volume of 300 µL of hot (100 °C) sodium dodecyl sulfate buffer (0.5% w/v SDS in Tris buffered saline) was added and cells were removed by a scrapper from the flask surface. The resulting cell lysates were transferred to 1.5 ml Eppendorf™ tubes in order to guarantee the total lysate. Cell lysates were then boiled for 10 min and samples stored at -20°C until required.

2.5.2 Protein estimation

Protein concentration in cell lysates was measured by Bicinchoninic acid (BCA) protein method (Bio- Rad laboratories, Hertfordshire, UK) . In brief, 5 µl of the sample cell lysate was added in duplicate to a 96 well plate. After which 200 µl of assay reagent B and 25 µl of assay reagent A (1 ml of reagent A, 20 µl of reagent S, and set according to the instructions of the manufacturer) were added. The samples were then covered with foil and placed in the shaker for 30 min at room temperature. Bovine serum albumin (BSA) protein standards were prepared in a range of 0–10 mg/ml. A standard plate reader was used to read the absorbance at 620 nm and the concentration of the protein samples were compared with standard curve produced of BSA.

2.5.3 SDS-PAGE

A volume of 75 µl of the sample lysate was mixed with 25 µl 4x Laemmli (8 % w/v SDS, 40 % (v/v) glycerol, 10 % (v/v) β-mercaptoethanol, 0.01 % (w/v) bromophenol blue, 250 mM Tris-HCl pH 6.8) in deionised water and boiled for 10 min. A 0.75 mm thickness 15 % (w/v) acrylamide gel was prepared, which contained the resolving gel (23 % (v/v) deionised water, 50 % (v/v) ProtoGel® acrylamide mix (30 % acrylamide solution 37.5:1 ratio, Geneflow Ltd, Staffordshire, UK), 25 % (v/v) 1.5 M Tris-HCl pH 8.8, 1 % (v/v) SDS solution, 10 % (w/v) Ammonium persulfate (APS) solution and 0.04 % (v/v) N,N,N',N'-tetramethylethylenediamine (TEMED) and were poured in to the gel cast (Bio-Rad Mini-Protean III system) and a space was left at the top of the gel cast for the stacking gel (Stacking gel; 68 % (v/v) deionised water, 17 % (v/v) ProtoGel® acrylamide mix, 12.5 % (v/v) 1.0 M Tris-HCl pH 6.8, 1 % (v/v) SDS solution (10 % (w/v) Sodium dodecyl sulphate in deionised water) 1 % (v/v) APS solution (10 % (w/v) Ammonium persulfate in deionised water), 0.1 % (v/v) TEMED) and the comp was added immediately. Once the gel was polymerized, 5 µl of protein ladder (Precision Plus Protein™ dual standards, Bio-Rad laboratories, Hertfordshire, UK) and the buffered lysate samples which contained 15 µg of protein were loaded into the gel wells. After that the gel was placed in electrophoresis container that contained 1x electrophoresis buffer (0.01 % (w/v) SDS, 2.5 mM Tris, 192 mM glycine, pH 8.3,). Gels were run at 200 V for 45 min. After protein separation, gels were placed in Western blot transfer buffer (25 mM Tris, 192 mM glycine and 20% (v/v) MeOH) at 4°C for 5 min.

2.5.4 Western blot

Proteins were transferred to nitrocellulose membranes using a Bio-Rad Trans-Blot system. A set up of a wet transfer was performed as follows; pre-wet sponge - filter paper - gel-nitrocellulose membrane - filter paper – pre-wet sponge. The layers were then placed into a western blotting cassette and closed gently to avoid air bubble and placed in the transfer tank that contained chilled transfer buffer. Proteins were transferred at 100 V for 1 h. After electrotransfer of the proteins, the nitrocellulose membrane was stained by Ponceau red stain (Sigma-Aldrich, UK) to confirm protein transfer from the gel. The membranes were then washed with PBS for 5 min with agitation to remove Ponceau staining. Un-occupied protein binding sites on the membrane were blocked using blocking buffer (5 % (w/v) skimmed milk powder and 0.1% v/v Tween-20 in TBS) for 1 h at room temperature with mild agitation. This will prevent nonspecific binding of the antibodies. Following blocking, the proteins of interest were detected by using primary antibodies diluted in a fresh blocking buffer (1:1000; see table 2.1) and incubated overnight at 4°C with mild agitation. After that, the antibody is removed and the membrane was washed with TBS/tween three times for 15 min. The membrane was then incubated for 2 hours at room temperature with mild agitation with secondary antibody conjugated with horseradish peroxidase diluted in a blocking buffer (1:1000; see table 2.2). The membrane was then washed at room temperature in TBS/Tween three times for 15 min. Blots were developed by Ultra Chemiluminescence Detection System (Cheshire Sciences Ltd, Chester, UK) and proteins were quantified by (Advanced Image Data Analysis). Software (Fuji; version 3.52). Target protein were normalized to GAPDH or to its total protein target to measure the value of target protein.

2.6 *Two-Dimensional Electrophoresis (2-DE)*

2D gel electrophoresis could separate proteins in a mixture according to their charge (*pI*) in the first dimension and their molecular weight in the second dimension. This reproducible technique enable protein identification when combined with mass spectrometry. and assessment of protein expression levels.

Differentiated H9c2 cells (7 days) were cultured in T25 culture flasks. Following experimentation, cells were washed twice with warm PBS (37 °C) and lysed in 300 µL of urea lysis buffer (8 M urea, 50 mM DTT, 4% w/v CHAPS, and 0.2% v/v Bio-Lyte 3/10 ampholyte;

Bio-Rad, UK) in deionised water. Cell lysates were then precipitated in a proportion of 10% (v/v) cell lysate to 90 % (v/v) acetone and kept overnight in -20 °C. After that, the precipitated cell lysates were then centrifuged at 10,000 RCF at 4°C for 10 min and the supernatant removed. The pellets were partially covered to prevent any contamination and left to dry for 1 h in the fume cupboard. To determine protein concentration, 5 µl of the sample was used for DC Lowry protein assay. An amount 300 µg of protein sample was added to 120 µL rehydration buffer (Biolite®ampholytes (pH 3-10), 8 M urea, 50 mM DTT, 0.0002% (w/v) bromophenol blue, 4% (w/v) CHAPS, 0.2% (v/v) Biolite®ampholytes (pH 3-10) in deionised water. In the first-dimension (isoelectric focusing), 120 µl of the sample was applied on to an IEF focusing tray making sure that the spreading of the protein sample was even and makes contact with the cathode and anode of the wires. Then a 7 cm 3-10 pH ReadyStrip™ IPG strips (pH 3−10; Bio-Rad, UK) was applied in the IEF tray in contact with the protein sample without any air bubbles and sample protein was absorbed into the IPG gel to allow a passive rehydration for 1 h at room temperature. After that, mineral oil (Bio-Rad laboratories, Hertfordshire, UK) was added on top of the IPG strip to avoid buffer evaporation. The protein sample then went through active rehydration at 50 V for 16 hours. Once the rehydration was completed, IEF system electrode wicks (Bio-Rad laboratories, Hertfordshire, UK) were added in-between the top of the electrodes in the focusing tray and the IPG strip to ensure an effective focusing and to get rid of excess salt. A linear voltage slope up to 250 V was then applied for 20 min. A second linear voltage slope increasing to 4000 V was applied for 2 h. A rapid voltage slope to 4000 V for 10,000 Volt-hours was then applied. Finally, a rapid voltage slope down to 500V was applied to the gel for 25 h. After that, IPG strips were equilibrated by placing the IPG strips in 2500 µl of equilibration buffer 1 (1.5 M Tris/HCl pH 8.8, 6 M urea, 50 % (v/v) glycerol, 2 % (w/v) DTT, 2 % (w/v) SDS, in deionised water) for 10 min at room temperature with gentle agitation. Equilibration buffer 1 was then removed and 2500 µl of equilibration buffer 2 added (2 % (w/v) SDS, 50 % (v/v) glycerol, 6 M urea, 2.5 % (w/v) iodoacetamide, 1.5 M Tris/HCl pH 8.8, in deionised water) for 10 min at room temperature with gentle agitation. After equilibration, proteins were resolved in IPG strips and applied for the second dimension gel, were proteins are separated according to their molecular size. IPG strips were placed on the top of 15 % (w/v) SDS acrylamide gel (including a stacking gel) as described in section 2.6.3. Then a 0.5 cm strip of filter paper was immersed in a mixture of 10 % (v/v) protein ladder (Precision Plus Protein™

dual standards, Bio-Rad laboratories, UK, Hertfordshire) and 90 % (v/v) 4x Laemmli buffer (40 % (v/v) glycerol, 8 % w/v SDS, 0.01 % (w/v) bromophenol blue, 250 mM TRIS-HCl pH 6.8, 10 % (v/v) β-mercaptoethanol, in deionised water) and placed at the IPG strips side for comparison of molecular weight. Gel molten ReadyPrep™ (Bio-Rad laboratories, UK, Hertfordshire) were then added over the IPG strip. A 1x electrophoresis buffer was added in to electrophoresis container (Bio-Rad laboratories, UK, Hertfordshire) and 200 V was applied for 45 min to allow protein separation. After electrophoresis, the gels were washed for 5 min in deionised water for three times. The gels were then stained by ProtoBlue™safe colloidal coomassie G-250 stain (Bio-Rad laboratories, IK, Hertfordshire), and the gel left for staining overnight at room temperature. After staining, the gel was then washed for 1 h in deionised water to remove any additional background staining. Stained gels were imaged by Syngene G-box with Genesnap software. The gels were then placed between two layers of acetate plastic that contain 0.001 % w/v sodium azide solution in deionised water at 4 °C to maintain the gel and avoid its breaking.

2.6.1 SameSpot analysis

The imaged gel was then analyzed by the software known as Progenesis SameSpot (V 3.1.3030.23662, Non- linear Dyramics, UK). The images of the gels were aligned to a gel picked to be a control, either untreated mitotic or untreated differentiated H9c2 cells. Densitometric analysis was then carried out to identify gel spots proteins which have decreased or increased in expression when compared to the control spot in the control gel. The significance of the change in density of the gel spots is then reported with $p < 0.05$ reported as a significant change and spots were circled with a defined number.

2.6.2 De-staining

Proteins whose expression was significantly altered were selected and excised from the gels using a pipette tip cut the exact size spot. Excised proteins were placed in a 1 ml Eppendorf™ tube containing a mixture of equal volumes of deionised water, 50 mM ammonium bicarbonate, and acetonitrile and incubated for 5 min at 37 °C with gentle agitation. The supernatant was poured carefully making sure that the gel spot is still inside the Eppendorf™ tube. A mixture containing equal volumes of 50 mM ammonium bicarbonate, deionised water and acetonitrile was added and incubated at room temperature for 15 min with gentle

agitation. After that, an equal volume of 100 % acetonitrile was added for spot dehydration and incubated for 5 min at room temperature with gentle agitation. The supernatant was removed and 50 mM ammonium bicarbonate solution was added and incubated for 5 min at room temperature with gentle agitation. The supernatant was again removed and 100 % acetonitrile was added for 1 min at room temperature poured. A volume of 100 µl of deionised water was added for 5 min to make sure that the proteins were completely rehydrated. The supernatant was removed and trypsin digestion mixture was added (16.6 µl 100 mM ammonium bicarbonate, 1 µl Mass spectrometry grade Promega gold trypsin, and 7.6 µl deionised water) and incubated at 37 °C for 16 h. 1 µl 1 % (v/v) Trifluoroacetic acid (TFA) was added to terminate the digestion reaction.

2.6.3 ZipTip reverse phase chromatography

After tryptic digestion of the proteins, samples were prepared for MALDI-TOF MS (matrix-assisted laser desorption/ionization mass spectrometry) using C18 ZipTips (200 Å pore size; Millipore, Hertfordshire, UK) to concentrate and sanitize the peptide sample. A Milllipore C18 ZipTip was set by cleaning in 80 % v/v acetonitrile with 10 µl pipette tip for three times cycling, followed by 10 µl pipette tip in 0.1 % v/v TFA for three times cycling. The peptide digest was then bound to the C18 ZipTip chromatography medium by 10 µl of the peptide digest sample for 25 times cycling. The C18 ZipTip was then washed in 0.1 % TFA 10 µl three times cycling. The bound peptides were then eluted from the chromatography medium by the up-take of 5 µl of 80 % acetonitrile and cycled 25 times into a sterile 0.5 ml Eppendorf™ tube. 1.5 µl of the peptide digested sample was then added onto the MTP 384 ground steel Mass Spectrometry target plate (Bruker, UK) and 1.5 µl of CHCA matrix mixture (5mg/ml α-Cyano-4- hydroxycinnamic acid (Bruker, UK), 50 % v/v acetonitrile, 0.1 % v/v TFA) was added to the peptide digest spot with a gentle mix by the pipette tip and covered to prevent contamination and left to dry at room temperature for 15 min. For calibration, a volume of 1 µl of peptide calibrate mixture (Bruker peptide calibration standard) was added next to the protein samples onto the MTP 384 ground steel Mass Spectrometry target plate along with 1 µl CHCA matrix mixture was spotted onto the target plate.

2.6.4 MALDI-TOF MS/MS

Target plate containing the digested peptides was analysed by Bruker Ultraflextreme MALDI-TOFTOF mass spectrometer (reflectron positive mode, ion suppression m/z 650, and mass range m/z 0−4000). Calibrate mixture spot was used to calibrate the mass spectrometer with a Laser power and shots (≈ 1000-3000 shots) to produce the best SNR (signal-to-noise ratio). Proteins were identified using Bruker-Daltonics Biotools (v 3.2, build 2.3) software, searched against the SwissProt database, rat species, using Mascot (version 2.3 server, Matrix Science, UK), PMF 100 ppm tolerance, and reported according to percentage sequence coverage (SC%). MS/MS search parameters: MS tolerance, 100 ppm; MS/MS tolerance, 0.8 Da; and three missed cleavages. All identified proteins exhibited Mascot scores that were considered statistically significant ($p < 0.05$).

2.7 *Binding of Dansylated PSP to Purified Tropomyosin.*

To validate the identification of one of the proteins labeled by dansylated PSP, 10 µl of purified human heart tropomyosin (10 µg; Lee Biosolutions, USA) was incubated with 10µl of 25 µM dansylated PSP or unlabeled PSP for 1 h at room temperature The sample was then mixed with 6 µl of 4x Laemmli and incubated for 5 min at 100 °C. The sample was then subjected to SDS/PAGE on a 0.75 mm thickness 10 % acrylamide gels, which contain resolving gel (40 % (v/v) deionised water, 33 % (v/v) ProtoGel® acrylamide mix (30 % acrylamide solution 37.5:1 ratio, Geneflow Ltd, Staffordshire, UK), 25 % (v/v) 1.5 M Tris-HCl pH 8.8, 1 % (v/v) SDS solution, 1 % (v/v) APS solution and 0.04 % (v/v) TEMED) and were poured in to the gel cast (Bio-Rad Mini-Protean III system) and a space was left at the top of the gel cast for the stacking gel (Stacking gel; 68 % (v/v) deionised water, 17 % (v/v) ProtoGel® acrylamide mix, 12.5 % (v/v) 1.0 M Tris-HCl pH 6.8, 1 % (v/v) SDS solution (10 % (w/v) Sodium dodecyl sulphate in deionised water) 1 % (v/v) APS solution (10 % (w/v) Ammonium persulphate in deionised water), 0.1 % (v/v) TEMED) and the comp was added immediately. Once the gel was polymerized, 5 µl of protein ladder (Precision Plus Protein™ dual standards, Bio-Rad laboratories, Hertfordshire, UK) and the sample was then loaded into the gel wells. After that the gel was placed in electrophoresis container that contain in a 1x electrophoresis buffer (0.01 % (w/v) SDS, 2.5 mM Tris, and pH 8.3, 19.2 mM glycine). Then, 200 Voltage was applied for 45 min. The gels were removed from the electrophoresis tank and from the glass casting frames and placed in 10% methanol for 15 minute to allow

fixation. The fluorescence visualized under UV light. Gels were imaged by Syngene G-box with Genesnap software. The same gel was then stained by ProtoBlue™safe colloidal coomassie G-250 stain (Bio-Rad laboratories, IK, Hertfordshire), and the gel left for staining overnight at room temperature. After staining, the gel was then washed for 1 h in deionised water to remove any additional background staining. Stained gels were imaged by Syngene G-box with Genesnap software.

2.8 *Statistical analysis*

Statistical analysis was performed using Prism software (GraphPad 6 version 6, California, USA). Statistical significance was determined by one-way ANOVA (analysis of variance of means) which compares three or more sets of data, with Student's t test being used to compare two sets of data. Tukey's multiple comparison post hoc analysis was used to further demonstrate significant differences between multiple data sets. ($p < 0.05$ was considered statistically significant and highlighted with an asterix (*). Organophosphate IC_{50} values (concentrations of drug producing 50% of the maximal inhibition) derived from MTT assays and EC_{50} values (concentrations of drug producing 50% of the maximal stimulation) derived from LDH assays were obtained by computer assisted curve fitting using Prism software. All data is presented as the mean ± SEM The n in the text refers to the number of separate experiments. The number of replicates within each experiment is indicated, where appropriate, in the figure ligends.

Chapter 3:

Differentiation of H9c2 Cardiomyoblasts

3.1 Introduction

H9c2 cells are cardiomyoblasts derived from embryonic rat heart cells that display skeletal muscle properties and cardiac-specific characteristics (Sardao *et al.*, 2007). In addition, these cells possess similar electrical signalling pathways to those present in adult cardiomyocytes. Therefore, they are widely used as an *in vitro* model to study molecular mechanisms associated with toxicology, hypertrophy and apoptosis (Pereira *et al*., 2011; Watkins *et al.,* 2011). Importantly, H9c2 cells have the ability to differentiate and develop into a more cardiomyocyte-like phenotype when treated with all-*trans* retinoic acid (RA) and in the presence of low-serum medium (Menard *et al.,* 1999). However, to date, the vast majority of toxicity studies use mitotic H9c2 cells as a model cell line, while differentiated H9c2 cells display the formation of myocytes/myotubes from H9c2 myoblasts (Pagano *et al.,* 2004). Furthermore, it has been shown that differentiated H9c2 cells display increased expression of cardiac-specific markers, such as troponin (Menard *et al.*, 1999), and cytoskeleton proteins, such as myogenin and actin (Pagano *et al.,* 2004). More interestingly, when comparing mitotic and differentiated H9c2 cells in toxicological studies. It has been found that differentiated H9c2 cells show more sensitivity to toxic agents such as doxorubicin (Branco *et al.,* 2012). This might relate to the observation that differentiated H9c2 cells showed increased levels of mitochondrial superoxide compared to their undifferentiated state (Branco *et al.*, 2012). In addition, another study also showed that differentiated H9c2 cells were found to be more susceptible to toxicity than their mitotic form when exposed to the β-receptor agonist isoproterenol (Branco *et al.*, 2011). However, no studies have investigated the effect of OPs using differentiated H9c2 cells. The use of differentiated H9c2 cells provides a better model to study the cytotoxic effect of OPs and facilitates a better understanding of the cellular mechanism(s) involved in OP-induced cardiac toxicity.

As reported previously, culturing mitotic H9c2 cells in low-serum medium and RA will induce differentiation of H9c2 cardiomyoblasts (Menard *et al.,* 1999). The present study has assessed the effective differentiation of H9c2 cells by morphological characterisation of cardiomyoblasts as they differentiate into cardiomyocytes. Moreover, it has monitored the expression of cardiac-specific markers, such as cardiac troponin 1. After assessment of the cardiomyocyte-like phenotype, further studies were conducted to identify novel proteins

expressed in differentiated cells; these novel proteins may be implicated in OP-induced toxicity.

3.2 *Aims*

The aim of the work in this chapter was to investigate the differentiation of mitotic H9c2 cells into a more cardiomyocyte-like phenotype. Initial experiments examined the morphological characteristics of differentiated cardiomyocyte-like H9c2 cells and confirmed the expression of known specific cardiac markers, such as troponin, during cardiogenic differentiation. Subsequently, mass spectrometry was used to identify novel proteins that were significantly expressed in differentiated H9c2 cells.

3.3 Methods

As described in chapter 2 section 2.2.5, 2.4, 2.5 and 2.6.

3.4 *Results*

3.4.1 Morphological characterisation of cardiomyocyte-like cells

Rat cardiomyoblast H9c2 cells were cultured in differentiation medium (containing 1% v/v foetal bovine serum [FBS] and 10 nM RA) for 7 days to induce differentiation into a more cardiomyocyte-like phenotype. Following 7 days differentiation, cells were stained with Coomassie Blue and cell morphology was assessed microscopically. As shown in Figure 3.1, after 24 h culture under normal culture conditions, mitotic cells exhibit a rounded cell mono-nucleated cell (control). H9c2 cells following 7 days in differentiation medium appeared larger, elongated and multinucleated.

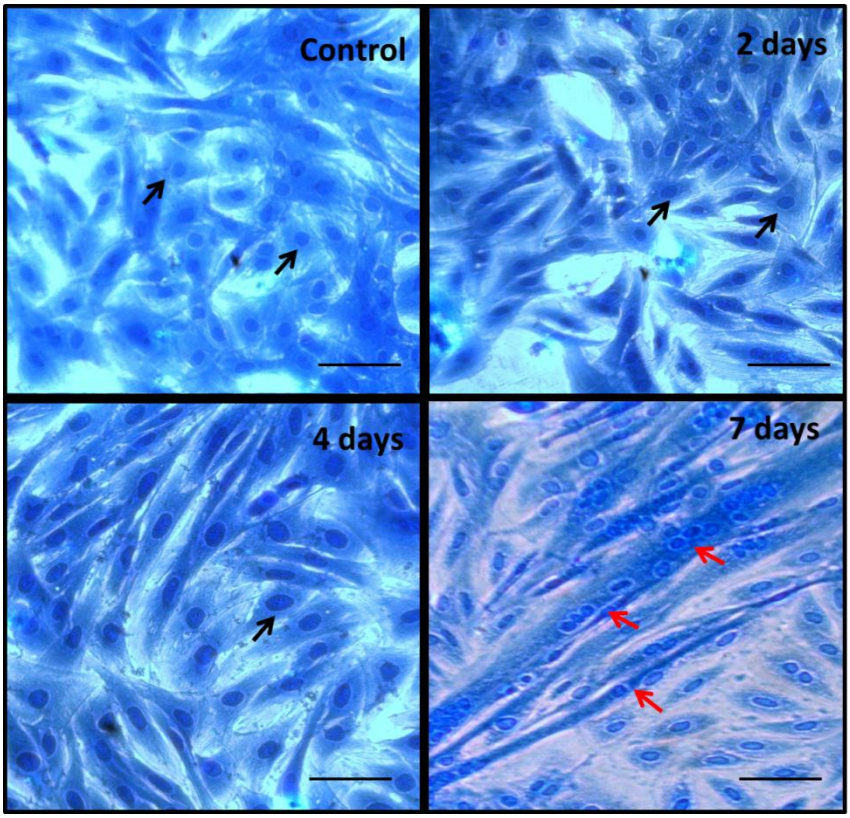

Figure 3.1 Light microscopy examination of H9c2 cells.

Mitotic H9c2 cells (control) cultured under normal culture conditions (medium alone) appear to be mono-nucleated rounded myoblasts (black arrow); differentiated cells undergo a morphological change when treated with 1% FBS and 10 nM RA in DMEM medium for 7 days. Cells appear elongated and some are multinucleated (red arrow). Images were visualised on days 2, 4 and 7 using a 20× objective lens. Scale bar = 100 µm.

3.4.2 Measurement of cardiac-specific troponin

To confirm mitotic H9c2 cell differentiation to a more cardiomyocyte-like phenotype, the expression of the cardiac-specific marker troponin 1 in cells cultured in differentiation medium was monitored over a period of 9 days using western blot analysis and compared with that of control mitotic cells. In agreement with previous studies, cardiac troponin 1 expression increased following H9c2 cardiomyocyte-like differentiation (Branco *et al.*, 2011). Quantitative values (in percentages) showed that troponin 1 expression peaked after 7days treatment (see Figure 3.2). Data was confirmed by immunocytochemistry, results showing significant increase in troponin 1 staining at 4, 7 and 9 days when compared to the control mitotic cells. In agreement with the western blot data, troponin 1 expression peaked after 7-day treatment. Structural examination of 7 and 9 day differentiated cells demonstrated large, long, multi-nucleated myotubes displaying clear myofilaments. This provided additional evidence that the cells had gained a cardiac-like phenotype (see Figure 3.3).

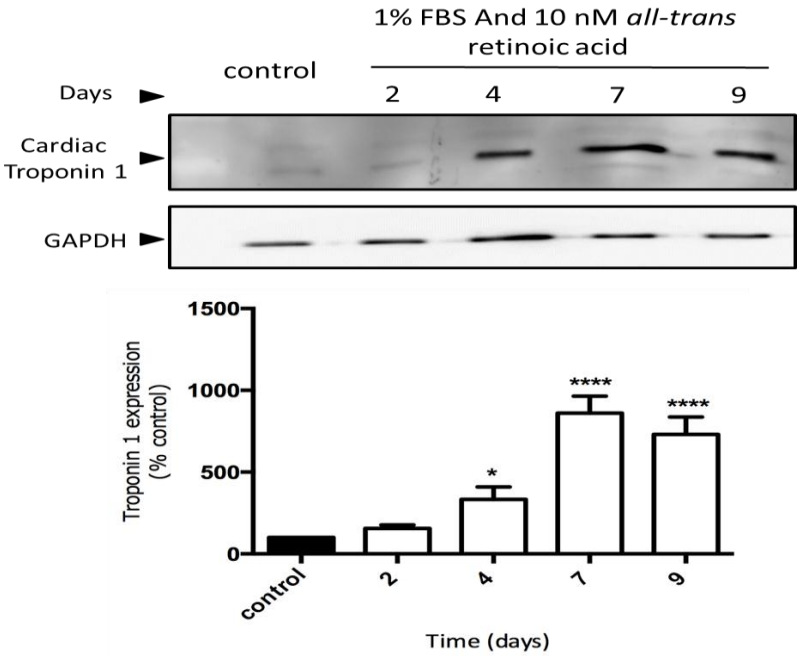

Figure 3.2 Cardiac-specific troponin 1 expression in differentiating H9c2 cells.

Mitotic H9c2 cells (control) were differentiated with RA (10 nM) in a 1% FBS medium. (A) Cell lysates (15 µg) were analysed for cardiac troponin 1 expression on days 1, 2, 4, 7 and 9 via western blotting using anti-cardiac troponin 1 antibody. Lysates were also analysed on separate blots for GAPDH expression to confirm equal protein loading. Quantified values are expressed as a percentage of troponin 1 expression in control mitotic cells (100 %) and represent the mean ± SEM of three independent experiments. *p<0.05 and ****p < 0.0001 versus control (mitotic) cells.

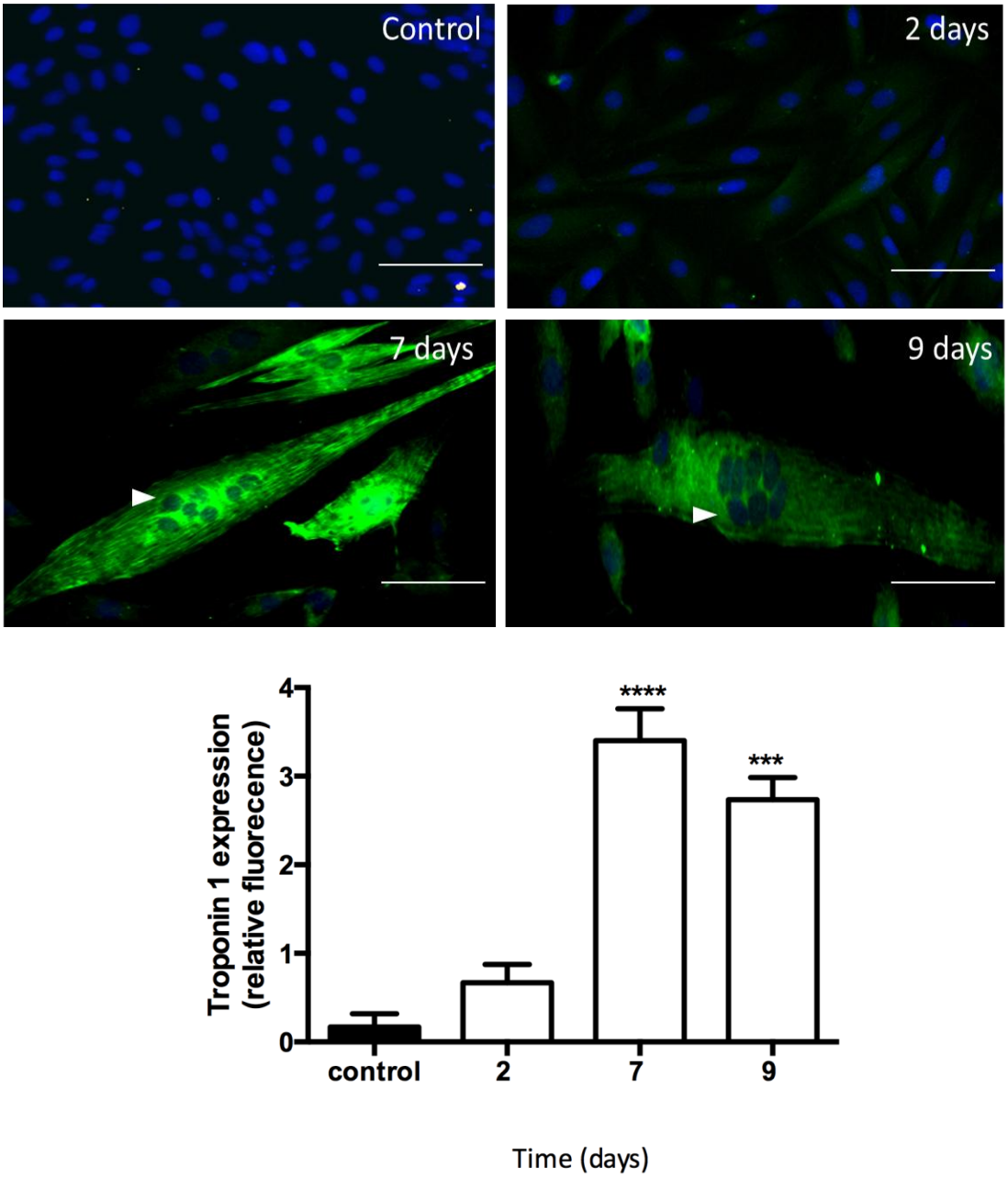

Figure 3.3 Cardiac-specific troponin expression of H9c2 cells upon differentiation.

Mitotic H9c2 cells (control) were cultured in differentiation medium and cardiac troponin 1 was assessed on days 1–9 via indirect immunofluorescence staining using a cardiac-specific troponin 1 antibody (green) and DAPI counterstain for nuclear visualisation (blue) of H9c2 cells. Scale bar = 100 µm. Images presented are from one experiment and are representative of four experiments. Quantified data are expressed as a percentage of control (mitotic) cell values and represent the mean ± SEM of four independent experiments. ***$p < 0.001$ and ****$p < 0.0001$ versus control (mitotic) cells.

3.4.3 Identification of proteins associated with H9c2 cell differentiation

The results presented thus far indicate that 1% FBS and 10 nM all-*trans* RA in DMEM medium induced differentiation of H9c2 cells to a cardiomyocyte-like phenotype. To identify other proteins and monitor changes in protein expression associated with H9c2 cell differentiation, 2D gel electrophoresis was performed as described in Chapter 2. Several protein spots, which were significantly increased in expression in differentiated H9c2 cells when compared to undifferentiated cells. Four protein spots (Spot ID: 1, 2, 3, 5) were significantly up regulated in differentiated H9c2 cells as determined by using Progenesis SameSpot software (see Table 3.1). Protein spots were visually distinct for spot picking (Figure 3.4). Protein spots were picked from the stained gel and digested with trypsin followed by MALDI-TOF mass spectrometry analysis of the peptides produced. Mass spectrometry analysis identified tropomyosin ß-chain, tropomyosin α4-chain, cytoplasmic α-actin and vimentin as novel proteins that exhibited a significant increase in levels in differentiated H9c2 cells when compared to mitotic H9c2 cells. The identified proteins are listed in Table 3.2. These proteins were also confirmed by comparison of their gel position with their theoretical molecular weights and isoelectric point (p*I*).

Table 3.1 Progenesis SameSpot analysis represent a significant increase in density of protein spot in differentiated H9c2 cells.

Spot number	ANOVA (p value)
1	2.88E-11
3	1E-09
5	4.07E-08
2	0.000725

Data table represent a significant increase in protein spots densities using ANOVA analysis of protein spot densities. Data values of 3 accumulated 2D gel electrophoresis, $*p < 0.05$ was viewed as significant.

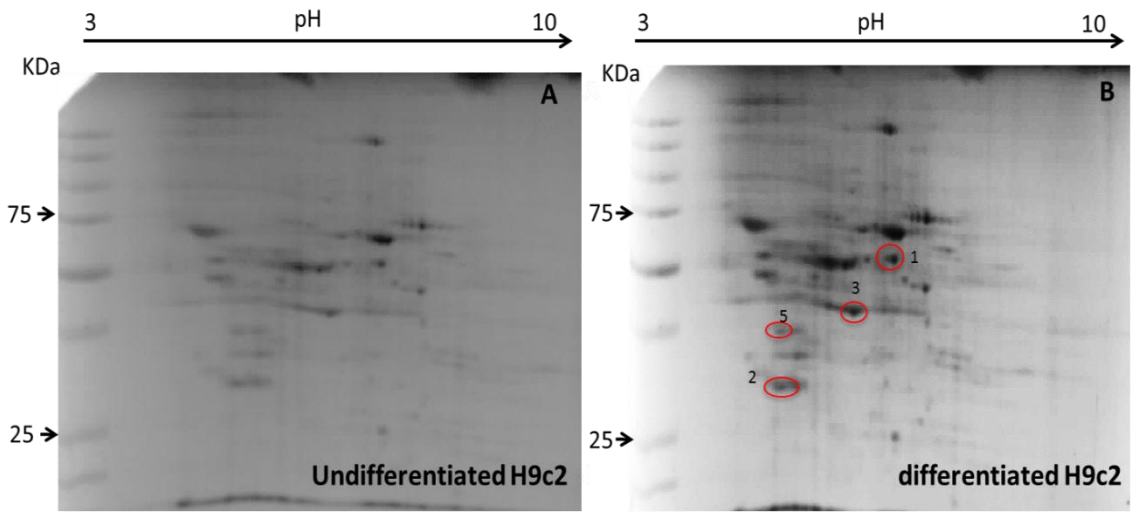

Figure 3.4 Representative 2D gel images of protein expression in H9c2 cells.

A) Mitotic cells and B) cells differentiated with 1% FBS and 10 nM all-*trans* RA in DMEM medium for 7 days. Cell lysates (300 µg) were analysed by 2D gel electrophoresis using pH 3–10 gradient strips. Gels were stained with ProtoBlue Safe colloidal Coomassie G-250 stain and Gel images analysed using Progenesis SameSpots software. Data values of 3 accumulated 2D gel electrophoresis and circled spots represent proteins that showed significantly stronger staining when compared to mitotic cells. Spot 1, vimentin; spot 3, cytoplasmic α-actin; spot 5, tropomyosin ß-chain; spot 2, tropomyosin α4-chain.

Table 3.2 Identification of novel proteins significantly expressed in differentiated H9c2 cells.

Spot number	Protein	Accession no.	PMF sequence coverage (%)	Mascot score	kDa	p*I*
1	vimentin	P20152	56	79.7	54	6.3
3	α-actin	P62737	53	76.2	42	4.72
5	tropomyosin ß-chain	P58774	9	73	33	4.2
2	tropomyosin α4-chain	P09495	45	92	28.5	4.4

Proteins significantly expressed in differentiated H9c2 cells were identified using MALDI-TOF MS (PMF) as described in the Material and Methods. Sequencing data were analysed using Mascot software and reported according to percentage sequence coverage (SC%) or Mascot score (ion scores for PMF > 51 indicate extensive homology). All identified proteins exhibited Mascot scores that were considered statistically significant (*$p < 0.05$).

To further validate the MALDI-TOF MS/MS data, α-actin and tropomyosin were selected to confirm their up-regulation in differentiated H9c2 cells via western blot. As shown in Figure 3.5 there was a significant increase in reactivity of cell lysates with anti-α-actin and anti-tropomyosin antibodies in the differentiated cells when compared to the undifferentiated control cells.

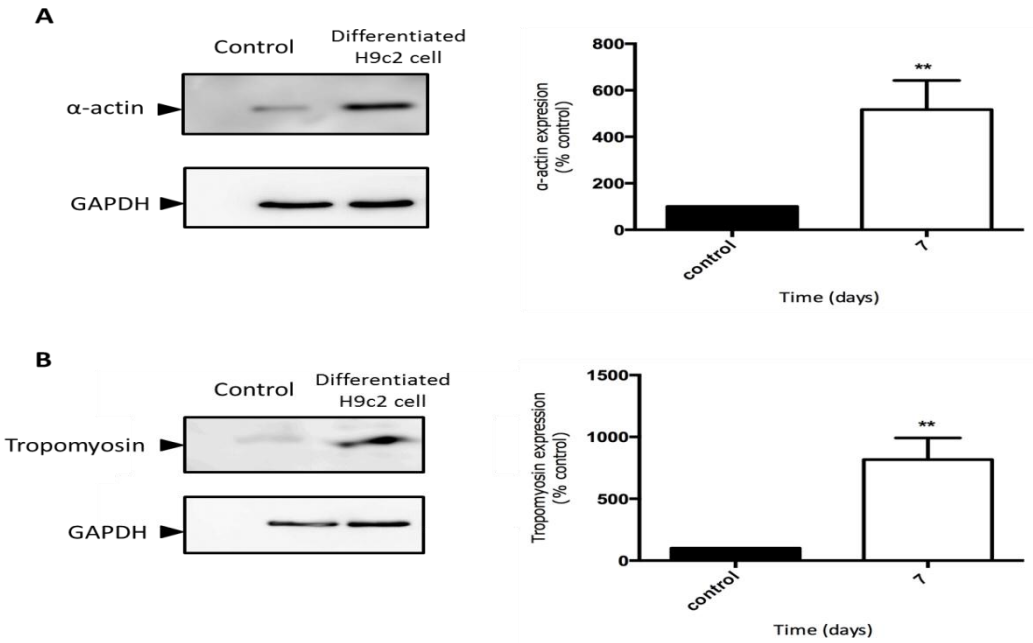

Figure 3.5 Cardiac cytoskeleton α-actin and tropomyosin expression in differentiating H9c2 cells.

Mitotic H9c2 cells (control) were differentiated with RA (10 nM) in a 1% FBS medium. Cell lysates (15 µg) were analysed for cardiac tropomyosin on day 7 via western blotting using anti-α-actin and anti-tropomyosin antibody. Lysates were also analysed on separate blot for GAPDH expression to confirm equal protein loading. Quantified densitometry values are expressed as the percentage of α-actin and tropomyosin expression in control mitotic cells (100 %) and represent the mean ± SEM of three independent experiments. **p < 0.01 versus control cells.

3.5 *Discussion*

3.5.1 Assessment of the differentiated H9c2 cardiomyocyte-like phenotype

In the present study, H9c2 myoblast cells were induced to differentiate to produce a well-established H9c2 cardiomyocyte-like phenotype *in vitro*. Establishment of a differentiated H9c2 cell model will enable further examination of OP toxicity in a cardiomyocyte-like cell line. The current results confirmed the differentiation of mitotic H9c2 cells to cardiomyocyte-like characteristics; cells expressed cardiomyocyte-specific markers, such as troponin 1. Troponin 1 expression increased during the time course of cell differentiation when cultured in low-serum medium and all-*trans* RA. In contrast, expression of troponin 1 was not detected in mitotic H9c2 cells. The data presented support the hypothesis that all-*trans* RA and low-serum medium enhance the differentiation of H9c2 myoblasts to myocytes/myotubes, as reported in previous studies (Menard *et al*., 1999; Pagano *et al.,* 2004; Comelli *et al.*, 2011).

Mitotic H9c2 cells have been used previously as an *in vitro* model in several toxicological studies (Spallarossa *et al*., 2005; Ellis *et al*., 2010; Hosseinzadeh *et al.*, 2011), since they display morphological, electrophysiological and biochemical properties that are similar to those of primary cardiac myocytes (Hescheler *et al.,* 1991). With regard to H9c2 mitotic cells, these may lack some cardiomyocyte properties, such as gap junction communication and T tubules, which will limit their use (Hescheler *et al.,* 1991). However, H9c2 cardiomyoblasts have the ability to differentiate into cardiac muscle cells under certain growth conditions. In their differentiated state, cells express specific cardiac proteins, such as L-type voltage-dependent Ca^{2+} channels and undergo morphological and physiological changes (Menard *et al*., 1999). These changes include the appearance of elongated multinucleated myotubes consistent with noticeable branched fibres and actin filaments (Kadivar *et al.,* 2006; Zara *et al*., 2010). These characteristics show that the H9c2 cell line is an appropriate model for studying the effects of OPs on the cardiomyocyte phenotype. More interestingly, H9c2 cardiac-like differentiation was shown to be more susceptible to toxicity when exposed to toxic compounds, such as isoproterenol, in comparison with their mitotic form (Branco *et al.,* 2011). Hence, the use of differentiated H9c2 cells to study OP-induced cytotoxicity represents a more physiologically relevant cellular model than mitotic H9c2 cells.

In the present study, the process of cellular differentiation proceeded by culturing mitotic H9c2 cells in low FBS and 10 nM RA medium for 7 days in a similar manner to that used in previously published studies investigating cardiomyocyte-like differentiation (Menard *et al*., 1999; Kageyama *et al*., 2002; Comelli *et al.*, 2011). Treatment of the cells confirmed successful cardiac differentiation into more cardiac-like phenotype characteristics. In terms of their morphological features, differentiated cells appeared to be thin and multinucleated cells, as shown by Coomassie staining and compared with the mitotic cell line (Figure 3.1). This is consistent with previous research that investigated cardiomyocyte-like differentiation (Menard *et al*., 1999; Kageyama *et al*., 2002). Moreover, as shown in Figure 3.2, western blot analysis demonstrated that differentiated cells expressed higher amounts of cardiac troponin 1, a specific marker of cardiac differentiation (Decker *et al.,* 2009; Kuzmenkin *et al*., 2009). This globular protein present in myocardial tissue plays an important role in actin–myosin interactions, which are necessary for muscle contraction (O'Brien, 2008). Troponin is released in serum as a result of myocardial injury; it is considered to be more specific than other cardiac biomarkers (Apple *et al.,* 1999; Brogan *et al.,* 1999). More interestingly, the OP fenthion induces cardiotoxicity and increased the levels of troponin 1 in blood rats (Yavuz *et al*., 2008). Therefore, troponin 1 expression and/or release can be monitored as a sensitive marker indicating the presence of OP poisoning.

Immunofluorescence staining confirmed the increase in troponin 1 expression in the cardiomyocyte-like phenotype induced by RA treatment of H9c2 cells. Cells appeared to change from rounded shaped to elongated multinucleated cells characterised by the parallel arrangement of the branched fibres. This was previously shown to be accompanied by the formation of myofibrils, intercalated disks and T tubules (Perissel *et al*., 1980; Isenberg & Klockner, 1982). The developed ultra-structural features were in accordance with those observed in the differentiation of primary cultures of cardiomyocytes (Borisov *et al*., 2008). Striated cardiac myofilaments are involved in the development of sarcomere assembly structure with appearance of dense Z-lines in the cardiac cytoskeleton (Niederreither *et al.*, 2001). In differentiated H9c2 cells, cells were characterised by the organised, linear arrangement of filamentous architecture in the cytoskeleton, indicating the formation of ultra-structural assemblies required for cardiac myogenesis. In contrast, undifferentiated H9c2 cells appear to be devoid of myofilaments.

3.5.2 Expression of proteins associated with differentiated H9c2 cardiomyocyte-like cells

It was apparent that differentiated H9c2 cells exhibited increased expression of cardiac-specific troponin 1. However, it would be of interest to investigate further proteins expressed in differentiated cells as these novel proteins may be implicated in OP-induced toxicity in differentiated H9c2 cells. The present study identified several other proteins that were expressed more highly in differentiated H9c2 cells; these proteins are listed in Table 3.2. They include α-actin, tropomyosin ß-chain, tropomyosin α4-chain and vimentin. Proteins were selected based on visual observation of spots from 2D gels electrophoresis and confirmed by their significant score in Progenesis SameSpot analysis and MALDI-TOF MS/MS. All proteins identified are cytoskeletal proteins, thereby confirming the cytoskeletal changes of mitotic cells adopting structural cardiomyocyte-like features. The increased expression of these cytoskeletal proteins may contribute to the process of myogenesis-like differentiation (Comelli *et al.*, 2011). Identifying significant protein expression changes in differentiated H9c2 cells gives the opportunity to study biochemical remodeling and specific pathways involved in the process of differentiation (Branco *et al*., 2015). Although 2D gel electrophoresis is a powerful tool in proteomic identification and cardiac troponin is a specific cardiac marker. This method occasionally under estimated the presence of proteins. However, failure to detect specific proteins such as troponin 1 does not confirm its absence from the sample and this may be due to several reasons. One reason may be that the troponin is less abundant in the samples prepared for 2D gel electrophoresis.

Tropomyosin isoforms represent important regulators of microfilament stability in both muscle and non-muscle cells (Robinson & Shoichiro, 2006). It regulates the interaction of some actin-binding proteins, such as, ADF-cofilin, Arp2/3, formin, and tropomodulin (Lehrer & Morris, 1984; Clayton *et al*., 2010). Tropomyosin is a component of contractile filaments known also as a sarcomeric contractile protein. In cardiac muscle, regulation of myosin binding to actin is achieved by tropomyosin and troponin complex. In the presence of troponin and the absence of elevated level of Ca^{2+}, tropomyosin blocks the interaction of myosin heads (thick filaments) with actin (thin filament) allowing filament sliding and subsequent muscle contraction (McKillop & Geeves; 1993). Generally, tropomyosin is a

muscle-specific marker protein and it has been previously used to evaluate differentiated cardiomyocytes derived from human embryonic stem cells (Hollweck *et al.*, 2011).

The α-actin is a cytoskeletal actin-binding protein and a member of the spectrin superfamily. It forms an anti-parallel rod-shaped dimer with one actin-binding domain at each end of the rod and join the actin filaments in multiple cell-type and cytoskeleton frameworks (Pollard & Cooper, 2009). In cardiac and muscle cells, it is localized at the Z-disk and stabilizes the muscle contractile mechanism and associates with a number of cytoskeletal and signaling molecules to form an important structural and regulatory roles in cytoskeleton organization (Sjoblom *et al.,* 2008). The up-regulation of α-actin expression observed as a consequence of RA treatment, reflects the increased expression of functional skeletal muscle actin that was observed in trans-differentiation of embryonic rat stem cells to adult cardiomyocytes (Swynghedauw, 1986). Furthermore, Yamada *et al.* (2007) also observed increased expression of cardiomyocyte specific genes such as, cardiac α-actin in cardiomyocytes derived from mesenchymal stem cells. More interestingly, disruption of α-actin levels may be a potential biomarker for OP exposure in differentiated H9c2 cells, as previous results have demonstrated that the OP pesticide malathion induced a decrease in α-actin expression and caused the re-distribution of cellular microfilaments in the human mammary carcinoma cell line MCF-7 (Cabello *et al*., 2003).

MALDI-TOF MS/MS analysis of 2D gels also identified increased levels of vimentin in differentiated H9c2 cells. Vimentin is a cytoskeletal protein that is normally expressed in mesenchymal cells; an increase in its expression can indicate the transition of epithelial cells to mesenchymal cells (Hendrix *et al*., 1997). Mesenchymal cells are precursor cells that are important in the formation of heart valves during embryonic development (Casper, 2004). Therefore, the increased expression of vimentin in the present study may further verified the transformation of mitotic cells into a more cardiomyocyte-like phenotype. A potential link between the effects of the OP sarin and vimentin has been previously investigated in the central nervous system of rats. Thus, the toxic effect of sarin leads to a change in level of vimentin that causes astrocyte dysfunction associated with astroglial dedifferentiation (Tirupapuliyar *et al.,* 2002). Since these cytoskeletal structural proteins, such as tropomyosin isoforms, α-actin and vimentin, are significantly expressed when compared to the

cardiomyoblast form of H9c2 cells, it will be worthwhile to study the effect of OPs on them during the differentiation of H9c2 cells.

3.6 *Conclusion*

H9c2 rat cardiomyoblasts treated with all-*trans*-RA and low-serum medium were investigated for cardiomyogenic differentiation. The results demonstrated morphological changes developing over a period of 7 days of differentiation. The cardiomyocyte-like phenotype was confirmed by the expression of the cardiac-specific marker troponin 1, which indicates the formation of cytoskeletal branched fibres and the development of myogenesis. Finally, differentiation of H9c2 cells was associated with the increased expression of several cytoskeletal proteins of which tropomyosin and α-actin were identified. These proteins are strongly linked with the development of the myofilament assembly, which contains tubular and Z-structure proteins.

Chapter 4:

Effects of Organophosphorus Compounds on Differentiated H9c2 Cells

4.1 *Introduction*

Diazinon and chlorpyrifos are highly toxic, commonly used pesticides that induce neurotoxicity by primary inhibition of acetylcholinesterase (AChE) activity in neuromuscular junctions and the central nervous system (Chambers, 1992; Hargreaves, 2012). Thus, adverse effects of OPs can be fatal to non-target species including humans. PSP is a structural analogue of saligenin cyclic-o-tolyl phosphate (SCOTP) an active metabolite of tri-ortho-cresyl phosphate (TOCP) which is commonly used in jet engine oils and jet hydraulic fluid due to its anti-wear properties under certain conditions of temperature and humidity (Liyasova *et al.*, 2011). However, they were found to be toxic to both passengers and aircrew, resulting in muscle weakness, dizziness, nausea, disorientation and memory loss (Schopfer *et al.*, 2010; Carletti *et al*., 2011; Liyasova *et al*., 2011). The appearance of neurological symptoms of OP-induced delayed neuropathy (OPIDN) is caused by bioactivation of TOCP to active the toxic metabolite SCOTP (Carletti *et al.*, 2011). The majority of studies have focused on the effects of OP toxicity on the central nervous system. However, there is very little information on the effect of OPs on muscle function, particularly toxic effects on cardiac muscle. Cardiotoxic effects are also of particular concern because it has not yet been established whether the latter effects are induced due to excessive accumulation of ACh, or due to the inhibition of the enzyme itself (Baskin & Whitmer, 1991).

A considerable number of studies have shown that OPs interfere with the signalling pathways associated with members of the MAPK family (Kaplan, 1995; Hargreaves *et al.,* 2006, Pomeroy-Black & Ehrich, 2012). For example, chlorpyrifos was found to induce apoptosis of rat cortical neurons via the activation of ERK1/2, p38 MAPK and JNK signalling (Caughlan *et al.*, 2004). On the other hand, PSP was found to cause a significant activation of PI-3K signalling, a pathway which plays an important role in neurite outgrowth (Pomeroy-Black & Ehrich, 2012). More importantly, other studies have reported that OPs may affect several biochemical pathways independently from inhibition of AChE activity (Akbarsha & Sivasamy, 1997). Therefore, it was important to further explore the cytotoxic effect of OPs at the molecular level. The present study will investigate the effects of OPs on protein kinase signalling cascades that play an important role in cell survival (PKB, ERK1/2) and cell death (JNK and p38 MAPK). Inhibitory studies will be directed to ascertain which MAPK pathway mediated the toxic effects of OPs. H9c2 cells will be exposed to OPs in the presence of

specific inhibitors of PKB, ERK1/2, JNK and p38 MAPK. Inhibitors are used are SP 600125 (10 µM; JNK1/2 inhibitor), LY294002 (30 µM, PI3K inhibitor), PD 98059 (50 µM, MEK1/2 inhibitor), SB 203580 (30 µM; p38 MAPK inhibitor) and Wortmannin (100 nM, PI-3K).

Organophosphates have also been found to induce apoptosis *in vivo* in mice, rats and *Drosophila melanogaster* and also *in vitro* in different cell types such as neuronal cells, fibroblasts and placental cells (Li, 2010). In particular, PSP induces apoptosis in a concentration dependent manner in human SH-SY5Y neuroblastoma cells, as determined by the measurement of activation of caspase-3, suggesting that apoptosis is a consequence of OP poisoning (Ehrich *et al*., 1997). Therefore, in the present study, the effect of OPs on caspase-3 will be investigated to establish the role of apoptosis.

Previous studies have reported possible covalent binding of OPs (e.g. chlorpyrifos oxon, diazoxon and dichlorvos) to target proteins other than AChE, such as albumin and transferrin (Peeples *et al.,* 2005; Li *et al.*, 2009). However, the identity of protein targets for OPs in cardiac cells has not been investigated. This study utilized fluorescently labeled OPs (dansylated OP) to identify critical proteins is required in order to fully understand the mechanisms of OP-induced cytotoxicity. This type of approach is an accurate, specific and sensitive means of detecting novel protein targets of toxic compounds (Greenbaum *et al.,* 2002).

4.2. Methods

As described in chapter 2 section 2.3, 2.5, 2.2.5, 2.6 and 2.7.

4.3 *Aims*

This study is designed to examine the effect of the OPs chlorpyrifos and diazinon, their corresponding metabolites (chlorpyrifos oxon and diazoxon), and PSP on the viability of mitotic and differentiated rat embryonic cardiomyoblast-derived H9c2 cells and to identify novel non-acetylcholinesterase protein targets of OPs to fully understand the mechanisms to determine the molecular mechanisms underlying their cytotoxicity.

4.3 Results

4.3.1 Effects of organophosphates on the viability of mitotic H9c2 cells

Initial experiments in this study investigated the cytotoxic effects of OPs and their metabolite on the viability of mitotic H9c2 cells, which display properties of skeletal muscle. The effects of OP treatment on cell viability were assessed by monitoring MTT reduction (a measure of cellular dehydrogenase activity) and measurement of LDH activity released into the culture medium. Chlorpyrifos at concentration of 200 µM and 100 µM inhibited MTT reduction following 24 and 48 h exposure (Figure 4.1a and c) but had no effect on LDH release at these time points (Figure 4.1b and d). In contrast, chlorpyrifos oxon at concentrations up to 200 µM had no significant effect (p> 0.05) on MTT reduction or LDH release after 48 h of exposure (Figure 4.2). Also, at concentrations up to 200 µM both diazinon and its acutely toxic metabolites diazoxon had no significant effect (p> 0.05) on MTT reduction or LDH release following 48 h of exposure (see Figures 4.3 to Figure 4.4).

Phenyl saligenin phosphate significantly (p<0.05) induced cell death in a concentration and time-dependent manner, as determined by MTT reduction and LDH release following 24 h and 48 h exposure (Figure 4.5). Therefore, subsequent experiments assessed the effects of PSP on LDH release and MTT reduction at earlier time points e.g. 1, 2, 4, and 8 h (see Figures 4.6 to Figure 4.7). The data from these experiments revealed that PSP induced inhibition of MTT reduction was first evident at 4 h (IC_{50} = 8.5 ± 5.5 µM), with comparable results obtained at 8 h exposure (IC_{50} = 7.1 ± 4.7 µM). Similarly, significant (p<0.05) LDH release was first evident at 4 h (EC_{50} = 13 ± 1.1 µM) and at 8 h (EC_{50} = 13 ± 1.5 µM), with levels of LDH release comparable to those observed following 24 h of treatment. Overall, these data indicate that PSP displays marked cytotoxicity towards mitotic H9c2.

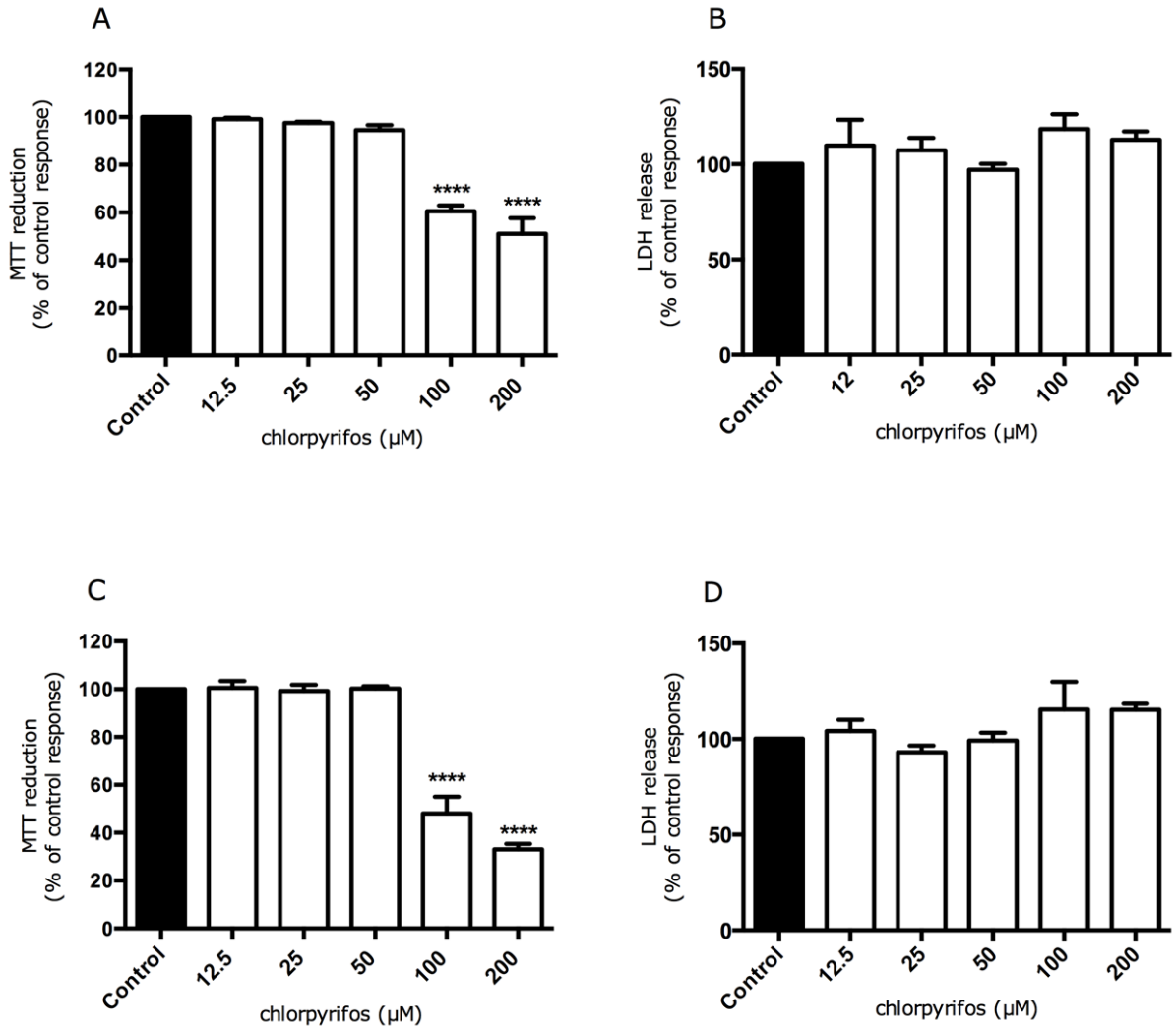

Figure 4.1 Effect of chlorpyrifos on the viability of mitotic H9c2 cells monitored by MTT reduction and LDH release.

Mitotic H9c2 cells were exposed to the indicated concentrations of chlorpyrifos for 24 h (panels A and B) and 48 h (panels C and D). Following chlorpyrifos exposure, cell viability was assessed by measuring the metabolic reduction of MTT by cellular dehydrogenases (A and C) and release of LDH (B and D). Data are expressed as a percentage of control cell values (=100%) and represent the mean ± SEM of four independent experiments each performed in quadruplicate (MTT) or sextuplicate (LDH). $^{**}p < 0.01$ $^{****}p < 0.0001$ versus the control response.

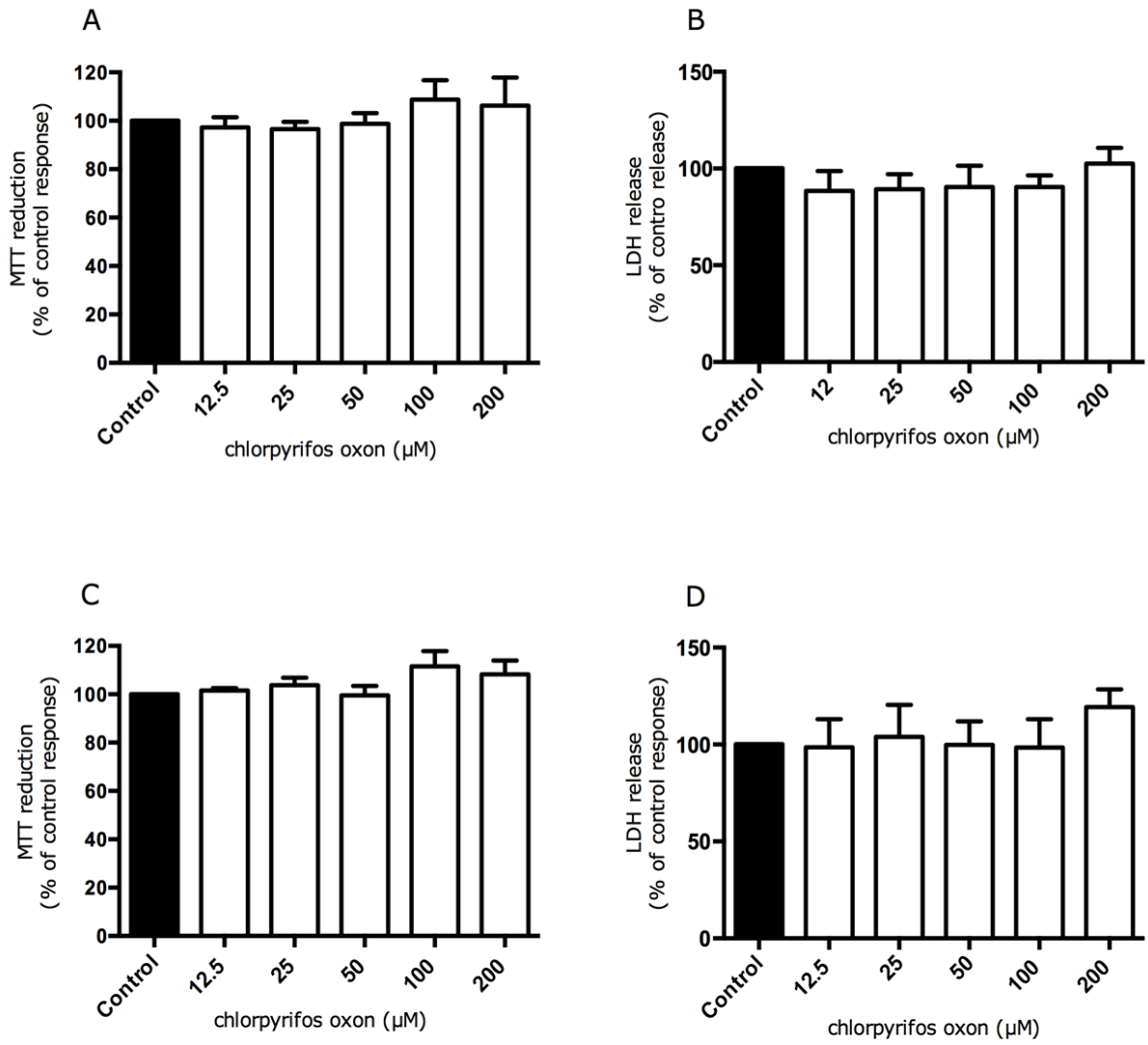

Figure 4.2 Effect of chlorpyrifos oxon on the viability of mitotic H9c2 cells monitored by MTT reduction and LDH release.

Mitotic H9c2 cells were exposed to the indicated concentrations of chlorpyrifos oxon for 24 h (panels A and B) and 48 h (panels C and D). Following chlorpyrifos oxon exposure, cell viability was assessed by measuring the metabolic reduction of MTT by cellular dehydrogenases (A and C) and release of LDH (B and D). Data are expressed as a percentage of control cell values (=100%) and represent the mean ± SEM of four independent experiments each performed in quadruplicate (MTT) or sextuplicate (LDH).

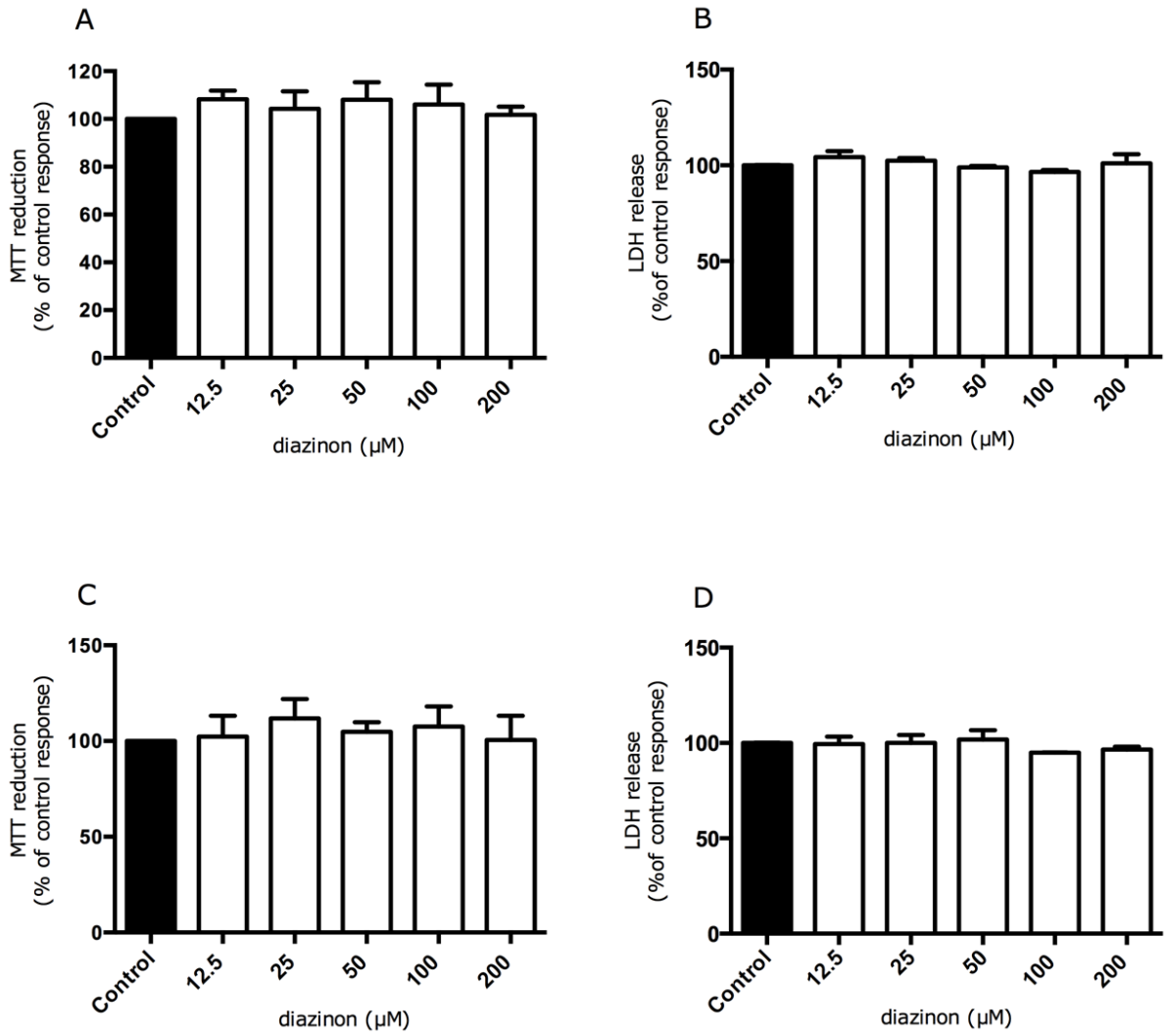

Figure 4.3 Effect of diazinon on the viability of mitotic H9c2 cells monitored by MTT reduction and LDH release.

Mitotic H9c2 cells were exposed to the indicated concentrations of diazinon for 24 h (panels A and B) and 48 h (panels C and D). Following diazinon exposure, cell viability was assessed by measuring the metabolic reduction of MTT by cellular dehydrogenases (A and C) and release of LDH (B and D). Data are expressed as a percentage of control cell values (=100%) and represent the mean ± SEM of four independent experiments each performed in quadruplicate (MTT) or sextuplicate (LDH).

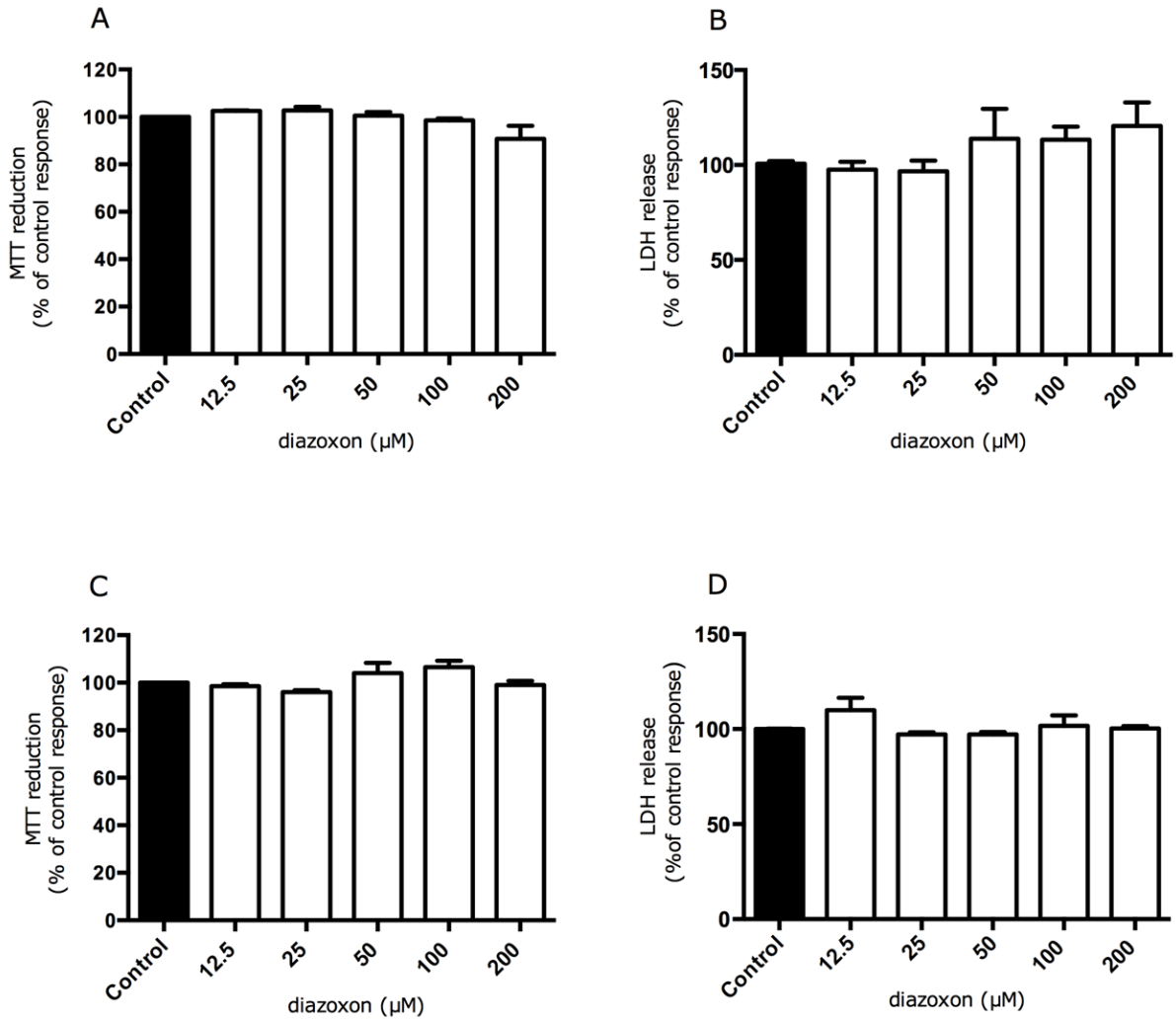

Figure 4.4 Effect of diazoxon on the viability of mitotic H9c2 cells monitored by MTT reduction and LDH release.

Mitotic H9c2 cells were exposed to the indicated concentrations of diazoxon for 24 h (panels A and B) and 48 h (panels C and D). Following diazoxon exposure, cell viability was assessed by measuring the metabolic reduction of MTT by cellular dehydrogenases (A and C) and release of LDH (B and D). Data are expressed as a the percentage of control cell values (=100%) and represent the mean ± SEM of four independent experiments each performed in quadruplicate (MTT) or sextuplicate (LDH).

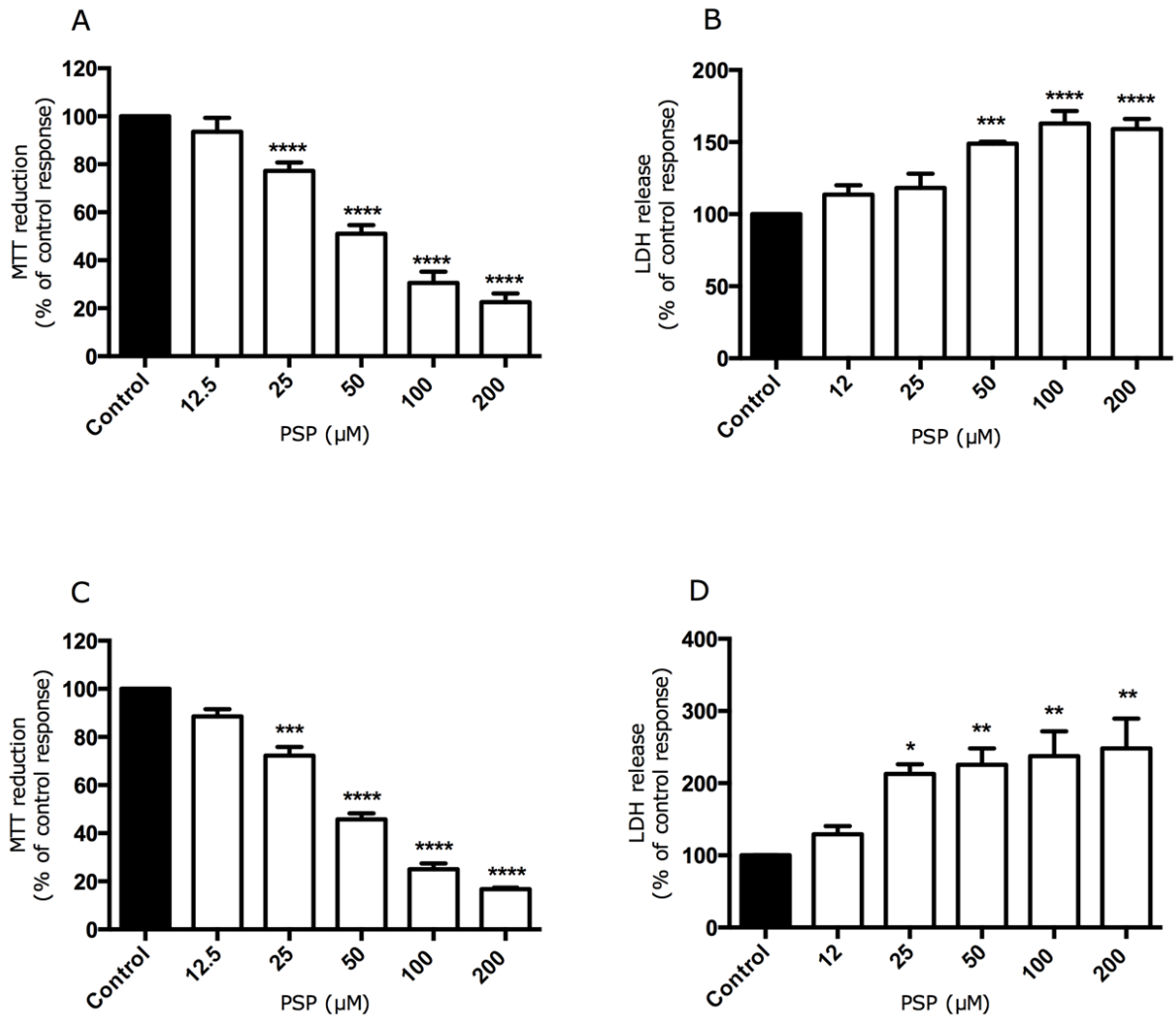

Figure 4.5 Effect of PSP on the viability of mitotic H9c2 cells monitored by MTT reduction and LDH release.

Mitotic H9c2 cells were exposed to the indicated concentrations of PSP for 24 h (panels A and B) and 48 h (panels C and D). Following PSP exposure, cell viability was assessed by measuring the metabolic reduction of MTT by cellular dehydrogenases (A and C) and release of LDH (B and D). Data are expressed as a percentage of control cell values (=100%) and represent the mean ± SEM of four independent experiments each performed in quadruplicate (MTT) or sextuplicate (LDH). *$p < 0.05$, **$p < 0.01$, ***$p < 0.001$, ****$p < 0.0001$ versus the control response.

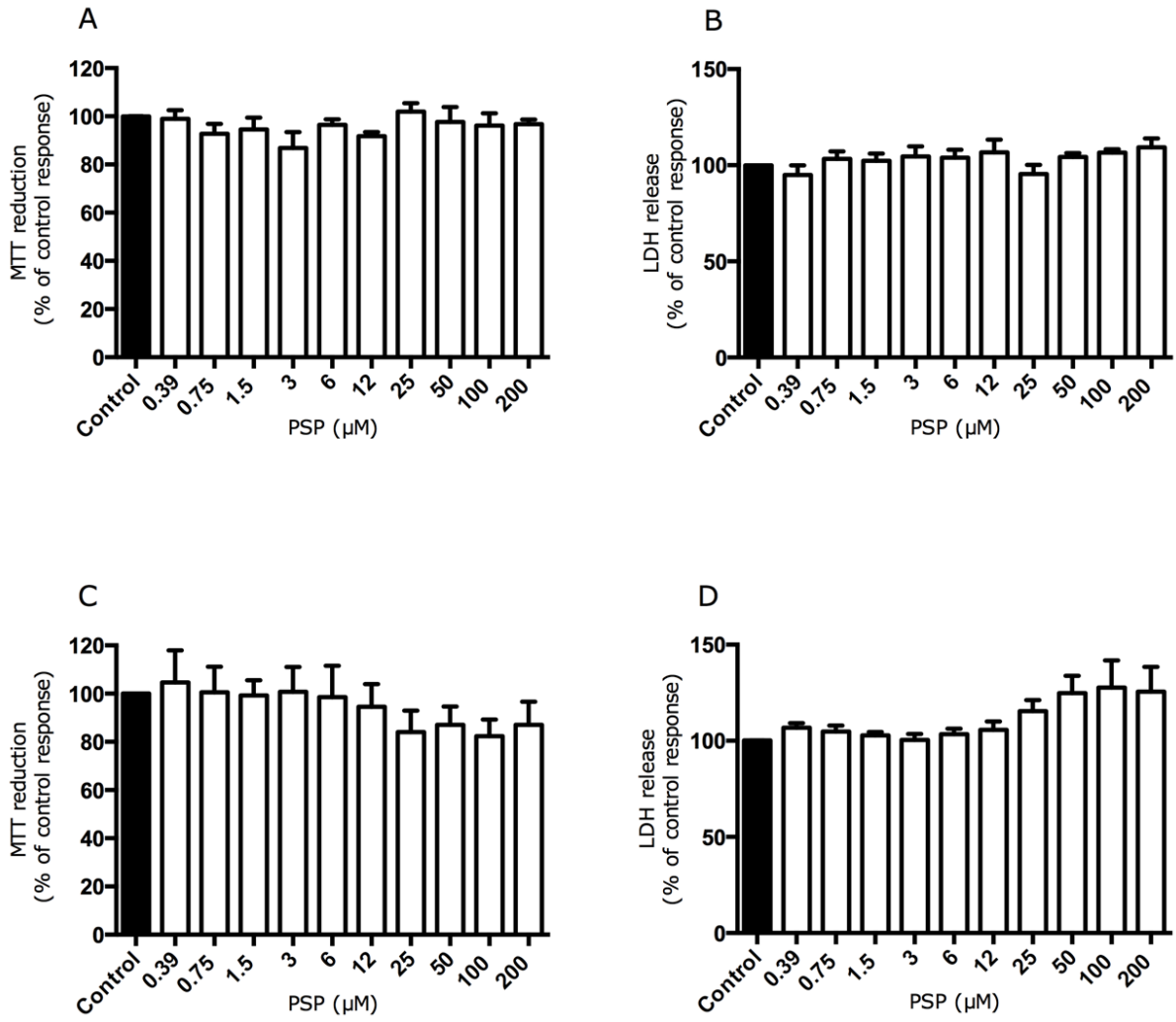

Figure 4.6 Effect of PSP on the viability of mitotic H9c2 cells monitored by MTT reduction and LDH release.

Mitotic H9c2 cells were exposed to the indicated concentrations of PSP for 1 h (panels A and B) and 2 h (panels C and D). Following PSP exposure, cell viability was assessed by measuring the metabolic reduction of MTT by cellular dehydrogenases (A and C) and release of LDH (B and D). Data are expressed as a percentage of control cell values (=100%) and represent the mean ± SEM of four independent experiments each performed in quadruplicate (MTT) or sextuplicate (LDH).

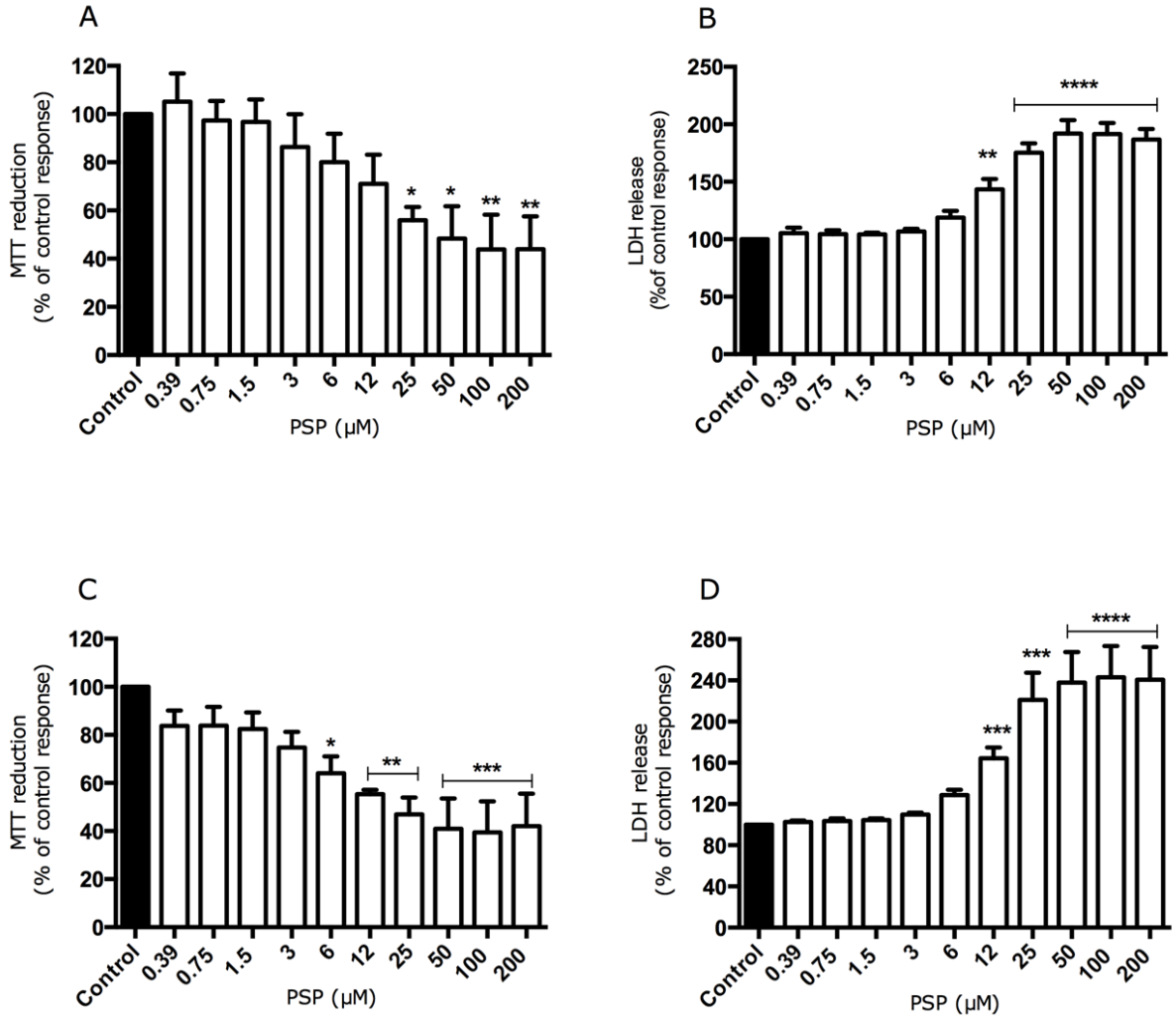

Figure 4.7 Effect of PSP on the viability of mitotic H9c2 cells monitored by MTT reduction and LDH release.

Mitotic H9c2 cells were exposed to the indicated concentrations of PSP for 4 h (panels A and B) and 8 h (panels C and D). Following PSP exposure, cell viability was assessed by measuring the metabolic reduction of MTT by cellular dehydrogenases (A and C) and release of LDH (B and D). Data are expressed as a percentage of control cell values (=100%) and represent the mean ± SEM of four independent experiments each performed in quadruplicate (MTT) or sextuplicate (LDH). *$p < 0.05$, **$p < 0.01$, ***$p < 0.001$, ****$p < 0.0001$ versus the control response.

4.3.2 Effects of organophosphates on the viability of differentiated H9c2 cells

Mitotic H9c2 cells can be differentiated into a more cardiomyocyte-like phenotype as shown in Chapter 3. Therefore, the effect of OP treatment on the viability of differentiated H9c2 cells was investigated. Chlorpyrifos at 200 µM and 100 µM inhibited MTT reduction following 24 and 48 h exposure (Figure 4.8a and c) and at 200 µM triggered a small but significant (p<0.05) release in LDH at these time points (Figure 4.8b and d). In contrast, chlorpyrifos-oxon at concentrations up to 200 µM had no significant effect on MTT reduction or LDH release after 48 h exposure (Figure 4.9). At concentrations up to 200 µM, both diazinon and diazoxon had no significant effect (p>0.05) on MTT reduction or LDH release following 48 h exposure (see Figures 4.10, Figure 4.11).

In differentiated cells, PSP significantly inhibited (p<0.05) the reduction of MTT and triggered the release of LDH following 24 h and 48 h of exposure (Figures 4.12). Subsequent experiments assessed the effects of PSP on MTT reduction and LDH release at earlier time points e.g. 1, 2, 4, and 8 h (see Figures 4.13, Figure 4.14). The data from these experiments revealed that PSP-induced MTT reduction and was first evident at 2 h (IC_{50} = 6.5 ± 1.2 µM), with further inhibition observed following 4 h (IC_{50} = 12.8 ± 4.9 µM) and 8h (IC_{50} = 25 ± 9.3 µM) exposure. In contrast, PSP-induced LDH release was first evident at 4 h (EC_{50} = 15.8 ± 6.1 µM) and increased at 8 h (EC_{50} = 15.1 ± 4.3 µM), when levels of LDH release were comparable to those observed following 24 h treatment. Overall, these data (summarised in Table 4.1) indicate that PSP displays greater toxicity towards differentiated H9c2 cells compared to the other OPs tested.

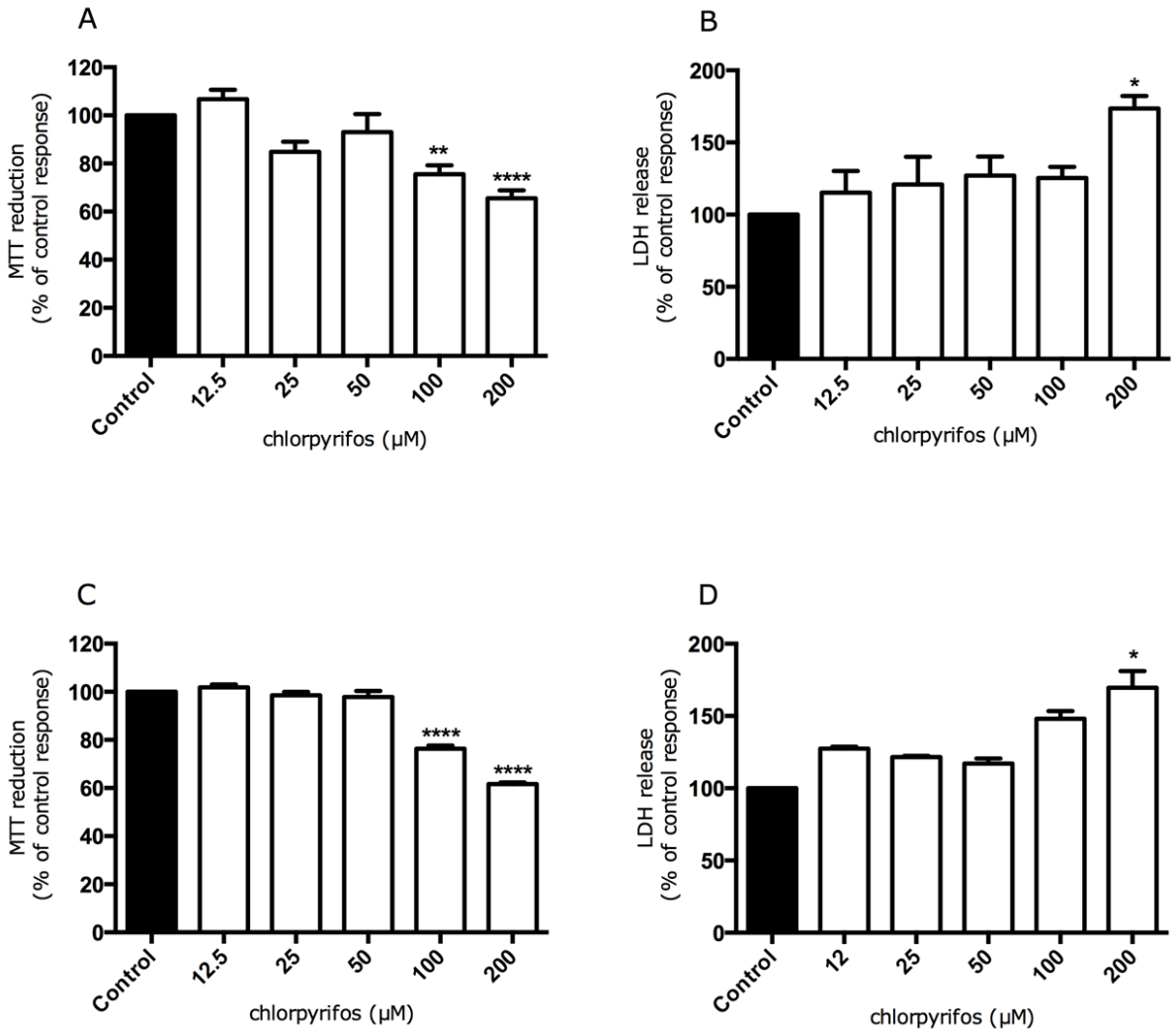

Figure 4.8 Effect of chlorpyrifos on the viability of differentiated H9c2 cells monitored by MTT reduction and LDH release.

Mitotic H9c2 cells were exposed to the indicated concentrations of chlorpyrifos for 24 h (panels A and B) and 48 h (panels C and D). Following chlorpyrifos exposure, cell viability was assessed by measuring the metabolic reduction of MTT by cellular dehydrogenases (A and C) and release of LDH (B and D). Data are expressed as a percentage of control cell values (=100%) and represent the mean ± SEM of four independent experiments each performed in quadruplicate (MTT) or sextuplicate (LDH). *$p < 0.05$, **$p < 0.01$, ****p < 0.0001 versus the control response.

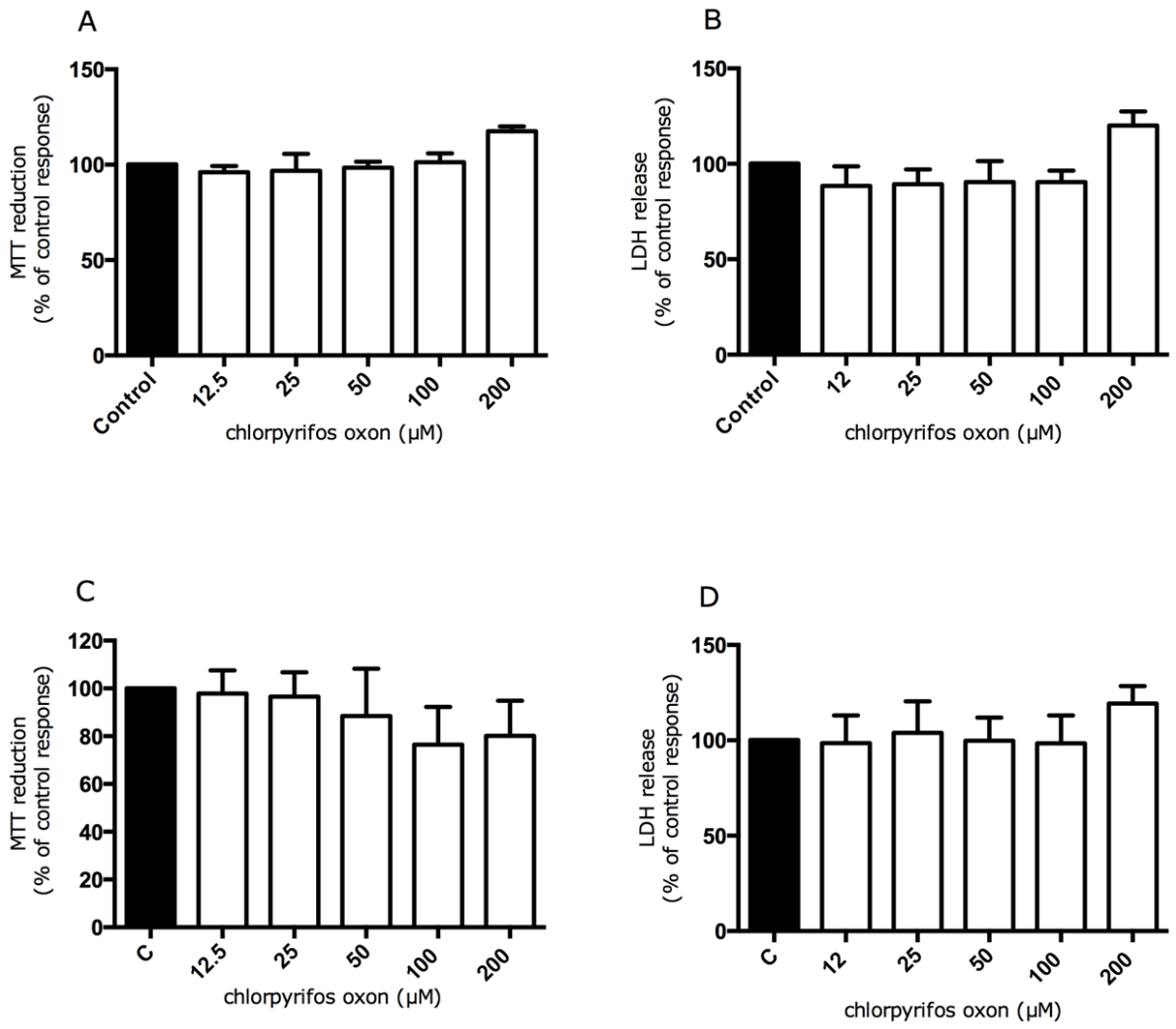

Figure 4.9 Effect of chlorpyrifos oxon on the viability of differentiated H9c2 cells monitored by MTT reduction and LDH release.

Differentiated H9c2 cells were exposed to the indicated concentrations of chlorpyrifos oxon for 24 h (panels A and B) and 48 h (panels C and D). Following chlorpyrifos oxon exposure, cell viability was assessed by measuring the metabolic reduction of MTT by cellular dehydrogenases (A and C) and release of LDH (B and D). Data are expressed as a percentage of control cell values (=100%) and represent the mean ± SEM of four independent experiments each performed in quadruplicate (MTT) or sextuplicate (LDH).

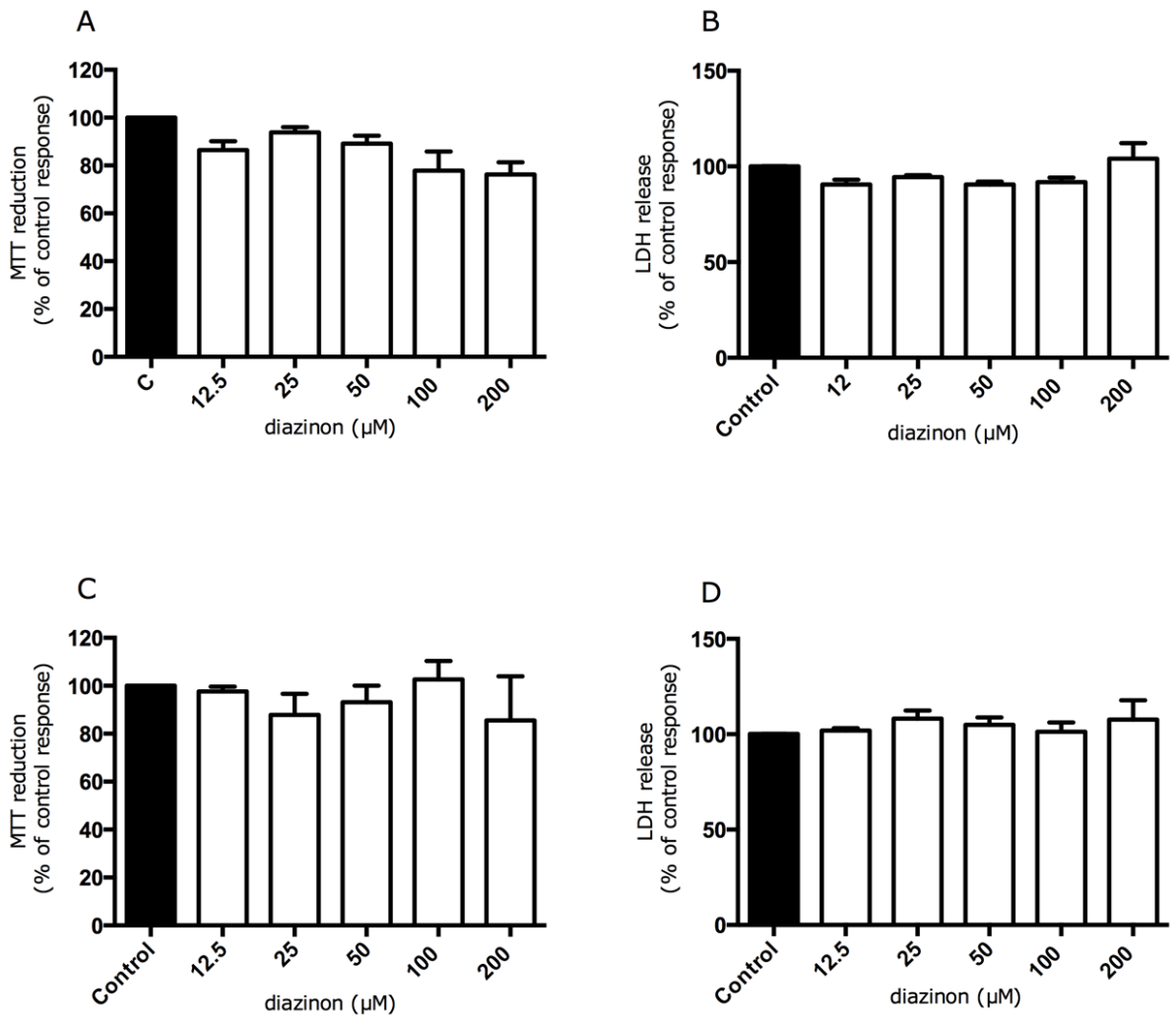

Figure 4.10 Effect of diazinon on the viability of differentiated H9c2 cells monitored by MTT reduction and LDH release.

Differentiated H9c2 cells were exposed to the indicated concentrations of diazinon for 24 h (panels A and B) and 48 h (panels C and D). Following diazinon exposure, cell viability was assessed by measuring the metabolic reduction of MTT by cellular dehydrogenases (A and C) and release of LDH (B and D). Data are expressed as a percentage of control cell values (=100%) and represent the mean ± SEM of four independent experiments each performed in quadruplicate (MTT) or sextuplicate (LDH).

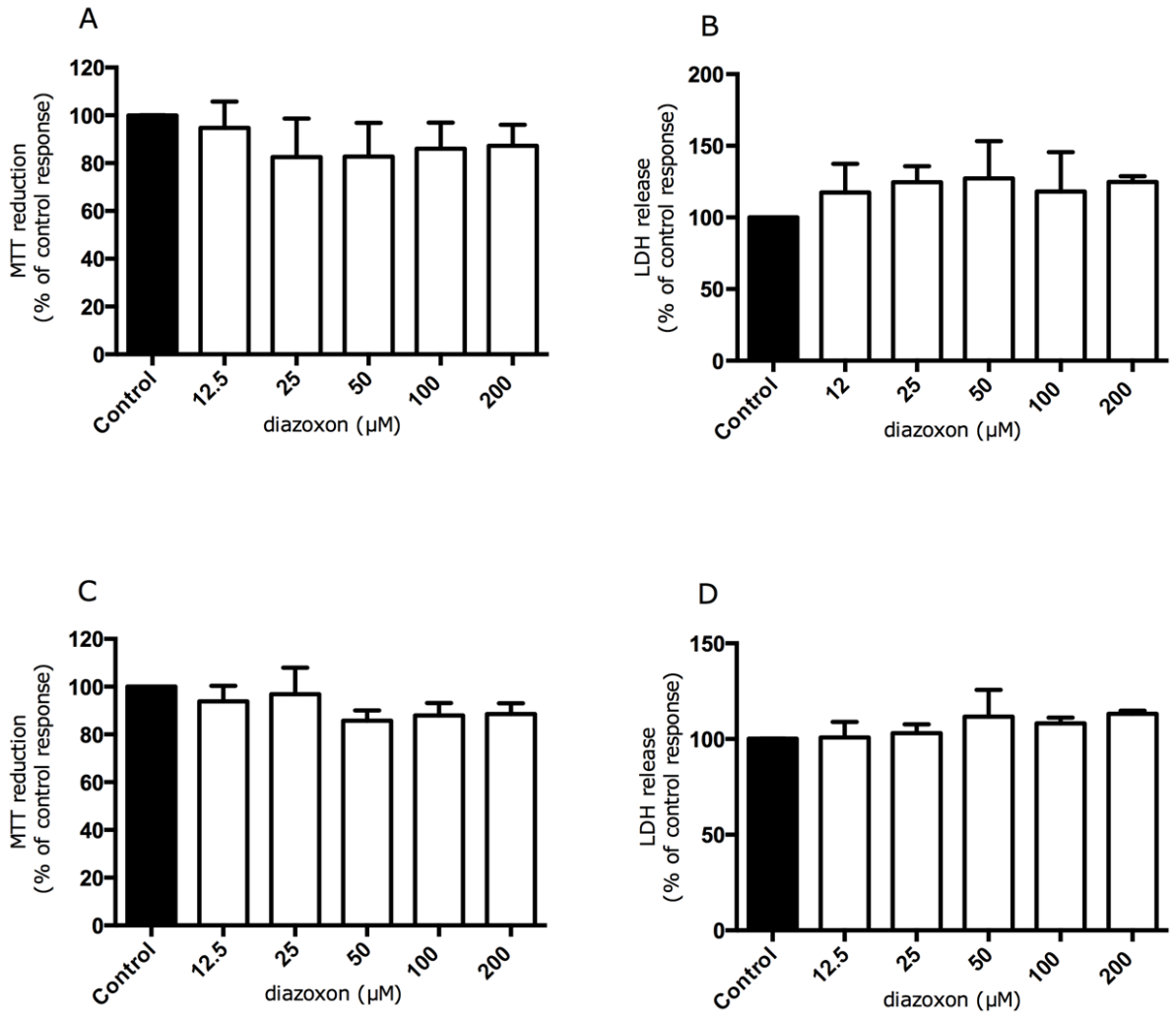

Figure 4.11 Effect of diazoxon on the viability of differentiated H9c2 cells monitored by MTT reduction and LDH release.

Differentiated H9c2 cells were exposed to the indicated concentrations of diazoxon for 24 h (panels A and B) and 48 h (panels C and D). Following diazoxon exposure, cell viability was assessed by measuring the metabolic reduction of MTT by cellular dehydrogenases (A and C) and release of LDH (B and D). Data are expressed as a percentage of control cell values (=100%) and represent the mean ± SEM of four independent experiments each performed in quadruplicate (MTT) or sextuplicate (LDH).

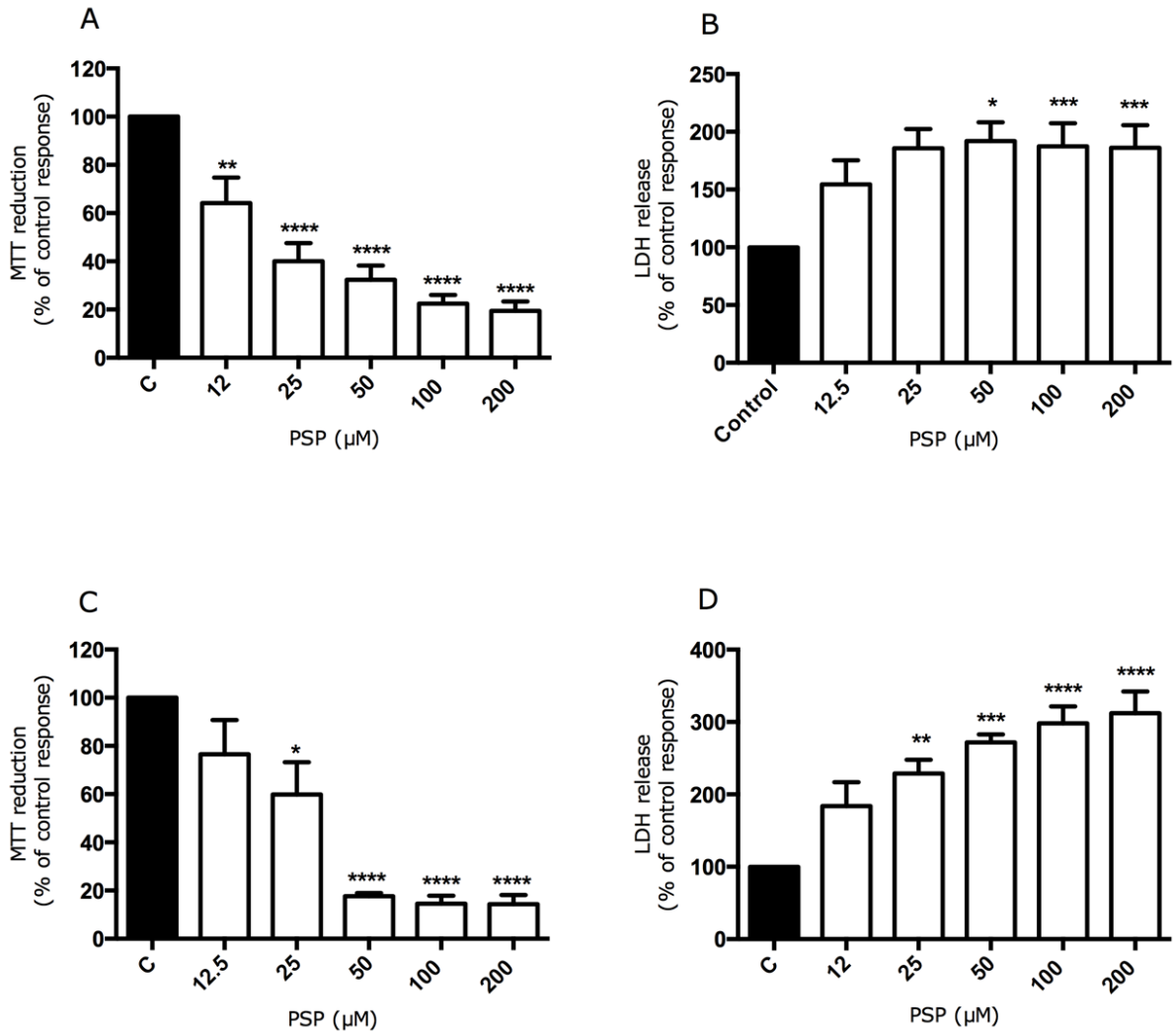

Figure 4.12 Effect of PSP on the viability of differentiated H9c2 cells monitored by MTT reduction and LDH release.

Differentiated H9c2 cells were exposed to the indicated concentrations of PSP for 24 h (panels A and B) and 48 h (panels C and D). Following PSP exposure, cell viability was assessed by measuring the metabolic reduction of MTT by cellular dehydrogenases (A and C) and release of LDH (B and D). Data are expressed as a percentage of control cell values (=100%) and represent the mean ± SEM of four independent experiments each performed in quadruplicate (MTT) or sextuplicate (LDH). *$p < 0.05$, **$p < 0.01$, ***p < 0.001 ****p < 0.0001 versus the control response.

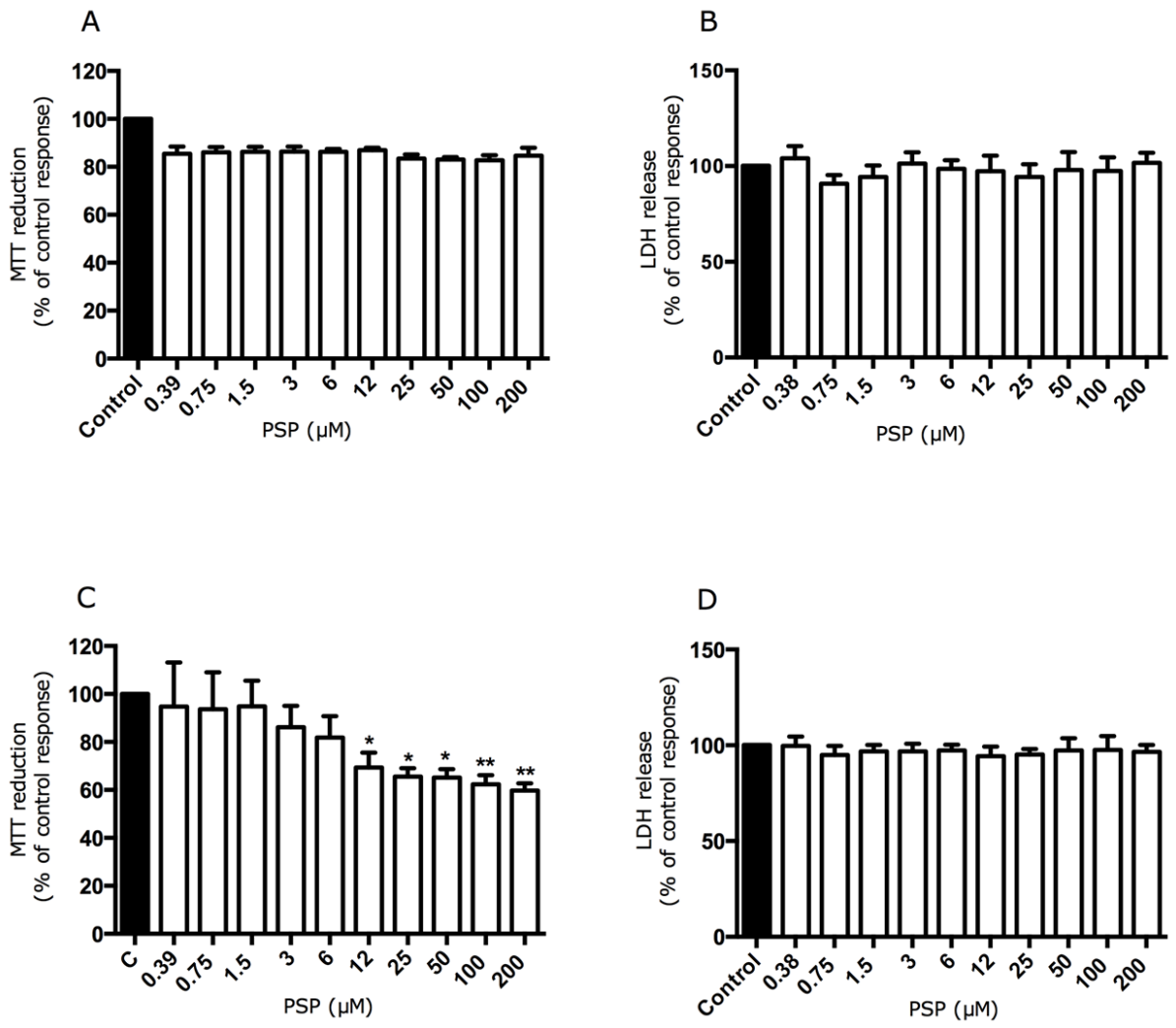

Figure 4.13 Effect of PSP on the viability of differentiated H9c2 cells monitored by MTT reduction and LDH release.

Differentiated H9c2 cells were exposed to the indicated concentrations of PSP for 1 h (panels A and B) and 2 h (panels C and D). Following PSP exposure, cell viability was assessed by measuring the metabolic reduction of MTT by cellular dehydrogenases (A and C) and release of LDH (B and D). Data are expressed as a percentage of control cell values (=100%) and represent the mean ± SEM of four independent experiments each performed in quadruplicate (MTT) or sextuplicate (LDH). *$p < 0.05$, **$p < 0.01$ versus the control response.

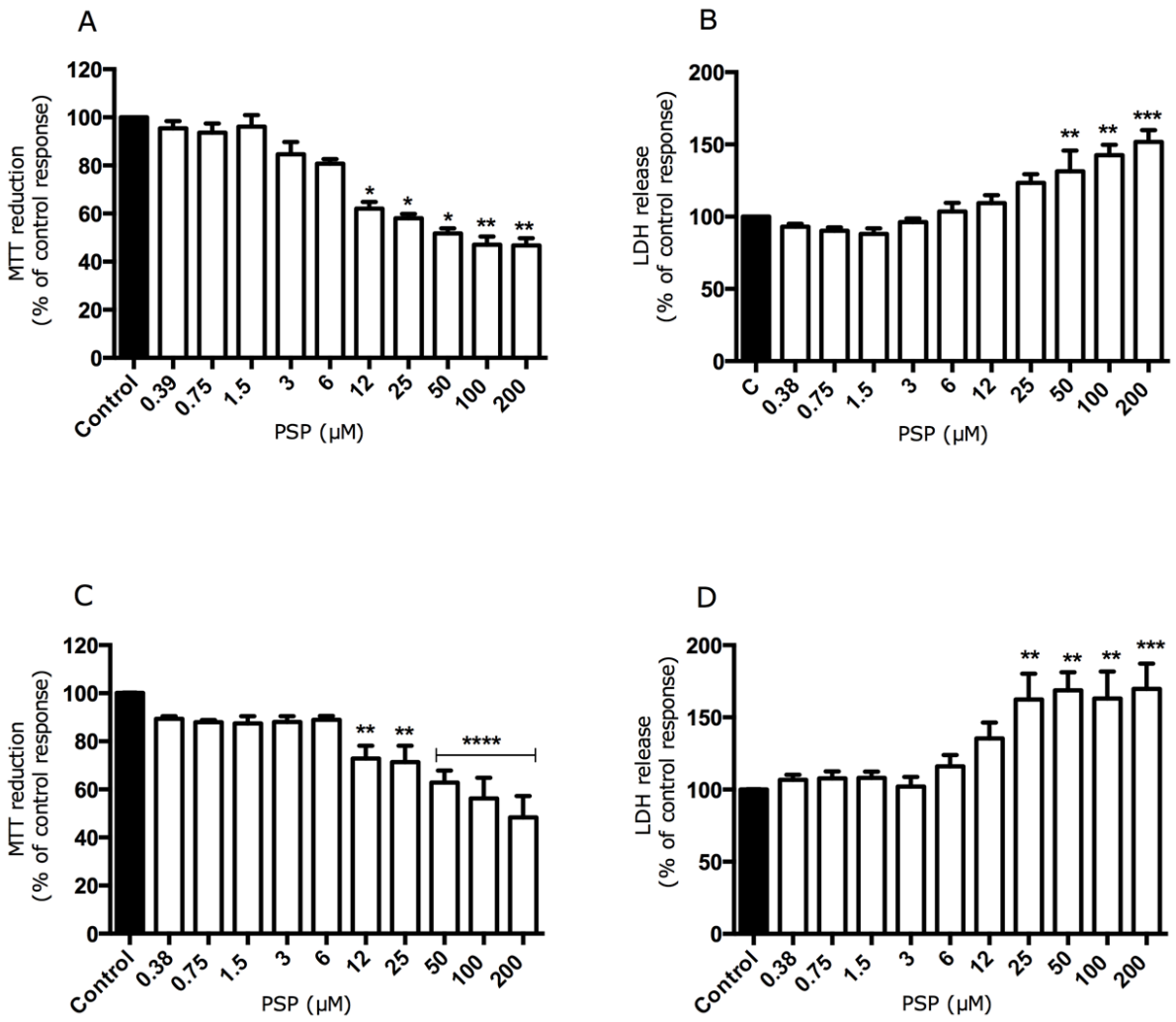

Figure 4.14 Effect of PSP on the viability of differentiated H9c2 cells monitored by MTT reduction and LDH release.

Differentiated H9c2 cells were exposed to the indicated concentrations of PSP for 4 h (panels A and B) and 8 h (panels C and D). Following PSP exposure, cell viability was assessed by measuring the metabolic reduction of MTT by cellular dehydrogenases (A and C) and release of LDH (B and D). Data are expressed as a percentage of control cell values (=100%) and represent the mean ± SEM of four independent experiments each performed in quadruplicate (MTT) or sextuplicate (LDH). *$p < 0.05$, **$p < 0.01$, ***$p < 0.001$, , ****$p < 0.0001$ versus the control response.

Table 4.1 Summary of effects of organophosphorous compounds on the viability of H9c2 cells. (+) represent significant effect (p<0.05) and (–) represent no significant effect (p>0.05) of four independent experiments.

ORGANOPHOSPHOR0US COMPOUND	Mitotic H9c2 cells				Differentiated H9c2 cells			
	MTT		LDH		MTT		LDH	
	24 h	48 h	24 h	4 8 h	24 h	48 h	24 h	48h
Chlorpyrifos	+	+	_	_	+	+	+	+
Chlorpyrifos oxon	–	–	–	–	–	–	–	–
Diazinon	–	–	–	–	–	–	–	–
Diazoxon	–	–	–	–	–	–	–	–
PSP	+	+	+	+	+	+	+	+
	1 h –	2h –	1 h –	2 h –	1 h –	2 h +	1 h –	2 h –
	4 h +	8 h +	4 h +	8 h +	4 h +	8 h +	4 h +	8 h +

4.4 Phenyl Saligenin Phosphate Induced Apoptosis in H9c2 Cells

From the previous results in this study it was found that PSP significantly induced H9c2 cell death in a concentration and time dependent manner in both mitotic and differentiated cells. Whilst MTT reduction and LDH release are widely used markers of cell viability, they do not discriminate between apoptotic and necrotic forms of cell death. To assess whether PSP-induced cell death involved apoptosis via caspase-3 activation following PSP exposure, caspase-3 activation was initially monitored by Western blotting at different time periods, (e.g., 1, 2, 4 and 8 h) using an antibody that recognises the large fragments (17/19 kDa) of activated caspase-3. As evident in Figure 4.15, treatment of differentiated H9c2 cells with 25 µM PSP for 4 h triggered a significant increase (p<0.05) in caspase-3 activation. Similar results were obtained when PSP-induced caspase-3 activation was monitored via immunocytochemistry as shown in Figure 4.16.

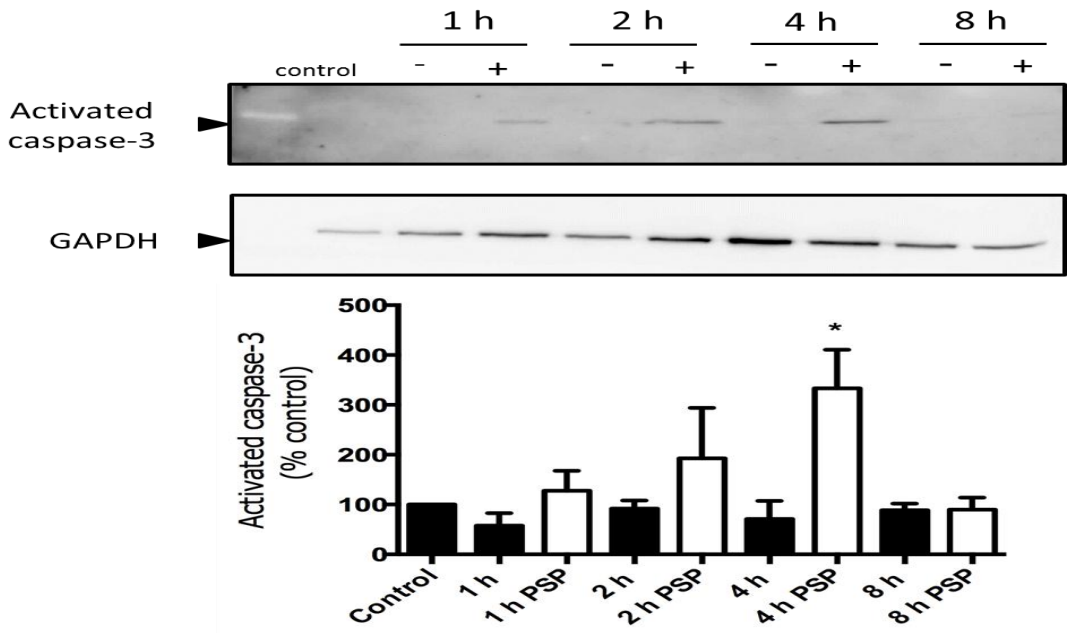

Figure 4.15 PSP-induced caspase-3 activation in differentiated H9c2 cells.

Differentiated H9c2 cells (7 days) were incubated without (-) or with (+) 25 µM PSP for the indicated time periods. Following PSP, exposure cell lysates (15 µg protein) were analysed for caspase-3 activation (17 kDa) by Western blot analysis using specific caspase-3 antibody. The same samples were consequently analysed to confirm equal loading of protein in each well using anti-GAPDH antibody. Quantified data are expressed as percentage of control cell values (100%) and represent the mean ± SEM of three independent experiments.*p < 0.05 versus untreated control cells.

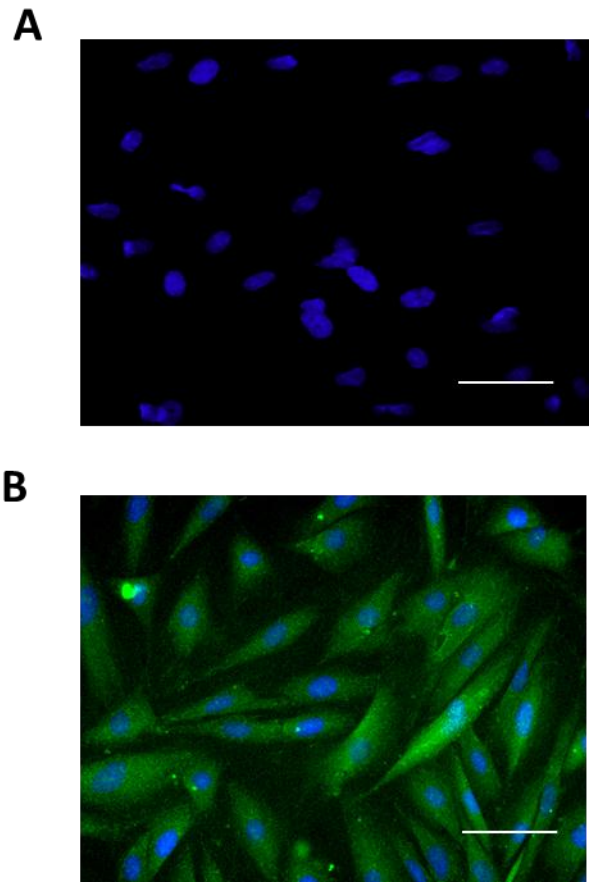

Figure 4.16 PSP-induced caspase-3 activation in differentiated H9c2 cells.

Differentiated H9c2 cells (7days) were exposed to 25 µM PSP for 4 h and assessed for caspase-3 activation via immunocytochemical staining. A) Untreated differentiated H9c2 control cells; only nuclei shown by DAPI staining (blue). B) Caspase-3 activity detected using FITC-labelled anti-activated caspase-3 (green) after 4 h incubation with 25 µM PSP. Scale bar = 100 µm. Images presented are from one experiment and are representative of three.

4.5 Effects of Phenyl Saligenin Phosphate on Protein Kinase Activation

PSP-induced cell death in mitotic and differentiated H9c2 cells may involve the modulation of pro-survival and/or pro-apoptotic signalling pathways. It is generally accepted that ERK1/2 and protein kinase B (PKB; also known as Akt) promote cell survival by activating anti-apoptotic signalling pathways, whereas the activation of JNK and p38 MAPK are associated with apoptotic cell death (Armstrong, 2004; Hausenloy & Yellon, 2007). PSP-induced modulation of protein kinase activity was assessed by Western blotting using phospho-specific antibodies that recognise phosphorylated motifs within activated ERK1/2 (pTEpY), p38 MAPK (pTGpY), JNK (pTPpY) and PKB (S^{473}). Exposure of differentiated H9c2 cells to PSP (25 µM) for 1 h, 2 h, 4 h and 8 h had no significant effect on the levels of phosphorylated PKB, ERK1/2, (Figure 4.17 and Figure 4.18) or p38 MAPK (no appearance of any bands). In marked contrast, PSP (25 µM) induced a time dependant increase in JNK1/2 activation in differentiated H9c2 cells with significant activation observed at 4 h (Figure 4.19).

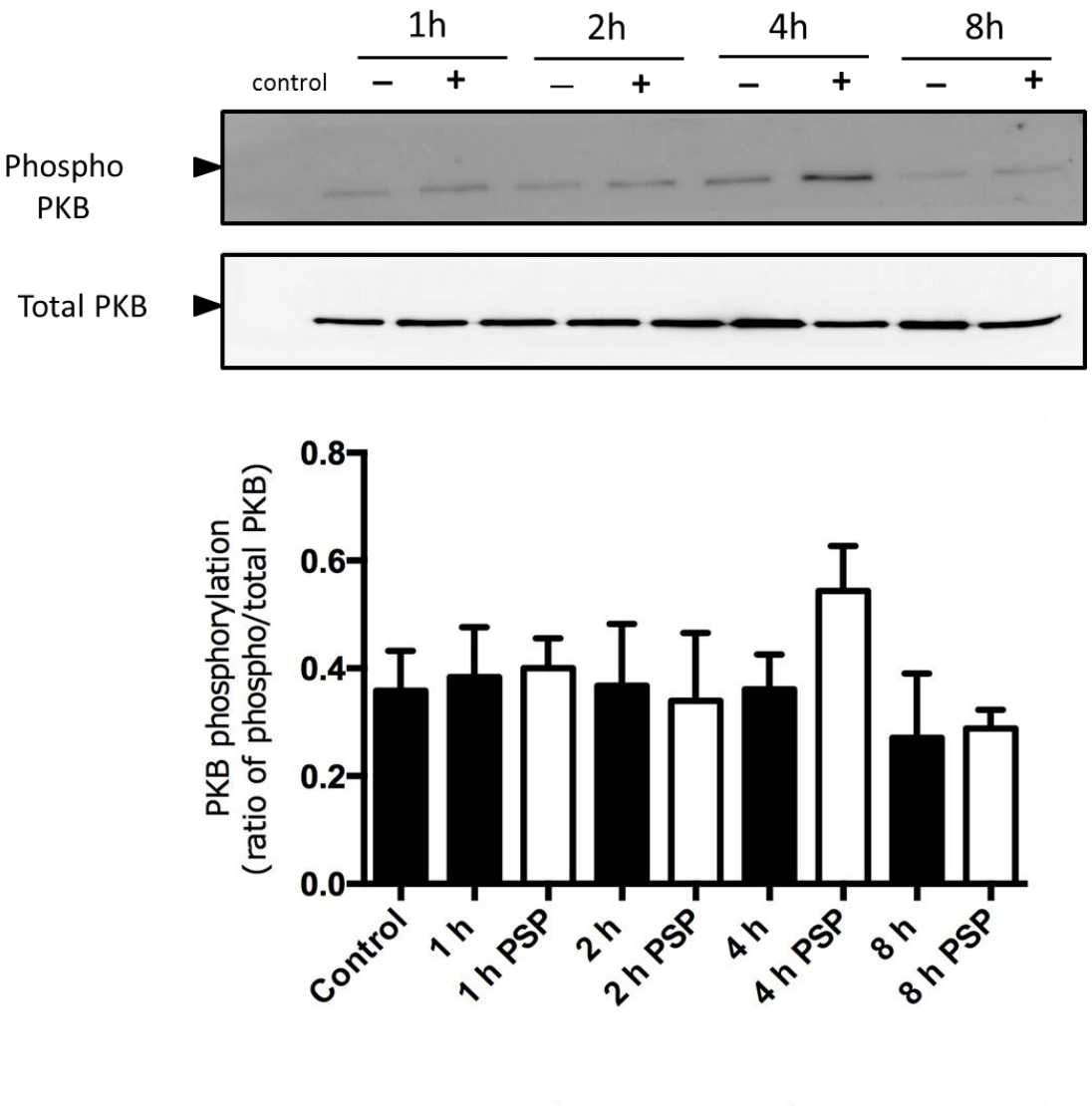

Figure 4.17 Effect of PSP on PKB activation in differentiated H9c2 cells.

Differentiated H9c2 cells (7 days) were exposed to 25 µM PSP for the indicated time periods after which cell lysates (15 µg protein) were analysed for PKB activation (56 kDa) by Western blot analysis using anti-phospho-specific PKB antibody. The same samples were consequently analysed to confirm equal loading of protein in each well using anti-total PKB antibody. Quantified data are expressed as the ratio of phosphorylated PKB to total PKB and represent the mean ± SEM of three independent experiments.

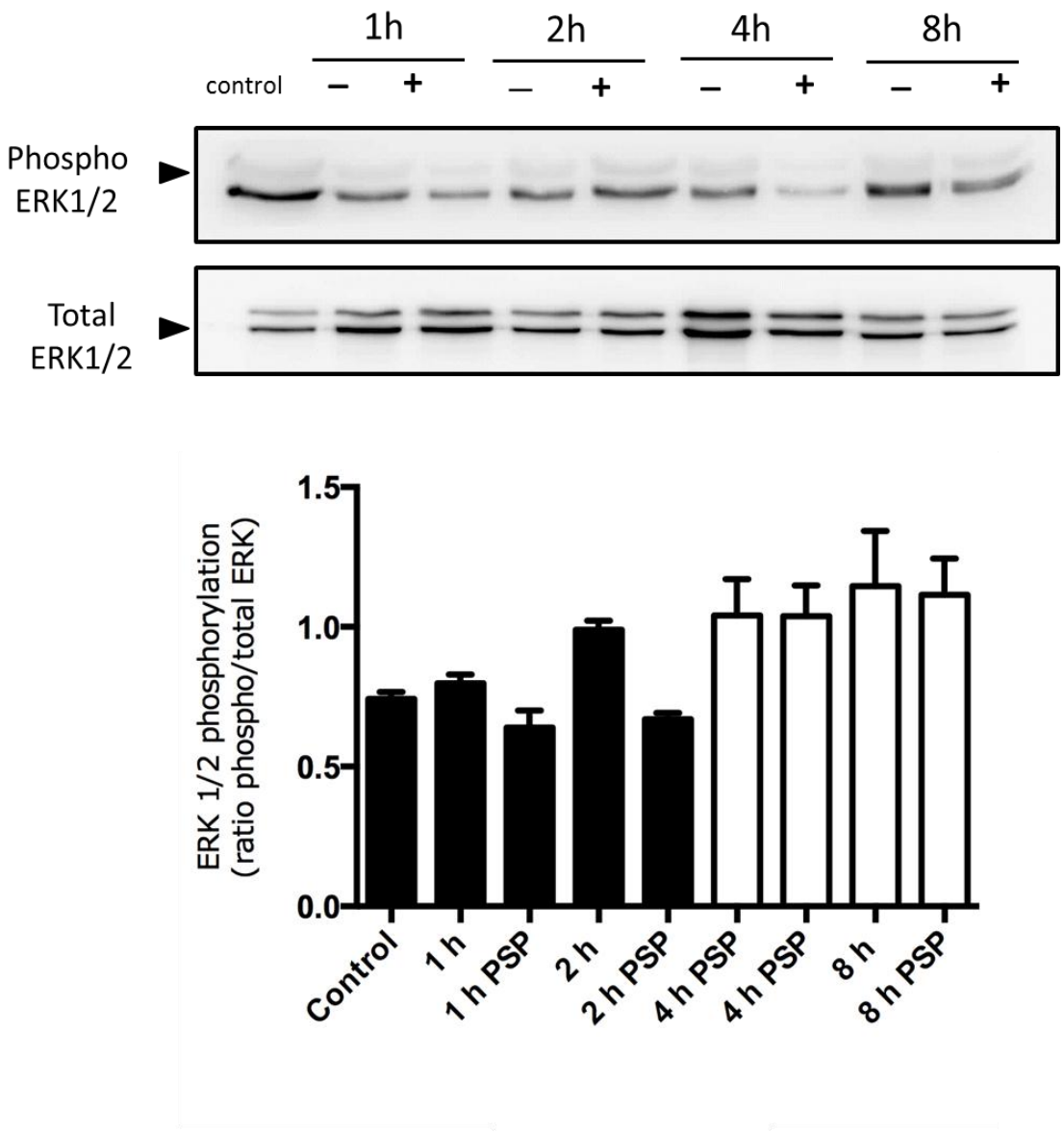

Figure 4.18 Effect of PSP on ERK1/2 activation in differentiated H9c2 cells.

Differentiated H9c2 cells (7 days) were exposed to 25 µM PSP for the indicated time periods after which cell lysates (15 µg protein) were analysed for ERK1/2 activation (42/44 kDa) by Western blot analysis using anti-phospho-specific ERK1/2 antibody. The same samples were consequently analysed to confirm equal loading of protein in each well using anti-total ERK1/2 antibody. Quantified data are expressed as the ratio of phosphorylated PKB to total PKB and represent the mean ± SEM of three independent experiments.

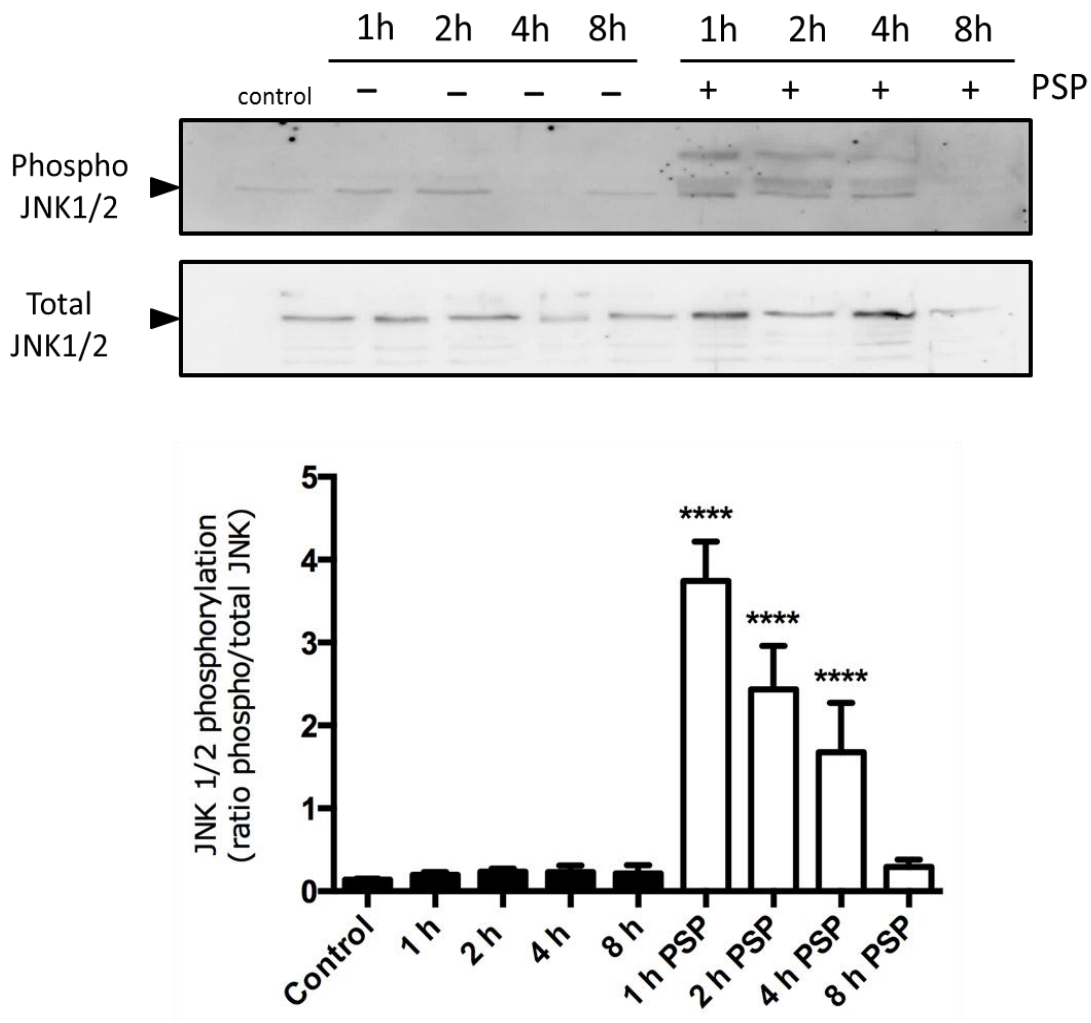

Figure 4.19 PSP induced JNK1/2 activation in differentiated H9c2 cells.

Differentiated H9c2 cells (7 days) were exposed to 25µM PSP for the indicated time periods after which cell lysates (15 µg protein) were analysed for JNK1/2 activation (46/54 kDa) by Western blot analysis using anti-phospho-specific JNK1/2 antibody. The same samples were consequently analysed on separate blots to confirm equal loading of protein in each well using anti-total JNK1/2 antibody. Quantified data are expressed as ratio of phosphorylated JNK1/2 to total JNK 1/2 and represent the mean ± SEM four independent experiments. ****$p < 0.0001$ versus untreated control cells.

4.6 *The Effect of the JNK1/2 Inhibitor SP600125 on PSP-Induced Cell Death and JNK 1/2 Activation*

To investigate further the role of JNK1/2 in PSP-induced cell death, differentiated H9c2 cells were pre-treated for 30 min with the JNK1/2 inhibitor SP 600125 (10 µM; Bennett *et al*. 2001) prior to OP exposure. As shown in Figure 4.20, SP 600125 had no significant effect on 25 µM PSP-induced inhibition of MTT reduction or LDH release following 4 h or 8 h OP exposure. Western blot analysis was subsequently used to establish whether SP 600125 (10 µM) had attenuated PSP-induced JNK1/2 activation in H9c2 cells. As depicted in Figure 4.21, SP 600125 pre-treatment significantly inhibited PSP (25 µM)-induced JNK1/2 activation following 1h and 2 h OP exposure. However, it did not block PSP-induced JNK1/2 activation after 4 h of exposure, which presumably accounts for the lack of effect observed with SP 600125 when monitoring PSP-induced inhibition of MTT reduction and release of LDH at 4 h and 8 h. Since PSP-induced caspase-3 activation was evident at 1 h and 2 h OP exposure, present study determined the effect of SP 600125 on PSP-induced caspase-3 activation at these earlier time points via immunocytochemistry. As shown in Figure 4.22, SP 600125 (10 µM) attenuated PSP-induced caspase-3 activation, confirming the involvement of JNK1/2 in PSP-mediated cell death in H9c2 cells. For comparison, the kinase inhibitors LY 294002 (30 µM; PI-3K inhibitor), PD 98059 (50 µM; MEK1/2 inhibitor), SB 203580 (30 µM; p38 MAPK inhibitor) and wortmannin (100 nM; PI-3K inhibitor) had no significant effect on PSP-induced caspase-3 activation (Figure 4.23).

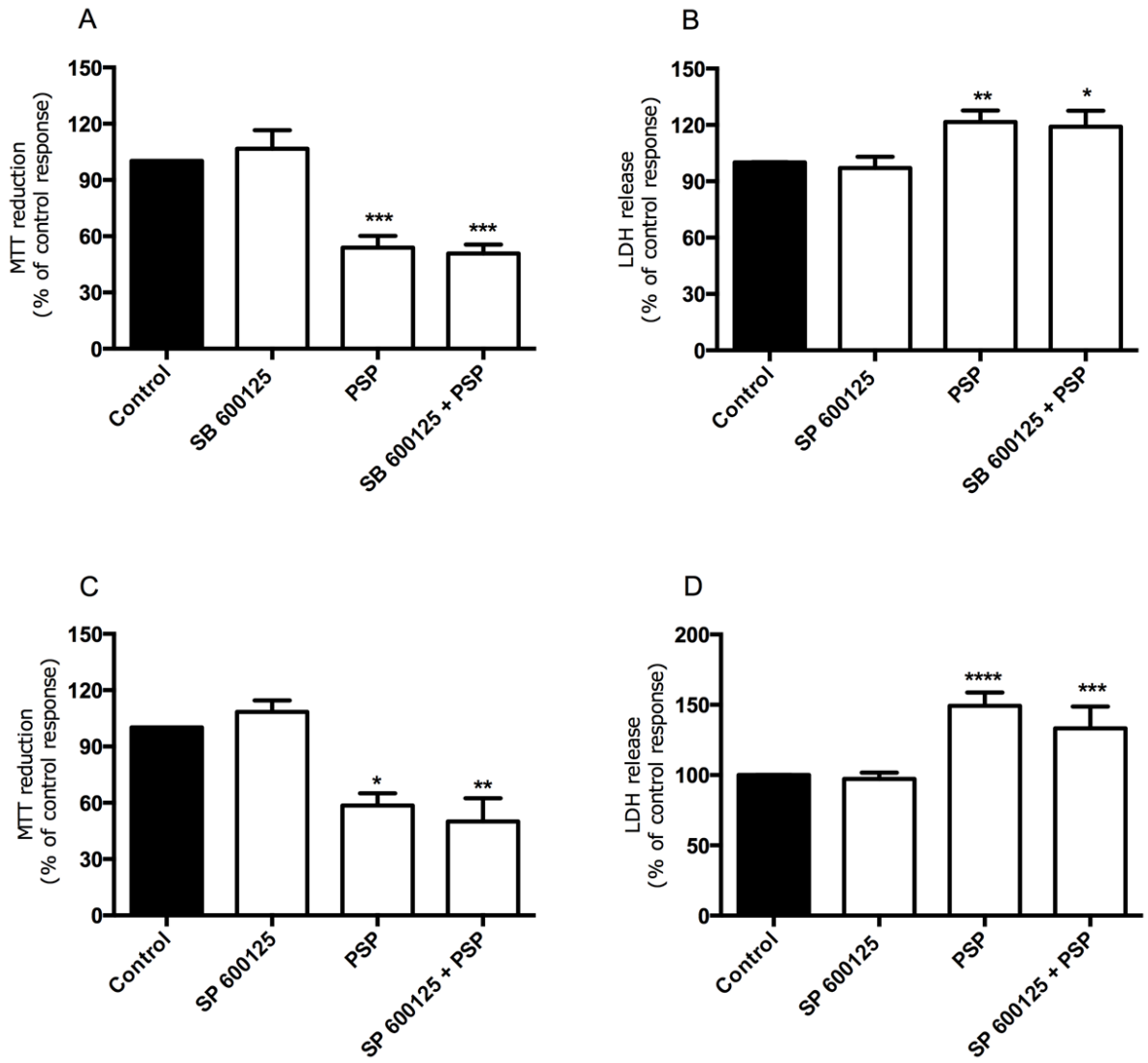

Figure 4.20 Effect of the JNK1/2 inhibitor SP 600125 on PSP-induced inhibition of MTT reduction and release of LDH.

Differentiated H9c2 cells (7 days) were pre-treated for 30 min with the JNK1/2 inhibitor SP 600 125 (10 µM) prior to exposure to 25 µM PSP for 4 h (panels A and B) and 8 h (panels C and D) in the presence and absence of SP 600125 as indicated. Following PSP exposure, cell viability was assessed by measuring the metabolic reduction of MTT by mitochondrial dehydrogenases (A and C) and release of LDH (B and D). Data are expressed as the percentage of control cell values (= 100%) and represent the mean ± SEM of at least three independent experiments each performed in quadruplicate (MTT) or sextuplicate (LDH). *$p < 0.05$, **$p < 0.01$ ***$p < 0.001$ and ****$p < 0.0001$ versus the untreated control response.

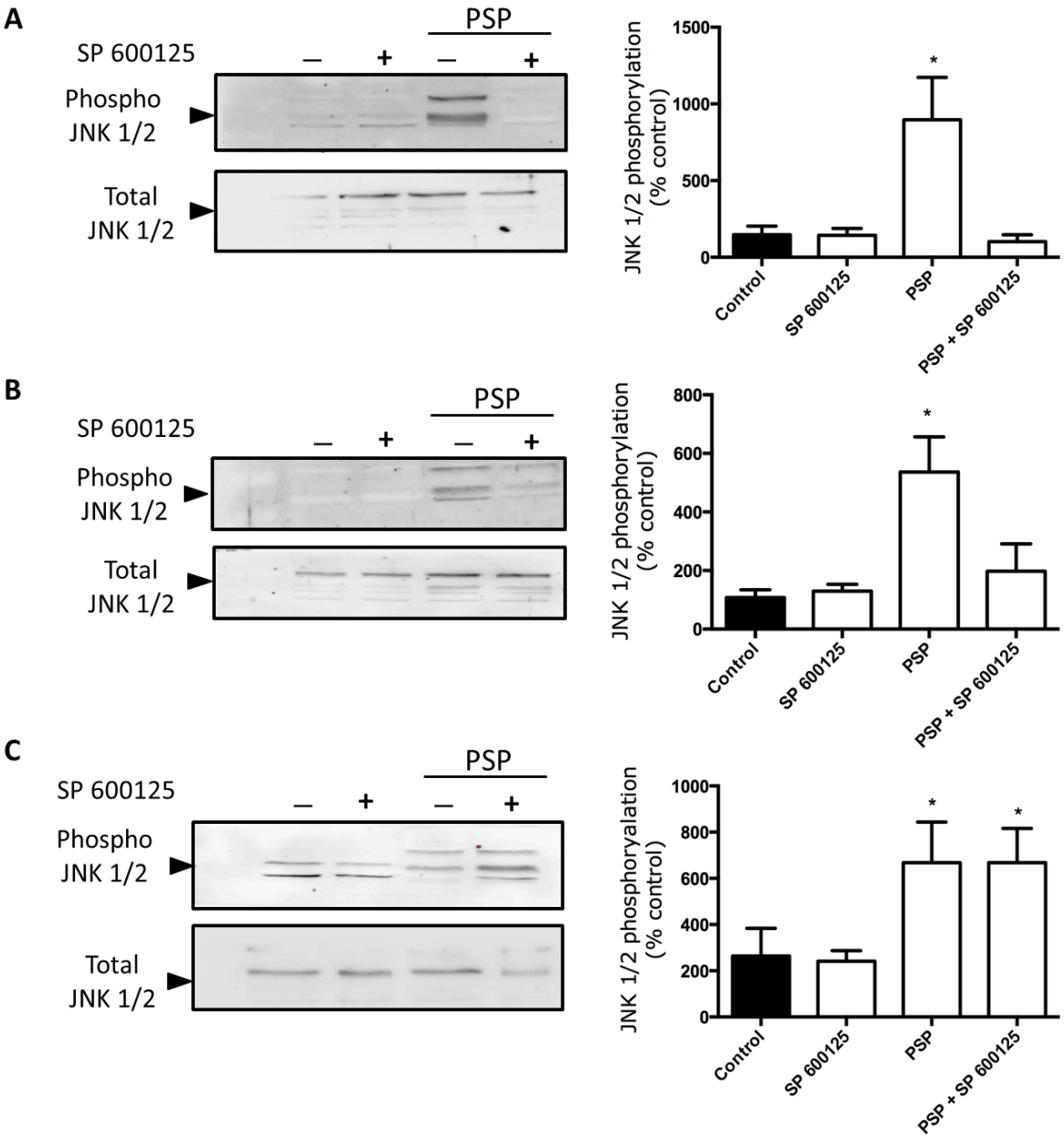

Figure 4.21 Effect of the JNK1/2 inhibitor SP 600125 on PSP-induced JNK1/2 activation.

Differentiated H9c2 cells (7 days) were pre-treated with SP 600125 (10 µM, JNK1/2 inhibitor) 30 min prior to stimulation with 25 µM PSP for A) 1h, B) 2h and C) 4h. Cell lysates (15 µg protein) were analysed for JNK1/2 activation (46/54 kDa) by Western blot using anti-phospho-specific JNK1/2 antibody. The same samples were consequently analysed to confirm equal loading of protein in each well using anti-total JNK antibody. Quantified data are expressed as the percentage of control cell values (100%) and represent the mean ± SEM of three independent experiments. *$p < 0.05$ versus the untreated control response.

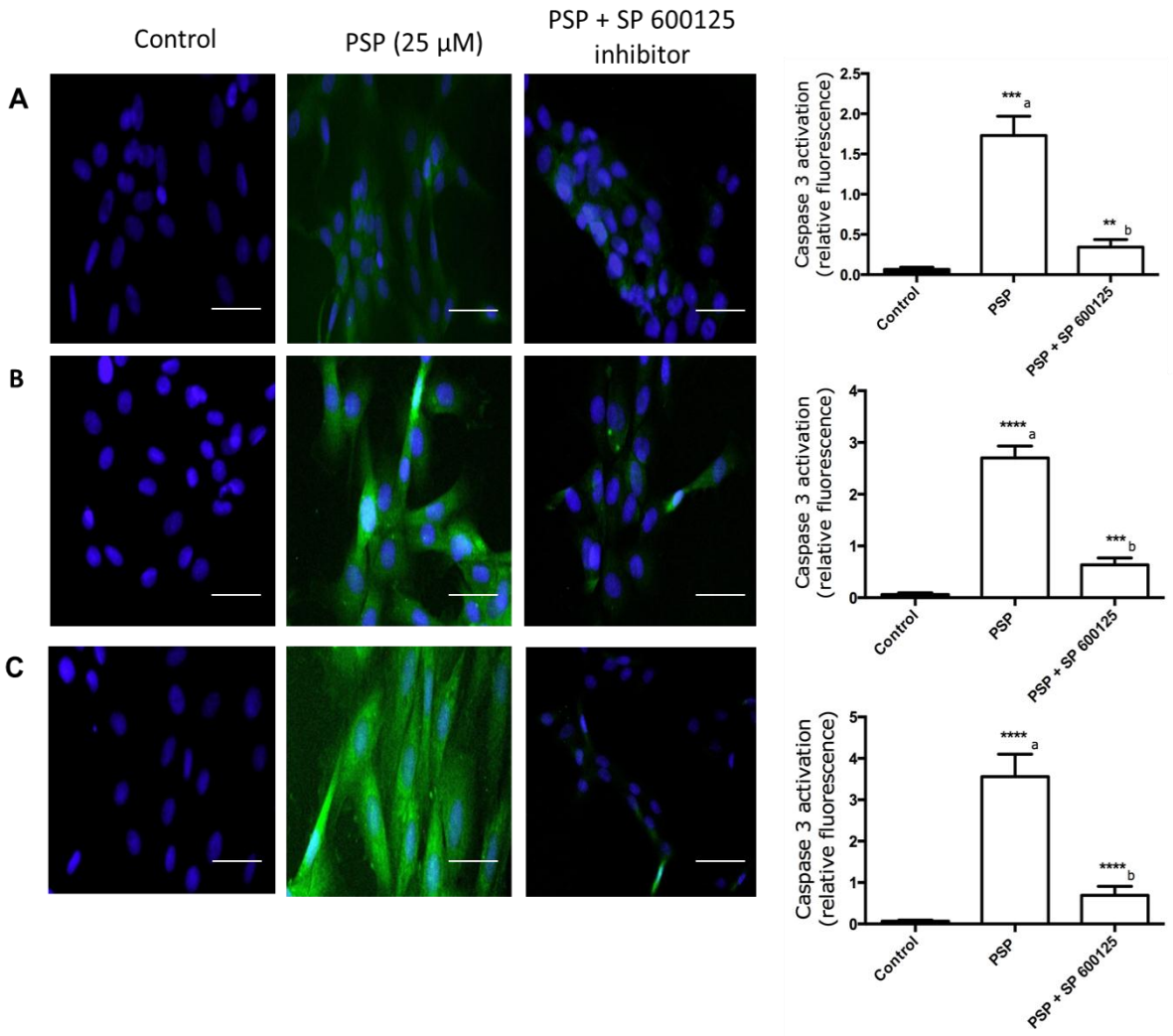

Figure 4.22 Effect of the JNK1/2 inhibitor SP 600125 on PSP-induced caspase 3 activation.

Differentiated H9c2 cells (7 day) were exposed to 25 µM PSP for A) 1 h, B) 2h, and C) 4 h in the presence and absence of SP 600125 (10 µM; 30 min pre-incubation). Following PSP exposure, caspase 3 activation was assessed via immunocytochemistry using anti-active caspase 3 antibody (green) and DAPI counterstain for nuclei visualisation (blue). Scale bar = 100 µm. Images presented are from one experiment and representative of four. Quantified data are expressed as a percentage of control cell values and represent the mean ± SEM of four independent experiments. **p<0.01, ***p<0.001, ****p<0.0001, (a) versus control and (b) versus PSP alone treated cells.

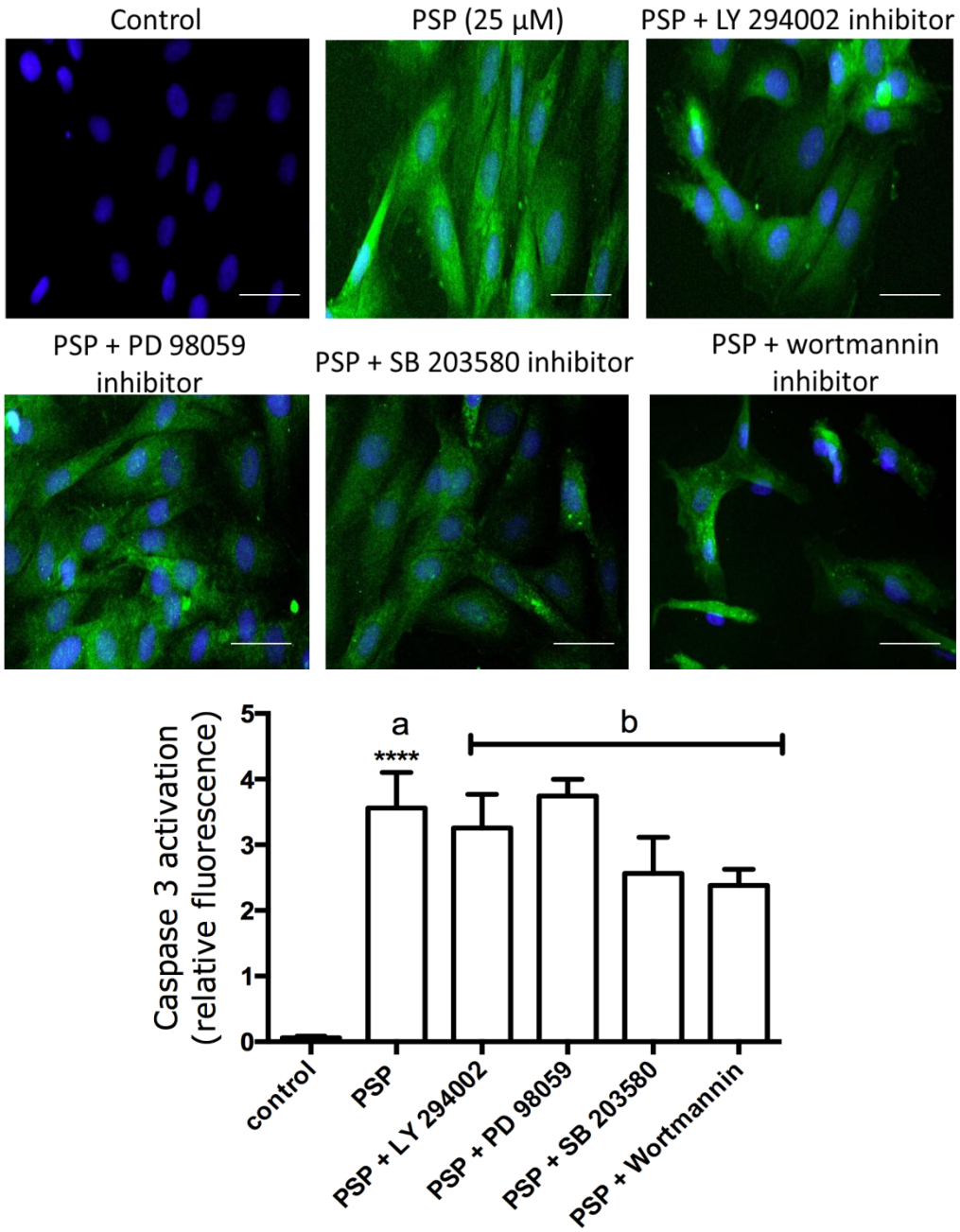

Figure 4.23 Effects of PI-3K, MEK1/2 and p38 MAPK inhibition on PSP-induced caspase 3 activation.

Differentiated H9c2 cells (7 day) were exposed to 25 µM PSP for 4 h in the presence and absence of LY 294002 (30 µM; PI-3K inhibitor), PD 98059 (50 µM; MEK1/2 inhibitor), SB 203580 (30 µM; p38 MAPK inhibitor;) and wortmannin (100 nM; PI-3K inhibitor) 30 min pre-incubation. Following PSP exposure, caspase 3 activation was assessed via immunocytochemistry using anti-active caspase 3 antibody (green) and DAPI counterstain for nuclei visualisation (blue). Scale bar = 100 µm. Images presented are from one experiment and representative of four. Quantified data are expressed as a percentage of control cell values and represent the mean ± SEM of four independent experiments. ****$p<0.0001$, (a) versus control and (b) versus PSP alone treated cells.

4.7 Effects of phenyl saligenin phosphate on AChE activity in differentiated H9c2 cells

In order to establish the relationship between the cytotoxic effects of OPs in differentiated H9c2 cells and the level of AChE activity, cholinesterase assays were performed in the presence and absence of 25 µM chlorpyrifos, diazinon and their metabolites (chlorpyrifos oxon, diazoxon) and PSP. Figure 4.24 shows that there was much stronger inhibition of AChE by the oxon forms chlorpyrifos oxon and diazoxon, followed by the parent compounds chlorpyrifos and diazinon. By contrast, PSP proved to be a very weak inhibitor of AChE activity in H9c2 cells, causing only approximately 30% inhibition compared to control levels of activity.

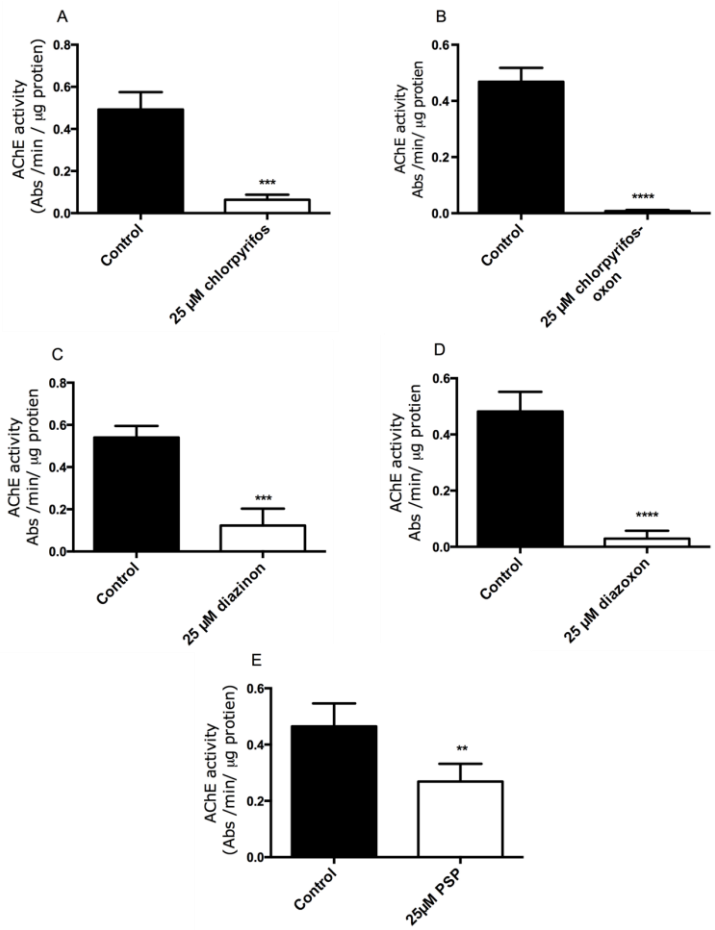

Figure 4.24 Effects of OP compounds on acetylcholinesterase activity.

Cells were induced to differentiate for 7 days and then exposed to A) chlorpyrifos B) chlorpyrifos oxon C) diazinon D) diazoxon E) PSP for (8 h,25 µM). Shown are the mean specific activities ± SEM from three independent experiments. **p<0.01, ***p<0.001, ****p<0.0001 versus non-OP-treated control cells (Student's t test).

4.8 Dansylated PSP

This study utilized fluorescently labeled PSP (dansylated PSP), which was a gift from Dr. Garner (Nottingham Tent University) as shown in Figure 4.25 This type of approach is an accurate, specific and sensitive means of detecting novel protein targets of toxic compounds (Greenbaum *et al.,* 2002).

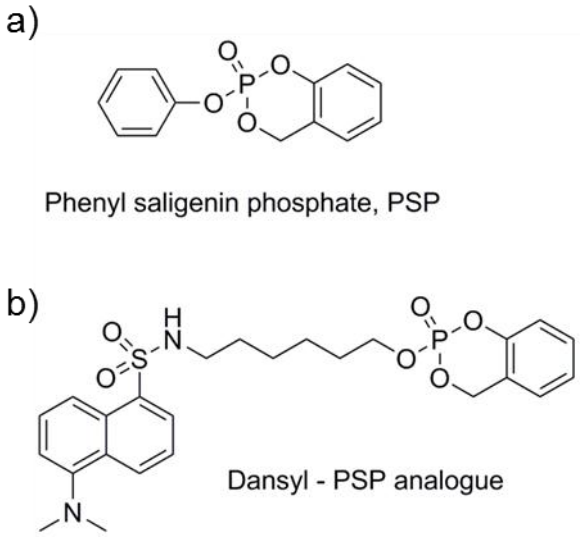

Figure 4.25 Chemical structures of A) PSP and B) dansylated PSP.

As illustrated in the current study that a concentration of 25 µM of PSP was incubated with differentiated H9c2 cells and produced optimal cardiotoxicity associated with the activation (phosphorylation) of JNK signalling pathways and the induction of apoptosis by caspase-3 activation. Proteins that bind to OPs can be separated by denaturing gel electrophoresis and visualized under UV transillumination as simplified in Figure 4.26. This was followed by 2D gel electrophoresis and MALDI-TOF mass spectrometry to identify tryptic peptides.

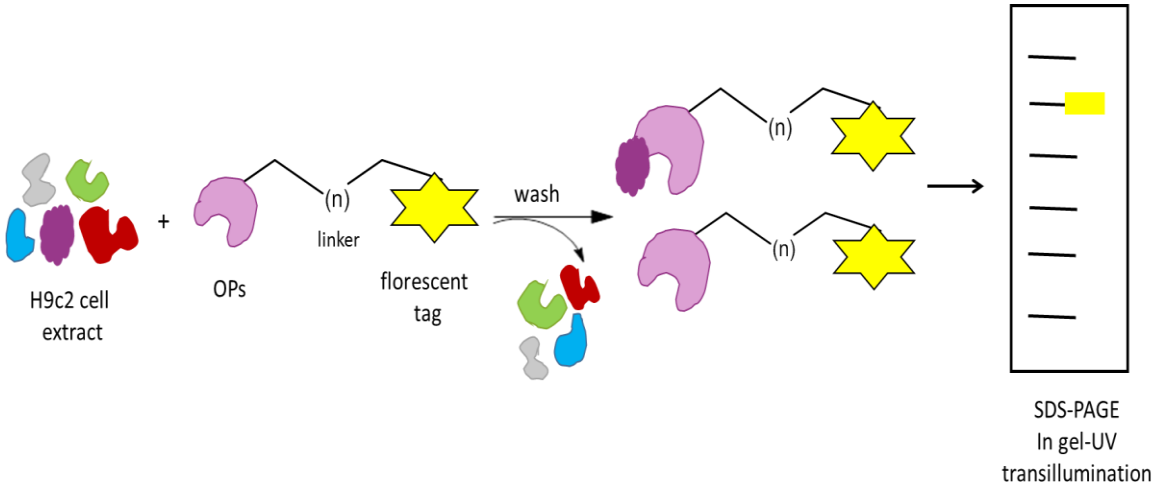

Figure 4.26 Strategy of using dansylated PSP for protein targeting.

The H9c2 cells enriched proteins are incubated with dansylated PSP, cell lysates are then separated by SDS PAGE and target proteins visualized under UV transillumination.

4.8.1 Dansylated-PSP induced cytotoxicity in H9c2 cells

Prior to investigation of novel protein targets of PSP, initially more thorough analyses were undertaken in order to compare the cytotoxic effects of dansylated PSP with those of PSP shown in section 4.3.2. Differentiated H9c2 cells were treated with different concentrations of dansylated PSP up to (200 µM) for 8 h. From the assay results obtained, it can be seen that dansylated PSP was shown to reduce significantly MTT reduction and increase the release of LDH in a concentration dependent manner, as indicated in Figure 4.27.

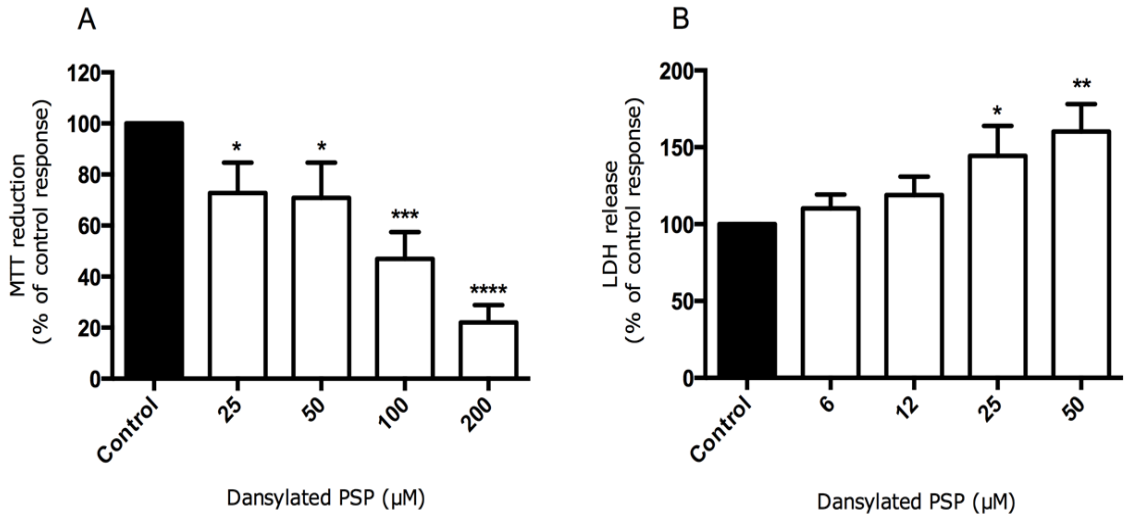

Figure 4.27 Effect of dansylated PSP on the viability of differentiated H9c2 cells monitored by MTT reduction and LDH release.

Differentiated H9c2 cells (7 days) were exposed to the indicated concentrations of dansylated PSP for 8 h. Following PSP exposure, cell viability was assessed by measuring the metabolic reduction of MTT by mitochondrial dehydrogenases (A) and the release of LDH (B). Data are expressed as a percentage of control cell values (=100%) and represent the mean ± SEM of three (MTT) or four (LDH) independent experiments, each performed in quadruplicate (MTT) or sextuplicate (LDH). *<p0.05, **p<0.01, ***p<0.001 and ****p<0.0001 versus control response.

4.8.2 SDS-PAGE analysis for dansylated-PSP binding to differentiated H9c2 cells

Differentiated H9c2 cells were incubated for 8 h with 25 µM dansylated-PSP. This concentration and time point were chosen based upon results obtained from the cytotoxicity experiments described in section 4.3.2. Following incubation, cell lysates were initially subjected to SDS-PAGE and dansylated PSP binding proteins visualised under UV light. In these experiments the presence of a detectable fluorescent band was defined as a positive test and hence the presence of protein targets, whereas undetectable fluorescence is defined as a negative result. As shown in Figure 4.28, several bright fluorescent bands were identified via SDS PAGE of dansylated-PSP treated cell lysates, indicating the presence of OP labeled target proteins, while in non-PSP treated control cells there were no fluorescent bands. Later, the gels were stained with Coomassie blue to confirm the presence of proteins in differentiated H9c2 cells. However, further experiments were required in order to identify these target proteins.

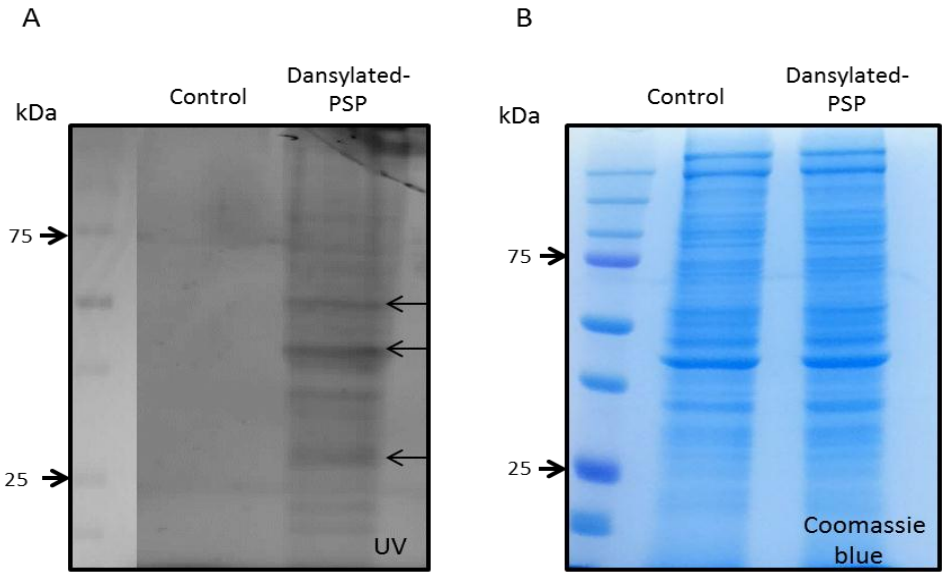

Figure 4.28 Visualisation of proteins labeled with dansylated-PSP.

Differentiated H9c2 cells were untreated or treated with dansylated PSP (8 h, 25 µM) and cell lysates (15 µg) were separated by SDS-PAGE. A) Gels were visualised under UV light. The arrows point to prominently dansylated-PSP labelled proteins. B) After visualisation of fluorescent bands, the same gels were stained with Coomassie blue to confirm the presence of protein bands. Images are presented from three independent experiments.

4.8.3 Identification of PSP labeled proteins by mass spectrometry

Identification of dansylated PSP labelled proteins was achieved by 2D gel electrophoresis followed by MALDI-TOF analysis of the peptides produced by trypsin digestion. Differentiated H9c2 cells were untreated (control) or treated with 25 µM dansylated-PSP, and cell lysates prepared and subjected to 2D gel electrophoresis. Visualisation of 2D gels under UV light revealed control cells did not show any fluorescent spots (Figure 4.29a). In comparison, treated cells showed several fluorescent protein spots (Figure 4.29b). After visualisation under UV light, gels were stained with ProtoBlue™ safe colloidal Coomassie G-250 stain and imaged as described in Chapter 2 (section 2.7). In order to identify dansylated-PSP labeled protein targets, Progenesis SameSpots software was used and was able to identify three protein spots that showed significant binding of labeled PSP (Figure 4.29d). To identify these spots, these proteins were excised from the stained gel and digested by trypsin, and analyzed by a MALDI-TOF/TOF mass spectrometry. Target protein spots showed significant similarities with searched databases; these identified proteins are listed in Table 4.2.

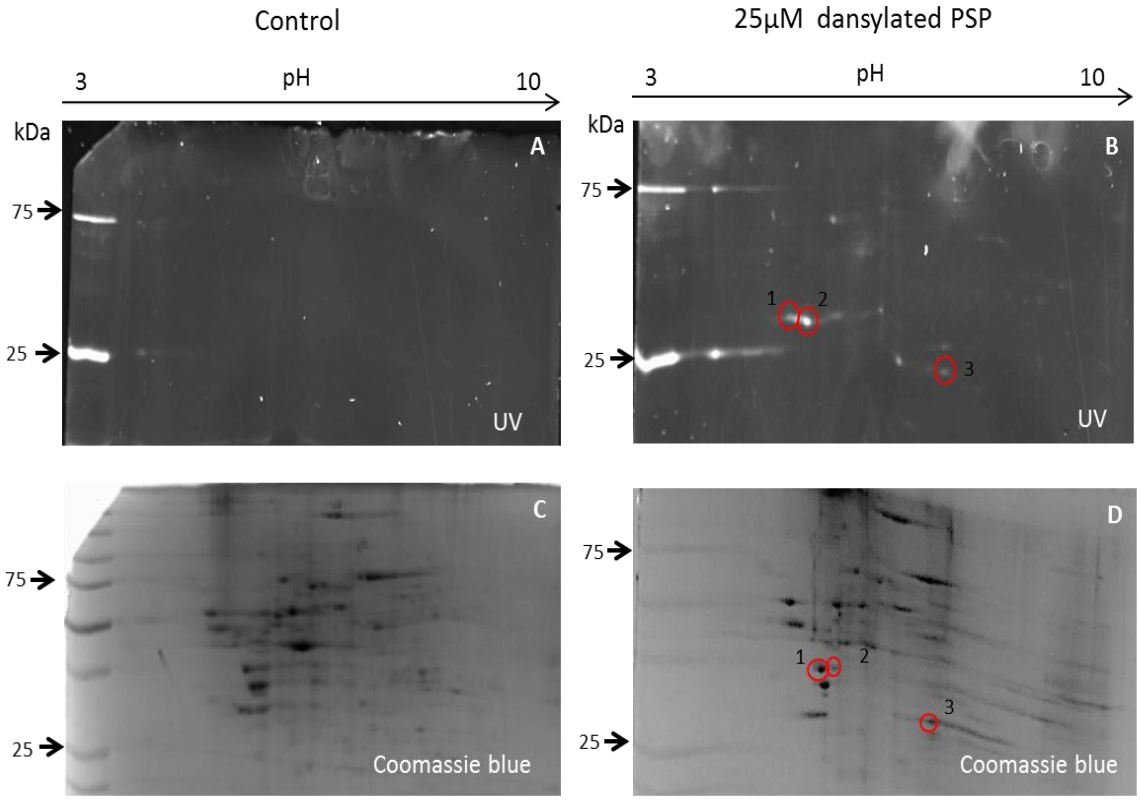

Figure 4.29 Visualisation of proteins labelled with dansylated PSP.

Differentiated H9c2 cells were untreated or treated with dansylated PSP (8 h, 25 µM) and cell lysates processed and analysed by 2D gel electrophoresis using pH 3-10 gradient strips. Gels were visualised under UV light (panels A and B) prior to staining with ProtoBlue™safe colloidal Coomassie G-250 stain (panels C and D). Gel images are presented from three independent experiments and were analysed using Progenesis SameSpots software and circled spots represent those labelled with dansylated PSP. Spot 1: nucleolar protein 58; Spot 2: tropomyosin α-4; Spot 3: heat shock protein β-1. A list of identified proteins labelled by dansylated PSP is provided in Table 6.1

Table 4.2 Identification of PSP-Binding proteins in differentiated H9c2 cells.

Spot no.	Protein	Accession no.	PMF sequence coverage (%)[a]	Identified peptide sequence (MS/MS)	Mascot score [b]	kDa	p*I*
2	tropomyosin α-4	P09495	39	-	52	28.5	4.4
3	Heat shock protein β-1 (HSP-27)	P42930	-	LFDQAFGVPR	80	22.9	6.1
1	nucleolar protein 58	Q9Q286	32	-	52	59.5	9.2

H9c2 cells treated with dansylated PSP (8 h, 25 µM) were analyzed by 2D gel electrophoresis and PSP-labeled proteins identified using MALDI- TOF MS (PMF) or MS/MS as described in chapter 2 (section 2.7.4). Sequence data were analyzed using Mascot software and reported according to percentage sequence coverage (SC%) or Mascot score (ion scores for MS/MS > 27 indicate identity or extensive homology; > 51 for PMF). All identified proteins exhibited Mascot scores that were considered statistically significant (*$p < 0.05$). [a]MALDI-TOF MS. [b]MS/MS.

4.9 Binding of dansylated PSP to purified tropomyosin

To confirm the identification of one protein labelled by dansylated PSP, tropomyosin was chosen for validation by incubation of purified human heart tropomyosin (10 µg) with or without dansylated PSP or unlabelled PSP. The purified tropomyosin was then subjected to SDS-PAGE and visualised under UV light followed by staining with Coomassie blue. As shown in Figure 4.30, purified tropomyosin was labelled with dansylated PSP.

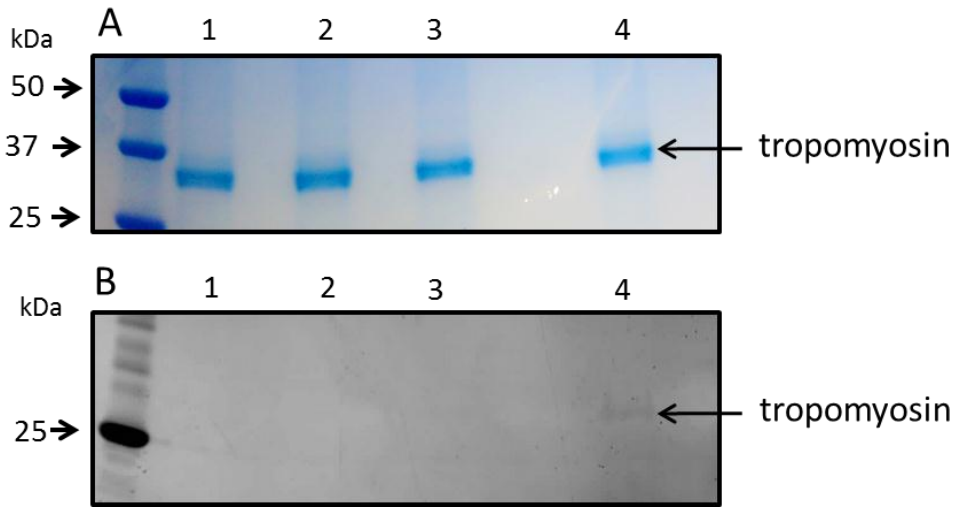

Figure 4.30 Labeling of purified human heart tropomyosin with dansylated PSP.

Human heart tropomyosin (10 µg) was incubated for 1 h in presence or absence of dansylated/unlabelled PSP (25 µM). Tropomyosin samples were then subjected to SDS-PAGE, visualised under UV light (B) and subsequently stained with Coomassie Blue (A). Lane 1: tropomyosin incubated with Tris-buffered saline; Lane 2: tropomyosin incubated with DMSO (the solvent for PSP); Lane 3: tropomyosin incubated with unlabeled PSP; Lane 4: tropomyosin incubated with dansylated PSP. Gel images are presented from three independent experiments.

4.10 Discussion

4.10.1 Phenyl saligenin phosphate-induced cytotoxicity

Organophosphate poisoning may affect heart function causing cardiac complications such as bradycardia due to enhanced cholinergic stimulation and conduction disturbance (Brill *et al*., 1984; Wang *et al*., 1998). Thus far, a limited number of studies have investigated cardiac toxicity induced by OPs, but still the detailed mechanisms underlying the cellular toxicity are not known (Ludomirsky *et al.*, 1982, Saadeh *et al.*, 1997) and there is very little information on the direct effect of OPs on muscle cell function.

Initial experiments in this study examined chlorpyrifos and diazinon and their *in vivo* metabolites chlorpyrifos oxon and diazoxon. It was found that chlorpyrifos showed toxic effects at the highest concentrations >100 µM in mitotic and differentiated H9c2 cells. Chlorpyrifos oxon, diazinon and diazoxon at concentrations up to 200 µM had no cytotoxic effects on mitotic and differentiated H9c2 cardiomyoblast cells. These results are in stark contrast to the cardiovascular consequences of acute OP poisoning, which reflects over-activity of sympathetic and parasympathetic pathways due to enhanced levels of acetylcholine (Roth *et al.* 1993; Anand *et al.*, 2009).

The oxon forms of chlorpyrifos and diazinon did not show any cytotoxic effects in H9c2 cells. Taking into account the fact that oxon metabolites of chlorpyrifos and diazinon are potent inhibitors of AChE (Eaton *et al*., 2008). This supports the view that the cytolethal effects of these compounds is not only associated with AChE inhibition (Masoud *et al.*, 2003). This is in agreement with the results of Saulsbury *et al.* (2008) who investigated the differences between chlorpyrifos and chlorpyrifos oxon, and found that chlorpyrifos induced a reduction in cell viability more than its oxon metabolite. Thus, OP intoxication depends on the physiological response of cells towards specific OP compounds (Rush *et al.*, 2010). In summary, OPs that mediate acute *in vivo* toxicity, primarily *via* AChE inhibition, display little cytotoxicity towards mitotic and differentiated H9c2 cardiomyoblasts. In marked contrast, PSP (a weak AChE inhibitor) displayed pronounced cytotoxicity towards both mitotic and differentiated H9c2 cells. PSP is an analogue of SCOTP, an active neuropathic metabolite of TOCP which is known to be a direct inhibitor of NTE (Chen *et al.*, 2012) and a weak inhibitor of AChE (Jortner & Ehrich 1987). Hence, the cytotoxic effects of PSP observed in this study

are presumably mediated via non-cholinergic mechanisms. As shown in Figure 4.7a, findings pointed to PSP cytotoxic effects on mitotic H9c2 cells at the shorter incubation time 4 h with MTT reduction and LDH release, whereas in differentiated H9c2 cells PSP-induced toxicity was evident at 2 h when monitoring MTT reduction (Figure 4.13c). Here, results showed that MTT reduction was more sensitive than LDH release in detecting cytotoxic events in differentiated cells. The difference in sensitivity between MTT and LDH assays is in agreement with previous studies, which have reported the MTT assay as being more sensitive in detecting cytotoxic effects (Fotakis & Timbrell, 2006). These cytotoxic effects are consistent with earlier studies that have shown that PSP inhibits MTT reduction in mouse N2a neuroblastoma cells and human hepatic HepG2 cells (IC_{50} values of approximately 10-15 µM; Harris *et al.,* 2009).

4.10.2 Phenyl saligenin phosphate-induced apoptosis

It has been questioned whether the observed PSP-induced cytotoxicity is associated with apoptosis or necrosis. Therefore, caspase-3 was measured following PSP exposure. The present findings showed that treatment with PSP (25 µM) triggered the rapid activation of intracellular caspase-3 (Figure 4.15 and Figure 4.16), indicating that PSP induced apoptosis in cultured differentiating H9c2 cells. These results are consistent with a previous study showing that PSP (10 and 100 µM) induced apoptosis in human SH-SY5Y cells via activation of caspase-3 (Carlson *et al.,* 2000). As PSP was found to be a weak inhibitor of AChE (Figure 4.24e), and this also supports the fact that OP-induced apoptosis can occur independently from AChE inhibition (Li, 2010). A review by Ehrich *et al.* (1997), which compared various OPs, concluded that PSP-induced apoptosis was inversely associated with the extent of AChE inhibition.

4.10.3 Phenyl saligenin phosphate-induced JNK1/2 signalling

There is increasing evidence showing that apoptosis is modulated by different members of the MAPK family (Hetman & Xia, 2000). However, there is very little known about the effect of OPs on MAPK signaling pathways in differentiated H9c2 cells. To determine whether various MAP kinase signaling pathways were involved with PSP-induced apoptosis, the current study investigated the effect of PSP exposure on protein kinase cascades associated with cell survival (ERK1/2 and PKB) and cell death (p38 MAPK and JNK1/2). It was presumed

that PSP induced cytotoxic effect may induce activation of ERK1/2, PKB, p38 MAPK and JNK1/2 signalling pathway. In the current study it appears that PSP did not significantly modulate PKB phosphorylation or ERK1/2 MAPK or p38 MAPK activation status in differentiated H9c2 cells (Figure 4.17; Figure 4.18; with anti-p38 no bands appeared). In contrast, previous reports provided evidence that administration of sub-lethal concentrations of PSP was able to modulate these important protein kinase signal transduction pathways. For example, in differentiating mouse N2a neuroblastoma cells, PSP triggered the transient activation of ERK1/2 (2.5 µM; 4 h; Hargreaves *et al.* 2006). Also, Pomeroy-Black & Ehrich (2012) observed elevated levels of phosphorylated PKB in human SH-SY5Y neuroblastoma cells following exposure to PSP (0.1 µM). It is notable that the effect of PSP on PKB activation in SH-SY5Y cells was a consequence of OP-induced activation of the low affinity neurotrophin p75 receptor (Pomeroy-Black & Ehrich 2012). Thus, neurotrophins play an important role in neuronal survival and development (Ginty, 2002).

Data from this study also showed that PSP administration to differentiated H9c2 cells was found to increase significantly the phosphorylation of JNK 1/2 (Figure 4.19) indicating that JNK1/2 activation plays a major role in PSP-induced apoptosis in differentiated H9c2 cells. As this is supported by previous study that reported that JNK1/2 pathway plays an important role in the induction of apoptosis (Dhanasekaran & Reddy, 2008). Thus, as JNK1/2 belongs to the MAPK family, any disturbance in MAPK pathways could lead to morphological changes which may induce loss of cell viability as observed in previous studies (Nostrandt *et al*., 1992; Carlson *et al.,* 2000). These results are consistent with an earlier study showing that sarin and soman-like organophosphate nerve agents ([bis(isopropyl methyl)phosphonate, BIMP and bis(pinacolyl methyl)phosphonate, BPMP]) induce JNK activation in rat brain cells (Niijima *et al.*, 2000). Interestingly, the activation of JNK by these two OPs was dependent upon phospholipase C and protein kinase C activation (Nijima *et al.*, 2000).

Moreover, activation of the JNK pathway initiates harmful inflammation and, if unabated, can lead to apoptosis (Abraham & Clark, 2006). Interestingly, in cultured adult rat cardiac ventricular myocytes, JNK activation triggers the release of pro-apoptotic molecules such as cytochrome c and AIF (apoptosis-inducing factor; Aoki *et al*., 2002). This may suggest the potential mechanism of PSP-induced apoptosis in differentiated H9c2 cells.

To ascertain the role of the JNK1/2 pathway in PSP-induced cytotoxicity, H9c2 cells were exposed to PSP in the presence of the JNK1/2 inhibitor SP 600125. However, pre-treatment with SP 600125 (10 μM) did not reverse the toxic effect of PSP in terms of either MTT reduction or LDH release following 4 h or 8 h exposure (Figure 4.20). In contrast, pre-administration of SP 600125 attenuated PSP-induced JNK1/2 activation at 1 h and 2 h (Figure 4.21a and b). However, SP 600125 ineffective to block JNK activation at 4 h (Figure 4.21c). The results showed that SP 600125 did not play a vital role in preventing cell death as shown in MTT and LDH assay. The reversible inhibition of PSP-induced JNK1/2 activation by SP 600125 may reflect removal of the inhibitor from the cell (although the inhibitor was present throughout the experiment) and/or its metabolism to an inactive metabolite. Another possibility may be that alternative pathways are involved in the death machinery of differentiated H9c2 cells.

However, SP 600125 did block caspase-3 activation at 1 h, confirming the involvement of JNK1/2 in PSP-induced apoptosis. It is interesting to note that although SP 600125 blocked caspase-3 activation at 4 h, it did not block PSP-induced JNK1/2 activation at 4 h (Figure 4 22). This is could potentially be a consequence of caspase-3 activation being downstream of JNK1/2 and hence inhibition of JNK1/2 at early time points (<2 h) prevents subsequent caspase-3 activation. Regarding the clinical relevance, a previous study has shown that similar levels of SCOTP (an analogue of PSP) can be achieved in the heart tissue after normal levels of accidental exposure (Somkuti & Abou-Donia, 1990). Since the present data showed that 25 μM PSP was able to induce caspase-3 activation at the first hour of exposure, it is most likely that such levels can be achieved transiently *in vivo.* More interestingly, previous study shown that 100 μM TOCP were observed in heart tissue in rats after a repeated oral doses (50 mg/kg) of TOCP, suggesting that high levels of metabolite are achievable and longer exposure of PSP at lower concentrations can induce caspase-3 activation (Somkuti & Abou-Donia, 1990).

Furthermore, pre-treatment with other kinase inhibitors LY 294002, PD 98059, SB 203580 and wortmannin did not block caspase-3 activation at 1,2 and 4 h, confirming that neither ERK 1/2 nor p38 MAPK and PKB are involved in PSP-induced cell death (Figure 4.23). Although this is the first report describing PSP-induced activation of JNK 1/2 in differentiated

H9c2 cells, further studies are required to reveal other molecular mechanisms implicated in PSP-induced cytotoxicity towards H9c2 cells.

4.10.4 Effect of OPs on cellular AChE activity in differentiating H9c2 cells

In the current study, the results from AChE activity assays showed that exposure to chlorpyrifos and diazinon and their acutely toxic metabolites (diazoxon and chlorpyrifos oxon) was associated with significant inhibition in AChE activity (Figure 4.24a, b, c and d). The extent of inhibition associated with each compound was in agreement with previous observations in nerve tissue treated with chlorpyrifos and diazinon showing significant inhibition of AChE activity (Murphy, 1986; Sultatos, 1994). In contrast, PSP confirmed to be a weak inhibitor of AChE under the same experimental conditions as used for LDH and MTT assays (Figure 4.24 e). These data pointed to the idea that cytotoxic effects of PSP on H9c2 cells were unrelated to significant cholinesterase inhibition and it is more likely that other cellular targets contribute to its toxicity. At present the cellular effect(s) of neuropathic OPs, such as PSP, on cardiomyocytes are largely unknown.

4.11 Identification of PSP Binding Proteins.

Over the years, OPs are known to be a highly reactive compounds that have been shown to bind to the active site of AChE causing hyper-stimulation of cholinergic receptors resulting in OP intoxication (Abdollahi & Karami-Mohajeri, 2012). However, OPs are also known to interact with non-cholinergic targets. For example, mass spectrometry analysis has demonstrated that OPs may bind to human albumin (Ding *et al.,* 2008; Li *et al*., 2007), alpha- and beta-tubulin (Grigoryan *et al.,* 2008), human transferrin and mouse transferrin (Li *et al.,* 2009). In a previous study, OPs were confirmed to form covalent adducts on tyrosine residues of these proteins (Grigoryan *et al.,* 2009). Binding of OPs such as chlorpyrifos-oxon with tubulin was found to inhibit tubulin polymerization, affecting neuronal cytoskeleton function resulting in neuronal cytotoxicity in the hippocampus of rodent brain (Prendergast *et al.,* 2007; Grigoryan *et al.,* 2008). On the other hand, other OP-binding proteins such as albumin and transferrin were not linked to any toxic effects. Thus OP adducts with these proteins may serve as biomarkers for OP exposure (B. Li *et al.*, 2009). Despite the variety of proteins identified as targets to different OPs, to date targets proteins of PSP in cardiac cells have not been investigated.

Exposure to PSP was found to induce OPIDN, in which NTE inhibition and found to be a primary target (Jortner & Ehrich, 1987). NTE is a member of the patatin-like phospholipase (PNPLA) family, whose functions include regulation of lipid metabolism and cell signalling (Chang *et al*., 2010; Richardson *et al.,* 2013). Although NTE (PNPLA6) has been detected in non-neuronal tissues including human heart (Wilson *et al.,* 2006), it is not known whether mitotic or differentiated H9c2 cells express NTE. Although beyond the scope of the present study, it would be of interest to investigate NTE expression and the effect of PSP on NTE activity in H9c2 cells. Previous studies have only focused on the effect of PSP on proteolytic enzymes, as well as cytoskeleton proteins and signalling molecules in neuronal cells (Hargreaves 2012; Pomeroy- Black & Ehrich 2012). However, the mechanism of PSP toxicity in differentiated cardiac cells remains unclear. For this purpose in the present study, modified (dansylated) PSP was used to facilitate the search of new biomarkers and identification of protein targets of PSP in differentiated H9c2 cells.

Several methods are available to tag proteins and molecules and the most commonly used tags on a chemical probe are biotin, fluorescent, and radioactive tags, which use simple labeling techniques to identify the protein of interest in gel electrophoresis with high protein selectivity (Patricelli *et al.,* 2001). However, both fluorescent and radioactive probes are known to be more sensitive for detection than biotin (Greenbaum *et al.,* 2002). Fluorescently labeled probes contain a reactive group which has the ability to covalently attach to a functional group on the molecule to be labelled, which gives the compound a detectable property (Probes, 2013). They are suitable for in vitro assay procedures to probe particular compounds that can be detected through fluorescence emission (Jeffery & Bogyo, 2003).

Mass spectrometry analysis identified tropomyosin, heat shock protein β-1 and nucleolar protein 58 as novel protein targets for PSP. Heat shock protein β-1 (also known as HSP-27) is a member of small heat shock protein family. These proteins are induced in response to stress and are known to have a cardioprotective effect. At the subcellular level they play an important role in preventing apoptosis and necrosis (Mymrikov *et al*., 2011; Wettstein *et al*., 2012). Moreover, they have been found to be associated with the regulation and stability of cytoskeleton proteins, by promoting their structural stability and increasing their resistance to stress (Huot *et al.,*1995; Guay *et al*.,1997). Based on the results presented in this chapter,

it is suggested that binding of PSP to HSP27 could lead to changes in its activation status, resulting in alterations in its protective function against apoptosis and cardiac toxicity.

Tropomyosin is known to play a central role as a contractile regulatory protein, which also plays an important role in actin stability in muscle and non-muscle cells (Yo & Ono, 2006). In vitro studies have suggested that tropomyosin functions to protect actin from actin depolymerizing factor proteins (ADF) such as cofilin (Bernstein & Bamburg, 1982; Broschat, 1990). Actin is known to be a core component of the microfilament network, which is involved in a number of biological function such as regulation of cell motility, contraction and cell shape (Khaitlina 2001; Yarar *et al,* 2005). *In vivo* studies showed that alteration in tropomyosin expression directly contributes to significant alteration in cardiac function, including cardiac hypertrophy, ventricular fibrosis and atrial enlargement (Prabhakar *et al*.,2003).

More interestingly, exposure to PSP (100 µM) induced *in vitro* cytotoxicity and apoptotic cell death mediated by caspase-3 activation in SH-SY5Y human neuroblastoma cells, suggesting that activation of caspase-3 is associated with numerous substrate degradation, such as actin (Carlson *et al.,* 2000). Later on, exposure to PSP (10 µM) was observed to significantly decrease the levels of cellular filamentous actin in human SH-SY5Y neuroblastoma cells (Carlson & Ehrich, 2001). Although, all these studies reported the effect of PSP using neuronal cells as a model system, none of them used cardiomyocytes. However, It is not known whether the changes in actin expression reported in the previous study is a result of the direct effect of PSP on actin or an indirect effect from PSP modification of tropomyosin or potentially other actin binding protein. Therefore, it is reasonable to suggest that PSP binding to tropomyosin may affect actin stabilization, which could in turn contribute to the development of cardiac toxicity.

Moreover, it is important to mention that there is clear evidence supporting the link between actin stability and apoptosis. For example, drugs that inhibit actin filament organization, such as Jasplakinolide, were found to trigger apoptosis in human Jurkat T cells (Bubb *et al*., 1994; Odaka *et al.,* 2000). Thus, changes in actin dynamics are associated with different stages of programmed cell death (Desouza *et al*., 2012). These observations are consistent with the possibility that the toxicity of PSP towards differentiated H9c2 may be

due to tropomyosin binding affecting actin polymerization, which could alter its activity status and induce the activation of downstream caspases that mediate apoptosis. Moreover, it is conceivable that PSP binding to tropomyosin attenuates its interaction with other actin binding proteins (e.g. cofilin) that are linked to cytoskeleton mediated modulation of apoptotic signalling (Desouza *et al*. 2012).

Finally, PSP also bound to nucleolar protein 58 which is MSP58 protein is found in the microspherules of the nucleolus (Ren *et al.*, 1998) and required for 60S ribosomal subunit biogenesis (Lyman *et al.* 1999). PSP binding to this protein might impair the translation of proteins essential for cell survival; thus, overexpression of MSP58 protein was suggested to be associated with alteration in nucleolus size and shape (Ren *et al.*, 1998). However, it remains to be established if there is a definitive link between any of these novel protein targets and PSP-induced cytotoxicity.

4.12 Conclusion

In summary the data presented in this chapter indicate marked differences between the effects of the tested OPs on mitotic and differentiated H9c2 cells. PSP was shown to be the most cytotoxic compound that induced significant increase in LDH release and inhibition of MTT reduction, without a major effect on AChE activity. Furthermore, the findings indicate that the toxic manifestations induced by PSP administration are associated with activation of JNK1/2 and caspase-3. However, the cytotoxic effects of PSP may involve other molecular mechanism and biological targets. Therefore, further investigations into the intracellular protein targets of PSP are necessary. Mass spectrometry identified tropomyosin, heat shock protein β-1 and nucleolar protein 58 as novel binding proteins that may be involved in PSP toxicity. PSP binding with such proteins may affect fundamental cardiac function. However a number of questions remain unanswered, such as the location and nature of the binding sites and whether PSP binding with these protein occur *in vivo*. Therefore, additional experiments are needed to determine the potential significance of these observations and whether the biomarkers identified could be of potential value for diagnostic purposes or as targets for the development of therapeutic approaches to attenuate OP-induced cardiac damage.

Chapter 5:

Sublethal Effects of OPs on Differentiating H9c2 Cells

5.1 Introduction

Organophosphate pesticides and nerve agents are chemical compounds that cause toxicity via inhibition of AChE, which results in overstimulation of cholinergic and nicotinic receptors in the central nervous system. In turn, they affects other organs including the heart (McDonough & Shih, 1997). In addition to their effects on AChE, such OPs may have direct or indirect effects on other target molecules (Silveira *et al.,* 1990; Jett *et al.,* 1991). For example, OPs were found to directly affect cytoskeleton proteins. For example, sublethal concentrations of chlorpyrifos oxon were found to bind covalently to tubulin and tubulin-associated proteins resulting in disruption of microtubule function in neuronal cells (Jiang *et al*., 2010). Organophosphates may also affect proteins involved in the regulation of axonal transport in neuronal cells, leading to neuronal dysfunction and cell death (Morfini *et al*., 2009). However, no studies conducted so far have examined the effect of sublethal concentrations of OPs and their metabolites on cytoskeleton proteins in differentiating H9c2 cells and on cardiomyocyte-like development.

Heart structural proteins can be divided into four types: normally contractile proteins, sarcomeric skeleton proteins, true cytoskeleton proteins and membrane-associated proteins (Kostin *et al.*, 2000). Cytoskeleton proteins, such as myosin, actin, tropomyosin and troponins, play a significant role in cardiac contractile function, morphological stability and signal transduction (Kostin *et al.,* 2000). Thus, any alterations in these structural and functional proteins may result in an increase in mechanical stress and morphological alterations in cardiac cells that can cause cardiac dysfunction (Ehler & Perriard, 2000). For example, in patients with heart failure, the expression of contractile proteins such as, actin and myosin was downregulated and accompanied by contractile and diastolic dysfunction (Kostin *et al.,* 2000). Also, tubulin and desmin expression increased in the early development of heart failure in guinea pig hearts, highlighting the importance of cytoskeletal changes associated with heart failure (Wang *et al*., 1999) and over expression of tropomyosin in hearts resulted in dilated cardiomyopathy (Rajan *et al*., 2010). Therefore, to study the effect of OPs on the development of differentiating H9c2 cells, it is important to evaluate the expression of cardiac cytoskeleton proteins, as the expression of these proteins is strongly correlated with functional alteration and structural degeneration. At present there are few reports on the effects of sublethal concentrations of OPs on cardiac cells. However, a recent

in vivo study demonstrated changes in heart rate and anatomical abnormalities in both *Xenopus* and zebrafish following exposure to low concentrations of chlorpyrifos and dichlorvos (Watson *et al*., 2014). Another study also demonstrated that sublethal doses methamidophos induced cardiac hypertrophy in rats (Calore *et al*., 2006). The importance of the OPs effect at different stages of developmental is of concern. For example, amphibian species were shown to be more susceptible to sublethal doses of OPs in their early stages of development when compared to later stages (van der Schalie *et al*., 1999). Some toxicity studies have found that sublethal doses of OPs cause morphological changes and behaviour problems (Zalizniak & Nugegoda, 2006). However, the exact molecular mechanism underlying the effect of sublethal concentrations of these compounds on cardiomyocytes is still unclear. Therefore, the present study aimed to investigate the sublethal effects induced by OPs by monitoring changes in cellular morphology, AChE activity and expression of cytoskeletal proteins.

5.2 Methods

As described in chapter 2 section 2.3, 2.4, 2.5, 2.6

5.3 Aims

This aims of this chapter were to assess the potential effects of sublethal concentrations of the OPs chlorpyrifos and diazinon, their corresponding metabolites (chlorpyrifos oxon and diazoxon), and PSP on differentiating mouse H9c2 cells, in order to understand the molecular basis for the potential long-term toxicity of these compounds. The study focussed on the effects of these OPs on morphological features, AChE activity and expression of cardiac cytoskeleton proteins.

5.4 Results

The sublethal concentrations of 3 µM and 0.3 µM were selected according to the previous result in chapter 4, which demonstrated that OPs compounds at these concentrations had no significant effect on MTT reduction or LDH release following 48 h exposure in differentiated H9c2 cells. Therefore, these sublethal concentrations 3 µM and 0.3 µM were used to investigate if repetitive exposure to sublethal concentrations of OPs can disrupt the differentiation of H9c2 cells. In the present study cultured mitotic H9c2 cells were induced to differentiate with the desired concentrations of OPs in differentiation medium. Every 48 h the differentiation medium was replaced along with the relevant concentration of OPs. Then, cells were assessed at days 7, 9 and 13, as shown in Figure 5.1.

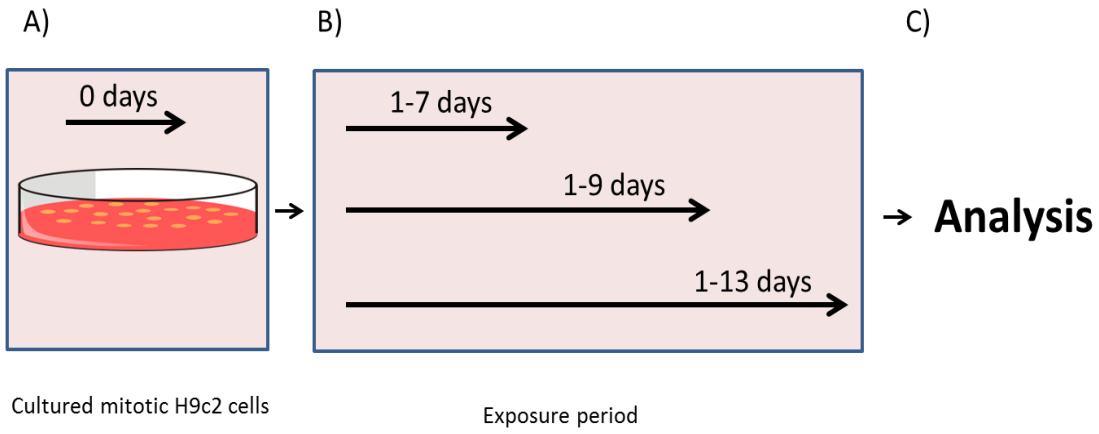

Figure 5.2 A schematic representation of the experimental procedure in the present chapter.

A) Cultured mitotic H9c2 cells. B) Cells were induced to diffrentiatiate in the presence of the disired concentration of OPs for 7 days, 9 days and 13 days . C) Different analyses were performed to study the effect of sublethal concentrations of OPs on differentiating H9c2 cells.

5.4.1 Effect of sublethal concentrations of OPs on cell morphology

Initial experiments assessed the effect of sublethal concentrations of OPs on morphological changes in differentiating H9c2 cells via Coomassie Brilliant Blue staining following 7, 9 and 13 day exposure periods. Overall, results showed variation in the size and shape of the cells according to the concentration of the OP, and the degree of cell deterioration ranged from slight to severe according to the type of OP used.

Exposure to 3 µM chlorpyrifos was shown to have a moderate effect on the morphology of differentiating H9c2 cells, which appeared to be more rounded rather than elongated with mild changes at days 7, 9 and 13 when compared to the control (Figure 5.2). By contrast, chlorpyrifos oxon proved to have a no observable effect on differentiating H9c2 cells at the 7-day and 9-day time point, as shown in Figure 5.3a and b. However, chlorpyrifos oxon had less observable effect than chlorpyrifos at 13-days as shown in Figure 5.3c. Exposure to diazinon showed similar effects to chlorpyrifos, in that some cells were shown to be to more rounded and less elongated at days 7, 9 and 13 when compared to control cells (Figure 5.4). More interestingly, the morphological effect of diazoxon was not observed at 7-days 9-day time point and at 13-days exposure had less effect than diazinon on differentiating H9c2 cells as shown in Figure 5.5.

Exposure of 3 µM PSP to differentiating H9c2 cells induced the most striking effect on cell morphology, when compared to other OP compounds (chlorpyrifos, chlorpyrifos oxon, diazinon and diazoxon). Cell deterioration was evident, since the PSP-treated cells did not exhibit a fibroblast-like structure, elongated spindle shape, or multiple nuclei at days 7, 9 and 13 (Figure 5.6). Lastly, treatment with 0.3 µM OPs did not cause any observable morphological changes and cells appeared to differentiate as normal. Therefore, further studies investigated the effects of 3 µM OPs on AChE activity and expression of cytoskeletal proteins.

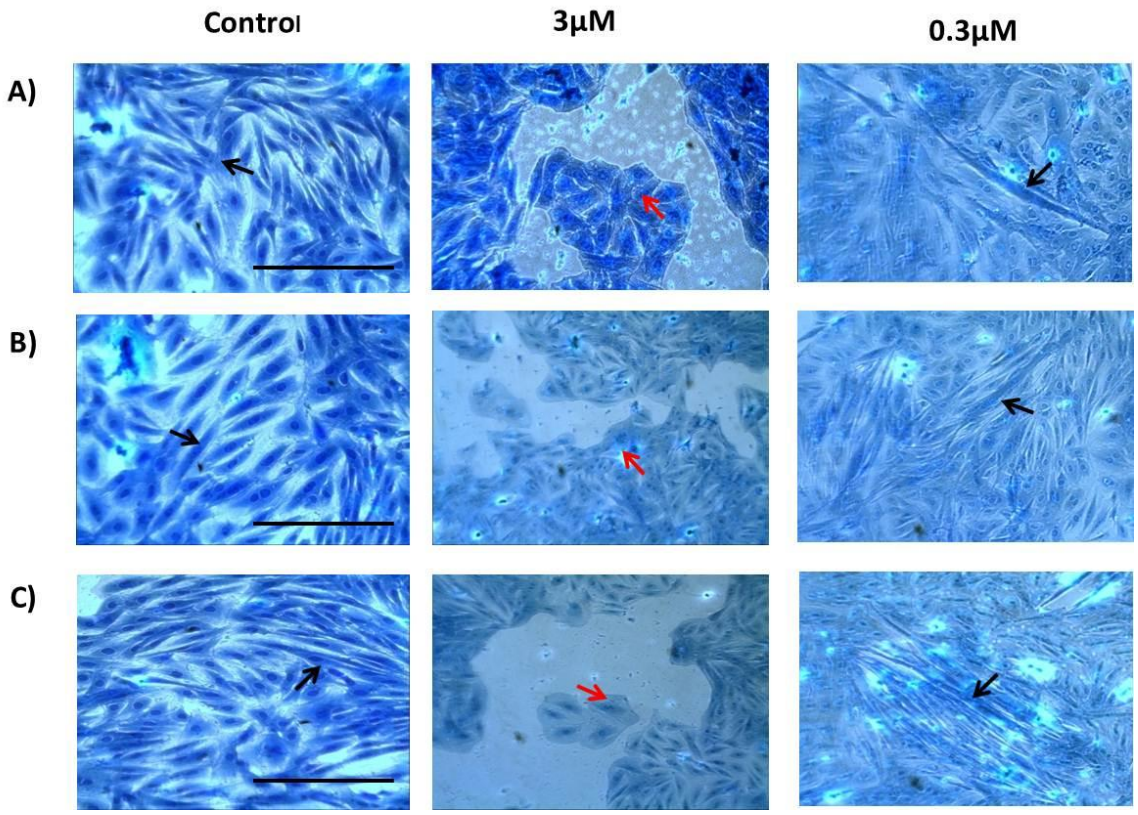

Figure 5.3 Effect of sublethal concentrations of chlorpyrifos on differentiating H9c2 cells.

Mitotic H9c2 cells were induced to differentiate in the presence of 3 µM and 0.3 µM chlorpyrifos for A) 7 days B) 9 days and C) 13 days. Following treatment cells were fixed with 90 % (v/v) methanol, stained with Coomassie brilliant Blue and then visualised using light microscopy (20x objective lens). The black arrow indicates elongated and multinucleated differentiated cells and red arrows indicate typical rounded and compact cells. Images presented are from one experiment and representative of three independent experiments. Scale bar = 100 µm.

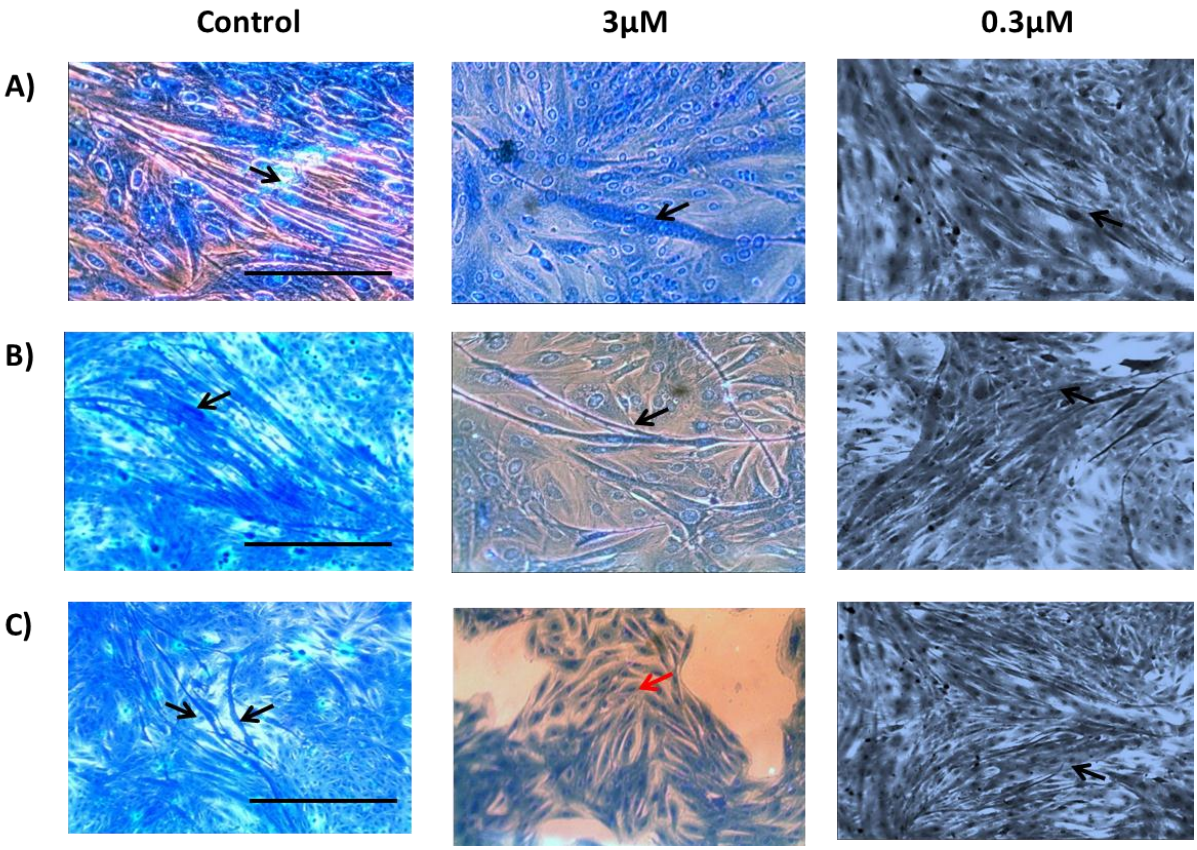

Figure 5.4 Effect of sublethal concentrations of chlorpyrifos oxon on differentiating H9c2 cells.

Mitotic H9c2 cells were induced to differentiate in the presence of 3 µM and 0.3 µM chlorpyrifos oxon for A) 7 days B) 9 days and C) 13 days. Following treatment, cells were fixed with 90 % (v/v) methanol, stained with Coomassie Brilliant Blue and then visualised using light microscopy (20x objective lens). The black arrow indicates typical elongated and multinucleated differentiated cells and red arrows indicate typical rounded and compact cells. Images presented are from one experiment and representative of three independent experiments. Scale bar = 100 µm.

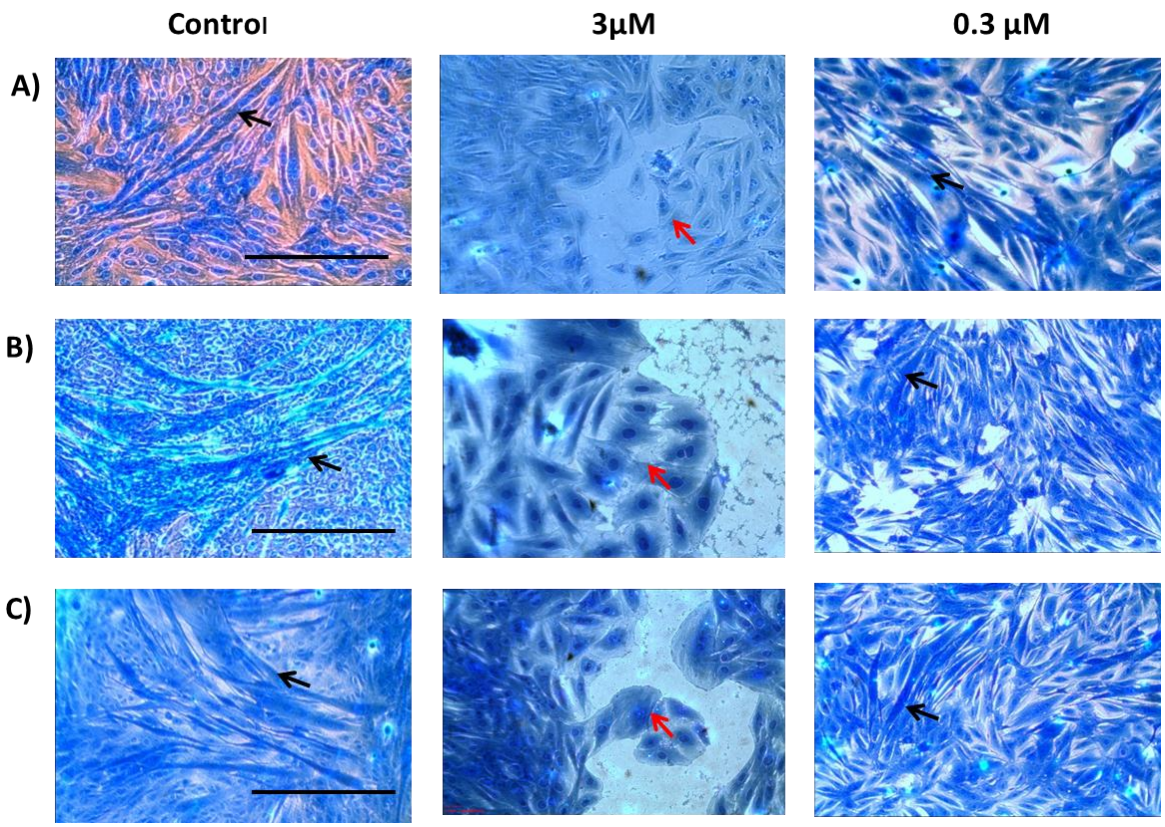

Figure 5.5 Effect of sublethal concentrations of diazinon on differentiating H9c2 cells.

Mitotic H9c2 cells were induced to differentiate in the presence of 3 µM and 0.3 µM diazinon for A) 7 days B) 9 days and C) 13 days. Following treatment cells were fixed with 90 % (v/v) methanol, stained with Coomassie Brilliant Blue and then visualised using light microscopy (20x objective lens). The black arrow indicates typical elongated and multinucleated differentiated cells and red arrows indicate rounded and compact cells. Images presented are from one experiment and representative of three independent experiments. Scale bar = 100 µm.

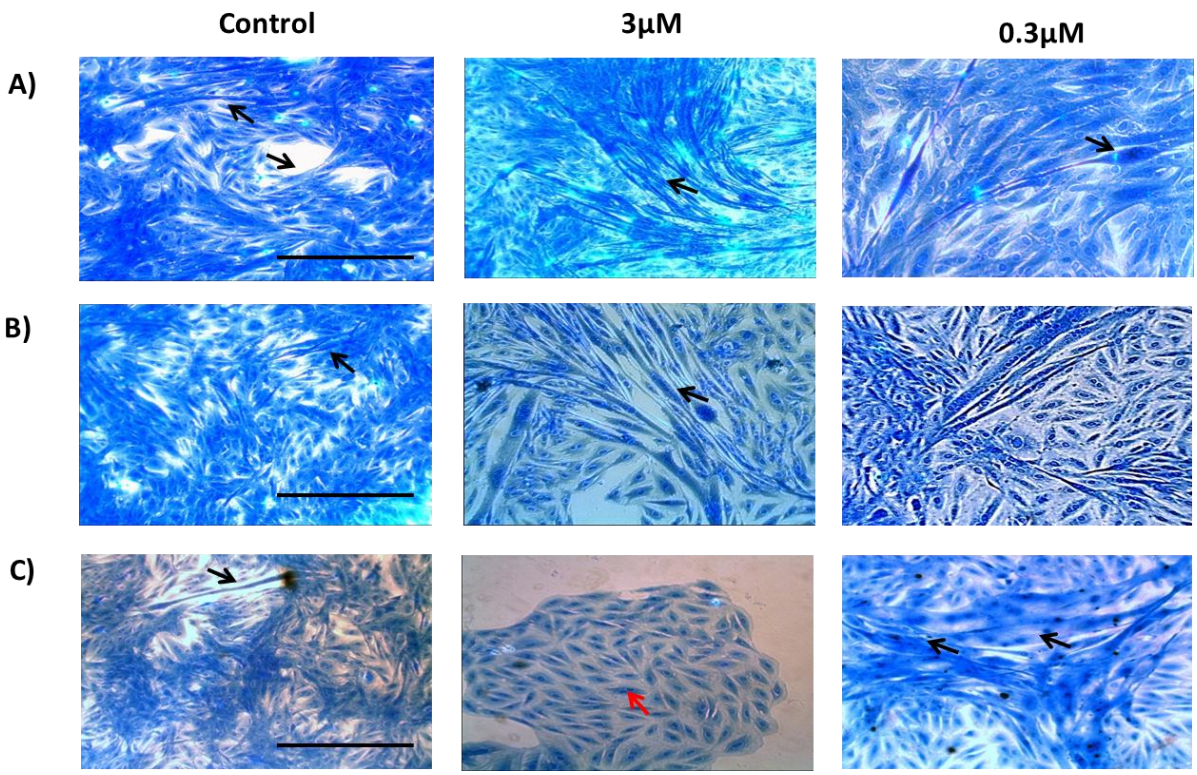

Figure 5.6 Effect of sublethal concentrations of diazoxon on differentiating H9c2 cells.

Mitotic H9c2 cells were induced to differentiate in the presence of 3 µM and 0.3 µM diazoxon for A) 7 days B) 9 days and C) 13 days. Following treatment cells were fixed with 90 % (v/v) methanol, stained with Coomassie Brilliant Blue and then visualised using light microscopy (20x objective lens). The black arrows indicate typical elongated and multinucleated differentiated cells and red arrows indicate typical rounded cells. Images presented are from one experiment and representative of three independent experiments. Scale bar = 100 µm.

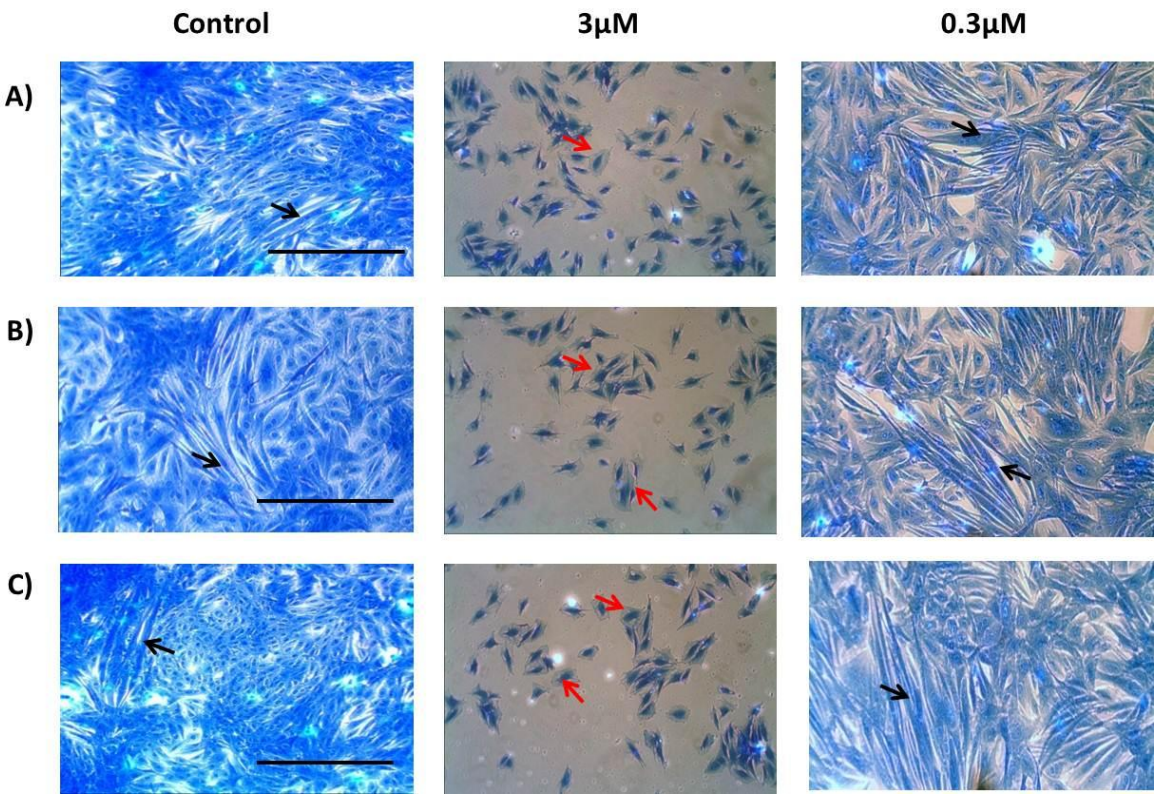

Figure 5.7 Effect of sublethal concentrations of PSP on differentiating H9c2 cells.

Mitotic H9c2 cells were induced to differentiate in the presence of 3 µM and 0.3 µM PSP for A) 7 days B) 9 days and C) 13 days. Following treatment cells were fixed with 90 % (v/v) methanol stained with Coomassie Brilliant Blue and then visualised using light microscopy (20x objective lens). The black arrows indicate typical elongated and multinucleated differentiated cells and red arrows indicate rounded compact cells. Images presented are from one experiment and representative of three independent experiments. Scale bar = 100 µm.

5.4.2 Effect of sublethal concentrations of OPs on cell viability

Under the same experimental conditions as described in section 5.3, the possible long-term effects of sub-lethal concentration of OPs on cell viability of differentiating H9c2 cells was assessed via MTT and LDH assays. Chlorpyrifos at a concentration 3 µM had no significant effect (p>0.05) on MTT reduction or LDH release following 7, 9 and 13-days exposure. Similarly, its acutely toxic metabolite chlorpyrifos oxon at the same concentration had no significant effect (p>0.05) on MTT reduction or LDH release following 7-days, 9-days and 13-days exposure (Figure 5.7). Also, diazinon and its metabolite at a concentration of 3 µM had no significant effect (p>0.05) on MTT reduction and LDH release following 7, 9 and 13-days exposure (Figure 5.8). Finally, 3 µM PSP had no significant effect on MTT reduction at 7-days. However, it had significant effect (p<0.05) on MTT reduction at 9-days and 13-days exposure. PSP had no significant effect (p>0.05) on LDH release following 7-days and 9-days exposure. However, it had significant effect (p<0.05) on LDH release following 13-days exposure. Thus, the MTT reduction assay was shown to be more sensitive than the LDH release assay for the detection of cytotoxic effects of PSP in differentiating H9c2 cells (Figure 5.9).

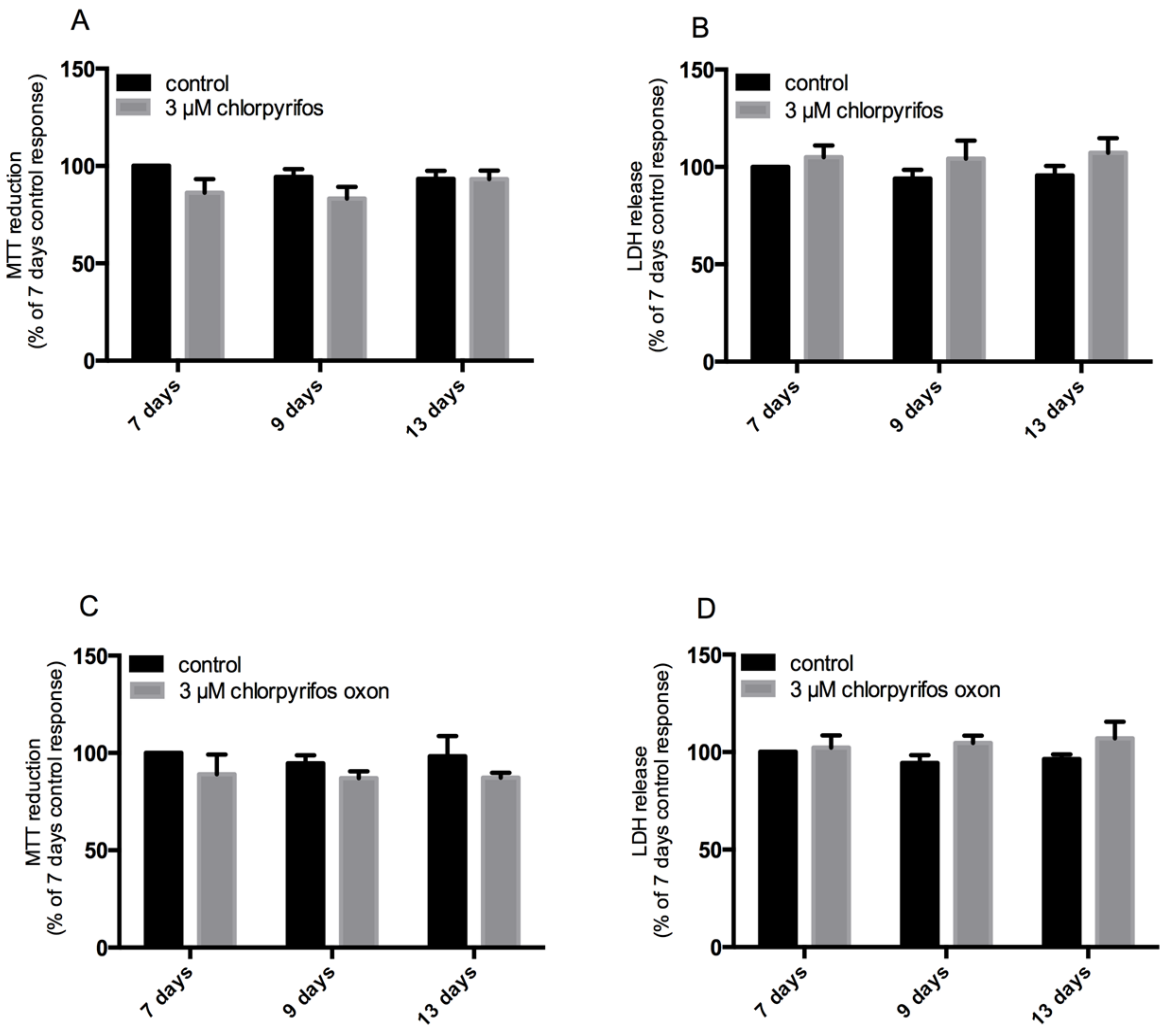

Figure 5.8 Effect of chlorpyrifos and chlorpyrifos oxon on the viability of differentiating H9c2 cells monitored by MTT reduction and LDH release.

H9c2 cells were induced to differentiate for 7 days, 9 days and 13 days in the presence and absence of 3 µM chlorpyrifos (A and B) and 3 µM chlorpyrifos oxon (C and D). Following chlorpyrifos and chlorpyrifos oxon exposure, cell viability was assessed by measuring the metabolic reduction of MTT by cellular dehydrogenases (A and C) and release of LDH (B and D). Data are expressed as a percentage of control cell values (= 100%) and represent the mean ± SEM of three independent experiments each performed in quadruplicate (MTT) or sextuplicate (LDH).

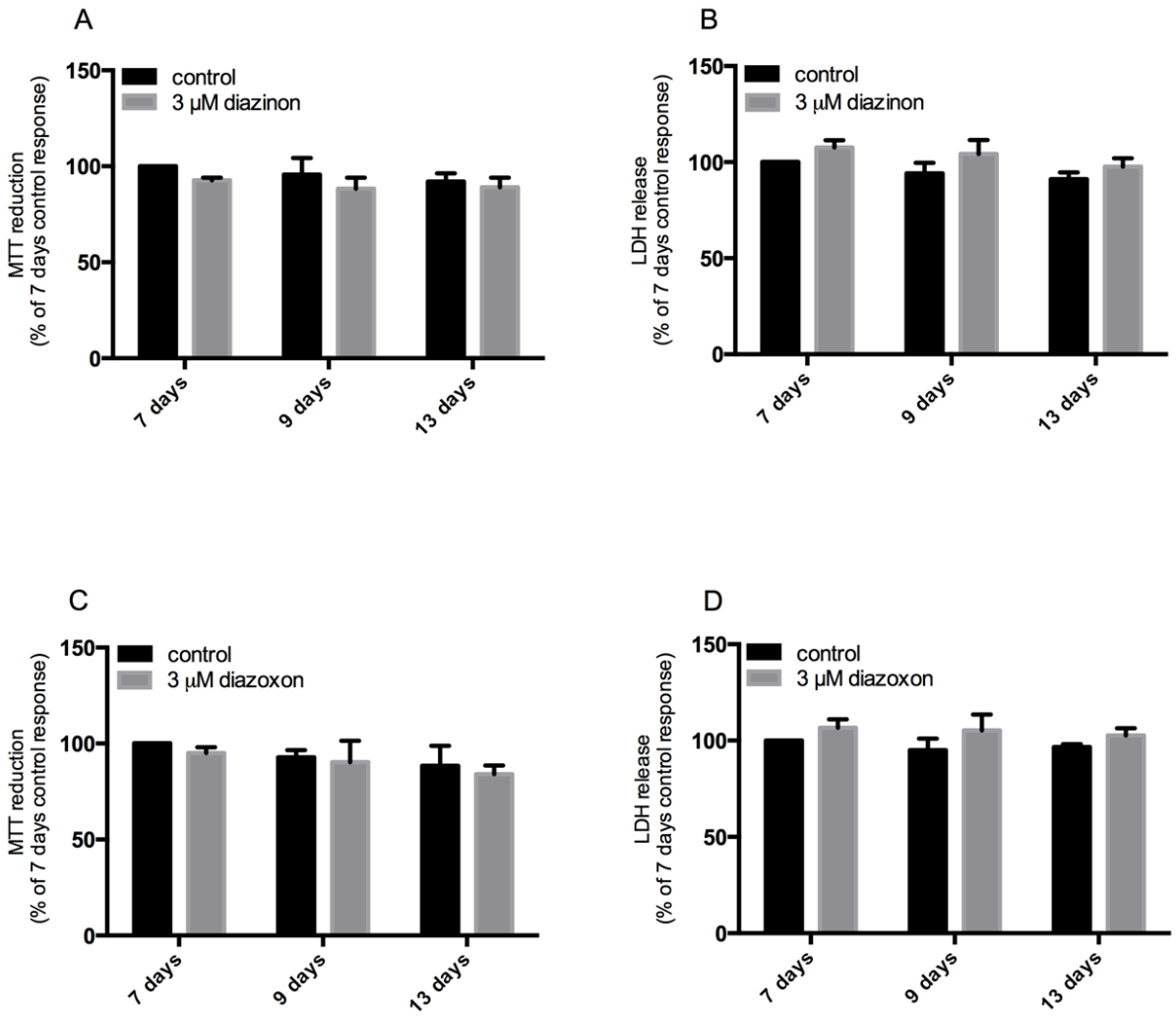

Figure 5.9 Effect of diazinon and diazoxon on the viability of differentiating H9c2 cells monitored by MTT reduction and LDH release.

H9c2 cells were induced to differentiate for 7 days, 9 days and 13 days in the presence and absence of 3 µM diazinon (A and B) or 3 µM diazoxon (C and D). Following diazinon and diazoxon exposure, cell viability was assessed by measuring the metabolic reduction of MTT by cellular dehydrogenases (A and C) and release of LDH (B and D). Data are expressed as a percentage of control cell values (= 100%) and represent the mean ± SEM of three independent experiments each performed in quadruplicate (MTT) or sextuplicate (LDH).

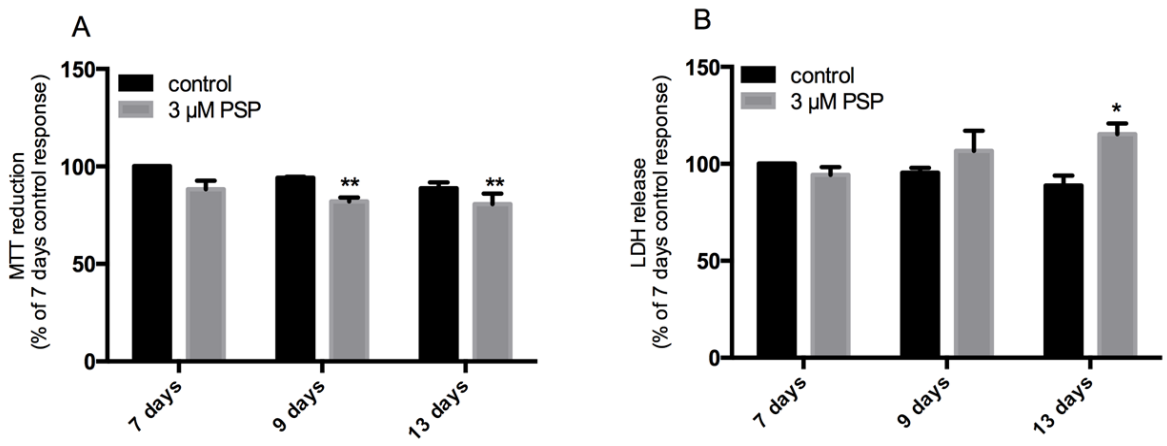

Figure 5.10 Effect of PSP on the viability of differentiating H9c2 cells monitored by MTT reduction and LDH release.

H9c2 cells were induced to differentiate for 7 days, 9 days and 13 days in the presence and absence of 3 µM PSP. Following PSP exposure, cell viability was assessed by measuring the A) metabolic reduction of MTT by cellular dehydrogenases and B) release of LDH. Data are expressed as a percentage of control cell values (= 100%) and represent the mean ± SEM of three independent experiments each performed in quadruplicate (MTT) or sextuplicate (LDH). *$p < 0.05$ and **$p < 0.01$ versus the control response.

5.4.3 Effect of sublethal concentrations of OPs on cellular AChE activity

Under the same experimental conditions as described in section 5.3, cellular AChE activity was measured to determine whether this enzyme was a molecular target of OPs (chlorpyrifos, diazinon chlorpyrifos oxon, diazoxon and PSP) at the sublethal concentration of 3 µM in differentiating H9c2 cells. Data from these experiments revealed that chlorpyrifos and diazinon and their metabolites chlorpyrifos oxon and diazoxon significantly inhibited (p<0.05) AChE activity; this inhibitory effect was observed at days 7, 9 and 13 (Figures 5.10 and 5.11). In contrast, PSP did not show significant inhibition of AChE activity at days 7, 9 or 13 (Figure 5.12).

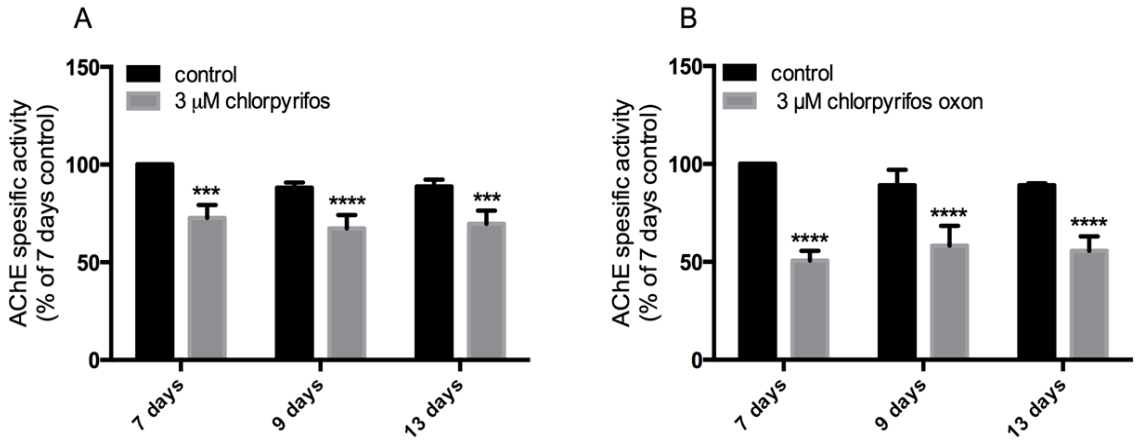

Figure 5.11 Effects of chlorpyrifos and chlorpyrifos oxon on AChE activity in differentiating H9c2 cells.

H9c2 cells were induced to differentiate in the presence of 3 µM A) chlorpyrifos and B) chlorpyrifos oxon for 7 days, 9 days and 13 days. AChE specific activities are expressed as a percentage of control cell values (=100%) and represent the mean ± SEM of three independent experiments. ***p < 0.001, and ****p < 0.0001 versus the control response.

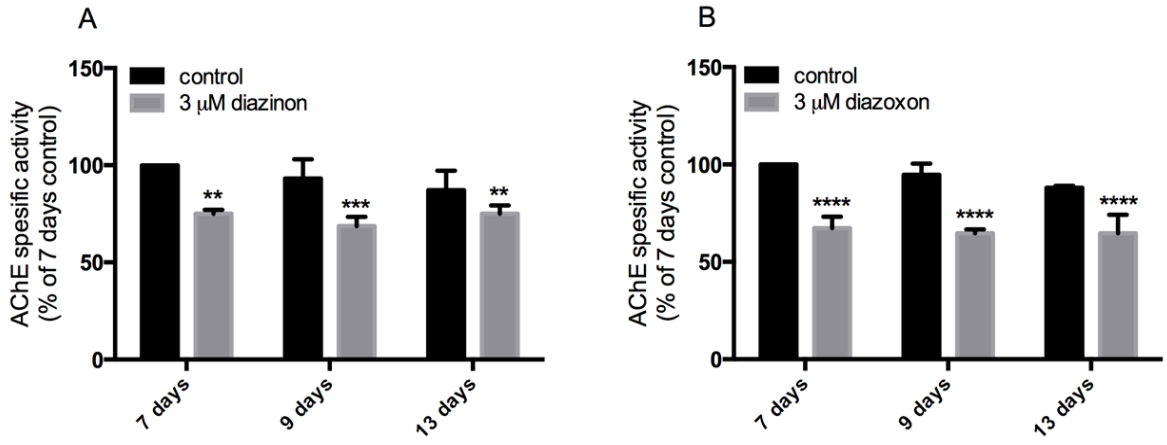

Figure 5.12 Effects of diazinon and diazoxon on AChE activity in differentiating H9c2 cells.

H9c2 cells were induced to differentiate in the presence of 3 μM A) diazoxon and B) diazoxon for 7 days, 9 days and 13 days. AChE specific activities are expressed as a percentage of control cell values (=100%) and represent the mean ± SEM of three independent experiments. $^{**}p < 0.01$, $^{***}p < 0.001$, and $^{****}p < 0.0001$ versus the control.

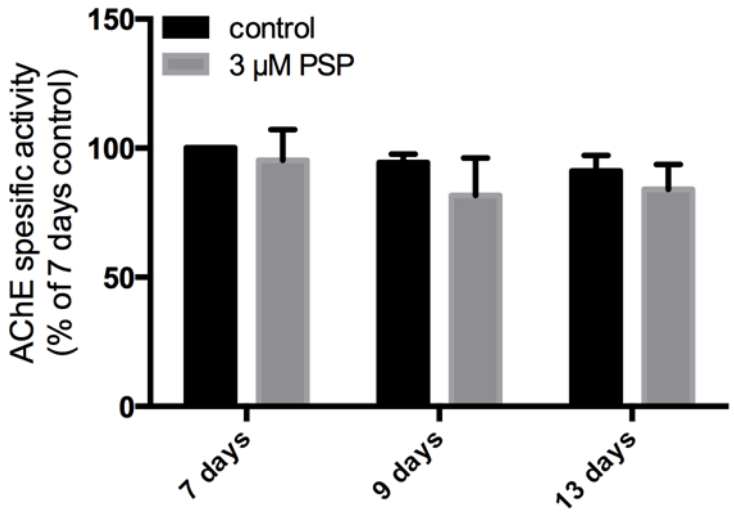

Figure 5.13 Effects of PSP on AChE activity in differentiating H9c2 cells.

H9c2 cells were induced to differentiate in the presence of 3 µM PSP for 7 days, 9 days and 13 days. AChE activities are expressed as a percentage of control cell values (=100%) and represent the mean ± SEM of three independent experiments.

5.4.4 Effect of sublethal concentrations of OPs on cardiac cytoskeleton proteins

In this section the effects of chlorpyrifos, diazinon chlorpyrifos oxon, diazoxon and PSP on cytoskeletal protein expression were investigated. Cells were induced to differentiate as detailed previously in section 5.3. Cells were exposed to a 3 µM OPs for 7, 9 and 13 days. The protein expression levels of cardiac cytoskeleton proteins (troponin 1, tropomyosin and α-actin) associated with H9c2 differentiation were measured via Western blot analysis. The parent compounds chlorpyrifos and diazinon had a significant effect (p<0.05) on cardiac cytoskeletal protein expression, whereas their oxon metabolites did not demonstrate such an effect. For example, treatment with chlorpyrifos resulted in a significant decrease (p<0.05) in troponin 1 levels in differentiating H9c2 cells at 13-days exposure, whereas other proteins such as tropomyosin and α-actin were not shown to be affected at 7, 9 or 13-days exposure (Figure 5.13). Chlorpyrifos oxon had no significant effect (p>0.05) on the levels any of the cytoskeleton proteins examined (Figure 5.14). In contrast, diazinon exposure resulted in a significant decrease in the levels of troponin 1 but had no significant effect (p>0.05) on tropomyosin or α-actin levels at 7, 9 and 13-days exposure (Figure 5.15). In contrast, its acutely toxic metabolite diazoxon had no significant effect (p>0.05) on any of the cytoskeleton proteins examined at any exposure time point (Figure 5.16). Finally, exposure to 3 µM PSP resulted in a significant decrease (p<0.05) in the levels of troponin 1, tropomyosin and α-actin at 7-days, 9-days or 13-days exposure (Figure 5.17). Table 5.1 summarizes the effects of OPs used in the present study on cytoskeletal protein expression in differentiating H9c2 cells.

Table 5.1 Summary of the effects of OPs (chlorpyrifos, diazinon, chlorpyrifos oxon, diazoxon and PSP) on cardiac protiens in differentiating H9c2 cells.

Organophospate	Cardiac sytoskelton protien								
	Troponin			Tropomyosin			α-Actin		
	Exposure time (days)								
	7 d	9 d	13 d	7 d	9 d	13 d	7 d	9 d	13 d
Chlorpyrifos	–	–	+	–	–	–	–	–	–
Chlorpyrifos oxon	–	–	–	–	–	–	–	–	–
Diazinon	+	+	+	–	–	–	–	–	–
Diazoxon	–	–	–	–	–	–	–	–	–
PSP	+	+	+	+	+	+	+	+	+

Effects of OPs on cardiac cytoskeleton protein (troponin 1, tropomyosin and α-actin) expression in differentiating H9c2 cells. H9c2 cells were induced to differentiate for 7 days, 9 days and 13 days in the presence of 3 µM OPs. (+) represent a significant (p<0.05)down regulating effect of OPs on cardiac cytoskeleton protiens and (-) represent no significant effect (p>0.05)of OPs on cardiac cytoskeleton protiens expression in differentiating H9c2 cells. These are total data of at least three independent experiments.

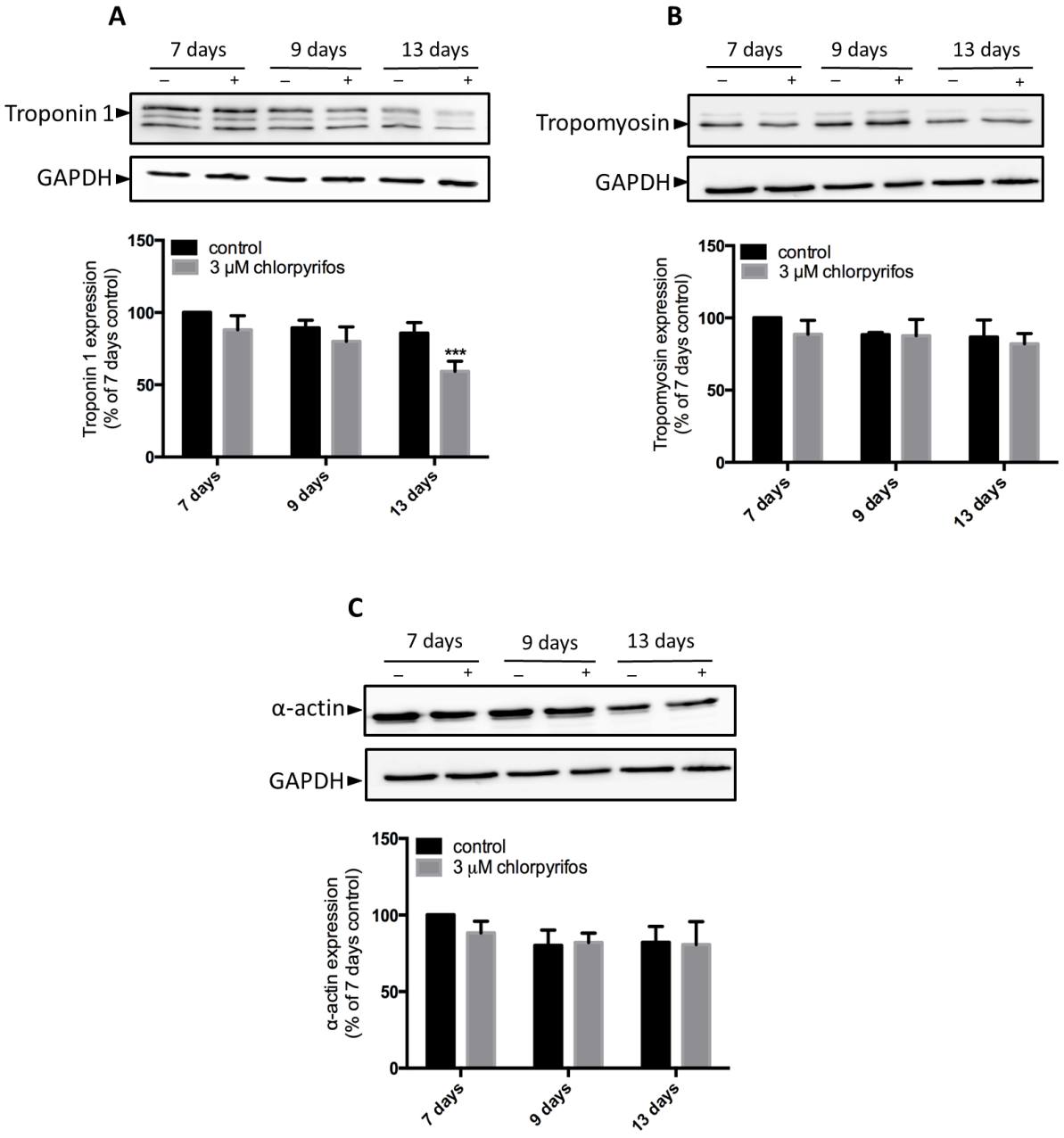

Figure 5.14 Effects of chlorpyrifos on cardiac cytoskeleton protein expression in differentiating H9c2 cells.

H9c2 cells were induced to differentiate for 7, 9 and 13 days in the presence (+) and absence (-) of 3 µM chlorpyrifos. Cell lysates (15 µg) were analysed via western blot and probed with antibodies that recognise A) cardiac troponin 1, B) tropomyosin and C) α-actin. All values were normalised to GAPDH levels and are expressed as mean % control values ± SEM of three independent experiments. ***p < 0.001 versus the control.

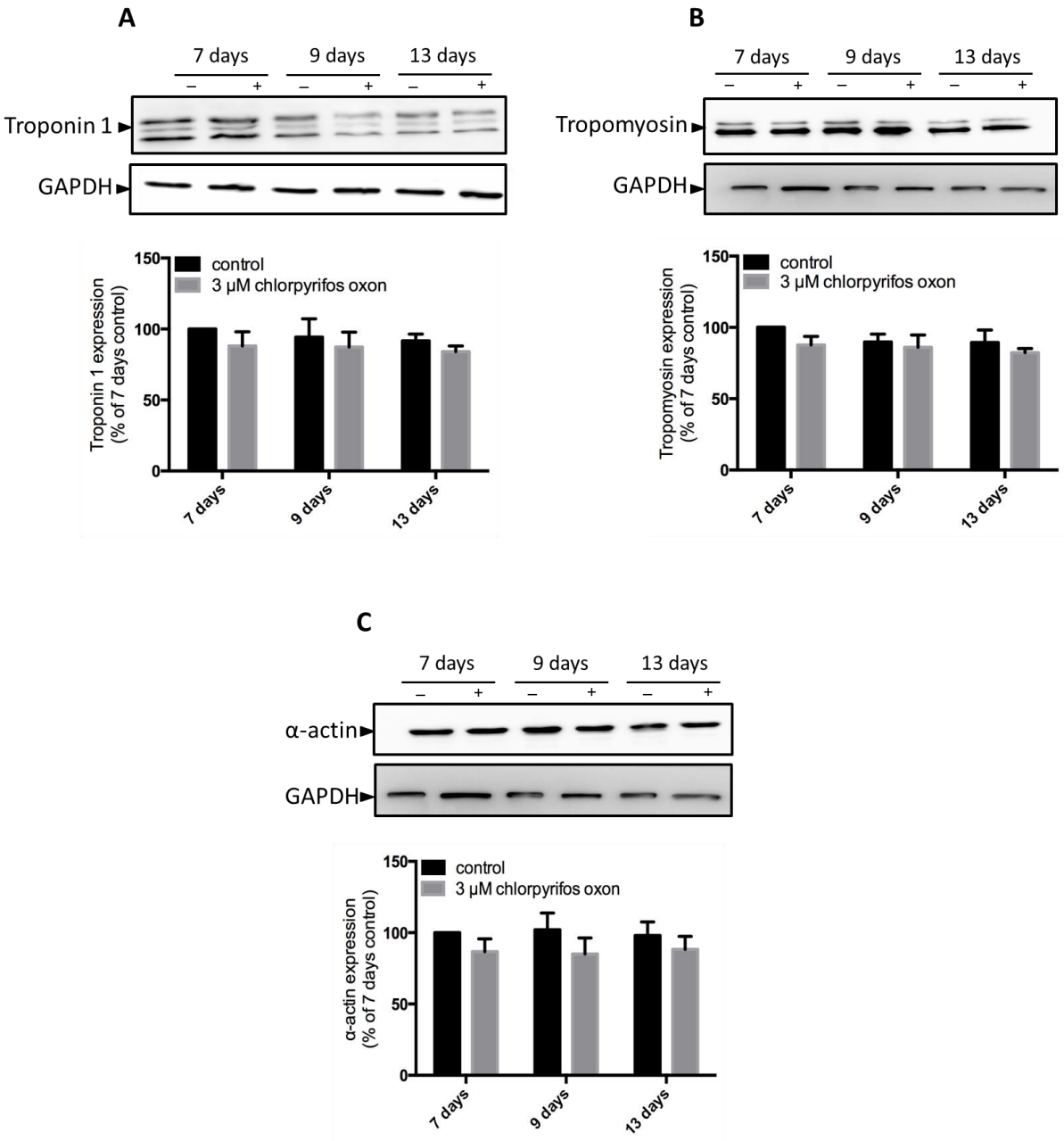

Figure 5.15 Effects of chlorpyrifos oxon on cardiac cytoskeleton proteins in differentiating H9c2 cells.

H9c2 cells were induced to differentiate for 7 days, 9 days and 13 days in the presence (+) and absence (-) of 3 μM chlorpyrifos oxon. Cell lysates (15 μg) were analysed via western blot and probed with antibodies that recognise A) cardiac troponin 1 B) tropomyosin C) α-actin. All values were normalised to GAPDH level and are expressed as mean % control values ± SEM of three independent experiments.

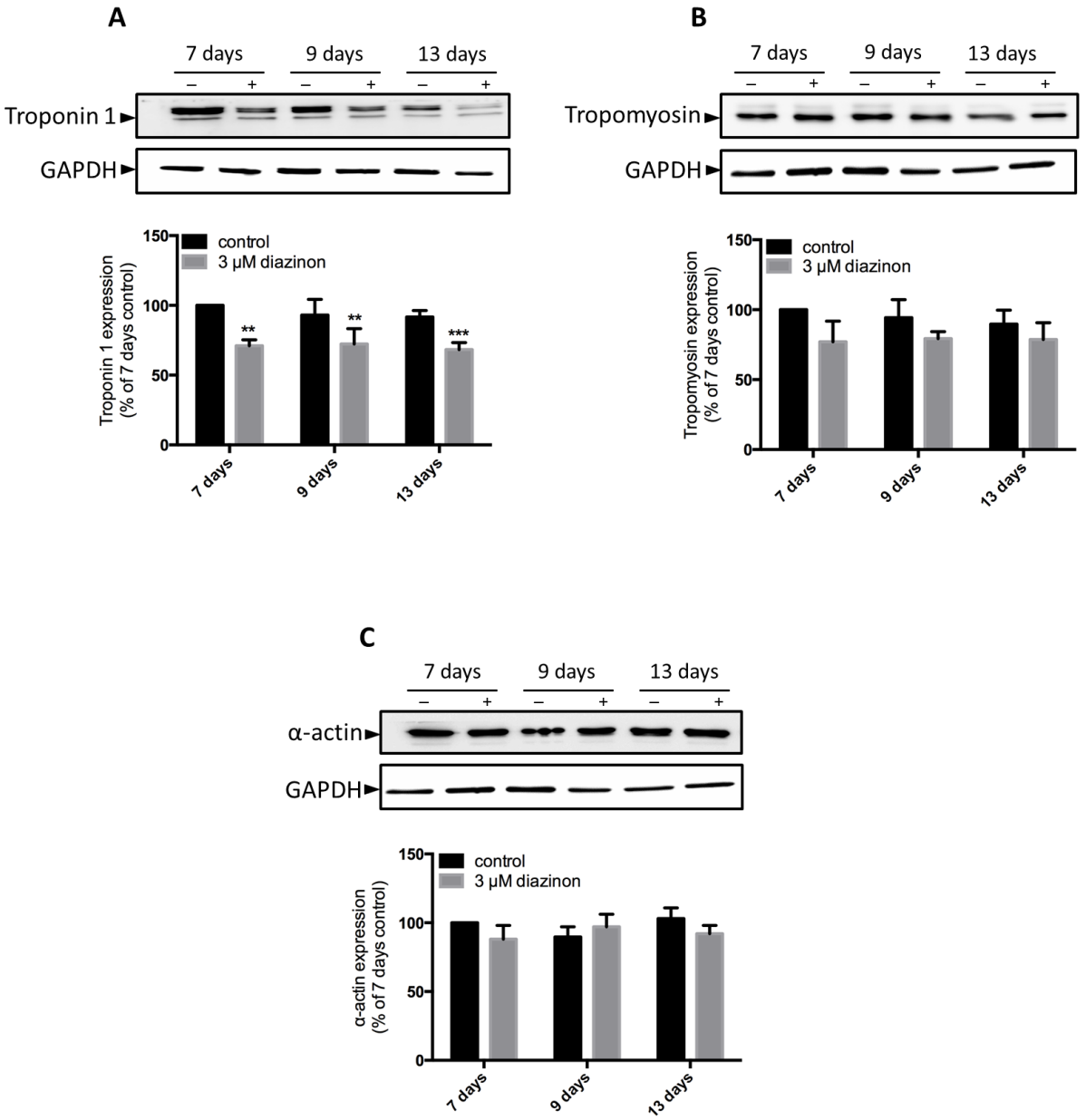

Figure 5.16 Effects of diazinon on cardiac cytoskeleton proteins in differentiating H9c2 cells.

H9c2 cells were induced to differentiate for 7 days, 9 days and 13 days in the presence (+) and absence (-) of 3 μM diazinon. Cell lysates (15 μg) were analysed via western blot and probed with antibodies that recognise A) cardiac troponin 1 B) tropomyosin C) α-actin. All values were normalised to GAPDH level and are expressed as mean % control values ± SEM of three independent experiments. $^{**}p < 0.01$, and $^{***}p < 0.001$ versus the control.

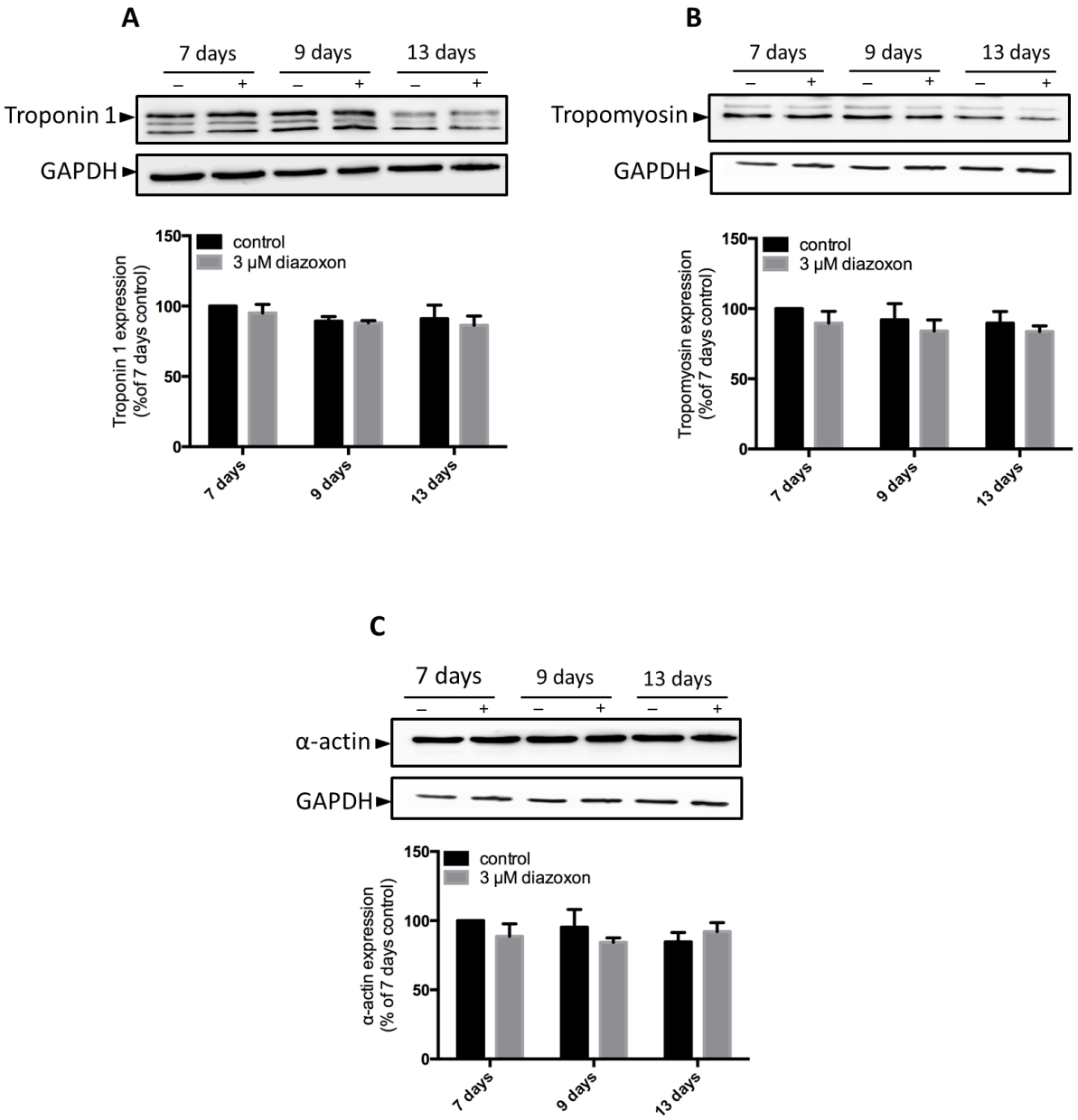

Figure 5.17 Effects of diazoxon on cardiac cytoskeleton proteins in differentiating H9c2 cells.

H9c2 cells were induced to differentiate for 7 days, 9 days and 13 days in the presence (+) and absence (-) of 3 μM diazoxon. Cell lysates (15 μg) were analysed via western blot and probed with antibodies that recognise A) cardiac troponin 1 B) tropomyosin C) α-actin. All values were normalised to GAPDH level and are expressed as mean % control values ± SEM of three independent experiments.

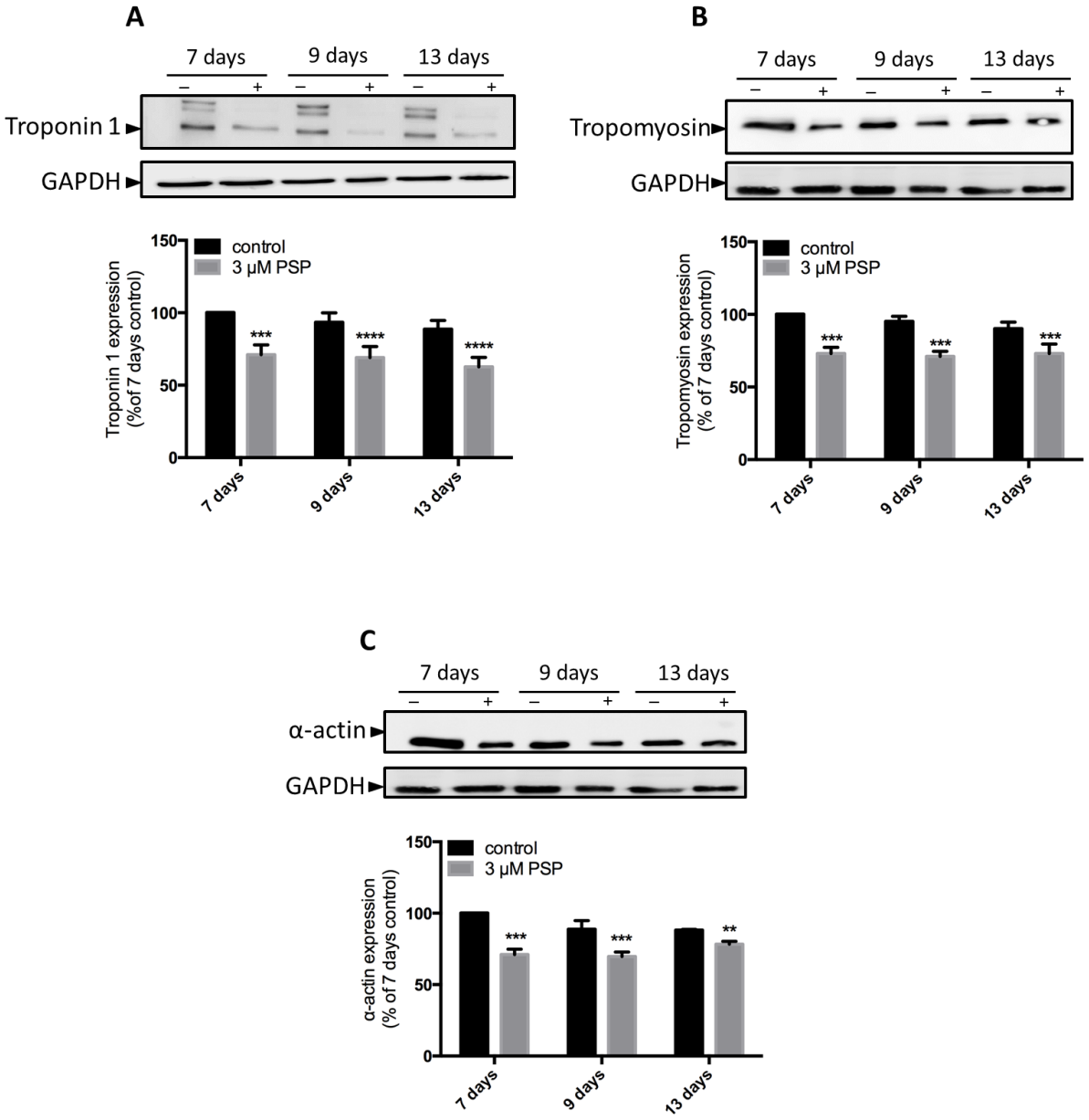

Figure 5.18 Effects of PSP on cardiac cytoskeleton proteins in differentiating H9c2 cells.

H9c2 cells were induced to differentiate for 7 day, 9 day and 13 day in the presence (+) and absence (-) of 3 μM PSP. Cell lysates (15 μg) were analysed via western blot and probed with antibodies that recognise A) cardiac troponin 1 B) tropomyosin C) α-actin. All values were normalised to GAPDH level and are expressed as mean % control values ± SEM of three independent experiments. $^{**}p < 0.01$, $^{***}p < 0.001$, and $^{****}p < 0.0001$ versus the control

5.4.5 Effect of sublethal concentrations of PSP on the proteome profile of H9c2 cells

The results presented thus far have shown that exposure to 3 µM PSP resulted in a more significant effect on cardiac cytoskeleton proteins: troponin1, tropomyosin and α-actin of differentiating H9c2 cells when compared to other OPs compound. Therefore, would be of interest to identify changes in the levels of other cardiac proteins that may be implicated in the toxic effect of PSP on differentiating H9c2 cells. These proteins can be considered as novel biochemical changes in H9c2 cells that were induced to differentiate for 7 days in the presence of 3 µM PSP. In the present study, 7 days was selected as a preliminary exposure period since H9c2 cardiomyoblasts were confirmed to be differentiated at 7-days in to a more cardiomyocyte-like phenotype and displayed cardiac-specific characteristics, as shown in chapter 3. Thus, long-term incubation such as 9-days and 13- days can be assessed for future adverse effect of PSP. 2D gel electrophoresis was performed as described in Chapter 2. Several protein spots showed a significant reduction in PSP-treated differentiating H9c2 cells when compared to untreated cells and the significant (p<0.05) in down regulating protein expression was determined by using Progenesis SameSpots software. Five protein spots (Spots ID 12, 16 , 14, 27 and 23) were identified as significantly decreased as shown in Table 5.2 and were visually distinct for spot picking (Figure 5.18). Protein pots were picked from the stained gel and digested with trypsin followed by MALDI-TOF mass spectrometry analysis of the peptides produced. Mass spectrometry analysis identified tropomyosin α-4 and α-actin, which is in agreement with previous findings in described in section 5.3.4. In addition, coiled-coil domain containing protein 61 (Ccdc61), calumenin and PDZ-LIM domain protein 1 were also identified as novel proteins that showed a significant decrease in density in treated differentiating H9c2 cells when compared to untreated H9c2 cells. The identified proteins are listed in Table 5.3. The identity of these proteins were also confirmed by comparison of their in gel position with their theoretical molecular weights and isoelectric point (p*I*).

Table 5. 2 Progenesis SameSpot analysis represent decrease in density of protein spot in 3 µM PSP treated cells.

Spot number	ANOVA (p value)
12	6.26E-09
14	2.85E-09
16	3.7E-09
23	2.55E-05
27	0.000132

Data table represent a significant decrease in protein spots densities using ANOVA analysis of protein spot densities. Data values of 3 accumulated 2D gel electrophoresis, $*p < 0.05$ was viewed as significant.

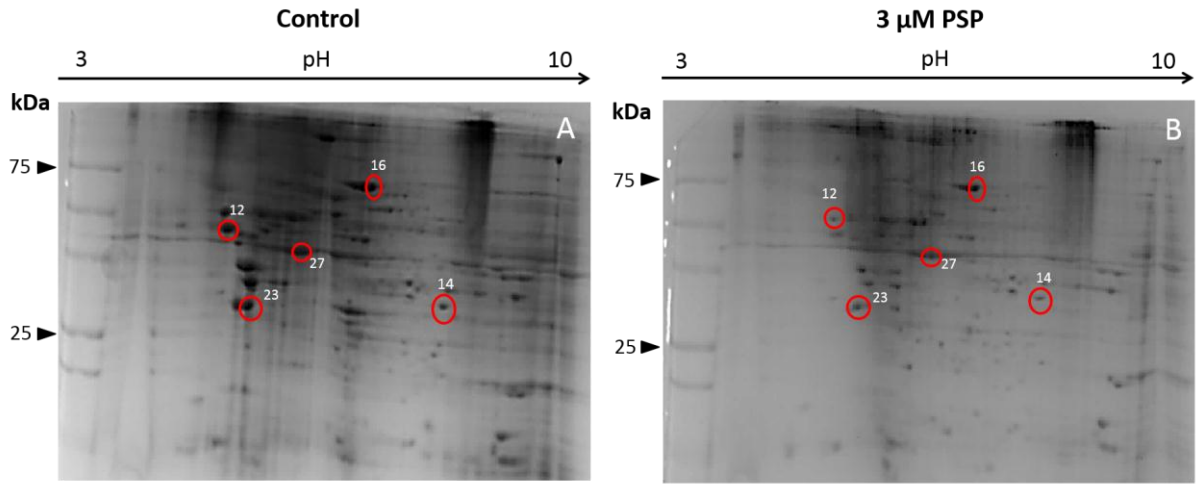

Figure 5. 19 Representative 2D gel images of PSP effects on cardiac protein expression in differentiating H9c2 cells.

H9c2 cells were induced to differentiate for 7 days in the A) absence and B) presence of 3 µM PSP: Cell lysates (300 µg) were analysed by 2D gel electrophoresis using pH 3–10 gradient strips. Gels were stained with Proto Blue Safe colloidal Coomassie G-250 stain and gel images analysed using Progenesis SameSpots software. Circled spots represent proteins that were significantly down regulated when compared to untreated cells. Spot 12, calumenin; spot 14, PDZ-LIM domain protein 1; Spot 16, coiled-coil domain containing protein 61; spot 23; tropomyosin α-4; spot 27, α- actin.

Table 5.3 Identification of proteins affected by sublethal concentrations of PSP in differentiating H9c2 Cells

Spot number	protein	accession no.	PMF sequence coverage (%)	Mascot score	kDa	p*I*	Fold change
16	Coiled-coil domain containing protein 61	A0JPP8	47%	54	57	5.52	11
12	Calumenin	O35783	37%	65	40	4.40	5
27	α-actin	P68035	55%	53	41	4.72	6
23	Tropomyosin α-4	P09495	45%	68	28.5	4.4	5
14	PDZ-LIM domain protein 1	P52944	47%	67	35	6.79	2

Mitotic H9c2 cells were induced to differentiate in the presence of 3 μM PSP for 7 days. Cells were analyzed by 2D gel electrophoresis. Proteins were identified using MALDI-TOF MS (PMF) as described in Materials and Methods. Sequence data were analyzed using Mascot software and reported according to percentage sequence coverage (SC%) or Mascot score (ion scores for PMF > 51 indicate extensive homology). All identified proteins exhibited Mascot scores that were considered statistically significant (*$p < 0.05$).

5.5 *Discussion*

The present study examined the morphological, enzymatic and molecular changes induced by chlorpyrifos and diazinon, their corresponding metabolites (chlorpyrifos oxon and diazoxon), and PSP in differentiating H9c2 cells. Numerous *in vivo* studies have examined the mechanism underlying the toxicity of low doses of OP compounds in the brain; these studies have shown that these compounds target neuronal cytoskeleton proteins and cause inhibition of neurite outgrowth (Gearhart *et al*., 2007; Prendergast *et al.,* 2007; Terry *et al.,* 2007). However, the molecular mechanism underlying the effects of sublethal concentrations of OPs on differentiating H9c2 cells were still unknown at the start of the current work. This is the first study to demonstrate the effect of OPs on cardiac cytoskeleton proteins in differentiating H9c2 cells. Figure 5.19 summarizes the major findings illustrated in the present study. Figure 5.20 represents a simple diagram outlining the possible sublethal effects of OPs in differentiating H9c2 cells.

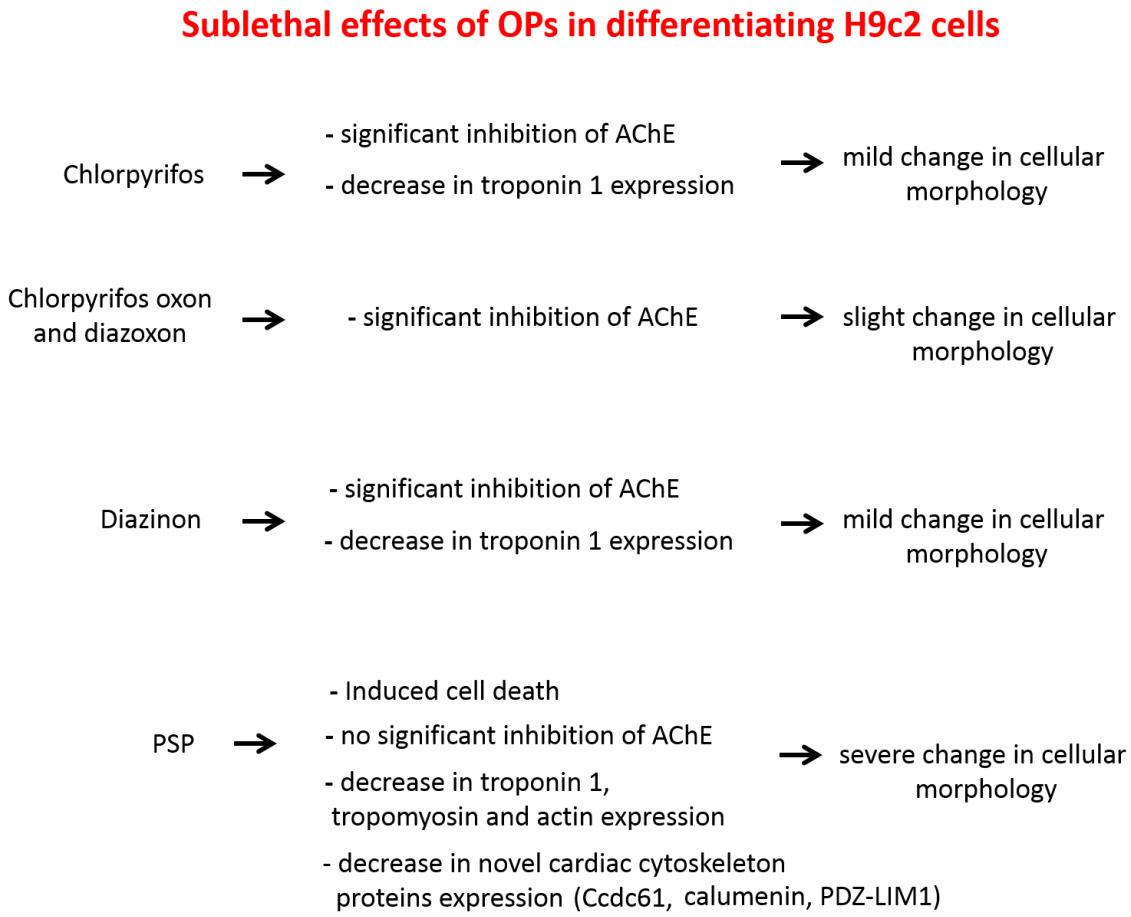

Figure 5.20 Summary of major finding of sublethal effects of OPs in differentiating H9c2 cells illustrated in the present study.

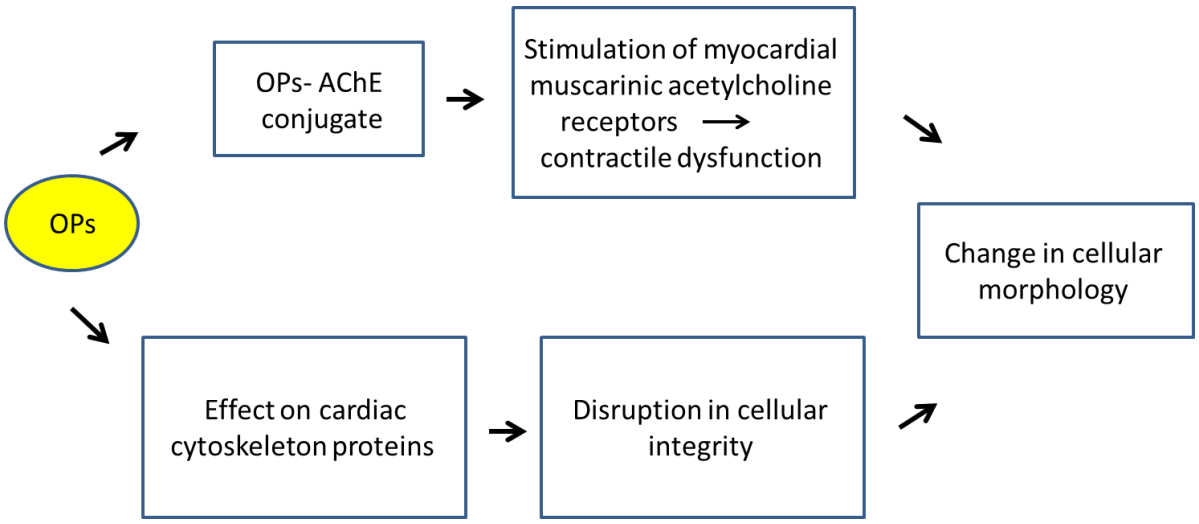

Figure 5.21 Simple diagrammatic representation of the sublethal effects of OPs (chlorpyrifos, diazinon, chlorpyrifos oxon, diazoxon and PSP) in differentiating H9c2 cells.

OPs may target AChE leading to enzyme activity inhibition and stimulation of myocardial muscarinic acetylcholine receptors and contractile dysfunction, resulting in changes in cellular morphology. OP exposure may also decrease cardiac cytoskeleton protein expression leading to disruption in cellular integrity and cellular morphology.

5.5.1 Effect of OPs on the morphological features of differentiating H9c2 cells

Two major OP concentrations (3 and 0.3 µM) were investigated for toxicity tests in differentiating H9c2 cells to determine which concentrations of OPs were harmful and which had no apparent effect after long- term exposure. Organophosphates at a concentration of 3 µM were shown to induce morphological changes in differentiating H9c2 cells, with the degree of deterioration ranging from mild to severe, whereas 0.3 µM of all OPs had no significant effect on differentiating H9c2 cells. Chlorpyrifos at a concentration of 3 µM had a moderate effect on differentiating H9c2 cells such as cell rounding or irregular cell shape at 7-days, 9-days and 13-days exposure as shown in Figure 5.2, These data are in agreement with previous studies that have reported the morphological change by sublethal concentrations of chlorpyrifos. For example, 3 µM chlorpyrifos was able to inhibit the outgrowth of axon-like processes in differentiating mouse N2a neuroblastoma (Sachana *et al.,* 2001). However, exposure to 3 µM chlorpyrifos oxon did not show major effect on H9c2 cell viability, and its effect on differentiating cells may be considered as non-cytotoxic (Figure 5.3).

Diazinon at a concentration of 3 µM was shown to have a moderate effect on differentiating H9c2 cells at 7-days, 9-days and 13-days exposure (Figure 5. 4). This is in agreement with a previous study in neuronal cells that showed that exposure to 1-10 µM diazinon induced selective inhibition of the outgrowth of neurites in differentiating mouse N2a neuroblastoma cells (Flaskos *et al.,* 2007). On the other hand, exposure to 3 µM diazoxon did not show any major effect on differentiating H9c2 cells and may be considered as the least toxic (Figure 5.5). In contrast, 5 µM diazoxon caused significant reductions in the number of axon-like processes produced by N2a neuroblastoma cells. This was associated with increased the expression of phosphorylated neurofilament heavy chain (NFH) when compared to controls (Sidiropoulou *et al.,* 2009).

The parents compounds chlorpyrifos and diazinon showed an observable effect on cellular morphology more than their oxon metabolites, this may be due to their low water solubility (lipophilic) and can be readily absorbed by cells (Bowman and Sans, 1983).On the other hand, the oxons are often more hydrophilic compounds (Gupta, 2006). Thus, Bioaccumulation chlorpyrifos and diazinon in cells of may be considered as an early exposure biomarker for adverse effect to toxic substances (Franke et al., 1994).

As indicated in Figure 5.6, exposure to PSP induced apparent deterioration in cell shape and size. Thus, 3 µM PSP inhibited the differentiation of these cells into a more cardiomyocyte-like phenotype characterised by an elongated spindle shape and multiple nuclei at days 7, 9 and 13. These effects are consistent with a previous study showing that 2.5 µM PSP for 24 h exposure decreased neurite outgrowth in differentiating N2a cells (Hargreaves *et al.*, 2006). Moreover, it is important to note that morphological change may be due to the alteration in the basic cell membrane mechanisms by OPs. For example, the OP parathion was found to stimulate Ca^{2+} uptake and ATP hydrolysis via Ca^{++} pump system in the sarcoplasmic reticulum, leading to alterations in cellular ionic balance and affecting myocardial conductivity and cellular structure (Ballantyne & Marrs, 1992). Overall, the data presented suggest that 3 µM levels of the OPs tested can be considered as sub-toxic toward differentiating H9c2 cells. Morphological analysis of the effect of OPs on differentiating H9c2 cells can be arranged from the most effective to the less effective, as shown PSP > diazinon > chlorpyrifos > chlorpyrifos oxon and diazoxon.

5.5.2 Effect of OPs on cell viability of differentiating H9c2 cells

Morphological changes are an indicator of OP-induced stress (Atale *et al*., 2014). The results indicated that cell morphology seemed to be affected by sublethal concentrations (i.e. 3 µM) of OP. Therefore, it would be of interest to investigate whether longer term exposure to OPs are associated with cell death. To the author's knowledge, no study has been conducted on the long- term toxicity of OPs in differentiating H9c2 cells. From the findings in this chapter, it is quite clear that chlorpyrifos and its toxic metabolite chlorpyrifos oxon at a sublethal concentration 3 µM had no significant effect on MTT reduction or LDH release following 7-day, 9-day and 13 day exposure (Figure 5.7). This is in agreement with previous study showed that sub-lethal concentrations 1–10 µM of chlorpyrifos and chlorpyrifos oxon had no effect on the level of MTT reduction in differentiating mouse N2a neuroblastoma concomitant with inhibition of the axon-like neurites outgrowth (Sachana *et al*., 2001; Flaskos *et al.*, 2011). Similarly, in the present study, chlorpyrifos treated cells exhibited rounded and irregular cell shape.

Diazinon and its toxic metabolite diazoxon at sublethal concentration 3 µM had no significant effect on MTT reduction or LDH release following 7-day, 9-day and 13-day exposure (Figure 5.8). In this study this may indicate that diazinon and diazoxon are not

cytotoxic under the conditions used. This is consistent with previous findings with differentiating mouse N2a neuroblastoma cells and sublethal concentration 1–10 µM diazinon and its oxon metabolite diazoxon, no significant MTT reduction. However, they inhibited the outgrowth of axon-like neurites (Flaskos *et al*., 2007; Sidiropoulou *et al.,* 2009).

PSP exposure showed significant effects on MTT reduction following 9-days and 13 days, whereas it showed significant effect on LDH release following 13-days exposure of differentiating H9c2 cells. Both exposure periods (9 and 13 days) can be considered as long-term. However, MTT reduction was shown to be more sensitive than LDH. This may be explained by the cytotoxicity mechanism of each assay. For example, the MTT reduction assay assesses cellular mitochondrial function whereas the LDH release assay measures loss of cell membrane integrity (Haider & Rauf, 2014). Therefore, the present results may possibly suggest that exposure to PSP may lead to impaired mitochondrial function (MTT reduction) in differentiating H9c2 cells prior to disturbance of cell membrane and loss of cell membrane integrity (LDH release). In a previous study, it has been reported that OPs were able to cause disturbance of mitochondrial integrity and permeability and led to the release of cytochrome c to the cytosol and ultimately activated caspase-3 and induced apoptosis through intrinsic pathway (Razavi *et al.,* 2013). In contrast in a previous study in neuronal cells, no cytotoxicity was observed when N2a neuroblastoma cells were exposed to PSP at concentrations 3 µM or lower (Harris *et al.*, 2009). The present findings clearly indicate that sub-lethal exposure to PSP for 13 days could cause deleterious effects in differentiating H9c2 cells and may disturb cell survivability and can considered cytotoxic.

5.5.3 Effect of OPs on AChE activity in differentiating H9c2 cells

AChE is a key enzyme biomarker of neurotoxicity and is known to be a primary target of OPs. Its inhibition can lead to accumulation of ACh and results in hyperstimulation of the sympathetic and parasympathetic pathways (Mileson *et al*., 1998). Therefore, it is important to investigate the effects of sublethal concentrations of OPs on AChE activity, as this is essential in understanding their cytotoxic effect more fully in differentiating H9c2 cells.

Chlorpyrifos and its metabolite chlorpyrifos oxon showed significant inhibition of AChE activity in differentiating H9c2 cells following 7, 9 and 13 days exposure (Figure 5.10). This is in agreement with a previous study showed that 10 µg/ml chlorpyrifos and 10 ng/ml

chlorpyrifos oxon caused a significant inhibition in the AChE activity in neuronal cells, resulting in significant inhibition of neurite outgrowth in the early differentiation process; suggesting that AChE activity is strongly associated with neurite outgrowth (Das & Barone, 1999).

In a previous study, chlorpyrifos oxon decreased the activity of AChE with a potency which was at least 100-fold higher than that of chlorpyrifos in brain cell cultures (Monnet-Tschudi *et al.,* 2000). However such a difference in potency was not observed in the current study. One possible explanation is that the surface of the peripheral anionic site of AChE varies between different species and cell types, although the esteratic site is similar. This may result in variation of the steric attraction of the oxon to the active site of the enzyme in each cell line (Kemp & Wallace, 1990). For example, AChE in rainbow trout possesses a smaller active site than that for rat AChE, which makes it less accessible than rat AChE to certain cholinesterase inhibitors (Kemp & Wallace, 1990). Thus, AChE in H9c2 cells may have less steric attraction for OPs compared to AChE in neuronal cells. Another possibility is that if the nucleophilic site of AChE is weak, the acidity of the phosphorus atom of the inhibitor determines the rate of phosphorylation of the enzyme and thereby determines the overall rate of inhibition (Kemp & Wallace, 1990). This may also determine the spontaneous reactivation of the inhibited enzyme, as shown previously in other cell lines using different OPs (Wallace & Herzberg, 1988). This raises the possibility that H9c2 cells have a relatively weak nucleophilic site in their AChE compared to that of neuronal cells. However, AChE characterization in H9c2 cells has not been previously addressed, further work in this area could be worthwhile. Onother point of view is that oxons are metabolically converted to less toxic compounds via hydrolysis by paraoxonase (A-esterase; Sogorb & Vilanova, 2010). Therefore, it can be assumed that the effectiveness of paraoxonase in differentiated H9c2 cells resulted in increase in oxon hydrolysis. Moreover, studies had indicated that the paraoxonase activity between different cell lines exhibit different expression level. Thus cell may express high, intermediate, or low paraoxonase activity (Eckerson *et al.,* 1983; Mueller *et al.,* 1983). However, expression level of paraoxonase in H9c2 cells have not been previously investigated.

chlorpyrifos and its toxic metabolite have been reported to display neurotoxic effects primarily via AChE inhibition, which may persist for days to weeks (McDonough & Shih,

1997; Wijeyaratne & Pathiratne, 2006). Although chlorpyrifos and chlorpyrifos oxon showed significant inhibition of AChE, they displayed little cytotoxicity against differentiating H9c2 cells even at very high concentrations (100 µM), as shown in Chapter 4. This may be because neuronal cells have higher AChE activity than muscle, eye and heart cells (Miron *et al.,* 2008). This may suggest that direct inhibition of AChE activity by chlorpyrifos and chlorpyrifos oxon may be associated with the mild to slight morphological changes observed in differentiating H9c2 cells.

The present study also showed that treatment of differentiating H9c2 cells with diazinon and its metabolite diazoxon induced significant inhibition of AChE activity in following 7, 9 and 13 days exposure (Figure 5.11). These results are consistent with a previous study that showed that 10 µM diazinon and its metabolite diazoxon inhibited AChE activity in human lymphocytes and fibroblast cells (Colovic *et al.,* 2010). Moreover, an *in vivo* study showed that sublethal doses of diazinon had toxic effects in rats which resulted in apoptotic cell death, mainly induced by lipid peroxidation, and the induction of oxidative stress (Ogutcu *et al.,* 2006). In stark contrast, diazinon and diazoxon did not induce cell death at the sublethal concentration of 3 µM in differentiating H9c2 cells, as illustrated in Chapter 4. One possible explanation is that *in vivo* a number of factors contribute to the development of cardiotoxicity and induction of cell death, such as over-activation of the sympathetic and parasympathetic nervous systems, hypoxia, acidosis and electrolyte derangement (Karki *et al*., 2004). Differences between *in vivo* and *in vitro* experiments are expected, given the differences in the physiological characteristics of cells and model animals in both experimental conditions (Aronzon *et al*., 2011; Sztrum *et al*., 2011; Hutler Wolkowicz *et al*., 2014). However, In this study, it may be suggested that significant inhibition of AChE activity by sublethal concentrations of diazinon and diazoxon may be correlated with the induction of sub-toxic effects that may result from long-term exposure without the induction of cell death. In summary, chlorpyrifos and diazinon and their metabolites showed significant inhibition of AChE activity in differentiating H9c2 cells. This effect may lead to stimulation of myocardial muscarinic acetylcholine receptors. In this respect, muscarinic acetylcholine receptors were found to be expressed in H9c2 cells and play an important role in cardioprotective mechanism in H9c2 cells (Pan *et al*., 2012). These receptors are strongly associated with dysautonomic symptoms such as decrease in cardiac contractility (Liang-

Xiong Fu *et al.*, 1995; Goin *et al*., 1997) and changes in the cardiac response to vagal innervation (Chemnitius *et al.,* 1999). Thus, this suggests that reversible or irreversible inhibition of AChE may reflect changes in cellular morphology in differentiating H9c2 cells. However, researches have shown that cholinergic hyperexcitability is not responsible for all of toxic effects of OP poisioning. For example, diazinon was showen to accumulates in different tissues leading to histological and biochemical damages (Handy *et al.,*2002) and Intoxication with diazinon was found to be associated with changes haematological parameters and induces genotoxicity (Hariri *et al.,* 2010). Changes in cellular morphology may also be associated with other non-cholinergic molecular targets, which it would be worthwhile to investigate in order to assess the long-term effect of sublethal concentrations of OPs.

PSP exposure did not show significant inhibition of AChE activity (Figure 5.12). Therefore, it is believed that the cytotoxic effect of PSP in differentiating H9c2 cells is not associated with AChE inhibition. However, failure of PSP to interfere significantly with AChE activity indicates that alternative proteins targets are involved, which could be useful biomarkers for evaluating the cardiac cytotoxicity of PSP.

5.5.4 Effect of OPs on the cardiac cytoskeleton proteins of differentiating H9c2 cells

Certain OPs may have long-term toxic effects and may interfere with brain development by binding to molecular targets other than AChE or by affecting neuronal cytoskeletal proteins and causing disruption of cellular integrity and cellular structure (Richardson, 1995; Crumpton *et al.,* 2000). The current study investigated the possible effects of chlorpyrifos and diazinon, their metabolites (chlorpyrifos oxon and diazoxon), and PSP on the cardiac cytoskeleton proteins troponin 1, tropomyosin, and α-actin. Changes in the expression of these proteins are considered an indicator of cardiac toxicity or cardiac failure (Rajan *et al.,* 2010).

The results of the present study showed that treatment with chlorpyrifos at a sublethal concentration of 3 µM induced a significant decrease in the expression of troponin 1 at 13 days exposure in differentiating H9c2 cells, as determined by Western blot analysis (Figure 5.13 a). Similarly, 3 µM chlorpyrifos exposure was shown to disrupt cytoskeletal protein (NF-

H; neurofilament heavy chain) in neuronal cells, which suggests that this compound is strongly correlated with the inhibition of neurite outgrowth and AChE activity inhibition (Schmuck & Ahr, 1997; Flaskos *et al*., 1998; Li & Casida, 1998, Sachana *et al*., 2001). In cardiac cells, troponin 1 is a sensitive biomarker of cardiac toxicity (O'Brien, 2008). Thus, reduction in troponin 1 expression could indicate an early development of a molecular lesion, which is directly proportional to the concentration of the toxic given (Ferrans *et al.* 1969). Thus, this may be the cause of morphological alterations in differentiating H9c2 cells.

The present results showed that chlorpyrifos oxon had no effect on the cardiac proteins examined on Western Blots of lysates from differentiating H9c2 cells (Figure 5.14). In contrast, 0.03 µM of chlorpyrifos oxon was shown to impair neurite outgrowth in cultures of rat PC12 cells (Das & Barone, 1999). Additionally, chlorpyrifos oxon was reported to have a more potent effect on differentiation/neurite outgrowth than chlorpyrifos in neuronal cell lines (Howard *et al.,* 2005). However, in differentiating H9c2 cells, although chlorpyrifos oxon did not show any significant effect on cardiac cytoskeleton proteins, it was shown to induce slight morphological changes that may be related to AChE inhibition. A previous study on neuronal cells reported that OPs, which interfere with the morphogenic activity of AChE, may cause a disruption in axonal outgrowth (Brimijoin & Koenigsberger, 1999).

In the present study, diazinon was found to have a significant effect on the expression of the cardiac cytoskeleton proteins troponin 1 at 7-days, 9-days and 13-days exposure in differentiating H9c2 cells (Figure 5.15a). This finding has not been previously reported in cardiac-like cells, as the majority of such studies use neuronal cells. For example, a previous study reported that sublethal concentrations of diazinon and diazoxon interfered with the outgrowth of differentiating mouse N2a neuroblastoma cells after 24 h of exposure (Axelrad *et al*., 2003; Flaskos *et al*., 2007; Sidiropoulou *et al.*, 2009). Thus, inhibition of neurite outgrowth is associated with changes in cytoskeleton proteins e.g. neurofilament heavy chain (NFH), microtubule associated protein MAP 1B and heat shock protein 70 (HSP-70; Flaskos *et al*., 2007; Flaskos, 2012). Based on the findings of previous studies, it can be assumed that the morphological changes induced by diazinon in differentiating H9c2 cells are brought about via its effect on cardiac cytoskeleton proteins.

The present data also showed that diazoxon did not have a significant effect on the expression of the cardiac proteins examined in differentiating H9c2 cells (Figure 5.16). In contrast, it was reported that diazoxon induced a decrease in the expression of cytoskeleton proteins such as, tubulin and MAP 1B during the differentiation of rat C6 glioma cells; this study also reported a transient decrease in AChE activity, which probably triggers the events that later lead to outgrowth impairment (Sidiropoulou *et al.,* 2009). Thus, diazoxon seems to have a more potent effect on cytoskeleton proteins in neuronal cells than cytoskeleton proteins in cardiac cells or it may affects different proteins to diazinon or it may affects the cytoskeleton through different signaling pathways. Such differences between cell lines are generally expected (Watson *et al*., 2014).

Western Blot analysis indicated that PSP exposure significantly decreased the level of troponin 1, tropomyosin and α-actin expression at 7, 9 and 13 days exposure (Figure 5.17). The present study, to the best of the author's knowledge, is the first to report the effect of PSP on cardiac cytoskeleton protein expression. In neuronal cells, PSP is believed to induce delayed neurotoxicity (Jortner *et al*., 1999). Sublethal concentrations of PSP were found to reduce neuronal cytoskeleton protein expression (neurofilaments), which was found to be clearly correlated with the inhibition of outgrowth of axon-like processes (Zhao *et al.,* 2006). Cardiac proteins such as troponin 1, tropomyosin and α-actin are proteins associated with the normal differentiation process of cardiac muscle contraction (O'Brien, 2008). A decrease in the level of these cytoskeleton proteins clearly suggests the presence of an early molecular lesion that may interfere with the differentiation of H9c2 cells into cardiomyocyte-like cells. This reinforces the idea that the observed effect of PSP may be one of the possible factors responsible for its cardiac cytotoxicity. Troponins are globular proteins that play an important role in cardiac muscle contraction (O'Brien, 2008). In human and animal studies, troponins have been reported to be a sensitive biomarker that is first released within minutes in myocardial infarct (Babuin & Jaffe, 2005). Thus, the troponin level in blood is not elevated in healthy people (O'Brien, 2008). The effect of OPs on troponin 1 have been previously studied *in vivo*. For example, 0.8 g/kg fenthion was found to induce myocardial injury and lead to a significant increase in troponin 1 levels in the blood of rats. Thus, troponin 1 could be a useful biomarker of OP-induced cardiotoxicity. These findings confirm that reduced troponin 1 expression is a key early event following exposure of

differentiating H9c2 cells to PSP. Tropomyosin is a central regulator of muscle contraction and cellular movement, and it acts in synergy with troponin in actin-myosin interactions (Barua *et al*., 2012). Changes in tropomyosin expression and it's phosphorylation status play an essential role during cardiac development and in response to cardiac hypertrophy and heart failure (Schiaffino *et al*., 1996).

α-actin, a basic regulator of muscle contraction, together with myosin, plays an important role in cell migration and cell structure (Pollard & Cooper, 2009). It has been shown that OPs such as triphenyl phosphite and parathion can affect the function of the actin cytoskeleton (Carlson & Ehrich, 1999; Carlson *et al,* 2000). More interestingly, caspase activation was shown to occur following actin degradation induced by OPs (Carlson *et al*., 2000).In this respect, long term exposure of 3 µM PSP was found to induce cell death in differentiating H9c2 cells. Exposure to this concentration in particular involves in α-actin instability and cellular structure deterioration leading to cell death. These findings seem to indicate that disruption of cardiac cytoskeleton proteins can be a sensitive indicator of PSP-induced cytotoxicity in differentiating H9c2 cells. Thus, prolonged exposure to PSP at the sublethal concentration of 3 µM may be considered to cause a sub-acute cytotoxic effect.

5.5.5 Effect of PSP on novel cardiac cytoskeleton proteins expression of differentiating H9c2 cells

It was apparent from blot analysis that sublethal concentrations of PSP induced changes in the expression of cardiac cytoskeleton proteins troponin 1, tropomyosin and α-actin. It was therefore of interest to further investigate the effects of 3 µM PSP on other cardiac proteins expressed in differentiating H9c2 cells. These proteins also may be implicated in the mechanisms underlying PSP-induced toxicity. Using 2D gel electrophoresis and mass spectrometry the present study identified several novel proteins, specifically coiled-coil domain-containing protein 61, calumenin, and PD-LIM domain protein 1, whose expression was down regulated in differentiating H9c2 cells in the presence of PSP. These proteins are listed in Table 5.3.

Coiled-coil domain-containing protein 61 (Ccdc61) is present in the centrosomes and plays an important role in centrosome function, specifically, in cell division and cell development (Kuhn *et al*., 2014). Ccdc61 connected to the centriole at the centre of the centrosomes and

functions as a scaffold and for recruiting various eukaryotic proteins, including kinases and phosphatases, thus serving as a signalling centre of multicellular development (Kuhn *et al*., 2014). During the current study, exposure to the sublethal concentration of PSP resulted in reduced expression of Ccdc61. This suggests that PSP may affect centrosome function in H9c2 cells by disrupting the mitotic spindle of dividing cells and thereby; blocking further progress of mitosis. PSP may also promote microtubules disassembly, thereby affecting the morphology of the entire cell. Moreover, Ccdc61 was found to play a critical role in the post-translational modification of proteins (Kuhn *et al.*, 2014); depletion of these proteins thus may impair the general structure of H9c2 rat cells during differentiation.

Calumenin is a calcium-binding protein expressed in various tissues and at particularly high levels in heart tissue (Yabe *et al*., 1997). Calumenin is located in the sarcoplasmic reticulum of the mammalian heart (Yabe *el al*., 1997; Jung & Kim, 2004;). Calumenin has been shown to interact with sarco(endo)plasmic reticulum Ca^{2+} ATPase and ryanodine receptor to maintain Ca^{2+} homeostasis in rat cardiac cell (Sahoo & Kim, 2010). Additionally, extracellular calumenin was reported to suppress cellular migration and tumour metastasis by inactivating ERK1/2 signalling. Calumenin depletion consequently induced cellular migration in hepatocellular and pancreatic carcinoma (Wang *et al*., 2015). In the present study, a sublethal concentration (3 µM) of PSP was shown to down regulate the expression of calumenin. As a result, PSP may alter Ca^{2+} haemostasis in differentiating H9c2 cells and thus also affect muscle contraction (Periasamy & Huke, 2001). Further, depletion of calumenin in cardiomyocytes is associated with enhancement of Ca^{2+} ion transient amplitude in a short period to reach peak levels (Koss & Kranias, 1996).

The PDZ-LIM domain protein 1 (PDZLIM 1) is a muscle-specific protein that interacts with the α-actin to form the Z-disc structure; disruption in its function results in skeletal myopathy as observed in the muscles of male mice (Pashmforoush *et al*., 2001; Zhou *et al*., 2001). Additional research in mice has revealed increased expression of PDZLIM 1 to be associated with the development of malignancy and migration of cancerous cells in the breast, while depletion of PDZLIM 1 has been shown to disrupt cell motility and cell migration (Liu *et al.,* 2015). Thus, PSP may exhibit similar effects in differentiating H9c2 cells, decreasing H9c2 cell motility and function.

5.6 *Conclusion*

The work presented in this chapter shows that exposure to sublethal concentrations of chlorpyrifos and diazinon and their metabolites (chlorpyrifos oxon and diazoxon) in differentiating H9c2 cells induced significant inhibition of AChE activity, which may be strongly associated with the morphological changes in these cells. However, only the parent compounds chlorpyrifos and diazinon had a significant effect on cardiac cytoskeleton proteins. In contrast, PSP did not show significant inhibition of AChE activity, but it had a significant effect on the levels of cardiac cytoskeleton proteins, which is probably closely associated with the morphological changes observed. Mass spectrometry data also presented novel proteins down regulated in response to PSP. Thus, these findings may represent a molecular mechanism for long-term OP-induced cytotoxicity in differentiating H9c2 cells.

Chapter 6:

Effects of OPs on human-induced pluripotent stem cell-derived cardiomyocytes

6.1 Introduction

Induced pluripotent stem cells are reprogrammed cells generated from differentiated adult human somatic cells, which are similar to human embryonic stem cells (Yamanaka, 2007). More interestingly, hiPSCs have the ability to form the three primary embryonic germ layers: the mesoderm, endoderm and ectoderm, and hence have the potential to differentiate into any cell type under certain conditions, including cardiomyocytes (Jq *et al.*, 2003; Yamanaka, 2007). The ability of immature cells to adopt the features of a mature cardiomyocyte provides a promising strategy for various aspects of cardiovascular research including drug screening, therapeutic testing and toxicity testing (Ma *et al.*, 2011). Several studies have recently evaluated the maturation *in vitro* of hiPSCs-CMs to the cardiac human phenotype (Liu *et al*., 2009; Sartiani *et al.,* 2007; Foldes *et al.*, 2011). A recent study involving ultrastructural analysis of cardiomyocytes derived from hiPSCs showed that they exhibited a highly-ordered contractile apparatus similar to that of mature structures of cardiomyocytes, such as *fascia adherens*, dense myofibrils that have clear A and I-bands, gap junctions and visible sarcomeres (Lundy *et al.*, 2013). Notably, at the molecular level, cardiomyocytes derived from hiPSCs exhibited cardiac structural biomarkers, which were similar to those reported in human cardiac myocytes, including connexin-43 and a *β*-myosin heavy chain (Lundy *et al.*, 2013).

In the previous chapters of this thesis, findings showed significant cytotoxic effects of OPs, in particular PSP, on differentiated H9c2 cells. However, an established rodent cell line may respond differently to xenobiotic exposure when compared to human cells, due to the marked physiological differences between animal and human models (Lewis & Kerry, 2015). Therefore, it is essential to assess the cardiotoxic response to OPs on a cellular model that is comparable to the functional cardiomyocytes of humans. In this respect, hiPSCs-CMs are considered to provide a reproducible, scalable and human-based model applicable for *in vitro* toxicity screening and drug discovery (Burridge *et al.*, 2012). The present study employed hiPSCs-CMs as an *in vitro* model system to assess the effect of OPs on cardiomyocytes. This is the first study to explore the toxicological effects of OPs on cardiomyocytes derived from hiPSCs; it forms a useful comparison with the toxicological effects of OPs that have been previously investigated in differentiated H9c2 cells, and may thus represent an opportunity for preclinical evaluation.

6.2 *Aims*

The aims of this study were to examine the morphological characteristics of mature human-induced pluripotent stem cell-derived cardiomyocytes (hiPSCs-CMs), to confirm the expression of known specific cardiac markers, such as troponin 1, tropomyosin and α-actin, and to validate cytotoxic effects of OPs (chlorpyrifos, diazinon and PSP) observed in earlier chapters in a more human-relevant cellular model.

6.3 Methods

As described in chapter 2 section 2.3, 2.4, 2.5.

6.4 *Results*

6.4.1 Characterisation of hiPSCs-CMs

In the present study, hiPSCs-CMs were passaged once and cultured for seven days to enrich the contracting cells, as a previous study reported that hiPSCs-CMs start to contract after 7 days of culture (Burridge *et al.*, 2014). Immunostaining studies were performed to confirm cardiomyocyte differentiation and assess the expression of the cardiac-specific proteins in myocardial contracting cells. As shown in Figure 6.1, hiPSCs-CMs were positively stained for the cardiac troponin 1, tropomyosin and sarcomeric α-actin. The positively-stained cardiomyocytes demonstrated mature striated myocytes. Structural examination also demonstrated large and elongated cells. This provided additional evidence that the cells had gained a mature adult cardiac phenotype.

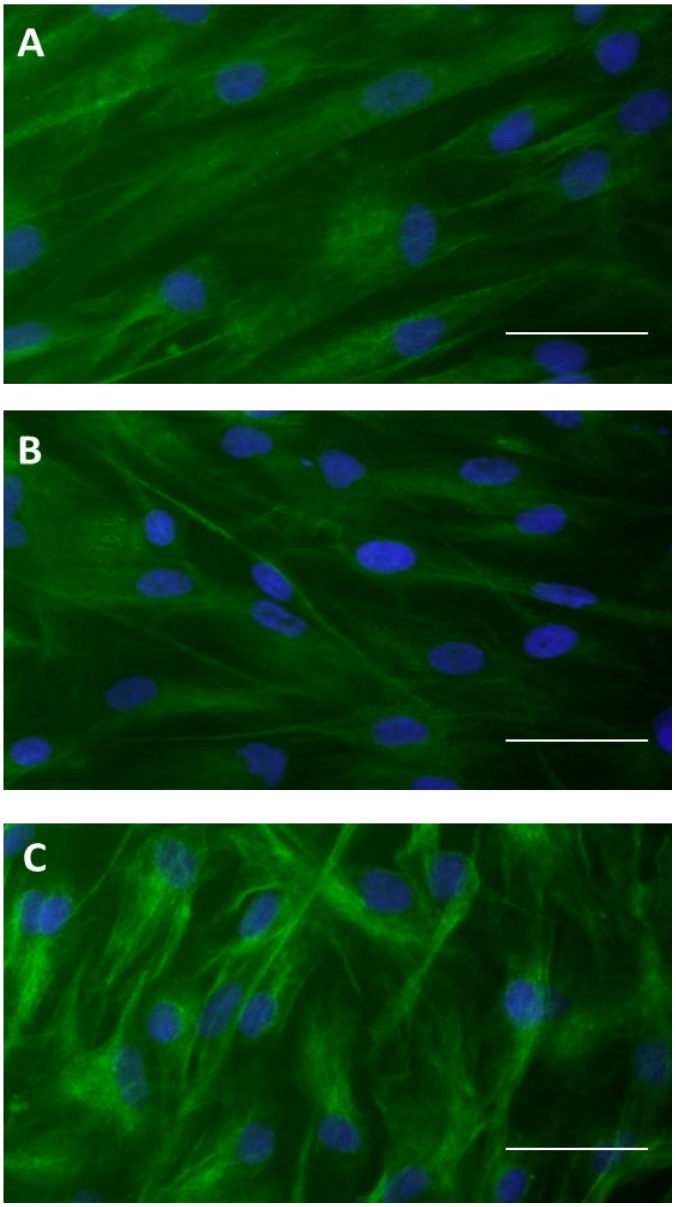

Figure 6.1 Structural characterisation of the hiPSCs-CMs.

The hiPSCs-CMs were passaged once and cultured for 7 days in cardiac myocyte medium. Immunofluorescence staining was performed with antibodies to A) cardiac troponin-1 (green), B) tropomyosin (green) and C) α-actin (green). Nuclei were stained with DAPI counterstain (blue). Scale bar = 100 µm. The images presented are from one experiment and are representative of four experiments.

6.4.2 Effects of OPs on the viability of hiPSCs-CMs

Initial experiments in this study assessed the effect of OP treatment on the viability of hiPSCs-CMs and this was investigated via monitoring MTT reduction and the release of LDH into the culture medium. Also, the morphological changes of hiPSCs-CMs were assessed via Coomassie Brilliant Blue staining following OP exposure. As a starting point, due to the limited number of cells, three concentrations of each selected OP (200 µM, 25 µM and 3 µM) were tested over a 48 h exposure period.

Chlorpyrifos at 200 µM significantly inhibited MTT reduction and triggered LDH release following 48 h exposure (Figure 6.2a and b). Coomassie Brilliant Blue staining, showed that cells appeared to be more rounded and compact, rather than elongated when compared to the control cells; also at 25 µM and 3 µM morphological changes were observed when compared to the control cells (Figure 6.2c).

Diazinon at a concentration of 200 µM had a significant effect on MTT reduction (Figure 6.3a), but had no significant effect on LDH release following 48 h exposure (Figure 6.3b). Also, at a concentration of 200 µM, stained cells appeared to be more rounded, without an appearance of elongated cells. Finally, at concentrations of 25 µM and 3 µM, changes in cell morphology suggested toxic effects when compared to control cells (Figure 6.3c).

PSP had a greater cytotoxic effect when compared to chlorpyrifos and diazinon. At concentrations of 200 µM and 25 µM PSP significantly inhibited the reduction of MTT and triggered the release of LDH following 48 h of exposure (Figure 6.4a and b). Cell deterioration was markedly evident at concentrations of 200 µM and 25 µM, followed by 3 µM PSP, since cells did not exhibit an elongated spindle shape typically observed in control cell cultures (Figure 6.4c).

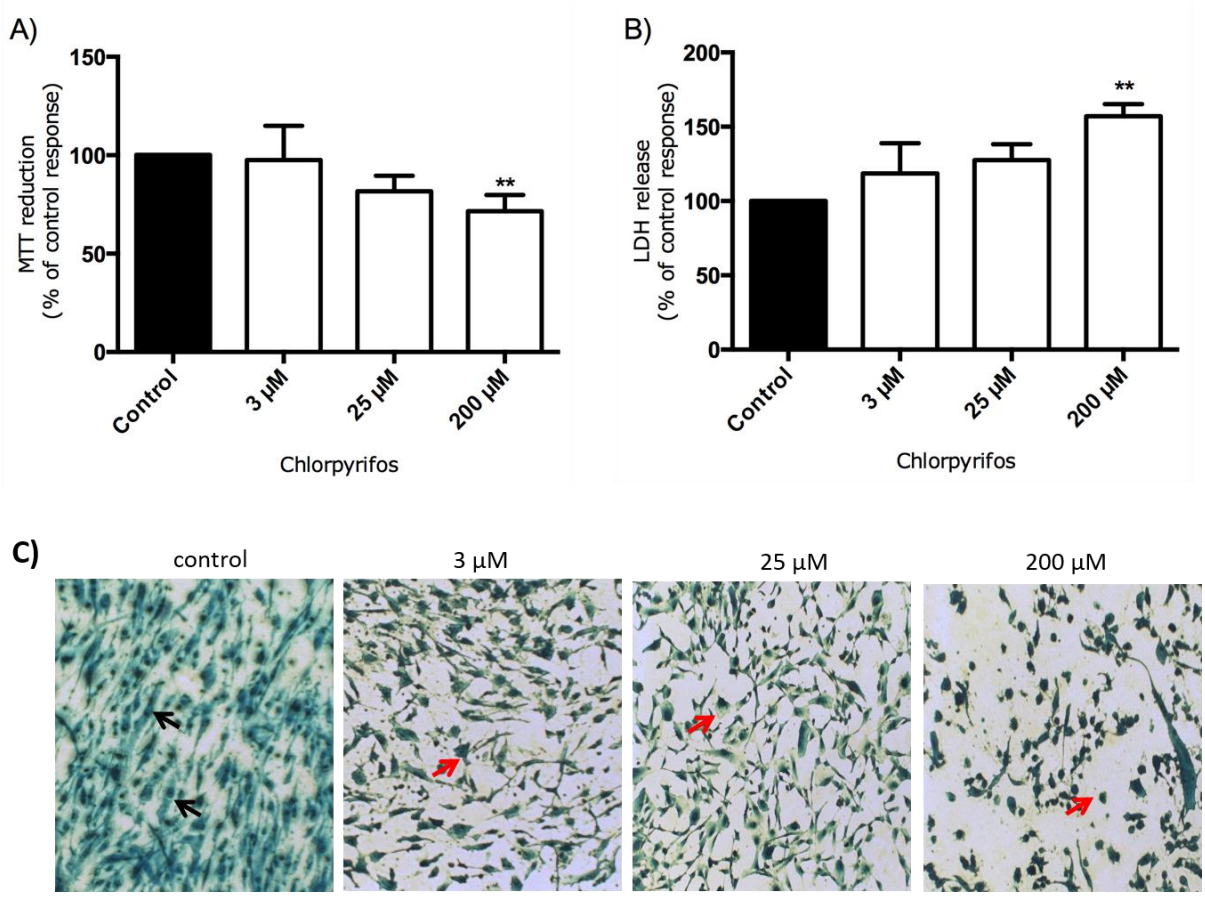

Figure 6.2 The effect of chlorpyrifos on the viability of hiPSCs-CMs monitored by MTT reduction and LDH release.

hiPSCs-CMs cells were exposed to the indicated concentrations of chlorpyrifos for 48 h. Following exposure, cell viability was assessed by measuring the metabolic reduction of MTT by cellular dehydrogenases (A) and the release of LDH (B). The data are expressed as a percentage of control cell values (=100%) and represent the mean ± SEM of three independent experiments, each performed in sextuplicate. $^{**}p < 0.01$ versus the control response. C) Following chlorpyrifos treatment with the indicated concentrations, cells were fixed (90 % (v/v) with methanol, stained with Coomassie Blue and then visualised using light microscopy (20x objective lens). The black arrows indicate typical elongated differentiated cells and the red arrows point to typical rounded compact cells. The images presented are from one experiment and are representative of three independent experiments.

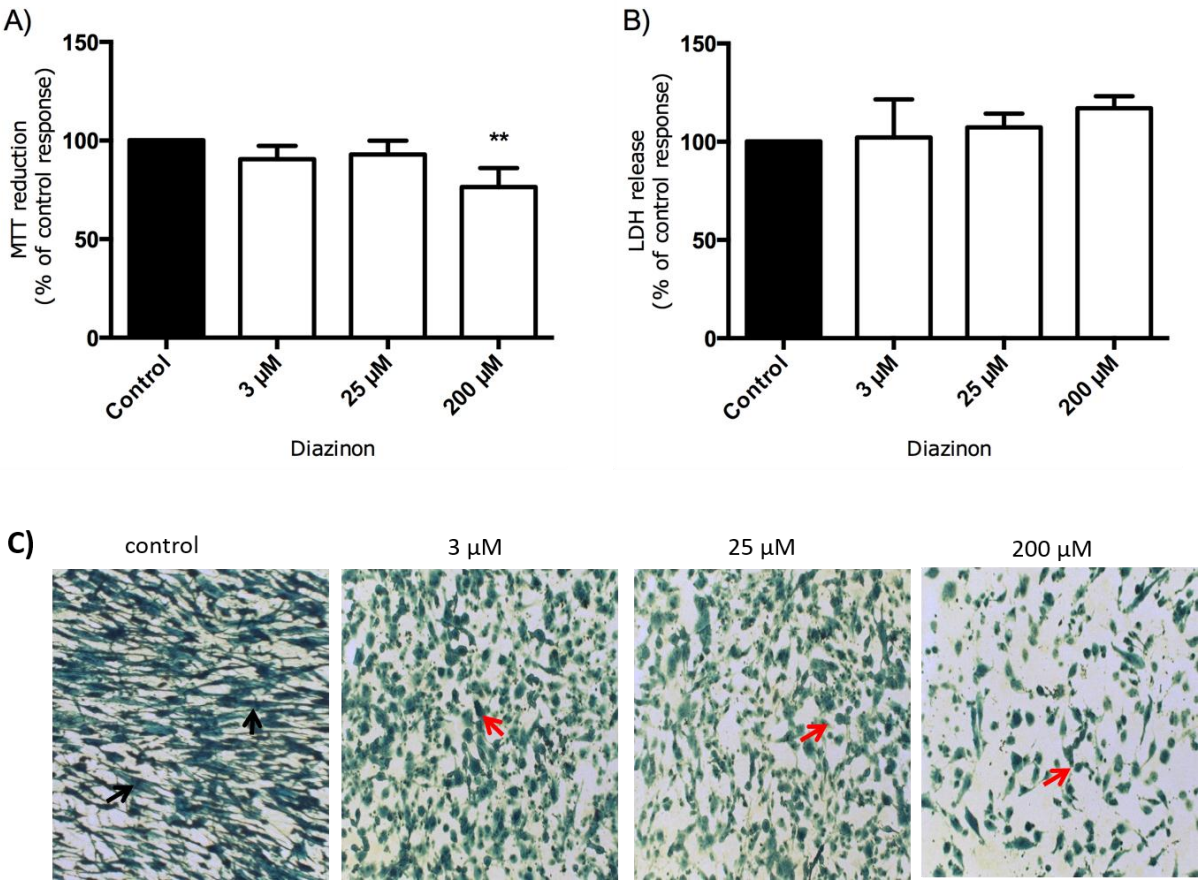

Figure 6.3 The effect of diazinon on the viability of hiPSCs-CMs as monitored by MTT reduction and LDH release.

hiPSCs-CMs cells were exposed to the indicated concentrations of diazinon for 48 h. Following exposure, cell viability was assessed by measuring the metabolic reduction of MTT by cellular dehydrogenases (A) and the release of LDH (B). Data are expressed as a percentage of control cell values (=100%) and represent the mean ± SEM of three independent experiments, each performed in sextuplicate. $^{**}p < 0.01$ versus the control response. C) Following diazinon treatment with the indicated concentrations, cells were fixed (90 % (v/v) with methanol, stained with Coomassie Blue and then visualised using light microscopy (20x objective lens). The black arrow indicates typical elongated differentiated cells and the red arrows point to typical rounded compact cells. The images presented are from one experiment and are representative of three independent experiments.

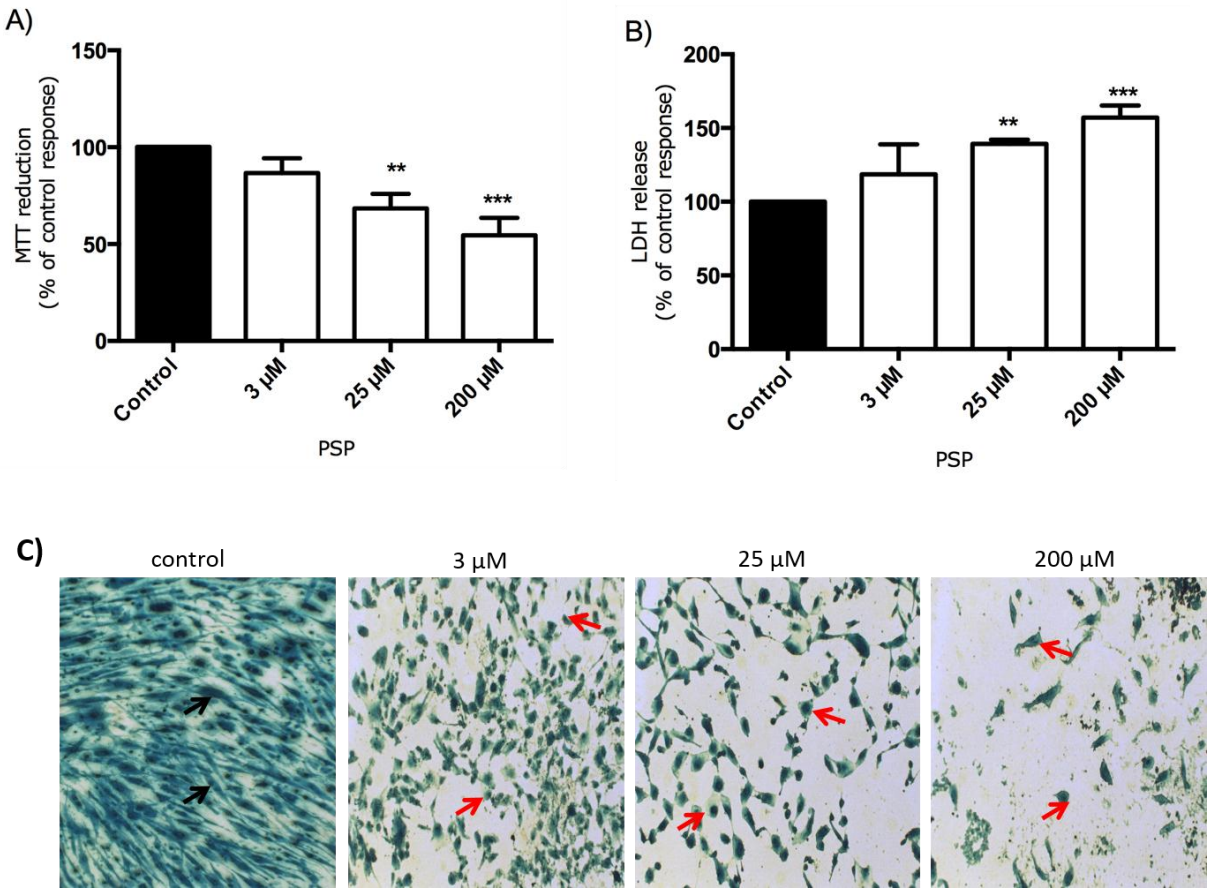

Figure 6.4 The effect of PSP on the viability of hiPSCs-CMs monitored by MTT reduction and LDH release.

Following exposure, cell viability was assessed by measuring the metabolic reduction of MTT by cellular dehydrogenases (A) and the release of LDH (B). Data are expressed as a percentage of control cell values (=100%) and represent the mean ± SEM of three independent experiments, each performed in sextuplicate. $^{**}p < 0.01$, $^{***}p < 0.001$ versus the control response. C) Following PSP treatment with the indicated concentrations, cells were fixed (90 % (v/v) with methanol, stained with Coomassie Blue and then visualised using light microscopy (20x objective lens). The black arrows indicate typical elongated differentiated cells and the red arrows point to typical rounded compact cells. The images presented are from one experiment and are representative of three independent experiments.

6.4.3 Phenyl Saligenin Phosphate induced Apoptosis in hiPSCs-CMs

From the previous results it was confirmed that PSP significantly induced hiPSCs-CMs cell death at concentration 25 µM and 200 µM. Therefore it is worth to assess whether PSP induce cell death via caspase-3 activation. Caspase-3 activation was monitored via immunocytochemistry at different time periods (eg, 1, 2 and 4 h). As evident in Figure 6.5, treatment of hiPSCs-CMs with 25 µM PSP triggered a significant activation of caspase-3 at 2 and 4 h of exposure.

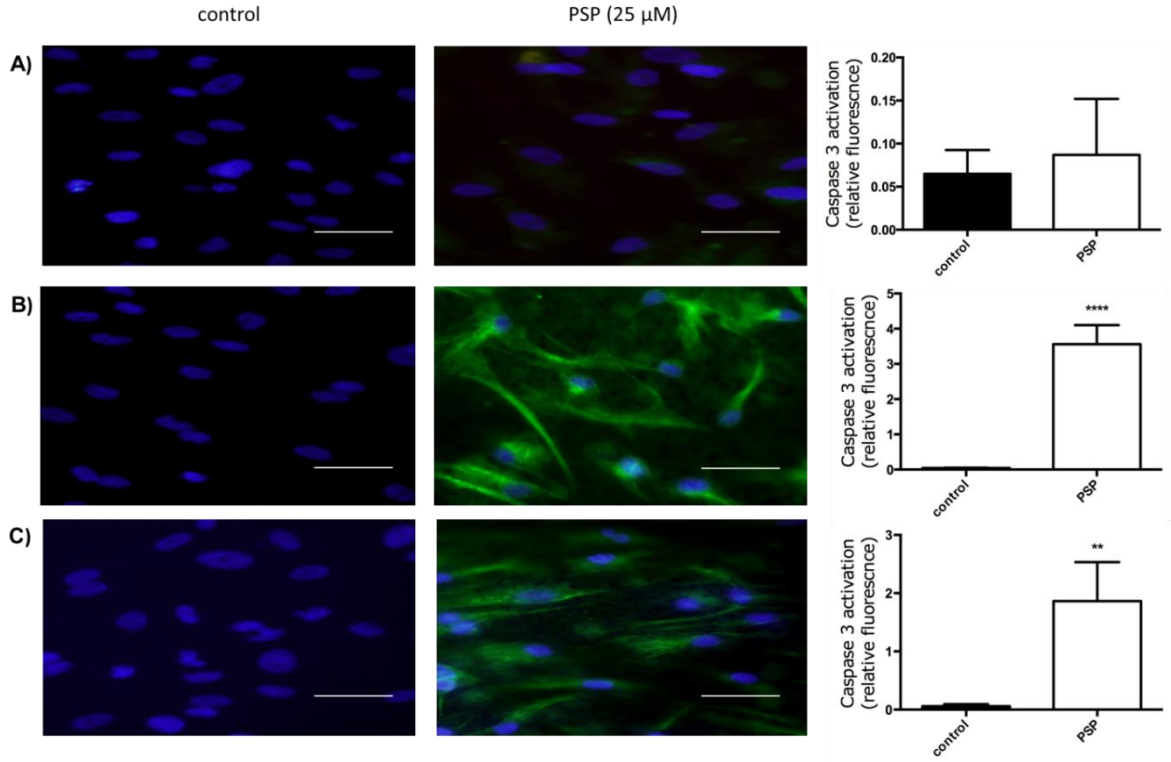

Figure 6.5 PSP-induced caspase-3 activation in hiPSCs-CMs.

hiPSCs-CMs were induced to differentiate for 7 days, then cells were exposed to 25 µM PSP for A) 1h, B) 2 h and C) 4 h. Following PSP exposure, caspase-3 activation was assessed via immunocytochemistry using an anti-active caspase-3 antibody (green) and DAPI counterstain for nuclei visualization (blue). Scale bar = 100 µm. The images presented are from one experiment and are representative of three. Quantified data are expressed as a percentage of control cell values and represent the mean ± SEM of four independent experiments. **p < 0.01 and ****p < 0.0001 versus the control.

6.4.4 The Effect of sublethal concentrations of PSP on hiPSCs-CMs

Previous results in chapter 5 showed 3 µM PSP caused a significant decrease in the expression level of cardiac cytoskeleton proteins; troponin 1, tropomyosin, and α-actin in differentiated H9c2 cells. Therefore it was worthwhile to assess if similar effect would apply with differentiating hiPSCs-CMs. hiPSCs-CMs were induced to differentiated in the presence of 3 µM PSP. As shown in Figure 6.6 troponin 1, tropomyosin, and α-actin expression were significantly decreased in PSP treated cell when compared to untreated cells.

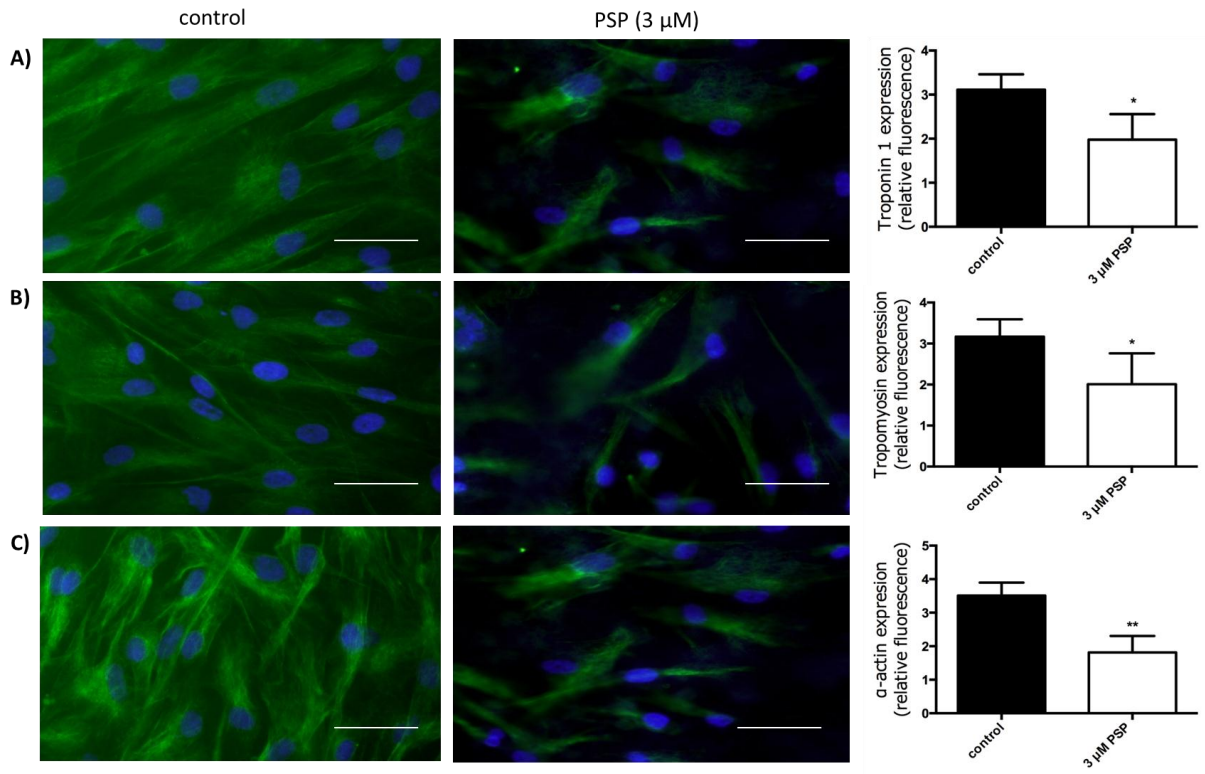

Figure 6.6 The effects of PSP on cardiac cytoskeleton protein expression s in differentiating hiPSCs-CMs.

hiPSCs-CMs were induced to differentiate for 7 days in the presence and absence of 3 µM PSP. Cells were analysed via immunofluorescence staining using antibodies that recognise A) cardiac troponin 1 B) tropomyosin C) α-actin (green) and DAPI counterstain for nuclei visualization (blue). Scale bar = 100 µm. The images presented are from one experiment and are representative of three. Quantified data are expressed as a percentage of control cells and represent the mean ± SEM of four independent experiments. *$p < 0.05$ and **$p < 0.01$ versus the control response.

6.5 *Discussion*

The current study evaluated the effects of the OPs chlorpyrifos, diazinon and PSP on cardiomyocytes derived from hiPSCs since these cells have been demonstrated to be one of the best models of choice for studies focusing on cardiac disease and cardiac toxicity (Liang *et al.,* 2013). hiPSCs-CMs have gained a high interest due to their superiority over heterologous studies and their spontaneous cardiac differentiation, during which they show cardiac beating, and their ability to address the effect of chronic exposure to toxic compounds in terms of morphological and physiological assessment (Dell'Era *et al.*, 2015). A number of studies have investigated the effect of OPs on different stem cell types, such as mesenchymal stem cells (Hoogduijn *et al.*, 2006), human umbilical cord blood-derived stem cells (hUCBSCs; Kashyap *et al.*, 2013) and adipose tissue-derived stem cells (Zarei *et al.*, 2015). However, cardiotoxic investigations of OPs on hiPSCs-CMs have not been previously assessed. A simple summary comparison between differentiated H9c2 cells and hiPSCs-CMs illustrating the major findings is shown in Table 6.1.

Table 6.1 Comparison of major findings of significant effect (p<0.05) of OPs in differentiated H9c2 cell and hiPSCs-CMs.

	MTT			LDH		
Differentiated H9c2 cell	3 µM -	25 µM ↓ PSP	200 µM ↓ CPF ↓ PSP	3 µM -	25 µM ↑ PSP	200 µM ↑CPF ↑PSP
hiPSCs-CMs	-	↓ PSP	↓ CPF ↓ PSP ↓Diazinon	-	↑PSP	↑ CPF ↑ PSP
Caspase-3 activation (25 µM PSP)						
Differentiated H9c2 cell	1 h -		2 h ↑		4 h ↑	
hiPSCs-CMs	-		↑		↑	
Sublethal effect of 3µM PSP on cardiac protein						
Differentiated H9c2 cell	Troponin ↓		Tropomyosin ↓		α-actin ↓	
hiPSCs-CMs	↓		↓		↓	

↑ represents a significant increase; ↓ represents significant decrease

6.5.1 Morphological characterisation of hiPSCs-CMs

The present findings showed that reproducibly differentiated cardiomyocytes derived from hiPSCs-CMs cells have the ability to express cardiac markers, such as troponin 1, tropomyosin and α-actin (Figure 6.1). Indeed, similar cardiac markers were shown to be expressed in adult human cardiomyocytes (Braam *et al.,* 2010). This is also in agreement with a study showing that hiPSCs-CMs displayed morphological maturation that involved expression of cardiac structural proteins, most notably troponin and α-actin (Zwi *et al.,* 2009; Ma *et al.*, 2011) Similar expression levels of these proteins were found in adult human heart (Lundy *et al.*, 2013). Moreover, the ultra-structural analysis provided additional evidence of cardiac maturation with cells displaying the appearance of highly ordered, dense filaments and long myotubes. Moreover, similar structural properties were shown in cultured adult human cardiomyocytes (Olivetti *et al.*, 1996).

6.5.2 The Effect of OPs on the viability of hiPSCs-CMs

Previous results demonstrated the effect of OPs on differentiated H9c2 cells, as shown in Chapter 4. Here, the effects of OPs were assessed on hiPSCs-CMs. Initial experiments assessed the effect of OPs on cell viability of hiPSCs-CMs by monitoring MTT reduction and LDH release. Interestingly, cell viability results for hiPSCs-CMs displayed a similar pattern to that observed in differentiated H9c2 cells. In the present study on hiPSCs-CMs, chlorpyrifos showed cytotoxicity at the highest concentration 200 µM, and Coomassie Blue staining indicated that they were more rounded and compact cells at 200 µM, 25 µM and 3 µM (Figure 6.2). Diazinon at concentration 200 µM caused significant inhibition of MTT reduction but had no significant effect on LDH release, suggesting that the former assays more sensitive than the latter (Figure 6.3a and b). This may be due to the earlier onset of metabolic effects than membrane leakage, consistent with the suggestion that MTT is a better predictor of cytotoxicity as observed in a previous study (Fotakis & Timbrell, 2006). Coomassie Blue Brilliant stain at 200 µM, 25 µM and 3 µM revealed the appearance of rounded rather than elongated cells when compared to the control cells (Figure 6.3c).

In comparison with differentiated H9c2 cells, chlorpyrifos induced cytotoxic effects at a concentration > 100 µM, whereas diazinon did not show any cytotoxicity effects at a concentration 200 µM. It is possible that hiPSCs are slightly more sensitive to OP toxicity than differentiated H9c2 cells due to the physiological differences between animal and

human models. Consequently, different responses may be observed, particularly in toxicity screening (Lewis *et al.*, 2013). However, stained cell images of chlorpyrifos and diazinon at sublethal concentration of 3 µM pointed to the idea that other cardiac parameters may be affected that influence cell morphology. Indeed, sublethal toxic effect of chlorpyrifos and diazinon towards hiPSCs-CMs cannot be excluded as a recent study showed that *in vitro* exposure to 10 and 200 µM of chlorpyrifos for 12 h was able to induce a significant gene alteration in mouse embryonic stem cells without inducing cell death or changes in the cellular structure (Estevan *et al*., 2013). Moreover, diazinon at concentrations 1 µM and 10 µM have been shown to decrease axonal cytoskeleton microtubule associated protein 1B **(**MAP 1B) expression, that may reflect inhibition of axon outgrowth in neuronal cells (Flaskos *et al.*, 2007). Also, in the current study sublethal concentrations of chlorpyrifos and diazinon (3 µM) significantly decreased the cardiac specific marker troponin 1 in differentiating H9c2 cells. This observations suggests that sublethal concentrations of chlorpyrifos and diazinon may interfere with myocellular contraction. In the muscle contraction process both troponin 1 and tropomyosin block the binding of actin to myosin preventing muscle contraction. At higher Ca^{2+} concentration, Ca^{2+} binds to troponin C, leading movement of tropomyosin which allows the myosin head interact with actin thus allowing contraction. This demonstrates the critical role of troponin in cardiac function (Metzger & Westfall, 2004). Therefore, it is likely that similar parameters may be affected in hiPSCs-CMs treated with chlorpyrifos or diazinon, which may subsequently affect cellular morphology. It would therefore be of interest in future work to determine if sublethal concentrations of OPs interfere with the reported contraction of hiPSCs-CMs. However, further work will be required to determine which targets are most altered that may relate to disruption of cardiac cellular differentiation or cellular function.

PSP was shown to be more potent than chlorpyrifos and diazinon in viability assays, since PSP cytoxicity was observed at lower concentrations (25 µM) in hiPSCs-CMs. Also, Coomassie Blue staining at 200 µM and 25 µM showed cell deterioration. This is strongly in agreement with the previous study that demonstrated cytotoxic effect of 25 µM PSP in differentiated H9c2 cells. Also, visualisation of Coomassie blue stained cells revealed that 3 µM PSP induced morphological changes which were not unexpected. In the previous chapter, it was shown that 3 µM PSP significantly down regulated cardiac cytoskeleton proteins, troponin 1,

tropomyosin and α-actin in differentiating H9c2 cells. Clinically, cardiac troponins have been found to be a sensitive biomarker of drug-induced skeletal muscle and myocardial toxicity (Smith *et al.*, 2013). Together, troponin with tropomyosin intertwine with thin filament G-actin and function to regulate contraction of cardiac muscle mediated by increases in intracellular Ca^{2+} (Barua *et al.,* 2012). Structural instability and conformational changes of tropomyosin was found to significantly affect proteins that control Ca^{2+} flux such as the sarcoplasmic Ca^{2+} ATPase (SERCA2a; Schulz *et al.,* 2012). Also, mutation in tropomyosin was found to affect its ability to activate the actin thin filament upon binding of Ca^{2+} to troponin (Mamidi *et al.*, 2013). Thus, functional diversity of actin cytoskeletal is strongly associated with alterations of tropomyosin expression (Gunning *et al.,* 2008). Presuming that local change of tropomyosin activity by PSP may be sufficient to modulate cardiac contractile function. Overall, the data support the idea that PSP exposure is more cytotoxic than the other OPs tested as it is observed in both the H9c2 cells (rat) and hiPSCs-CMs.

6.5.3 PSP-induced caspase activation in hiPSCs-CMs

In the present study, 25 µM PSP was found to induce a significant increase in caspase-3 activation at the earlier time point of 2 h exposure (Figure 6.5). This is in agreement with the data obtained from studies with differentiated H9c2 cells, in which 25 µM PSP was shown to induce apoptosis mediated by significant activation of caspase-3 and JNK1/2. Thus, similar molecular mechanisms of PSP-induced cell death in hiPSCs-CMs may be observed. However, hiPSCs-CMs appeared to show more sensitivity to PSP than differentiated H9c2 cells, as caspase-3 was found to be significantly activated at 2 h, while in differentiated H9c2 cells caspase-3 was significantly activated at 4 h. One reasonable explanation for this could be the minor variations in DNA repair between mouse embryonic stem cells (mESC) and human embryonic stem cells (hESC) which might lead to differences in cell fate during cell development (Mahler & Butcher *et al.*, 2011; Arabadjiev *et al.*, 2012). Therefore, it can be possible that compounds that may show toxicity towards human cells may not be seen to have any toxic effects towards mice cells and vice versa (Xia *et al.*, 2008; Malik *et al.*, 2014). However, due to the limited number of hiPSCs-CMs, the present study was not able to investigate further the molecular mechanism(s) of PSP toxicity in hiPSCs-CMs. Hence, in future work, it would be interesting to validate the human cardiac cellular response against PSP and to explore the role of protein kinases e.g. JNK1/2 in the regulation of apoptosis in

hiPSCs-CMs. Moreover, the ability to engineer iPSC lines by different techniques makes it an advantageous source to study genetic alterations caused by toxic compounds (Zhu *et al.*, 2011; Zeng *et al.*, 2014).

6.5.4 The Effect of sublethal concentrations of PSP on hiPSCs-CMs

The fact that 25 µM PSP was shown to induce apoptotic cell death suggests that it is necessary to assess the risk of exposure to sublethal concentrations of 3 µM PSP during the development of contracting hiPSCs-CMs. In the present study, PSP was shown to significantly decrease the level of troponin 1, tropomyosin and α-actin at 7 days of exposure (Figure 6.6). Similarly, in differentiating H9c2 cells, 3 µM PSP was also found to reduce the expression of troponin 1, tropomyosin and α-actin at 7 days of exposure. Since, hiPSCs-CMs start to contract after 7 days in culture, and troponin 1, tropomyosin and α-actin are important myofilament proteins (Burridge *et al.*, 2014; Kempf *et al.*, 2016), these findings strongly support the idea that a non-cytotoxic concentration of PSP may disrupt cardiac development processes, such as cell proliferation and differentiation, through direct interference with cardiac proteins; thus a decrease in their expression may indicate an early sign of cardiotoxicity (Yavuz *et al.*, 2008).

6.6 *Conclusion*

Overall, the work presented in this chapter successfully demonstrated concordance with the results presented in chapters 4 and 5 on the effect of chlorpyrifos, diazinon and PSP on cardiac stem cells with respect to parameters such as MTT reduction, LDH release and caspase-3 pathway activation. The findings of this study revealed the toxic effects of OPs in differentiated H9c2 cells was similar to the presently reported hiPSCs-derived cardiomyocytes, indicating that hiPSCs-CMs represent a suitable model for *in vitro* toxicity testing although with considerable differences in potency amongst different OPs. The evaluation of PSP concentrations lower than 25 µM and their manifestations of effects would be very helpful in establishing a basic mechanism of PSP toxicity towards cardiac cell proliferation and differentiation. Such types of future testing paradigms could help to improve understanding of the possible differences in sensitivity of different cell types after exposure to OPs, which could be critical in developing measures or procedures for the effective management of OP poisoning cases.

Chapter 7:

General Discussion, Conclusion and Future Work

7.1 *General Discussion*

7.1.1 Differentiation of H9c2 cells

The present study used H92c cells to investigate the effect of OPs on cardiac myocytes. Mitotic H9c2 cells were reported to be suitable for use in the study of cardiac ischemia/reperfusion, diabetes and cardiac toxicity (Yu *et al.,* 2011; Zhu *et al*., 2011). However, they were shown to differentiate into more cardiomyocyte-like phenotype cells when treated with all-*trans*-RA (Menard *et al.*, 1999). In both previous studies and in the current work, the generation of cardiomyocyte-like phenotype cells was confirmed by monitoring the morphological alteration and the expression of a cardiac-specific markers, such as troponin 1, which developed over a period of 7 days of cell differentiation. Proteomic analysis also showed that differentiated H9c2 cells expressed significantly higher levels of cardiac cytoskeleton proteins, such as tropomyosin and α-actin, when compared to undifferentiated H9c2 cells. Thus, the use of differentiated H9c2 cells as an *in vitro* model could provide a potential application in toxicity screening and will aid in understanding the molecular mechanisms that contribute to OP-induced cardiotoxicity (Pagano *et al.,* 2004).

7.1.2 Effect of OPs on differentiated H9c2 cells

The clinical effects of OP poisoning can range from neurological complications to intermediate syndrome and cardiac conduction disorders (Abdollahi & Karami-Mohajeri, 2012). Most scientific studies have examined the effect of neuropathic OPs on neuronal cells. In contrast, the mechanisms underlying cardiotoxicity are not fully known. Therefore, the present study assessed the effects of PSP, chlorpyrifos and diazinon and their *in vivo* metabolites (chlorpyrifos oxon and diazoxon) on mitotic and differentiated H9c2 cells. The findings revealed considerable differences in potency among the different OPs. Chlorpyrifos diazinon and their oxon metabolites, which display acute toxicity *in vivo* as a result of the inhibition of AChE, were shown to have little cytotoxic effect on H9c2 cell cardiomyoblasts. Similarly, previous study showed that subacute exposure chronic administration of 15 and 30 mg/kg diazinon did not activate caspase-3 and caspase- 9 in diazinon treated rat groups. Moreover, no significant changes were observed in Bax and Bcl-2 ratios. Moreover, apoptosis induction was not observed in rat brain (Rashedinia *et al.,* 2013).

In contrast, PSP (a weak inhibitor of AChE) was shown to have a significant cytotoxic effect on both mitotic and differentiated H9c2 cells.

7.1.3. Cytotoxic effect of PSP on differentiating H9c2 cells

In the present study, PSP was found to induce a cytotoxic effect in both mitotic and differentiated H9c2 cells, as determined by the MTT and LDH assays. In mitotic cells, cell death occurred from 4 h exposure to concentrations of 25 µM–200 µM; in differentiating cells, cell death occurred from 2 h exposure to concentrations of 25 µM–200 µM. It was also determined that 25 µM PSP induced apoptotic cell death independently from AChE inhibition. As a previous study showed, the JNK1/2 pathway plays an essential role in the apoptotic pathway (Dhanasekaran & Reddy, 2008). Therefore, the present study investigated the effect of PSP on protein kinase signalling pathways such as, AKt ERK and JNK1/2. It was showen that PSP-induced apoptosis occurs via JNK 1/2 mediated caspase-3 activation. A similar phenomenon was observed in a previous study, in which PSP (10 and 100 µM) induced apoptosis in human neuroblastoma SH-SY5Y cells via the activation of caspase-3 (Carlson *et al.,* 2000). In agreement with a previous study revealed that some OPs such as, chlorpyrifos and dimethoate have an effect on MAPK pathway. Protein kinases like the Akt family or ERK was significantly down regulated after OPs poisoning, these proteins are essential for cell survival and proliferation (Schafer *et al.,* 2013)

Pre-treatment with the specific JNK1/2 inhibitor SP 600125 abolished PSP-induced JNK1/2 activation and was also able to block caspase-3 activation, indicating the involvement of the JNK 1/2 pathway. More interestingly, the results showed that other specific kinase inhibitors were unable to block the apoptotic pathway induced by PSP, thus excluding the involvement of other protein kinases, such as ERK1/2 and PKB. Since ERK1/2 and PKB pathways are associated with the regulation of cell survival (Xia *et al.*, 1995; Brunet *et al*., 2001), it is conceivable that increased ERK 1/2 and PKB activation are not essential to PSP-induced cell death.

The current study identified novel non-cholinesterase targets of PSP that may contribute to its cytotoxicity, including tropomyosin, heat shock protein β-1 and nucleolar protein 58. Tropomyosin is essential to muscle contraction and responsible for regulation of the interaction of actin binding proteins, such as myosin, with microfilaments (Yo & Ono, 2006),

Variation in tropomyosin expression can be caused by disease-related substitutions or naturally occurring amino acid substitutions in tissue-specific tropomyosin isoforms that may lead to unlikly physiological functions. Thus, structural instability in the central region of tropomyosin modulates cardiac contractile function (Mamidi *et al.,* 2014). In addition, Mutations in alpha-tropomyosin, a thin filament protein involved in structural and regulatory roles in muscle cells, are associated with Dilated cardiomyopathy (van de Meerakker *et al.,* 2013). Dilated cardiomyopathy is characterized by idiopathic dilatation and systolic contractile dysfunction of the ventricles leading to an impaired systolic function. Mutation in tropomyosin significantly weakens the binding of tropomyosin to actin by 25% (van de Meerakker *et al.,* 2013). Suggesting that binding to PSP may affect actin stabilisation, leading to impaired cell motility and cell contraction.

Heat shock protein β-1 is expressed in response to stress to mediate the cytoprotection effect that may prevent cell death (Mymrikov *et al*., 2011). This protein is found to be related to stress and metabolism in skeletal muscles (Kim *et al.,* 2010). Thus, the binding of heat shock protein β-1 to PSP may impair its ability to promote cell survival. Nucleolar protein 58 is located in microspherules in the nucleolus (Ren *et al.*, 1998), which is essential for 60S ribosomal subunit biogenesis (Lyman *et al.*, 1999). Therefore, it is suggested that binding to PSP may affect the nucleolus and protein translation.

7.1.4 Sublethal effect of OPs on differentiating H9c2 cells

A number of toxicity studies revealed that sublethal doses of OPs might cause morphological changes and behaviour problems (Zalizniak & Nugegoda, 2006). Therefore, the possible ability of sublethal concentrations of OPs to induce long-term toxicity cannot be neglected. The experiments performed in this study were designed to determine whether sublethal concentrations of OPs might have a measurable effects on the differentiation process of H9c2 cells. Mitotic H9c2 cells were induced to differentiate in the presence of 3 µM OPs and the effect of OPs was observed at 7, 9 and 13 days.

Results showed that both chlorpyrifos and diazinon induced morphological changes and elicited significant reduction in cardiac specific marker troponin 1. On the other hand, their oxon forms did not show any toxic effects toward differentiating H9c2 cells. Simirlay, sublethal concentration of 1, 5 and 10 µM diazinon had no effect on the expression of

neuronal cytoskeletal proteins β-tubulin in differentiating N2a neuroblastoma cells, it also failed to affect the levels neurofilament light (NFL) and neurofilament medium (NFM) chain levels (Sachana *et al.,* 2014). Indicating that the parent compounds were potent to interfere with H9c2 cell differentiation. Importantly, changes in a such a protein level is applied in clinical diagnostic for cardiomyopathies (O'Brien, 2008) and for chemical induced low dose toxicity (Reagan *et al.*, 2013). However, troponin 1 cannot alone account for adverse consequences of chlorpyrifos and diazinon, particularly following long-term exposure. These data suggest that chlorpyrifos and diazinon may affect other cytoskeleton proteins involved in the fundamental cardiac contractile function.

Although both parent compounds chlorpyrifos and diazinon and their metabolites are eliminated relatively rapidly in humans (i.e., metabolized and then eliminated primarily through the kidneys; Hill *et al.,* 1995), previous studies in rats indicate that chlorpyrifos and diazinon are redistributed to adipose tissue, forming a depot for slow release. More intristing, sublethal exposures to diazinon interfered with influence on the adipose tissue most probably via stimulation of muscarinic receptors (Pakzad *et al.,* 2013). Thus, the OPs may be retained for longer periods than is evident using plasma measurements (Gallo & Lawryk, 1991; Abu-Quare *&* Abou-Donia*,* 2001). Therefore, it is also important to note that chlorpyrifos and diazinon itself may have toxic properties in the absence of conversion to their oxon metabolites (Terry *et al.,* 2003). More recently, a study has reported lethal cardiac complications and severe histological alterations in the cardiac tissue with diazinon-chlorpyrifos treated animals. In addition, diazinon and chlorpyrifos tested increased the oxidative stress and oxidative modifications in the genomic DNA content of the cardiac tissues, data provided possible evidence of the cardiotoxicity mechanism (Zafiropoulos *et al.,* 2014). This may suggest that chlorpyrifos and diazinon may be stored in cardiac cells resulting in a sub lethal effect that may be longer lasting.

As mentioned previously, PSP was shown to have a potent effect on the viability of differentiating cells when compared to chlorpyrifos and diazinon. Interestingly, PSP was also found to affect the differentiation of H9c2 cells, as observed using a light microscope at 7, 9 and 13 days. Thus, cells appeared more rounded following exposure, rather than elongated or spindle-shaped. One explanation for this may be is the effect of PSP was also able to significantly decrease in the expression of cardiac cytoskeletal proteins, such as cardiac

troponin 1, tropomyosin and α-actin, at 7, 9 and 13 days, resulting in the loss of cell integrity and morphological alterations, as described above (Hamm & Hinton, 2000; Osterauer & Köhler, 2008). Morphological alterations were also induced by PSP in the study of Hargreaves *et al.* (2006), who showed a decrease in neurite outgrowth in differentiating N2a cells induced by 2.5 μM PSP. The attenuation of these cytoskeleton protein levels might reflect early molecular lesions in cardiac cells (O'Brien, 2008). Therefore, it is conceivable there is a continuous reduction in cell integrity and cardiac cytoskeletal protein expression resulting in PSP-induced cell death of differentiating H9c2 cells after 13 days.

A proteomic investigation revealed the first report on the effect of sublethal PSP exposure on novel protein expression in differentiating H9c2 cells when compared to control. Identified proteins included, coiled-coil domain-containing protein 61, calumenin, and PDZ-LIM domain protein 1.

Coiled-coil domain-containing protein 61 is abundant in the centrosomes and acts as a scaffold to recruit various eukaryotic proteins, such as kinases and phosphatases into the centrosomes for vital multicellular development (Kuhn *et al.,* 2014). A sublethal concentration of PSP was shown to induce a significant reduction in coiled-coil domain-containing protein 61 expression that may affect centrosome in H9c2 cells, thus affecting cell division and cell differentiation.

Calumenin is a Ca^{2+}-binding protein located in the endo/sarcoplasmic reticulum of mammalian hearts and regulates Ca^{2+} homeostasis in hearts (Sahoo & Kim, 2010). It is highly expressed during the early developmental stage of the heart and regulates the activity of sarco/endoplasmic reticulum Ca^{2+}-ATPase and of the ryanodine receptor in the endoplasmic reticulum (Sahoo & Kim, 2010). Therefore, calumenin is a Ca^{2+} sensor, which folds into a compact structure, capable of interacting with its molecular partners, when Ca^{2+} concentration within the ER reaches the millimolar range. (Mazzorana *et al*., 2016). In addition, previous study showed that overexpression of calumenin decreased ER stress and reduced ER-initiated apoptosis neonatal rat ventricular cardiomyocytes. Thus, calumenin may serve as a therapeutic target against various heart diseases (Lee *et al*., 2013). Thus, changes in the expression of calumenin could alter Ca^{2+} cycling (Sahoo & Kim, 2008).

Therefore, a decrease in calumenin expression induced by PSP in cardiomyocytes may disturb Ca^{2+} regulation and thus interferes with heart contraction.

PDZ-LIM domain protein 1 is a protein expressed in the early stage of heart development (Kotaka *et al.,* 2001). Furthermore, it is implicated in cytoskeleton organization and plays an important role in myofibrillogenesis (Kotaka *et al.,* 2001). PDZLIM1 binds to α-actinin and transfers as PDZLIM1/α-actinin complex to the newly formed actin cytoskeleton during migration and contraction of endothelial cells (Bauer *et al.,* 2000). PDZLIM1 is one of the proteins that found to increase its expression dramatically in breast cancer cell progression, thus disruption in the PDZLIM1/α-actinin complex may significantly affect signaling pathways which are relevant to cell migration and invasion (Liu *et al*., 2014). The observed decrease of PDZLIM1 expression in PSP-treated cells point to the idea that PSP is a developmental toxicant that may interfere with the early developmental process of cardiomyocytes. However, further work is required to validate the effect of PSP on the expression levels of these novel identified proteins and to establish the consequences of PSP interaction on their biochemical properties/function.

7.1.5 Effects of OPs on cardiomyocyte derived from human-induced pluripotent

The present study investigated the effect of OPs on differentiating H9c2 cells, which were derived from an embryonic rat. However, it is possible that cells derived from a human model when compared to cells derived from animals may respond differently, due to the physiological differences between the two species (Lewis & Falconer, 2015). Therefore, hiPSCs-CMs were used in the later stages of the current work to provide a model more similar to the functional cardiac cells in humans (Burridge *et al.*, 2012). A recent study charecterized the biophysical and pharmacological properties of hiPS-CMs. the Na^{+} and Ca^{2+} channels were evaluated and a pattern of increasing Na^{+} and L-type Ca^{2+} current density in hiPSCs-CMs was observed with increasing time in cell culture. hiPSCs-CMs also exhibited action potential heterogeneity, likely reflecting cell types (atrial, ventricular, and pacemaker) and a range of cellular maturation in the culture. hiPSCs-CMs showed prominent diastolic depolarization and action potentials spontaneously. hiPS-CMs are immature cells that proven with time in culture can progressively develop to a more mature phenotype without signs of dedifferentiation (Rashedinia *et al.,* 2013).

Initial experiments assessed the effect of chlorpyrifos, diazinon and PSP on the cell viability of hiPSCs-CMs at three different concentrations (3, 25 and 200 µM).

The findings revealed that chlorpyrifos and diazinon induced toxicity at a high concentration (200 µM), while PSP also showed a potent cytotoxic effect at a lower concentration (25 µM) in hiPSCs-CMs. Thus, the cell viability changes were comparable with the cytotoxic effect of 25 µM PSP on differentiated H9c2 cells. However, morphological changes at sublethal concentrations of chlorpyrifos, diazinon and PSP cannot be ruled out, as visualised stained cells appeared to be compact rather that elongated cells. This may reflect their toxic effects at sublethal concentration in hiPSCs-CMs as shown with differentiated H9c2 cells. Chlorpyrifos and diazinon exposure significantly reduced troponin 1 expression in differentiated H9c2 cells. However, other proteins and signaling pathways may be involved in OP-induced cardiotoxicity. For example, histological and morphometric studies in rats showed the development of hypertrophy in cardiac muscular cells exposed to OPs (Calore *et al.* 2007). Previous studies have shown that calcineurin may play a critical role in the signaling of cardiac hypertrophy in many experimental models (Kamiya *et al.,* 2001). Cardiotrophin-1 (CT-1), a member of the IL-6 family of cytokines that induces hypertrophy of cardiac myocytes *in vitro*. Furthermore, levels of CT-1 are elevated in the serum of patients with ischemic heart disease and valvular heart disease (Freed *et al.,* 2003). Therefore, it may be of value to study these biochemical pathways in chlorpyrifos and diazinon induced sublethal effect in hiPSCs-CMs.

More interestingly, 25 µM PSP was shown to induce apoptotic cell death mediated by caspase-3 activation in differentiated H9c2 cells, which provided further validation of the results obtained in hiPSCs-CMs. The current study also investigated the effect of a sublethal concentration of 3 µM PSP on the cardiac cytoskeletal proteins troponin 1, tropomyosin and α-actin in hiPSCs-CMs that may contribute to PSP toxicity. Exposure to PSP was shown to decrease significantly the expression of troponin 1, tropomyosin and α-actin at 7 days exposure, and this was consistent with the findings shown in differentiating H9c2 cells. These findings showed that sublethal exposure to PSP might affect the cardiac development processes and may interfere with cardiac function. On this basis, it can be confirmed that PSP exhibited cardiotoxicity, and this highlights concerns regarding human cardiomyocytes.

7.2 *Concluding Remarks*

The present research provides valuable insights into the effect of OPs on cardiac cells. PSP was found to have a potent cytotoxic effect on rodent and human cardiomyocyte-like cells when compared to other compounds, and to induce apoptosis in differentiating cells in a JNK1/2 activation related manner. Novel binding proteins (e.g. tropomyosin) were identified for PSP that may contribute to its cytotoxicity. Furthermore, long-term exposure to sublethal concentrations of chlorpyrifos, diazinon and PSP was able to attenuate the expression of cardiac cytoskeletal proteins that are important in cardiac differentiation, proliferation and migration. The data from the present study will help to establish a basic mechanism of cardiotoxicity following exposure to OPs. Figure 7.1 summaries the present study.

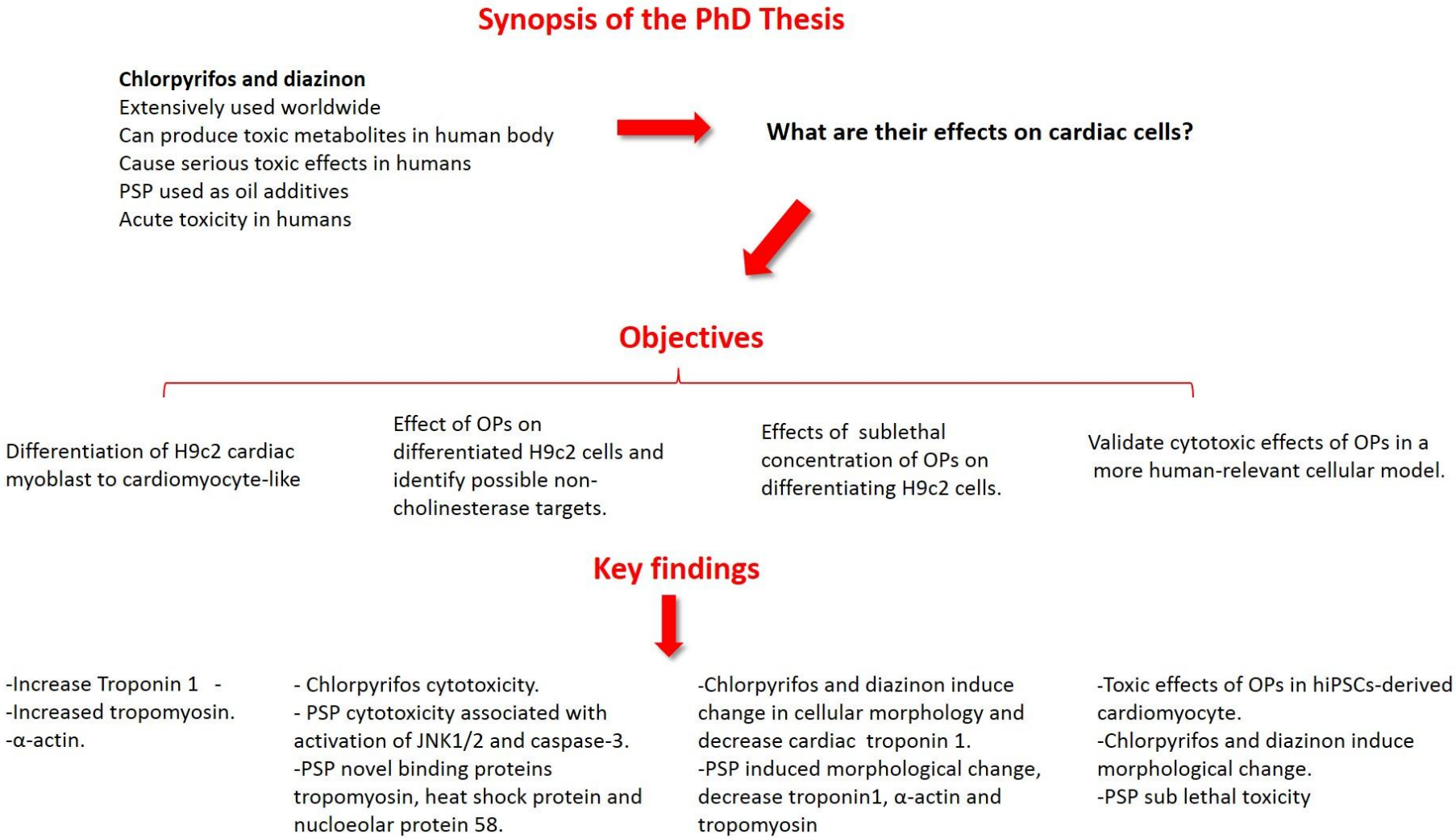

Figure 1.7 summary of results in the present study.

7.3 *Future work*

- As some organophosphates showed severe cholinergic toxicity resulting from the inhibition of acetylcholinesterase and butyrylcholinesterase and leading to an enhanced activation of the autonomic pathways (Lyzhnikov *et al.,* 1975, Ludomirsky *et al*., 1982, Anand *et al*., 2009), an evaluation of the effects of chlorpyrifos, diazinon and PSP on butyrylcholinesterase activity levels could help to further elucidate targets in differentiated H9c2 cells that may be involved in cardiac cytotoxicty.
- Organophosphates are highly reactive compounds and can interact with proteins at very low (nanomolar range) concentrations, as determined *in vitro* (Huff *et al*., 1994; Howard & Pope, 2002). Further research is needed to investigate lower concentrations of PSP that can bind to cardiac-specific proteins and whether similar binding occurs *in vivo.*
- The type of PSP binding to proteins and the possible motifs involved could be identified by mass spectrometry, in particular, with low concentration toxicity. Thus, the effect of a concentration less than 3 μM might be examined to identify a new molecular mechanism and provide novel strategies to control cardiac toxicity.
- *In vivo* models, such as mouse, rat, porcine and rabbit are available for toxicity screening and were proven to address similar cardiovascular complications in humans (Zaragoza *et al*., 2011). Thus, such types of future testing paradigms could also help in the understanding of possible differences in sensitivity between different species and their physiological behaviours after exposure to OPs, which could be critical in developing measures or procedures in the effective management of OP poisoning cases.
- Further studies are also required to establish time course and dose effects of OPs *in vivo.* It would also be worth determining the lethal dose of OPs, as the LD_{50} of some OPs were reported to be very low (1 mg/kg) in rats (Klaassen, 2007). Thus, this dose may evoke adverse consequences in humans and might likely lead to the development of cardiotoxicity.
- Understanding the molecular mechanisms associated with gene expression alterations or DNA damage in response to OPs exposure. Further experiments could

explore genetic biomarkers that can be detected following early exposure. Thus, this would improve the diagnostic tool and clinical treatment.

- Future studies should focus on the identification of possible non-cholinergic targets of OP compounds, which will help to increase understanding of the molecular mechanisms of OP-induced toxicity.
- General physiological studies to provide substantial evidence of that the two cardiac cells H9c2 and hiPSCs-CMs such as calcium channels and potassium channels.
- Measuring gene expression of cardiac proteins including calcium, potassium and sodium transport (channel proteins, SERCA, RyR ect)

REFERENCES

Abdollahi, M., & Karami-Mohajeri, S. (2012). A comprehensive review on experimental and clinical findings in intermediate syndrome caused by organophosphate poisoning. *Toxicology and Applied Pharmacology*, 258(3), pp.309-314.

Abou-Donia, M. (1993). The cytoskeleton as a target for organophosphorus ester-induced delayed neurotoxicity (OPIDN). *Chemico-Biological Interactions*, 87(1-3), pp.383-393.

Abou-Donia, M.B., & Lapadula, D.M. (1990). Mechanisms of organophosphorus ester-induced delayed neurotoxicity: type I and type II. *Annual Review in Pharmacology and Toxicology*, 30(1), pp.405-440.

Abraham, S.M., & Clark, A.R. (2006). Dual-specificity phosphatase 1: A critical regulator of innate immune responses. *Biochemical Society Transactions*, 34(6), pp.1018-1023.

Abu-Quare, A.W., & Abou-Donia, M.B. (2001). Inhibition and recovery of maternal and fetal cholinesterase enzyme activity following a single cutaneous dose of parathion and diazinon, alone and in combination, in pregnant rats. *Journal of Applied Toxicology*, 21(4), pp.307-316.

Akassoglou, K., Malester, B., Xu, J., Tessarollo, L., Rosenbluth, J., & Chao, M.V. (2004). Brain-specific deletion of neuropathy target esterase/Swiss cheese results in neurodegeneration. *Proceedings of the National Academy of Sciences*, 101(14), pp. 5075-5080.

Akbarsha, M.A., & Sivasamy, P. (1997). Apoptosis in male germinal line cells of rat in vivo: caused by phosphamidon, *Cytobios*, 91(364), pp.33-44.

Anand, S., Singh, S., Nahar Saikia, U., Bhalla, A., Paul Sharma, Y., & Singh, D. (2009). Cardiac abnormalities in acute organophosphate poisoning. *Clinical Toxicology*, 47(3), pp.230-235.

Anderson, R. (1993). Plasmalemmal caveolae and GPI-anchored membrane proteins. *Current Opinion in Cell Biology*, 5(4), pp.647-652.

Aoki, H., Kang, P., Hampe, J., Yoshimura, K., Noma, T., Matsuzaki, M., & Izumo, S. (2002). Direct Activation of Mitochondrial Apoptosis Machinery by c-Jun N-terminal Kinase in Adult Cardiac Myocytes. *Journal of Biological Chemistry*, 277(12), pp.10244-10250.

Apple, F.S., Christenson, R.H., Valdes, R. (1999). Simultaneous rapid measurement of whole blood myoglobin, creatine kinase MB, and cardiac troponin I by the triage cardiac panel for detection of myocardial infarction. *Clinical Chemistry*, 45(2), pp.199-205.

Arabadjiev, B., Petkova, R., Momchilova, A., Chakarov, S., & Pankov, R. (2012), Of mice and men differential mechanisms of maintaining the undifferentiated state in mESC and hESC, *Biodiscovery*, 3(1), pp.1-13.

Aronzon, C.M., Marino, D.J., Ronco, A.E., & Perez Coll, C.S. (2014). Differential toxicity and uptake of Diazinon on embryo-larval development of Rhinella arenarum. *Chemosphere*, 100(5), pp.50-56.

Ashkenazi, A., & Dixit, V. (1998). Death Receptors: Signaling and Modulation. *Science*, 281(5381), pp.1305-1308.

Atala, A. & Lanza, R.P. (2001). *Handbook of pesticide toxicology: Principles and agents*, Krieger R., Wayland J. & Hayes J. (ed.), San Diego, Academic Press, pp.215-235.

Atale, N., Gupta, K., & Rani, V. (2014). Protective effect of Syzygium cumini against pesticide-induced cardiotoxicity. *Environmental Science and Pollution Research International*, 21(13), pp.7956-7972.

Avasthi, S., Srivastava, R., & Singh, A. (2008). Stem cell: Past, present and future. *Internet Journal of Medical Update*, 3(1). pp.22-30.

Axelrad, J.C., Howard, C.V., & McLean, W.G. (2003). The effects of acute pesticide exposure on neuroblastoma cells chronically exposed to diazinon. *Toxicology*, 185(1-2), pp.67-78

Babuin, L., & Jaffe, A.S (2005). Troponin: The biomarker of choice for the detection of cardiac injury. *Canadian Medical Association Journal*, 173(10), pp. 1191-1202.

Baker, P.E., Cole, T.B., Cartwright, M., Suzuki, S.M., Thummel, K.E., Lin, Y.S., Co, A.L., Rettie, A.E., Kim, J.H., & Furlong, C.E. (2013). Identifying safer anti-wear triaryl phosphate additives for jet engine lubricants. *Chemico-Biological Interactions*, 203(1), pp.257-264.

Bakry, N.M., El-Rashidy, A.H., Eldefrawi, A.T., & Eldefrawi, M.E. (1988). Direct actions of organophosphate anticholinesterases on nicotinic and muscarinic acetylcholine receptors. *Journal of Biochemical Toxicology*, 3(4), pp.235-259.

Balaban, R.S., Bose, S., French, S.A. & Territo, P.R. (2003). Role of calcium in metabolic signaling between cardiac sarcoplasmic reticulum and mitochondria in vitro. *Cell Physiology*, 284(2), pp.285-293.

Barrett, K., & Jaward, F. (2012). A review of endosulfan, dichlorvos, diazinon, and diuron--pesticides used in Jamaica. *International Journal of Environmental Health Research*, 22(6), pp.481-99.

Barua, B., Pamula, M.C., & Hitchcock-DeGregori, S.E. (2011). Evolutionarily conserved surface residues constitute actin binding sites of tropomyosin. *Proceedings of the National Academy of Sciences,* 108(25), pp.10150-10155.

Barua, B., Winkelmann, D., White, H.D., & Hitchcock-DeGregori, S.E. (2012). Regulation of actin-myosin interaction by conserved periodic sites of tropomyosin. *Proceedings of the National Academy of Sciences of the United States of America*, 109(45), pp.18425-18430.

Bauer, K., Kratzer, M., Otte, M., de Quintana, K. L., Hagmann, J., Arnold, G. J., & Siess, W. (2000). Human CLP36, a PDZ-domain and LIM-domain protein, binds to alpha-actinin-1 and associates with actin filaments and stress fibers in activated platelets and endothelial cells. *Blood*, 96(13), pp.4236-4245.

Baskin, S. I., & Whitmer, M. P. (1991). The cardiac toxicolology of organophosphorous agents. In: *Principles of Cardiac Toxicology,* Boca Raton, CRC Press, pp.275-293.

Batalov I., & Feinberg A.W. (2015). Differentiation of Cardiomyocytes from human Pluripotent stem cells using Monolayer culture. *Biomarker Insights*, 10(1), pp.71-76.

Bowman, B. & Sans, W. (1983). Further water solubility determinations of insecticidal compounds. *Journal of Environmental Science and Health, Part B*, 18(2), pp.221-227.

Bernstein, B.W., & Bamburg, J.R. (1982). Tropomyosin binding to F-actin protects the F-actin from disassembly by brain actin-depolymerizing factor (ADF). *Cell Motility*, 2(1), pp.1-8.

Blin, G., Nury, D., Stefanovic, S., Neri, T., Guillevic, O., Brinon, B., Bellamy, V., Rücker-Martin, C., Barbry, P., Bel, A., Bruneval, P., Cowan, C., Pouly, J., Mitalipov, S., Gouadon, E., Binder, P., Hagege, A., Desnos, M., Renaud, J.-F., Menasche, P., & Puceat, M. (2010). A purified population of multipotent cardiovascular progenitors derived from primate pluripotent stem cells engrafts in postmyocardial infarcted nonhuman primates. *Journal of Clinical Investigation*, 120(4), pp.1125-1139.

Boggs, J.M. (2006). Myelin basic protein: a multifunctional protein. *Cellular and Molecular Life Science*, 63(17), pp.1945-1961.

Bogoyevitch, M.A., Gillespie-Brown, J., Ketterman, A.J., Fuller, S.J., Ben-Levy, R., Ashworth, A., Marshall, C.J., & Sugden, P.H. (1996). Stimulation of the stress-activated mitogen-activated protein kinase subfamilies in perfused heart. p38/RK mitogen-activated protein kinases and c-Jun N-terminal protein kinases are activated by ischemia/reperfusion. *Circulation Research*, 79(2), pp.162-173.

Borisov, A.B., Martynova, M.G., & Russel, M.W. (2008). Early incorporation of obscurin into nascent sarcomeres: Implication for myofibril assembly during cardiac myogenesis. *Histochemistry and Cell Biology*, 129, pp.463-478.

Bornfeldt, K.E. (1996). Platelet-derived growth factor stimulates protein Kinase A through a Mitogen-activated protein Kinase-dependent pathway in human arterial smooth muscle cells. *Journal of Biological Chemistry*, 271(1), pp.505-511.

Bozulic, L.D., Malik, M.T., Powell, D.W., Nanez, A., Link, A.J., Ramos, K.S., & Dean, W.L. (2007). Plasma membrane ca2+ ATPase associates with CLP36, α-actinin and actin in human platelets. *Thrombosis and Haemostasis*, 97(4), pp.587-597.

Braam, S.R., Tertoolen, L., van de Stolpe, A., Meyer, T., Passier, R., & Mummery, C.L. (2010). Prediction of drug-induced cardiotoxicity using human embryonic stem cell-derived cardiomyocytes. *Stem Cell Research*, 4(2), pp.107-116.

Ballantyne, B., & Marrs, T (1992). Clinical and eperimrntal toxicology of organophosphate and carbamates. Oxford, Butterworth-Heinemann, pp.3-27.

Branco, A.F., Pereira, S.L., Moreira, A.C., Holy, J., Sardao, V.A., & Oliveira, P.J. (2011). Isoproterenol cytotoxicity is dependent on the differentiation state of the cardiomyoblast H9c2 cell line. *Cardiovascular Toxicology*, 11(3), pp.191-203.

Branco, A.F., Pereira, S.P., Gonzalez, S., Gusev, O., Rizvanov, A.A., & Oliveira, P.J. (2015). Gene expression profiling of H9c2 Myoblast differentiation towards a cardiac-like Phenotype. *Plos One*, 10(6), pp.1-18.

Branco, A.F., Sampaio, S.F., Moreira, A.C., Holy, J., Wallace, K.B., Baldeiras, I., Oliveira, P.J., & Sardao, V.A. (2012). Differentiation-dependent Doxorubicin toxicity on H9c2 Cardiomyoblasts. *Cardiovascular Toxicology*, 12(4), pp.326-340.

Brazil, D.P., & Hemmings, B.A. (2001). Ten years of protein kinase B signalling: a hard Akt to follow. *Trends in Biochemistry science*, 26(11), pp.657-664.

Brill, D.M., Maisel, A.S., & Prabhu, R. (1984). Polymorphic ventricular tachycardia and other complex arrhythmias in organophosphate insecticide poisoning. *Journal of Electrocardiology*, 17(1), pp.97-102.

Brimijoin, S., & Koenigsberger, C. (1999). Cholinesterases in neural development: New findings and toxicologic implications. *Environmental Health Perspectives*, 107(1), pp.59-64.

Brogan, G.X, Hollander, J.E., & McCuskey, C.F. (1997). Evaluation of a new assay for cardiac troponin I vs creatine kinase–MB for the diagnosis of acute myocardial infarction. *Academic Emergency Medicine*, 4(1), pp.6-12.

Broschat, K.O. (1990). Tropomyosin prevents depolymerization of actin filaments from the pointed end. *Biochemistry,* 265(34), pp.21323-21329.

Brunet, A., Datta, S.R., & Greenberg, M.E. (2001). Transcription-dependent and -independent control of neuronal survival by the PI-3K-Akt signaling pathway. *Current Opinion in Neurobiology*, 11(3), pp.297-305.

Bubb, M.R, Senderowicz, A.M, Sausville, E.A., Duncan, K.L., & Korn, E.D. (1994). Jasplakinolide, a cytotoxic natural product, induces actin polymerization and competitively inhibits the binding of phalloidin to F-actin. *Journal of Biological Chemistry*, 269(21), pp.14869-14871.

Burridge, P.W., Keller, G., Gold, J.D., & Wu, J.C. (2012). Production of de novo Cardiomyocytes: Human Pluripotent stem cell differentiation and direct Reprogramming. *Cell Stem Cell*, 10(1), pp.16-28.

Burridge, P.W., Matsa, E., Shukla, P., Lin, Z.C., Churko, J.M., Ebert, A.D., & Wu, J.C. (2014). Chemically defined generation of human cardiomyocytes. *Nature Methods*, 11(8), pp.855-860.

Burridge, P.W., Keller, G., Gold, J.D., & Wu, J.C. (2012). Production of De Novo Cardiomyocytes: Human Pluripotent Stem Cell Differentiation and Direct Reprogramming. *Cell Stem Cell*, 10(1), pp.16-28.

Burridge, P.W., Matsa, E., Shukla, P., Lin, Z.C., Churko, J.M., Ebert, A.D., Lan, F., Diecke, S., Huber, B., Mordwinkin, N.M., Plews, J.R., Abilez, O.J., Cui, B., Gold, J.D., & Wu, J.C. (2014). Chemically defined generation of human cardiomyocytes. *Nature Methods*, 11(8), pp.855-860.

Cabello, G., Galaz, S., Botella, L., Calaf, G., Pacheco, M., Stockert, J., Villanueva, A., Canete, M., & Juarranz, A. (2003). The pesticide malathion induces alterations in actin cytoskeleton and in cell adhesion of cultured breast carcinoma cells. *International Journal of Oncology*, 23(3), pp.697-704.

Calore, E.E., Perez, N.M., & Herman, M.M. (2007). Morphometric studies of cardiac myocytes of rats chronically treated with an organophosphate. *Ecotoxicology and Environmental Safety*, 66(3), pp.447-450.

Cardona, D., Lopez-Granero, C., Canadas, F., Llorens, J., Flores, P., Pancetti, F., & Sanchez-Santed, F. (2013). Dose-dependent regional brain acetylcholinesterase and acylpeptide hydrolase inhibition without cell death after chlorpyrifos administration. *The Journal of Toxicological Sciences*, 38(2), pp.193-203.

Carey, J.L., Dunn, C., & Gaspari, R.J. (2013). Central respiratory failure during acute organophosphate poisoning. *Respiratory Physiology & Neurobiology*, 189(2), pp.403-410.

Carletti, E., Schopfer, L.M., Colletier, J.P., Froment, M.T., Nachon, F., Weik, M., Lockridge, O., & Masson, P. (2011). Reaction of Cresyl Saligenin phosphate, the Organophosphorus agent implicated in Aerotoxic syndrome, with human Cholinesterases: Mechanistic studies employing Kinetics, mass Spectrometry, and x-ray structure analysis. *Chemical Research in Toxicology*, 24(6), pp.797-808.

Carlson, K., & Ehrich, M. (1999). Organophosphorus Compound-Induced Modification of SH-SY5Y Human Neuroblastoma Mitochondrial Transmembrane Potential. *Toxicology and Applied pharmacology*, 160(1), pp.33-42.

Carlson, K., & Ehrich, M. (2001). Organophosphorus Compounds Alter Intracellular F-Actin Content in SH-SY5Y Human Neuroblastoma Cells. *Neurotoxicology*, 22(6), pp.819-827.

Carlson, K., Jortner, B.S., & Ehrich, M. (2000). Organophosphorus compound-induced apoptosis in SH-SY5Y human neuroblastoma cells. *Toxicology and Applied Pharmacology*, 168(2), pp.102-113.

Casida, J.E., & Quistad, G.B. (2005). Serine hydrolase targets of organophosphorus toxicants. *Chemeco-Biological Interaction*, 157(2), pp.277-283.

Caughlan, A., Newhouse, K., Namgung, U., & Xia, Z. (2004). Chlorpyrifos induces apoptosis in rat cortical neurons that is regulated by a balance between p38 and ERK/JNK MAP kinases. *Toxicological Sciences : An Official Journal of the Society of Toxicology*, 78(1), pp.125-134.

Chambers, J.E., & Levi, P.E. (1992). *Organophosphates: Chemistry, Fate and Effects*. San Diego, Academic Press, pp.3-18.

Chambers, J.E. (2004). Organophosphates, Serine Esterase Inhibition, and Modeling of Organophosphate Toxicity. *Toxicological Sciences*, 77(2), pp.185-187.

Chambers, J.E., & Chambers, H.W. (1989). Oxidative desulfuration of chlorpyrifos, chlorpyrifos-methyl, and leptophos by rat brain and liver. *Journal Biochemistry Toxicol*. 4(3), pp.201-203.

Chambon, P. (1996). A decade of molecular biology of retinoic acid receptors. *Federation of American Societies for Experimental Biology journal*, 10(9), pp.940-954.

Chang, P.A., & Wu, Y.J. (2010). Neuropathy target esterase: An essential enzyme for neural development and axonal maintenance. *The International Journal of Biochemistry & Cell Biology*, 42(5), pp.573-575.

Chemnitius, J.M., Sadowski, R., Winkel, H., & Zech, R. (1999). Organophosphate inhibition of human heart muscle cholinesterase isoenzymes. *Chemico-Biological Interactions*, 119(120), pp.183-192.

Chen, J., Kubalak, S.W., & Chien, K.R. (1998). Ventricular muscle restricted targeting of the RXRα genes reveals a non-cell autonomous requirement s in cardiac chamber morphogenesis. *Development*, 125(10), pp.1943-1949.

Chen, J.X., Xu, L.L., Mei, J.H., Yu, X.B., Kuang, H.B., Liu, H.Y., Wu, Y.J., & Wang, J.L. (2012). Involvement of neuropathy target esterase in tri-ortho-cresyl phosphate-induced testicular spermatogenesis failure and growth inhibition of spermatogonial stem cells in mice. *Toxicology Letters*, 211(1), pp.54-61.

Chen, Y.R., & Tan, T.H. (1998). Inhibition of the c-Jun N-terminal kinase (JNK) signaling pathway by curcumin. *Oncogene*, 17(2), pp.173-178.

Cheng, J., Godwin, A., Bellacosa, A., Taguchi, T., Franke, T., Hamilton, T., Tsichlis, P., & Testa, J. (1992). AKT2, a putative oncogene encoding a member of a subfamily of protein-serine/threonine kinases, is amplified in human ovarian carcinomas. *Proceedings of the National Academy of Sciences*, 89(19), pp.9267-9271.

Cherian, M.A., Roshini, C., Peter, J.V, & Cherian, A.M. (2005). Oximes in organophosphorus poisoning, *Veterinary Record*, 7(4), pp.155-163.

Chicheportiche, Y., Bourdon, P., Xu, H., Hsu, Y., Scott, H., Hession, C., Garcia, I., & Browning, J. (1997). TWEAK, a new secreted ligand in the tumor necrosis factor family that weakly induces apoptosis. *Journal of Biological Chemistry*, 272(51), pp.32401-32410.

Choudhary, S., & Gill, K.D. (2001). Protective effect of nimodipine on dichlorvos-induced delayed neurotoxicity in rat brain. *Biochemical Pharmacology*, 62(9), pp.1265-1272.

Choudhary, S., Verma, K., Raheja, G., Kaur, P., Joshi, K., & Gill, D. (2006). The l-type calcium channel blocker Nimodipine mitigates Cytoskeletal proteins Phosphorylation in Dichlorvos-Induced delayed Neurotoxicity in rats. *Basic and Clinical Pharmacology and Toxicology*, 98(5), pp.447-455.

Classen, W., Gretener, P., Rauch, M., Weber,E., & Krinke, G.J. (1996). Susceptibility of various areas of the nervous system of hens to TOCP-induced delayed neuropathy. *Neurotoxicology*, 17(3-4), pp.597-604.

Clayton, E., Sammons, R., Stark, C., Hodges, R., & Lord, M. (2010). Differential regulation of unconventional fission yeast myosins via the actin track. *Current Biology*, 20(16), pp.1423-1431.

Colovic, M., Krstic, D., Petrovic, S., Leskovac, A., Joksic, G., Savic, J., Franko, M., Trebse, P., & Vasic, V. (2010). Toxic effects of diazinon and its photodegradation products. *Toxicology Letters*, 193(1), pp.9-18.

Comelli, M., Domenis, R., Bisetto, E., Contin, M., Marchini, M., Ortolani, F., Tomasetig, L., & Mavelli, I. (2011). Cardiac differentiation promotes mitochondria development and ameliorates oxidative capacity in H9c2 cardiomyoblasts, *Mitochondrion*, 11(2), pp.315-326.

Cory, S., & Adams, J.M. (2002). The Bcl2 family: regulators of the cellular life-or-death switch. *Nature Reviews Cancer*, 2(9), pp.647-656.

Costa L.G., Li, W.F., Richter, R.J., Cole, T., Guizzetti, M., & Furlong, C.E. (2003). PON1 as a biomarker of susceptibility for organophosphate toxicity. *Biomarkers*, 8(1), pp.1-12.

Costa, L.G. (2006). Current issues in organophosphate toxicology. *International Journal of Clinical Chemistry*, 366(1-2), pp.1-13.

Cox, C. (2000). Diazinon: Toxicolgy, *Journal of Pesticide Reform*, 20(2), pp.15-21.

Crumpton, T.L., Seidler, F.J., & Slotkin, T.A. (2000). Developmental neurotoxicity of chlorpyrifos in vivo and in vitro: effects on nuclear transcription factor involved in cell replication and differentiation. *Brain Research*, 857(1-2), pp.87-98.

Das, K.P., & Barone, S. (1999). Neuronal differentiation in PC12 cells is inhibited by Chlorpyrifos and its metabolites: Is Acetylcholinesterase inhibition the site of action?. *Toxicology and Applied Pharmacology*, 160(3), pp.217-230.

Davies, S.P., Reddy, H., Caivano, M., & Cohen, P. (2000). Protein kinase inhibitors. *Biochemistry Journal*, 351(1), pp.95-105.

Debosch, B., Treskov, I., Lupu, T.S., Weinheimer, C., Kovacs, A., Courtois, M., & Muslin, A.J. (2006). Akt1 is required for physiological cardiac growth. *Circulation*, 113(17), pp.2097-2104.

Decker, R.S., Rines, A.K., Nakamura, S., Naik, T.J., Wassertsrom, J.A., & Ardehali, H. (2009). Phosphorylation of contractile proteins in response to alpha and beta-adrenergic stimulation in neonatal cardiomyocytes. *Translational Research*, 155(1), pp.27-34.

Dell'Era, P., Benzoni, P., Crescini, E., Valle, M., Xia, E., Consiglio, A., & Memo, M. (2015). Cardiac disease modeling using induced pluripotent stem cell-derived human cardiomyocytes. *World Journal Stem Cells,* 7(2), pp.329-342.

Demorais, S., Wilkinson, G.R., Blaisdell, J., Nakamura, K., Meyer, U.A., & Goldstein, J.A. (1994). The major genetic defect responsible for the polymorphism of S-mephenytoin metabolism in humans. *Journal Biological Chemistry*, 269(22), pp.15419-15422.

Derijard, B., Hibi, M., Wu, I.H., Barrett, T., Su, B., Deng, T., Karin, M., & Davis, R.J. (1994). JNK1: a protein kinase stimulated by UV light and Ha-Ras that binds and phosphorylates the c-Jun activation domain. *Cell*, 76(6), pp.1025-1037.

Desouza, M., Gunning, P.W., & Stehn, J.R. (2012). The actin cytoskeleton as a sensor and mediator of apoptosis. *Bio-Architecture*, 2(3), pp.75-87.

Dhanasekaran, D.N., & Johnson, G.L. (2007). MAPKs: function, regulation, role in cancer and therapeutic targeting. *Oncogene*, 26(22), pp.3097-3099.

Dhanasekaran, D.N., & Reddy, E.P. (2008). JNK signaling in apoptosis. *Oncogene*, 27(48), pp. 6245-51.

Dillon, R.L., White, D.E., & Muller, W.J. (2007). The phosphatidyl inositol 3-kinase signaling network: implications for human breast cancer. *Oncogene*, 26(9), pp.1338-1345.

Dimmeler, S., Burchfield J., & Zeiher A.M. (2008). Cell-based therapy of myocardial infarction. *Arteriosclerosis, Thrombosis and Vascular Biology*,28,(2), pp.208-216.

Duester, G. (2013). Retinoid signaling in control of progenitor cell differentiation during mouse development. *Seminars in Cell and Developmental Biology*, 24(10-12), pp.694-700.

Dyer, L.A., Makadia, F.A., Scott, A., Pegram, K., Hutson, M.R., & Kirby, M.L. (2010). BMP signaling modulates hedgehog-induced secondary heart field proliferation. *Developmental Biology*, 348(2), pp.167-176.

Eaton, D.L., Daroff, R.B., Autrup, H., Bridges, J., Buffler, P., Costa, L.G., Coyle, J., McKhann, G., Mobley, W.C., Nadel, L., Neubert, D., Schulte-Hermann, R., & Spencer, P.S. (2008). Review of the toxicology of Chlorpyrifos with an emphasis on human exposure and Neurodevelopment. *Critical Reviews in Toxicology*, 38(2), pp.1-125.

Eckerson, H.W., Wyte, C.M., & LaDu, B.N. (1983). The human serum paraoxonase/arylesterase polymorphism. *American Journal of Human Genetics,* 35(6), pp.1126-1138.

Eddleston, M., Buckley, N., Eyer, P., & Dawson, A.H. (2008). Management of acute organophosphorus pesticide poisoning. *Lancet*, 371(9612), pp.597-607.

Ehrich, M., & Jortner, B.S. (2010). Chapter 69 Organophosphorus-Induced delayed neuropathy. In: *Handbook of Pesticide Toxicology*, pp.1479-1504.

Ehrich, M. (1997). Acetylcholinesterase and neuropathy target Esterase inhibitions in neuroblastoma cells to distinguish Organophosphorus compounds causing acute and delayed neurotoxicity. *Fundamental and Applied Toxicology*, 38(1), pp.55-63.

Ehrich, M., & Jortner, B. S. (2001). Delayed Neuropathy. In: *Handbook of Pesticide Toxicology*, Elsevier, 2, 987-1012.

Ehler E., & Perriard J.C (2000). Cardiomyocyte Cytoskeleton and Myofibrillogenesis in Healthy and Diseased Heart. *Herat Failure Reviews*, 5(3), pp.259-269.

El-Fawal, H.A., & McCain, W.C. (2008). Antibodies to neural proteins in organophosphorus-induced delayed neuropathy (OPIDN) and its amelioration. *Neurotoxicology and Teratology*, 30(3), pp.161-166.

El-Fawal, H.A., Correll, L., Gay, L., & Ehrich, M. (1990). Protease activity in brain, nerve, and muscle of hens given neuropathy-inducing organophosphates and a calcium channel blocker. *Toxicology Applied Pharmacology*, 103(1), pp.133-142.

El-Fawal, H.A., & Ehrich, M.F. (1993). Calpain activity in Organophosphorus-induced delayed neuropathy (OPIDN): Effects of a Phenylalkylamine calcium channel blocker. Annals of the New York *Academy of Sciences*, 679(1), pp.325-329.

Ellis, C.E., Naicker, D., Basson, K.M., Botha, C.J., Meintjes, R., & Schultz, R.A. (2010). Cytotoxicity and ultrastructural changes in H9c2(2-1) cells treated with pavetamine, a novel polyamine. *Toxicon : Official Journal of the International Society on Toxinology*, 55(1), pp.12-19.

Elmore, S. (2007). Apoptosis: a review of programmed cell death. *Toxicological Pathology*, 35(4), pp.495-516.

Elersek, T., & Filipic, M. (2011). Organophosphorous Pesticides: Mechanisms of Their Toxicity. *National Institute of Biology*, 12(2)*,* pp.256-*245.*

Erices, A., Conget, P., & Minguell J.J. (2000). Mesenchymal progenitor cells in human umbilical cord blood. *British Journal of Haematology*, 109(1), pp.235-242.

Eskenazi, B., Harley, K., Bradman, A., Weltzien, E., Jewell, N.P., Barr, D.B., Furlong, C.E., & Holland, N.T. (2004). Association of in utero organophosphate pesticide exposure and fetal growth and length of gestation in an agricultural population. *Environmental Health Perspective*, 112(10), pp.1116-1124.

Estevan, C., Vilanova, E., & Sogorb, M.A. (2013). Chlorpyrifos and its metabolites alter gene expression at non-cytotoxic concentrations in D3 mouse embryonic stem cells under in vitro differentiation: Considerations for embryotoxic risk assessment. *Toxicology Letters*, 217(1), pp.14-22.

Fagnou, D.D., & Tuchek J.M., (1995). The biochemistry of learning and memory. *Molecular Cell Biochemistry*, 149(150), pp.279-286.

Fenske, R.A., Lu, C., Barr, D., & Needham, L. (2002). Children's exposure to chlorpyrifos and parathion in an agricultural community in central Washington State. *Enviromental Health Perspective*, 110(5), pp.549-553.

Ferrandi, C., Ballerio, R., Gaillard, P., Giachetti, C., Carboni, S., Vitte, P.A., Gotteland, J.P. & Cirillo, R. (2004). Inhibition of c-jun n-terminal kinase decreases cardiomyocyte apoptosis and infarct size after myocardial ischemia and reperfusion in anaesthetized rats. *British Journal of Pharmacology*, 142(6), pp.953-960.

Ferrans, V.J., Hibbs, R.G., Walsh, J.J., & Burch, G.E. (1969). Histochemical and electron microscopical studies on the cardiac necroses produced by sympathomimetic agents. *Annals of the New York Academy of Sciences* ,156(5) , pp.309-332.

Flaskos, J. (2012). The developmental neurotoxicity of organophosphorus insecticides: A direct role for the oxon metabolites. *Toxicology Letters*, 209(1), pp.86-93.

Flaskos, J., Harris, W., Sachana, M., Munoz, D., Tack, J., & Hargreaves, A.J. (2007). The effects of diazinon and cypermethrin on the differentiation of neuronal and glial cell lines. *Toxicology and Applied Pharmacology*, 219(2-3), pp.172-180.

Flaskos, J., McLean, W.G., & Hargreaves, A.J. (1994). The toxicity of organophosphate compounds towards cultured PC12 cells. *Toxicology Letters*. 70(1), pp.71-76.

Flaskos, J., McLean, W.G., Fowler, M.J., & Hargreaves, A.J. (1998). Tricresyl phosphate inhibits the formation of axon-like processes and disrupts neurofilaments in cultured mouse N2a and rat PC12 cells. *Neuroscience Letters*, 242(2), pp.101-104.

Flaskos, J., Nikolaidis, E., Harris, W., Sachana, M., & Hargreaves, A.J. (2011). Effects of sub-lethal neurite outgrowth inhibitory concentrations of chlorpyrifos oxon on cytoskeletal proteins and acetylcholinesterase in differentiating N2a cells. *Toxicology and Applied Pharmacology*, 256(3), pp.330-336.

Flucher, B.E. & Franzini-Armstrong, C. (1996). Formation of junctions involved in excitation-contraction coupling in skeletal and cardiac muscle. *Proceedings of the National Academy of Sciences,* 93(15), pp.8101-8106.

Foldes, G., Mioulane, M., Wright, J.S., Liu, A.Q., Novak, P., Merkely, B., Gorelik, J., Schneider, M.D., Ali, N.N., & Harding, S.E. (2011). Modulation of human embryonic stem cell-derived cardiomyocyte growth: A tested for studying human cardiac hypertrophy?. *Journal of Molecular and Cellular Cardiology*, 50(2), pp.367-376.

Fotakis, G., & Timbrell, J.A. (2006). In vitro cytotoxicity assays: Comparison of LDH, neutral red, MTT and protein assay in hepatoma cell lines following exposure to cadmium chloride. *Toxicology Letters*, 160(2), pp.171-177.

Fowler, M.J., Flaskos, J., McLean, W.G., & Hargreaves, A.J. (2008). Effects of neuropathic and non-neuropathic isomers of tricresyl phosphate and their microsomal activation on the production of axon-like processes by differentiating mouse N2a neuroblastoma cells. *Journal of Neurochemistry*, 76(3), pp.671-678.

Franke, C., Studinger, G., Berger, G., Böhling, S., Bruckmann, U., Cohors-Fresenborg, D. and Johncke, U. (1994). The assessment of bioaccumulation. *Chemosphere*, 29(7), pp.1501-1514.

Freed, D.H., Moon, M.C., Borowiec, A.M., Jones, S.C., Zahradka, P., & Dixon, I.M. (2003). Cardiotrophin-1: Expression in experimental myocardial infarction and potential role in post-MI wound healing. *Molecular and Cellular Biochemistry*, 254(1-2), pp.247-256.

Fu, M., Schulze, W., Wallukat, G., Hjalmarson, A., & Hoebeke, J. (1995). Functional epitope analysis of the second extracellular loop of the human heart muscarinic acetylcholine receptor. *Journal of Molecular and Cellular Cardiology*, 27(1), pp. 427-436.

Gallo MA & Lawryk, N.J. (1991). Organic phosphorus pesticides. Hayes, W.J., & Laws E.R. (ed) In: *Handbook of Pesticide Toxicology*, New York, Academic Press, 2, pp.917-1123.

Gassanov, N., Er, F., Zagidullin, N., Jankowski, M., Gutkowska, J., & Hoppe, U. C. (2008). Retinoid acid-induced effects on atrial and pacemaker cell differentiation and expression of cardiac ion channels. Differentiation, *Research in Biological Diversity*, 76(9), pp.971-980.

Gearhart, D.A., Sickles, D.W., Buccafusco, J.J., Prendergast, M.A., & Terry Jr., A.V. (2007).Chlorpyrifos, chlorpyrifos-oxon, and diisopropylfluorophosphate inhibit kinesin- dependent microtubule motility. *Toxicology and Applied Pharmacology*, 218(1), pp.20-29.

Gendron, T.F., & Petrucelli, L. (2009). The role of tau in neurodegeneration. *Molecular Neurodegeneration*, 4(1), pp.13-19.

Ginty, D. (2002). Retrograde neurotrophin signaling: Trk-ing along the axon. *Current Opinion in Neurobiology*, 12(3), pp.268-274.

Glynn, P. (2000). Neural development and neurodegeneration: Two faces of neuropathy target Esterase. *Progress in Neurobiology*, 61(1), pp.61-74.

Goin, J.C., Borda, E., Perez Leiros, C., Storino, R., & Sterin-Borda, L. (1994). Identification of antibodies with muscarinic cholinergic activity in human Chagas' disease: Pathological implications. *Journal of the Autonomic Nervous System*, 47(1-2), pp.45-52.

Gokalp, O., Buyukvanlı, B., Cicek, E., Ozer, M.K., Koyu, A., Altuntas, I. & Koylu, H. (2005). The effects of diazinon on pancreatic damage and ameliorating role of vitamin E and vitamin C. *Biochemistry and Physiology*, 81(2), pp.123-128.

Gown, A.M., & Willingham, M.C. (2002). Improved detection of Apoptotic cells in archival Paraffin sections: Immunohistochemistry using antibodies to cleaved Caspase 3. *Journal of Histochemistry and Cytochemistry*, 50(4), pp.449-454.

Greenbaum, D.C., Arnold, W.D., Lu, F., Hayrapetian, L., Baruch, A., Krumrine, J., Toba, S., Chehade, K., Brömme, D., Kuntz, I.D., & Bogyo, M. (2002). Small molecule affinity fingerprinting. *Chemistry and Biology*, 9(10), pp.1085-1094.

Grigoryan, H., & Lockridge, O. (2009). Nanoimages show disruption of tubulin polymerization by chlorpyrifos oxon: implications for neurotoxicity. *Toxicology and Applied Pharmacology*, 240(2), pp.143-148.

Grigoryan, H., Schopfer, L.M., Thompson, C.M., Terry, A.V, Masson, P., & Lockridge, O. (2008). Mass spectrometry identifies covalent binding of soman, sarin, chlorpyrifos oxon, diisopropyl fluorophosphate, and FP-biotin to tyrosines on tubulin: a potential mechanism of long term toxicity by organophosphorus agents. *Chemico-Biological Interactions*, 175(1-3), pp.180-186.

Gross, A., McDonnell, J.M., & Korsmeyer, S.J. (1999). BCL-2 family members and the mitochondria in apoptosis. *Genes and Development*, 13(15), pp.1899-1911.

Guay, J., Lambert, H., Gingras, B.G., Lavoie J.N., Huot J., & Landry J. (1997). Regulation of actin filament dynamics by p38 MAPK-mediated phosphorylation of heat shock protein 27. *Journal of Cell Science*, 110, pp.357-368.

Gunning, P., O'neill, G., & Hardeman, E. (2008). Tropomyosin-Based regulation of the Actin Cytoskeleton in time and space. *Physiological Reviews*, 88(1), pp.1-35.

Guo-Ross, S. (1998). Elevation of cerebral proteases after systemic administration of aluminum. *Neurochemistry International*, 33(3), pp.277-282.

Gupta, M.K., Illich, D.J., Gaarz, A., Matzkies, M., Nguemo, F., Pfannkuche, K., Liang, H., Classen, S., Reppel, M., Schultze, J.L., Hescheler, J., & Saric, T. (2010). Global transcriptional profiles of beating clusters derived from human induced pluripotent stem cells and embryonic stem cells are highly similar. *Biomed Central Developmental Biology*, 10(1), pp.98-117.

Gupta, R. (2006). *Toxicology of organophosphate and carbamate compounds*. Amsterdam,Elsevier Academic Press, pp.183.

Gupta, R.C., & Milatovic, D. (2012). Organophosphates and carbamates. *Veterinary Toxicology*, 5(6), pp.573-585.

Gupta, S., Barrett, T., Whitmarsh, A.J., Cavanagh, J., Sluss, H.K., Derijard, B., & Davis, R.J. (1996). Selective interaction of JNK protein kinase isoforms with transcription factors. *European Molecular Biology Organization Journal*, 15(6), pp.2760-2770.

Haas, P.J., Buck, W.B., Hixon, J.E., Shanks, R.D.,Wagner, W.C., Weston, P.G., & Whitmore, H. L. (1983). Effect of chlorpyrifos on Holstein steers and testosterone-treated Holstein bulls. *American Journal of Veterinary Research*, 44(5), pp.879-881.

Hamm, J.T. (2001). Increasing uptake and Bioactivation with development positively modulate Diazinon toxicity in early life stage Medaka (Oryzias latipes). *Toxicological Sciences*, 61(2), pp.304-313.

Hamm, J.T., & Hinton, D.E. (2000). The role of development and duration of exposure to the embryotoxicity of diazinon. *Aquatic Toxicology*, 48(3), pp.403-418.

Handy, R.D., Abd-El Samei, H.A., Bayomy, M.F.F., Mahran, A.M., Abdeen, A.M., & El-Elaimy, E.A. (2002). Chronic diazinon exposure: Pathologies of spleen, thymus, blood cells, and lymph nodes are modulated by dietary protein or lipid in the mouse. *Toxicology*, 172(1), pp.13-34.

Hargreaves, A.J. (2012). Neurodegenerations Induced by Organophosphorous Compounds. In: Chapter Neurodegenerative Diseases. In: *series Advances in Experimental Medicine and Biology,* 724(2) pp, 189-204.

Hargreaves, A.J., Fowler, M.J., Sachana, M., Flaskos, J., Bountouri, M., Coutts, I.C., Glynn, P., Harris, W., & Graham McLean, W. (2006). Inhibition of neurite outgrowth in differentiating mouse N2a

neuroblastoma cells by phenyl saligenin phosphate: Effects on MAP kinase (ERK 1/2) activation, neurofilament heavy chain phosphorylation and neuropathy target esterase activity. *Biochemical Pharmacology*, 71(8), pp.1240-1247.

Hariri, A.T., Moallem, S.A., Mahmoudi, M., Memar, B., & Hosseinzadeh, H. (2010) 'Sub-acute effects of diazinon on biochemical indices and specific biomarkers in rats: Protective effects of crocin and safranal. *Food and Chemical Toxicology*, 48(10), pp.2803-2808.

Harris, W., Munoz, D., Bonner, P. L., & Hargreaves, A.J. (2009). Effects of phenyl saligenin phosphate on cell viability and transglutaminase activity in N2a neuroblastoma and HepG2 hepatoma cell lines. *Toxicology in Vitro*, 23(8), pp.1559-63.

Hasan, M., Maitra, S.C., & Ali, S.F. (1979). Organophosphate pesticide DDVP-induced alterations in the rat cerebellum and spinal cord an electron microscopic study. *Experimental Pathology*, 17(2), pp.88-94.

He, J.Q., Ma, Y., Lee Y, Lee, Y., Thomson, J.A., & Kamp, T. J.(2003). Human embryonic stem cells develop into multiple types of cardiac Myocytes: Action potential characterization. *Circulation Research*, 93(1), pp.32-39.

Hendrix, M.J., Seftor, E.A., Seftor, R.E., & Trevor, K.T. (1997). Experimental co-expression of vimentin and keratin intermediate filaments in human breast cancer cells results in phenotypic interconversion and increased invasive behaviour. *American Journal of Pathology*, 150(2), pp.483-495.

Hescheler, J., Meyer, R., Plant, S. Krautwurst, D., Rosenthal, W., & Schultz, G. (1991). Morphological, biochemical, and electrophysiological characterization of a Clonal Cell (H9c2) Line From Rat Heart. *Circulation Research*, 69(3), pp.1476-1487.

Hetman, M., & Xia, Z. (2000). Signaling pathways mediating anti-apoptotic action of neurotrophins. *Acta Neurobiologiae Experimentalis*, 60(8), pp.531-545.

Hida, N., Nishiyama, N., Miyoshi, S., Kira, S., Segawa, K., Uyama, T., Mori, T., Miyado, K., Ikegami, Y., Cui, C., Kiyono, T., Kyo, S., Shimizu, T., Okano, T., Sakamoto, M., Ogawa, S., & Umezawa, A. (2008). Novel cardiac precursor-like cells from human menstrual blood-derived Mesenchymal cells. *Stem Cells*, 26(7), pp.1695-1704.

Hill, M.M., Adrain, C., Duriez, P.J., Creagh, E.M., & Martin, S.J. (2004). Analysis of the composition, assembly kinetics and activity of native Apaf-1 apoptosomes. *Embo Journal*, 23, pp.2134-2145.

Hill, R., Head, S., Baker, S., Gregg, M., Sheely, D., Baily, S., Williams, C., Sampson, E., & Needham, L. (1995) Pesticide residues in urine of adults living in the United States; reference range concentrations. *Environmental Research*, 71(8), pp.88-108.

Hollweck, T. (2011). Cardiac differentiation of human Wharton's jelly stem cells experimental comparison of protocols. *The Open Tissue Engineering and Regenerative Medicine Journal*, 4(1), pp.95-102.

Honda, M., Hamazaki, T.S., Komazaki, S., Kagechika, H., Shudo, K., & Asashima, M. (2005). RXR agonist enhances the differentiation of cardiomyocytes derived from embryonic stem cells in serum-free conditions. *Biochemical and Biophysical Research Communications*, 333(4), pp.1334-1340.

Hoogduijn, M.J., Rakonczay, Z., & Genever, P.G. (2006). The effects of Anticholinergic insecticides on human Mesenchymal stem cells. *Toxicological Sciences*, 94(2), pp.342-350.

Hosseinzadeh, L., Behravan, J., Mosaffa, F., Bahrami, G., Bahrami, A., & Karimi, G. (2011). Curcumin potentiates doxorubicin-induced apoptosis in H9c2 cardiac muscle cells through generation of reactive oxygen species. *Food and Chemical Toxicology*, 49(5), pp.1102-1109.

Howard, A.S., Bucelli, R., Jett, D. , Bruun, D., Yang, D., & Lein, P.J. (2005). Chlorpyrifos exerts opposing effects on axonal and dendritic growth in primary neuronal cultures. *Toxicology and Applied Pharmacology*, 207(2), pp.112-124.

Howard, M.D., & Pope, C.N. (2002). In vitro effects of chlorpyrifos, parathion, methylparathion and their oxons on cardiac muscarinic receptor binding in neonatal and adult rats. *Toxicology*, 170(8), pp.1-10.

Huang, S., Ma, J., Liu, X., Zhang, Y., & Luo, L. (2011). Retinoic acid signaling sequentially controls visceral and heart laterality in zebrafish. *The Journal of Biological Chemistry*, 286(32), pp.28533-28543.

Huangfu, D., Osafune, K., Maehr, R., Guo, W., Eijkelenboom, A., Chen, S., Muhlestein, W., & Melton, D.A. (2008). Induction of pluripotent stem cells from primary human fibroblasts with only Oct4 and Sox2. *Nature Biotechnology*, 26(11), pp.1269-1275.

Huff, R.A., Corcoran, J.J., Anderson, J.K., & Abou-Donia, M.B. (1994). Chlorpyrifos oxon binds directly to muscarinic receptors and inhibits cAMP accumulation in rat striatum. *The Journal of Pharmacology and Experimental Therapeutics*, 289(3), pp.329-335.

Huot, J., Lambert, H., Lavoie, J.N., Guimond, A., Houle, F., & Landry, J. (1995). Characterization of 45-kDa/54-kDa HSP27 Kinase, a stress-sensitive Kinase which may activate the Phosphorylation-Dependent protective function of mammalian 27-kDa heat-shock protein HSP27. *European Journal of Biochemistry*, 227(1-2), pp.416-427.

Hynx, D., & Hemmings, B.A. (2004). Physiological functions of protein kinase B/Akt. *Biochemical Society Transactions*, 32(2), pp.350-354.

Igney, F.H., & Krammer, P.H. (2002). Death and anti-death: tumour resistance to apoptosis. *Nature Reviews Cancer*, 2(4), pp.277-288.

Inui, K., Mitsumori K., Harada, T., & K. Maita (1993). Quantitative analysis of neuronal damage induced by Tri-ortho-cresyl phosphate in Wistar rats. *Toxicological Sciences*, 20(1), pp.111-119.

Isenberg, G., & Klockner, U. (1982). Calcium tolerant ventricular myocytes prepared by preincubation in a "KB medium". *European Journal of Physiology*, 395(1), pp.6-18.

Jeffery, D.A., & Bogyo, M. (2003). Chemical proteomics and its application to drug discovery. *Current Opinion in Biotechnology*, 14(1), pp.87-95.

Jett, D.A., Abdallah, E.A., El-Fakahany, E.E., Eldefrawi, M.E., & Eldefrawi, A.T. (1991). High-affinity activation by paraoxon of a muscarinic receptor subtype in rat brain striatum. *Pesticide Biochemistry and Physiology*, 39(2), pp.149-157.

Jha, V., Garcia-Garcia, G., Iseki, K., Li, Z., Naicker, S., Plattner, B., Saran, R., Wang, A.Y., & Yang, C.W. (2013). Chronic kidney disease: global dimension and perspectives. *Lancet*, 382(9888), pp.260-272.

Jia, Z., & Misra, H.P. (2007). Exposure to mixtures of endosulfan and zineb induces apoptotic and necrotic cell death in SH-SY5Y neuroblastoma cells, in vitro. *Journal of Applied Toxicology*, 27(5), pp.434-446.

Jiang, W., Duysen, E.G., Hansen, H., Shlyakhtenko, L., Schopfer, L.M., & Lockridge, O. (2010). Mice treated with chlorpyrifos or chlorpyrifos oxon have organophosphorylated tubulin in the brain and

disrupted microtubule structures, suggesting a role for tubulin in neurotoxicity associated with exposure to organophosphorus agents. *Toxicological Sciences*, 115(1), pp.183-193.

Johnson, G.L., & Lapadat, R. (2002). Mitogen-Activated Protein Kinase Pathways Mediated by ERK , JNK, and p38 Protein Kinases The Protein Kinase Complement of the Human Genome. *Science,* 298(5600), pp.1911-1912.

Jordaan, M.S., Reinecke, S.A., & Reinecke, A.J. (2013). Biomarker responses and morphological effects in juvenile tilapia Oreochromis mossambicus following sequential exposure to the organophosphate azinphosmethyl. *Aquatic Toxicology*, 144(2), pp.133-140.

Jortner, B.S., & Ehrich, M. (1987). Neuropathological effects of phenyl saligenin phosphate in chickens. *Neurotoxicology*, 8(8), pp.303-314.

Jortner, B.S., Perkins, S.K., & Ehrich, M. (1999). Immunohistochemicals study of phosphorylated neurofilaments during the evolution of organophosphorus ester-induced delayed neuropathy (OPIDN). *Neurotoxicology*, 20(5), pp.971-976.

Jung, D.H., & Kim, D.H. (2004). Characterization of isoforms and genomic organization of mouse calumenin. *Gene*, 327(2), pp.185-194.

Kadivar, M., Khatami, S., Mortazavi, Y., Shokrgozar, M.A., Taghikhani, M., & Soleimani, M. (2006). In vitro cardiomyogenic potential of human umbilical vein-derived mesenchymal stem cells. *Biochemical and Biophysical Research Communications*, 340(2), pp.639-647.

Kalender, Y., Kalender, S., Uzunhisarcikli, M., Ogutcu, A., Açikgoz, F., & Durak, D. (2004). Effects of endosulfan on B cells of Langerhans islets in rat pancreas. *Toxicology*, 200(5), pp.205-211.

Kallunki, T., Su, B., Tsigelny, I., Sluss, H.K., Derijard, B., Moore, G., Davis, R. & Karin, M. (1994). JNK2 contains a specificity-determining region responsible for efficient c-jun binding and phosphorylation. *Genes and Development*, 8(24), pp.2996-3007.

Kamiya, H., Okumura, K., Ito, M., Saburi, Y., Tomida, T., Hayashi, K., Matsui, H., & Hayakawa, T. (2001). Calcineurin inhibitor attenuates cardiac hypertrophy due to energy metabolic disorder. *The Canadian Journal of Cardiology*, 17(12), pp.1292-1298.

Kang, J.O., & Sucov, H.M. (2005). Convergent proliferative response and divergent morphogenic pathways induced by epicardial and endocardial signaling in fetal heart development. *Mechanisms of Development*, 122(1), pp.57-65.

Kaplan, D. (1995). Life and death in the nervous system: Role of Neurotrophic factors and their receptors. *Elsevier Science* ,73(2), pp.37-53.

Kappers, W., Edwards, R.J., Murray, S., & Boobis, R. (2001). Diazinon is activated by CYP2C19 in human liver. *Toxicology and Applied Pharmacology*, 177(1), pp.68-76.

Karalliedde, L. (1999). Organophosphorous poisoning and anesthesia. *Anaesthesia*, 54(3), pp.1073-1088.

Karami-Mohajeri, S., & Abdollahi, M. (2013). Mitochondrial dysfunction and organophosphorus compounds. *Toxicology and Applied Pharmacology*, 270(1), pp.39-44.

Karki, P., Ansari, J., Bhandary, S., & Koirala, S. (2004). Cardiac and electrocardiographical manifestations of acute organophosphate poisoning. *Singapore Medical Journal*, 45(8), pp.385-389.

Kataoka, T., Schroter, M., Hahne, M., Schneider, P., Irmler, M., Thome, M., Froelich, C. J., & Tschopp, J. (1998). FLIP prevents apoptosis induced by death receptors but not by perforin/granzyme B, chemotherapeutic drugs, and gamma irradiation. *Journal of Immunology*. 161(8), pp.3936-3942.

Katz, A. (1992). Excitation-contraction coupling and cardiac contractile force Bers, D. M. Kluwer, Dordrecht. *Journal of Molecular and Cellular Cardiology*, 24(1), p.105-107.

Kaur, P., Radotra, B., Minz, R.W., & Gill, K.D., (2007). Impaired mitochondrial energy metabolism and neuronal apoptotic cell death after chronic dichlorvos (OP) exposure in rat brain. *Neurotoxicology*, 28(6), pp.1208-1219.

Kehat, I., Kenyagin-Karsenti, D., Snir, M., Segev, H., Amit, M., Gepstein, A., Livne, E., Binah, O., Itskovitz-Eldor, J., & Gepstein, L. (2001). Human embryonic stem cells can differentiate into myocytes with structural and functional properties of cardiomyocytes. *Journal of Clinical Investigation*, 108(3), pp.407-414.

Kemp, J. R., & Wallace, K. B. (1990). Molecular determinants of the species-selective inhibition of brain acetylcholinesterase. *Toxicology and Applied Pharmacology*, 104(2), pp.1-12.

Kempf, H., Andree, B., & Zweigerdt, R. (2016). Large-scale production of human pluripotent stem cell derived cardiomyocytes. *Advanced Drug Delivery Reviews*, 96(7), pp.18-30.

Khaitlina, S.Y. (2001). Functional specificity of actin isoforms. *International Review of Cytology*, 202(3), pp.35-98.

Kim, E.K., & Choi, E.J. (2010). Pathological roles of MAPK signaling pathways in human diseases. *Molecular Basis of Disease*, 1802(4), pp.396-405.

Kim, J.M., Yoon, M., Kim, S.S., Kang, I., & Ha, J. (1999). Phosphatidylinositol 3-Kinase regulates differentiation of H9c2 Cardiomyoblasts mainly through the protein Kinase B/Akt-Independent pathway. *Archives of Biochemistry and Biophysics*, 367(1), pp.67-73.

Kim, N.K., Park, H.-R., Lee, H.C., Yoon, D., Son, E.S., Kim, Y.S., Kim, S.R., Kim, O.H. and Lee, C.S. (2010). Comparative studies of skeletal muscle proteome and transcriptome profilings between pig breeds. *Mammalian Genome*, 21(5-6), pp.307-319.

Kim, S.J., Kim, J.E., Ko, B.H., & Moon, I.S. (2003). Carbofuran induces apoptosis of rat cortical neurons and down-regulates surface alpha7 subunit of acetylcholine receptors. *Molecular Cells*, 17(2), pp.242-247.

Kimes, B.W., & Brandt, B.L. (1976). Properties of a clonal muscle cell line from rat heart. *Experimental Cell Research*, 98(2), pp.367-381.

King R.J. (2000). *cancer biology*. Harlow, UK: pearson Education, pp.198.

Kischkel, F.C., Hellbardt, S., Behrmann, I., Germer, M., Pawlita, M., Krammer, P.H., & Peter, M.E. (1995). Cytotoxicity-dependent APO-1 (Fas/CD95)-associated proteins from a death-inducing signaling complex (DISC) with the receptor. *European Molecular Biology Organization Journal*, 14(3), pp.5579-5588.

Kiss. Z., & Fazekas, T. (1979). Arrhythmias in organophosphate poisonings. *Acta Cardiology*, 34(8), pp.323-330.

Klaassen, C.D. (2007). *Casarett and Doull's Toxicology: The Basic Science of Poisons*. New York: Mcgraw-Hill, pp.135.

Kogler, G., Sensken, S., Airey, J.A., Trapp, T., Muschen, M., Feldhahn, N., Liedtke, S., Sorg, R.V., Fischer, J., Rosenbaum, C., Greschat, S., Knipper, A., Bender, J., Degistirici, O., Gao, J., Caplan, A.I., Colletti, E.J., Almeida-Porada, G., Müller, H.W., Zanjani, E., & Wernet, P. (2004). A new human

somatic stem cell from Placental cord blood with intrinsic Pluripotent differentiation potential. *The Journal of Experimental Medicine*, 200(2), pp.123-135.

Kolomeichuk, S.N., Terrano, D.T., Lyle, C.S, Sabapathy, K., & Chambers, T.C. (2008). Distinct signaling pathways of microtubule inhibitors vinblastine and Taxol induce JNK-dependent cell death but through AP-1-dependent and AP-1-independent mechanisms, respectively. *Federation of European Biochemical Societies Journal*, 275(3), pp.1889-1899.

Kolossov, E., Fleischmann, B.K., Liu, Q., Bloch, W., Viatchenko-Karpinski, S., Manzke, O., Ji, G.J., Bohlen, H., Addicks, K., & Hescheler, J. (1998). *journal of Cell Biology*, 143(2), pp.2045-2056.

Kose, A., Gunay, N., Yildirim, C., Tarakcioglu, M., Sari, I., & Demiryurek, A. T. (2009). Cardiac damage in acute organophosphate poisoning in rats: effects of atropine and pralidoxime. *The American Journal of Emergency Medicine*, 27(2), pp.169-175.

Koss, K.L., & Kranias, E.G. (1996). Phospholamban: A prominent regulator of myocardial Contractility. *Circulation Research*, 79(6), pp.1059-1063.

Kostin, S. Hein, E., Arnon, D., Scholz, J., & Schaper, A. (2000). The cytoskeleton and related proteins in the human failing heart. *Heart Failure Reviews*, 5(6), pp.271-280.

Kotaka, M., Lau, Y., Cheung, K., Lee, S.M.Y., Li, H., Chan, W., Fung, K., Lee, C., Waye, M. & Tsui, S.K.W. (2001). Elfin is expressed during early heart development. *Journal of Cellular Biochemistry*, 83(3), pp.463-472.

Kouloumbos, V.N., Tsipi, D.F., Hiskia, A.E., Nikolic, D., & van Breemen, R.B. (2003). Identification of photocatalytic degradation products of diazinon in TiO2 aqueous suspensions using GC/MS/MS and LC/MS with quadrupole time-of-flight mass spectrometry. *Journal of the American Society for Mass Spectrometry*, 14(8), pp.803-817.

Krysko, D.V, Vanden Berghe, T., D'Herde, K., & Vandenabeele, P. (2008). Apoptosis and necrosis: detection, discrimination and phagocytosis. *Methods (San Diego, Calif),* 44(3), pp.205-221.

Ku, P.M., Chen, L.J., Liang, J., Cheng, K.C., Li, Y.X., & Cheng, J.T. (2011). Molecular role of GATA binding protein 4 (GATA-4) in hyperglycemia-induced reduction of cardiac contractility. *Cardiovascular Diabetology*, *10*(1), pp.57-63.

Kuhn, M., Hyman, A.A., & Beyer, A. (2014). Coiled-Coil Proteins Facilitated the Functional Expansion of the Centrosome. *Plos Computational Biology*, 10(6), pp.1003657.

Kumar, S., & Duester, G. (2011). Retinoic acid signaling. *Cell*, 147(2), pp.1411-1422.

Kurosaka, K., Takahashi, M., Watanabe, N., & Kobayashi, Y. (2003). Silent cleanup of very early apoptotic cells by macrophages. *Journal of Immunology*, 171(8), pp.4672-4679.

Kuzmenkin, A., Liang, H., Xu, G., Pfannkuche, K., Eichhorn, H., Fatima, A., Luo, H., Saric, T., Wernig, M., Jaenisch, R., & Hescheler, J. (2009). Functional characterization of cardiomyocytes derived from murine induced pluripotent stem cells in vitro. *The Federation of European Biochemical Societies Journal*, 23(12), pp.4168-4180.

Laflamme, M.A., Chen, K.Y., Naumova, A.V., Muskheli, V., Fugate, J.A., Dupras, S.K., Reinecke, H., Xu, C., Hassanipour, M., Police, S., O'Sullivan, C., Collins, L., Chen, Y., Minami, E., Gill, E.A., Ueno, S., Yuan, C., Gold, J., & Murry, C.E. (2007). Cardiomyocytes derived from human embryonic stem cells in pro-survival factors enhance function of infarcted rat hearts. *Nature Biotechnology*, 25(9), pp.1015-1024.

Lalonde, R., & Strazielle, C. (2003). Neurobehavioral characteristics of mice with modified intermediate filament genes. *Reviews in the Neurosciences*, 14(4). pp.369-385.

Lavine, K.J., Yu, K., White, A.C., Zhang, X., Smith, C., Partanen, J., & Ornitz, D.M. (2005). Endocardial and epicardial derived FGF signals regulate myocardial proliferation and differentiation in vivo. *Developmental Cell*, 8(1), pp.85-95.

Lee, J.H., Kwon, E.J. & Kim, D.H. (2013). Calumenin has a role in the alleviation of ER stress in neonatal rat cardiomyocytes. *Biochemical and Biophysical Research Communications*, 439(3), pp. 327-332.

Lee, S., Chanoit, G., McIntosh, R., Zvara, D., & Xu, Z. (2009). Molecular mechanism underlying Akt activation in zinc-induced cardioprotection. *American Journal of Physiology, Heart and Circulatory Physiology*, 297(2), pp.569-575.

Lehrer, S.S., & Morris, E.P. (1984). Comparison of the effects of smooth and skeletal tropomyosin on skeletal actomyosin subfragment 1 ATPase. *Journal of Biology Chemistry*, 259(4), pp.2070-2072.

Lewis, K., & Falconer, K. (2015). Human pluripotent stem-cell-derived cardiomyocytes in cardiovascular drug discovery and development. *Biodiscovery*, 16(3), pp,1-9.

Li, B., Ricordel, I., Schopfer, L.M., Baud, F., Megarbane, B., Nachon, F., Masson, P., & Lockridge, O. (2010). Detection of Adduct on tyrosine 411 of albumin in humans poisoned by Dichlorvos. *Toxicological Sciences*, 116(1), pp.23-31.

Li, B., Schopfer, L.M., Hinrichs, S.H., Masson, P., & Lockridge, O. (2007). Matrix-assisted laser desorption/ionization time-of-flight mass spectrometry assay for organophosphorus toxicants bound to human albumin at Tyr411. *Analytical Biochemistry*, 361(2), pp.263-272.

Li, B., Schopfer, L.M., Grigoryan, H., Thompson, C.M., Hinrichs, S.H., Masson, P., & Lockridge, O. (2008). Tyrosines of human and mouse transferrin covalently labeled by organophosphorus agents: a new motif for binding to proteins that have no active site serine. *Toxicological Sciences : An Official Journal of the Society of Toxicology*, 107(1), pp.144-155.

Li, D., Huang, Q., Lu, M., Zhang, L., Yang, Z., Zong, M., & Tao, L. (2015). The organophosphate insecticide chlorpyrifos confers its genotoxic effects by inducing DNA damage and cell apoptosis. *Chemosphere*, 135(2), pp.387-393.

Li, Q., Kobayashi, M., & Kawada, T. (2007). Organophosphorus pesticides induce apoptosis in human NK cells. *Toxicology*, 239(1-2), pp.89-95.

Li, Q., Kobayashi, M., & Kawada, T. (2009). Chlorpyrifos induces apoptosis in human T cells. *Toxicology*, 255(1-2), pp.53-57.

Li, Qing. (2010). Apoptosis induced by anticholinesterase pesticides. In: *Anticholinesterase Pesticides: Metabolism, Neurotoxicity and Epidemiology*, pp.165-174.

Li, W., & Casida, J.E., (1998). Organophosphorus neuropathy target esterase inhibitors selectively blockoutgrowth of neurite-like and cell processes in cultured cells. *Toxicology Letters*, 98(3), pp.139-146.

Liang, P., Lan, F., Lee, A.S., Gong, T., Sanchez-Freire, V., Wang, Y., & Wu, J.C. (2013). Drug screening using a library of human induced Pluripotent stem cell-derived Cardiomyocytes reveals disease-specific patterns of cardiotoxicity. *Circulation*, 127(16), pp.1677-1691.

Lin, S.C., Dolle, P., Ryckebüsch, L., Noseda, M., Zaffran, S., Schneider, M.D., & Niederreither, K. (2010). Endogenous retinoic acid regulates cardiac progenitor differentiation. *Proceedings of the National Academy of Sciences of the United States of America*, 107(20), pp.9234-9239.

Lisanti, M.P., Tang, Z., Scherer, P.E., Kübler, E., Koleske, A.J., & Sargiacomo, M. (1995). Caveolae, transmembrane signalling and cellular transformation. *Molecular Membrane Biology*, 12(1), pp.121-124.

Liu, J., Lieu, D.K., Siu, C.W., Fu, J., Tse, H., & Li, R.A. (2009). Facilitated maturation of ca2+ handling properties of human embryonic stem cell-derived cardiomyocytes by calsequestrin expression. *Cell Physiology*, 297(1), pp.152-159.

Liu, Z., Zhan, Y., Tu, Y., Chen, K., & Wu, C. (2014). PDZ and LIM domain protein 1(PDLIM1)/CLP36 promotes breast cancer cell migration, invasion and metastasis through interaction with α-actinin. *Oncogene*, 34(10), pp.1300-1311.

Liyasova, M., Li, B., Schopfer, L.M., Nachon, F., Masson, P., Furlong, C.E., & Lockridge, O. (2011). Exposure to tri-o-cresyl phosphate detected in jet airplane passengers. *Toxicology and Applied Pharmacology*, 256(3), pp.337-347.

Lockridge, O., & Schopfer, L.M. (2010). Review of tyrosine and lysine as new motifs for organophosphate binding to proteins that have no active site serine. *Chemico-Biological Interactions*, 187(1-3), pp.344-348.

Lopachin, R.M. (2005). Protein Adduct formation as a molecular mechanism in Neurotoxicity. *Toxicological Sciences*, 86(2), pp.214-225.

Lotti, M. (1992). The pathogenesis of organophosphate neuropathy. *Critical Review in Toxicology*, 21(3), pp.465-487.

Lotti, M. (1993). Interactions between neuropathy target Esterase and its inhibitors and the development of Polyneuropathy. *Toxicology and Applied Pharmacology*, 122(2), pp.165-171.

Lotti, M. (2000). Clinical Toxicology of Anticholinesterase Agents in Humans. In: *Handbook of Pesticide Toxicology,* Elsevier, 2, pp.140.

Ludomirsky, A., Klein, H.O., Sarelli, P., Becker, B., Hoffman, S., Taitelman, U., Barzilai, J., Lang, R., David, D., DiSegni, E., & Kaplinsky, E. (1982). Q-T prolongation and polymorphous "torsade de pointes" ventricular arrhythmias associated with organophosphorus insecticide poisoning. *The American Journal of Cardiology*, 49(7), pp.1654-1658.

Lundy, S.D., Zhu, W.Z., Regnier, M., & Laflamme, M.A. (2013). Structural and functional maturation of Cardiomyocytes derived from human Pluripotent stem cells. *Stem Cells and Development*, 22(14), pp.1991-2002.

Lyman, S. K., Gerace, L., & Baserga, S. J. (1999). Human Nop5/Nop58 is a component common to the box C/D small nucleolar ribonucleoproteins. *RNA*,5(12), pp.1597-1604.

Lyzhnikov, E.A., Savina, A.S., & Shepelev V.M. (1975). Pathogenesis of disorders of cardiac rhythm and conductivity in acute organophosphate insecticide poisoning. *Kardiologia*, 15(9),pp.126-129.

Ma, J., Guo, L., Fiene, S.J., Anson, B.D., Thomson, J. , Kamp, T.J. (2011). High purity human-induced pluripotent stem cell-derived cardiomyocytes : electrophysiological properties of action potentials and ionic currents. *Heart and Circulatory Physiology*, 301(5), pp.2006-2017.

Mahler, G.J., & Butcher, J.T. (2011). Cardiac developmental toxicity. *Birth Defects Research C Embryo Today*, 93(4), pp.291-297.

Majno, G., & Joris, I. (1995). Apoptosis, oncosis, and necrosis: an overview of cell death. *American Journal of Pathology*, 146(1), pp.3-15.

Malik, N., Efthymiou, A.G., Mather, K., Chester, N.,Wang, X., Nath, A., Rao, M.S., & Steiner, J.P. (2014). Compounds with species and cell type specific toxicity identified in a 2000 compound drug screen of neural stem cells and rat mixed cortical neurons. *Neurotoxicology*, 45(3), pp.192-200.

Mamidi, R., Muthuchamy, M., & Chandra, M. (2013). Instability in the central region of tropomyosin modulates the function of its overlapping ends. *Biophysical Journal*, 105(9), pp.2104-2113.

Maness, P.F., & Schachner, M. (2007). Neural recognition molecules of the immunoglobulin superfamily: Signaling transducers of axon guidance and neuronal migration. *Nature Neuroscience*, 10(1), pp.19-26.

Maroney, A.C., Finn, J.P., Bozyczko-Coyne, D., O'Cane, T.M, Neff, N.T., Tolkovsky, A.M., Park, D.S., Yan, C.Y., Troy, C.M., & Greene, L.A. (1999). CEP-1347 (KT7515), an inhibitor of JNK activation, rescues sympathetic neurones and neuronally differentiated PC12 cells from death evoked by three distinct insults. *Journal of Neurochemistry*, 73(3), pp.1901-1912.

Marques, S.R., Lee, Y, Poss, K.D., & Yelon, D. (2008). Reiterative roles for FGF signaling in the establishment of size and proportion of the zebrafish heart. *Developmental Biology*, 321(2), pp.397-406.

Marsillach, J., Richter, R.J., Kim, J.H., Stevens, R.C., MacCoss, M.J., Tomazela, D., Suzuki, S.M., Schopfer, M.L., Lockridge, O., & Furlong, C. E. (2011). Biomarkers of organophosphorus (OP) exposures in humans. *Neurotoxicology*, 32(5), pp.656-660.

Martin, U. (2015). Pluripotent stem cells for disease modeling and drug screening: new perspectives for treatment of cystic fibrosis. *Molecular and Cellular Pediatrics*, 2(1), pp.15-21.

Martinez-Fernandez, A., Beraldi, R., Cantero, Peral, S., Terzic, A. & Nelson, T.J. (2014). The Developmental and stem sell biology approach in regenerative medicine applications in organ transplantation. In: *Heart Regeneration,* Elsevier, pp.457-477.

Masoud, L., Vijayasarathy, C., Fernandez-Cabezudo, M., Petroianu, G., & Saleh, A.M. (2003). Effect of malathion on apoptosis of murine L929 fibroblasts: a possible mechanism for toxicity in low dose exposure. *Toxicology*, 185(3), pp.89-102.

Massicotte, C., Jortner, B., & Ehrich, M. (2003). Morphological effects of neuropathy-inducing organophosphorus compounds in primary dorsal root ganglia cell cultures. *Neurotoxicology*, 24(6), pp.787-796.

Mazzorana, M., Hussain, R. & Sorensen, T. (2016). Ca-dependent folding of human Calumenin. *Plos One*, 11(3), p.0151547.

Mcconnell, R., Delgado-Tellez, E., Cuadra, R., Torres, E., Keifer, M., Almendaraz, J., Miranda, J., El-Fawal, H., Wolff, M., Simpson, D., & Lundberg, I. (1999). Organophosphate neuropathy due to metamidophos: biochemical and neurophysiologic markers. *Archive Toxicology*, 73(8), pp.296-300.

Mcdonough, J.H., & Shih, T.M., (1997). Neuropharmacological mechanisms of nerve agent-induced seizure and neuropathology. *Neuroscience and Biobehavioral Reviews*, 21(5), pp.559-579.

Mckillop, D.F. & Geeves, M.A. (1993). Regulation of the interaction between actin and myosin subfragment 1: Evidence for three states of the thin filament. *Biophysical Journal*, 65(2), pp.693-701.

Mclaren, A. (2001). Ethical and social considerations of stem cell research. *Nature*, 414(6859), pp.129-131.

McLaughlin, R., Kelly, C. J., Kay, E., & Bouchier-Hayes, D. (2001). The role of apoptotic cell death in cardiovascular disease. *Irish Journal of Medical Science*, 170(2), pp.132-140.

Menard, C., Pupier, S., Mornet, D., Kitzmann, M., Nargeot, J., & Lory, P. (1999). Modulation of L-type calcium channel expression during retinoic acid-induced differentiation of H9C2 cardiac cells. *The Journal of Biological Chemistry*, 274(41), pp.29063-29070.

Metzger, J.M., & Westfall, M.V. (2004). Covalent and Noncovalent modification of thin filament action: The essential role of Troponin in cardiac muscle regulation. *Circulation Research*, 94(2), pp. 146-158.

Metzstein, M. M., Stanfield, G. M., & Horvitz, H. R. (1998). Genetics of programmed cell death in C. elegans: past, present and future. *Trends in Genetics*, 14(10), pp.410-416.

Michaelis, S. (2011). Contaminated aircraft cabin air. *The journal of biological Physic*, 11(3), pp.132-145.

Mikkelsen, T.S., Hanna, J, Zhang, X, Ku, M.,Wernig, M., Schorderet, P., Bernstein, B.E., Jaenisch, R., Lander, E.S., & Meissner, A. (2008). Dissecting direct reprogramming through integrative genomic analysis. *Nature*, 454(6), pp.49-55.

Mileson, B. (1998). Common mechanism of toxicity: A case study of Organophosphorus pesticides. *Toxicological Sciences*, 41(1), pp.8-20.

Mima, T., Ueno, H., Fischman, D.A., Williams, L.T., & Mikawa, T. (1995). Fibroblast growth factor receptor is required for in vivo cardiac myocyte proliferation at early embryonic stages of heart development. *Proceedings of the National Academy of Sciences*, 92(2), pp.467-471.

Miron, D., Pretto, A., Crestani, M., Glusczak, L., Schetinger, M.R., Loro, V.L., & Morsch, V.M. (2008). Biochemical effects of clomazone herbicide on piava (Leporinus obtusidens). *Chemosphere,* 74(1), pp.1-5.

Mitsui, K., Tokuzawa, Y., Itoh, H., Segawa, K., Murakami, M., Takahashi, K., Maruyama, M., Maeda, M., & Yamanaka, S. (2003). The Homeoprotein Nanog is required for maintenance of Pluripotency in mouse Epiblast and ES cells. *Cell,* 113(5), pp.631-642.

Monnet-Tschudi, F., Zurich, M.G., Schilter, B., Costa, L.G., & Honegger, P. (2000). Maturation-dependent effects of chlor- pyrifos and parathion and their oxygen analogs on acetylcholinesterase and neuronal and glial markers in aggregating brain cell cultures. *Toxicology and Applied Pharmacology,* 165(8), pp.175-183.

Montgomery, M.R., Wier, G.T., Zieve, F.J., & Anders, M.W. (1977). Human intoxication following inhalation exposure to synthetic jet lubricating oil. *Clinical Toxicology.* 11(3), pp.423-426.

Morfini, G.A., Burns, M., Binder, L.I., Kanaan, N.M., LaPointe, N., Bosco, D.A., Brown, R.H., Jr, Brown, H., Tiwari, A., & Hayward, L., (2009). Axonal transport defects in neurodegenerative diseases. *Journal of Neuroscience*. 29, pp.12776-12786.

Moser, M., Stempfl, T., Li, Y., Glynn, P., Büttner, R., & Kretzschmar, D. (2000). Cloning and expression of the murine sws/NTE gene. *Mechanisms of Development*, 90(2), pp.279-282.

Mueller, R., Hornung, S., Furlong, C., Anderson, J., Giblett, E., Motulsky, A. (1983). Plasma paraoxonase polymorphism: a new enzyme assay, population, family biochemical and linkage studies. *Journal of Human Genetics*. 35(2), pp.393-408

Mummery, C. (2003). Differentiation of human embryonic stem cells to Cardiomyocytes: Role of Coculture with visceral Endoderm-Like cells. *Circulation*, 107(21), pp.2733-2740.

Mutch, E., & Williams, F. (2006). Diazinon, chlorpyrifos and parathion are metabolised by multiple cytochromes P450 in human liver. *Toxicology*, 224(1-2), pp.22-32.

Mymrikov, E.V., SeitNebi, A.S., & Gusev, N.B. (2011). Large potentials of small heat shock proteins. *Physiological Reviews*, 91(4), pp.1123-1159.

Naito, A.T., Tominaga, A., Oyamada, M., Oyamada, Y., Shiraishi, I., Monzen, K., Komuro, I., & Takamatsu, T. (2003). Early stage-specific inhibitions of cardiomyocyte differentiation and expression of Csx/Nkx-2.5 and GATA-4 by phosphatidylinositol 3-kinase inhibitor LY294002. *Experimental Cell Research*, 291(8), pp.56-69.

Niederreither, K., & Dolle, P. (2010). Development and Aging of the Drosophila Heart. *Heart Development and Regeneration*, 2(3), pp. 47-86.

Niederreither, K., Vermot, J., Messaddeq, N., Schuhbaur, B., Chambon, P., & Dolle, P. (2001). Embryonic retinoic acid synthesis is essential for heart morphogenesis in the mouse. *Development*, 128(7), pp.1019-311031.

Niijima, H., Nagao, M., Nakajima, M., Takatori, T., Iwasa, M., Maeno, Y., Koyama, H., & Isobe, I. (2000). The effects of sarin-like and soman-like organophosphorus agents on MAPK and JNK in rat brains. *Forensic Science International*, 112(2-3), pp.171-178.

Niijima, H., Nagao, M., Nakajima, M., Takatori, T., Matsuda, Y., Iwase, H., & Kobayashi, M. (1999). Sarin-like and Soman-like Organophosphorous agents activate PLCγ in rat brains. *Toxicology and Applied Pharmacology*, 156(1), pp.64-69.

Nishiyama, N., Miyoshi, S., Hida, N., Uyama, T., Okamoto, K., Ikegami, Y., Miyado, K., Segawa, K., Terai, M., Sakamoto, M., Ogawa, S. & Umezawa, A. (2007). The significant Cardiomyogenic potential of human Umbilical cord blood-derived Mesenchymal stem cells in vitro. *Stem Cells*, 25(8), pp.2017-2024.

Nomeir, A., & Abou-Donia, M. (1986). Studies on the metabolism of the neurotoxic tri-o-cresyl phosphate: distribution, excretion and metabolism in male cats after a single dermal application. *Toxicology*, 38(4), pp.15-33.

Norbury, C., & Hickson, I. (2001). Cellular responses to DNA damage. *Annual Review of Pharmacology and Toxicology*, 41(8), pp.367-401.

Nostrandt, A., Rowles, T., & Ehrich, M. (1992). Cytotoxic effects of organophosphorus esters and other neurotoxic chemicals on cultured cells. *In Vitro Toxicology*,5(3), pp.127-136.

Nsoukpoe-Kossi, C., Bourassa, P., Mandeville, J., & Tajmir-Riahi, H. (2014). Modelling of vitamin A binding to tRNA. *Journal of Pharmaceutical and Biomedical Analysis*, 99(5), pp.28-34.

O'Brien, P. (2008). Cardiac troponin is the most effective translational safety biomarker for myocardial injury in cardiotoxicity. *Toxicology*, 245(3), pp.206-218.

Odaka, C., Sanders, M.L., & Crews, P. (2000). Jasplakinolide induces Apoptosis in various transformed cell lines by a Caspase-3-Like protease-dependent pathway. *Clinical and Vaccine Immunology*, 7(6), pp.947-952.

Odorico, J., Kaufman, D., &Thomson, J. (2001). Multilineage differentiation from human embryonic stem cell lines. *Stem Cells*, 19(3), pp.193-204.

Ogutcu, A., Uzunhisarcikli, M., Kalender, S., Durak, D., Bayrakdar, F., & Kalender, Y. (2006). The effects of organophosphate insecticide diazinon on malondialdehyde levels and myocardial cells in rat heart tissue and protective role of vitamin E. *Pesticide Biochemistry and Physiology*, 86(2), pp.93-98.

Olivetti, G., Cigola, R., Maestri, D., Corradi, C., Lagrasta, S., & Anversa, P. (1996). Aging, cardiac hypertrophy and ischemic cardiomyopathy do not affect the proportion of mononucleated and

multinucleated myocytes in the hypertrophy and ischemic cardiomyopathy do not affect the proportion of mononucleated and multinucleated myocytes in the human heart. *Molecular and Cellular Cardiology*, 28(7), pp.1463-1477.

Olmos, C., Sandoval, R., Rozas, C., Navarro, S., Wyneken, U., Zeise, M., Morales, B., & Pancetti, F. (2009). Effect of short-term exposure to dichlorvos on synaptic plasticity of rat hippocampal slices: involvement of acylpeptide hydrolase and alpha(7) nicotinic receptors. *Toxicology and Applied Pharmacology,* 238(6), pp.37-46.

Osterauer, R., & Kohler H. (2008). Temperature-dependent effects of the pesticides thiacloprid and diazinon on the embryonic development of zebrafish (Daniorerio). *Aquatic Toxicology*, 86(4), pp.485-494.

Otakis, G., & Timbrell, J.A. (2006). In vitro cytotoxicity assays: comparison of LDH, neutral red, MTT and protein assay in hepatoma cell lines following exposure to cadmium chloride. *Toxicology Letters*, 160(6), pp.171-177.

Pagano, M., Naviglio, S., Spina, A., Chiosi, E., Castoria, G., Romano, M., Sorrentino, A., Illiano, F., & Illiano, G. (2004). Differentiation of H9c2 cardiomyoblasts: The role of adenylate cyclase system. *Journal of Cellular Physiology*, 198(3), pp.408-416.

Pakzad, M., Fouladdel, S., Nili-Ahmadabadi, A., Pourkhalili, N., Baeeri, M., Azizi, E., Sabzevari, O., Ostad, S.N. & Abdollahi, M. (2013). Sublethal exposures of diazinon alters glucose homostasis in Wistar rats: Biochemical and molecular evidences of oxidative stress in adipose tissues. *Pesticide Biochemistry and Physiology*, 105(1), pp.57-61.

Pan, Z., Guo, Y., Qi, H., Fan, K., Wang, S., Zhao, H., Fan, Y., Xie, J., Guo, F., Hou, Y., Wang, N., Huo, R., Zhang, Y., Liu, Y., & Du, Z. (2012). M3 subtype of Muscarinic Acetylcholine receptor promotes Cardioprotection via the suppression of miR-376b-5p. *Plos One*, 7(3), pp.32571-32580.

Pashmforoush, M., Pomies, P., Peterson, K., Kubalak, S., Ross, J., Hefti, A., Aebi, U., Beckerle, M., & Chien, K. (2001). *Nature Medicine*, 7(5), pp.591-597.

Patricelli, M.P., Giang, D.K., Stamp, L.M., & Burbaum, J.J. (2001). Direct visualization of serine hydrolase activities in complex proteomes using fluorescent active site-directed probes. *Proteomics*, 1(8), pp.1067-1071.

Peeples, E., Schopfer, L., Duysen, E., Spaulding, R., Voelker, T., Thompson, C., & Lockridge, O. (2005). Albumin, a new biomarker of organophosphorus toxicant exposure, identified by mass spectrometry. *Toxicological Sciences*, 83(2), pp.303-312.

Pereira, S.L., Ramalho-Santos, J., Branco, A.F., Sardao, V.A., Oliveira, P.J., & Carvalho, R.A. (2011). Metabolic remodeling during H9c2 myoblast differentiation: Relevance for in vitro toxicity studies. *Cardiovascular Toxicology*, 11(2), pp.180-190.

Periasamy, M., & Huke, S. (2001). SERCA pump level is a critical determinant of ca2+Homeostasis and cardiac Contractility. *Journal of Molecular and Cellular Cardiology*, 33(6), pp.1053-1063.

Perissel, B., Charbonne, F., Moalic, J.M., & Malet, P. (1980). Initial stages of trypsinized cell culture of cardiac myoblasts: Ultrastructural data. *Journal of Molecular and Cellular Cardiology*, 12(1), pp.63-75.

Pernigo, S., Lamprecht, A., Steiner, R., & Dodding, M. (2013). Structural basis for kinesin-1:cargo recognition. *Science*, 340(6130), pp.356-359.

Perrone Capano, C., Pernas-Alonso, R., & di Porzio, U., (2001). Neurofilament homeostasis and motoneurone degeneration. *Bioessays*, 23(1), pp.24-33.

Pierre, S., Bats, A.S., & Coumoul, X. (2011). Understanding SOS (Son of Sevenless). *Biochemical Pharmacology*, 82(9), pp.1049-1056.

Pimentel, J. M., & Carrington da Costa, R. B. (1992). Effects of organophosphates on the heart. In: Ballantyne and T. C. Marrs, (ed.) *Clinical and Experimental Toxicology of Organophosphates and Carbamates,* Butterworth-Heinemann, Oxford, pp.145-148.

Poet, T., Wu, H., Kousba, A., & Timchalk, C. (2003). In vitro rat hepatic and intestinal metabolism of the organophosphate pesticides chlorpyrifos and diazinon. *Toxicological Sciences*, 72(2), pp.193-200.

Pollard, T., & Cooper, J. (2009). Actin, a central player in cell shape and movement. *Science* 326(5957), pp.1208-1212.

Pomeroy-Black, M., & Ehrich, M. (2012). Organophosphorus compound effects on neurotrophin receptors and intracellular signaling. *Toxicology in Vitro : An International Journal Published in Association with BIBRA*, 26(5), pp.759-65.

Pope, C., Di Lorenzo, K., & Ehrich, M. (1995). Possible involvement of a neurotrophic factor during the early stages of organophosphate-induced delayed neurotoxicity. *Toxicology Letters*, 75(3), pp.111-117.

Prabhakar, R., Petrashevskaya, N., Schwartz, A., Aronow, B., Boivin, G.P., Molkentin, J.D., & Wieczorek, D.F. (2003). *Molecular and Cellular Biochemistry*, 251(1-2), pp.33-42.

Prall, O., Menon, M., Solloway, M., Watanabe, Y., Zaffran, S., & Bajolle, F. (2007). An Nkx2-5/Bmp2/Smad1 negative feedback loop controls heart progenitor specification and proliferation. La *Cellule Journal*, 128(5), pp.947-959.

Prendergast, M., Self, R., Smith, K., Ghayoumi, L., Mullins, M., Butler, T., Buccafusco, J., Gearhart, D., & Terry, A. (2007). Microtubule-associated targets in chlorpyrifos oxon hippocampal neurotoxicity. *Neuroscience*, 146(1), pp.330-339.

Qiao, J., Paul, P., Lee, S., Qiao, L., Josifi, E., Tiao, J.R., & Chung, D.H. (2012). PI3K/AKT and ERK regulate retinoic acid-induced neuroblastoma cellular differentiation. *Biochemical and Biophysical Research Communications*, 424(3), pp.421-426.

Quistad, G., Klintenberg, R., & Casida, J. (2005). Blood Acylpeptide Hydrolase Activity Is a Sensitive Marker for Exposure to Some Organophosphate Toxicants. *Toxicological Sciences*, 86(2), pp.291-299.

Rajan, S., Jagatheesan, G., Karam, C., Alves, M., Bodi, I., Schwartz, A., & Wieczorek, D. (2010). Molecular and functional characterization of a novel cardiac-specific human tropomyosin isoform. *Circulation*, 121(3), pp.410-418.

Raman, M., Chen, W., & Cobb, M. (2007). Differential regulation and properties of MAPKs. *Oncogene*, 26(3), pp.3100-3112.

Rashedinia, M., Hosseinzadeh, H., Imenshahidi, M., Lari, P., Razavi, B.M. & Abnous, K. (2013). Effect of exposure to diazinon on adult rats brain. *Toxicology and Industrial Health*, 32(4), pp.714-720.

Ray, D., & Richards, P. (2001). The potential for toxic effects of chronic, low-dose exposure to organophosphates. *Toxicology Letters*, 120(1-3), pp.343-351.

Read, R.W., Riches, J.R., Stevens, J.A., Stubbs, S.J., & Black, R.M. (2010). Biomarkers of organophosphorus nerve agent exposure: comparison of phosphylated butyrylcholinesterase and phosphylated albumin after oxime therapy. *Archives Toxicology*, 84(6), pp.25-36.

Razavi, B.M., Hosseinzadeh, H., Movassaghi, A.R., Imenshahidi, M. & Abnous, K. (2013). Protective effect of crocin on diazinon induced cardiotoxicity in rats in subchronic exposure. *Chemico-Biological Interactions*, 203(3), pp.547-555.

Reagan, W.J., York, M., Berridge, B., Schultze, E., Walker, D., & Pettit, S. (2013). Comparison of cardiac Troponin I and T, including the evaluation of an Ultrasensitive assay, as indicators of Doxorubicin-induced Cardiotoxicity. *Toxicologic Pathology*, 41(8), pp.1146-1158.

Ren, Y., Busch, R.K., Perlaky, L., & Busch, H. (1998). The 58-kDa microspherule protein (MSP58), a nucleolar protein, interacts with nucleolar protein p120. *European Journal of Biochemistry*, 253(3), pp.734-742.

Reszka, A.A., Seger, R., Diltz, C.D., Krebs, E.G., & Fischer, E.H. (1995). Association of mitogen-activated protein kinase with the microtubule cytoskeleton. *Proceedings of the National Academy of Sciences,* 92(19), pp.8881-8885.

Richards, P.G., Johnson, M.K., & Ray, D.E. (2000). Identification of Acylpeptide Hydrolase as a Sensitive Site for Reaction with Organophosphorus Compounds and a Potential Target for Cognitive Enhancing Drugs. *Molecular Pharmacology*, 58(3), pp.577-583.

Richardson, R.J. (1995). Assessment of the neurotoxic potential of chlorpyrifos relative to other organophosphorus compounds: A critical review of the literature. *Journal of Toxicology and Environmental Health,* 44(2), pp.135-165.

Richardson, R.J., Hein, N.D., Wijeyesakere, S.J., Fink, J.K., & Makhaeva, G.F. (2013). Neuropathy target esterase (NTE): Overview and future. *Chemico-Biological Interactions*, 203(1), pp.238-244.

Road, D. (2010). Molecular toxicology of neuropathy, *Toxicology Letters*, 5(3), pp.109-120.

Rogers, I., & Casper, R.F. (2004). Umbilical cord blood stem cells. *Best Practice and Research Clinical Obstetrics and Gynaecology*, 18(2), pp.893-908.

Rose, R.L., & Hodgson, E. (2005). Pesticide metabolism and potential for metabolic interactions. *Journal of Biochemistry Molecular Toxicology*, 19(6), pp.276-277.

Rosenblum, J.S., & Kozarich, J.W. (2003). Prolyl peptidases: A serine protease subfamily with high potential for drug discovery. *Current Opinion in Chemical Biology*,7(4), pp.496-504.

Roskoski, R. (2012). ERK1/2 MAP kinases: Structure, function, and regulation. *International Journal of Molecular Science*, 11(2), pp.4348-4360.

Roth, A., Zellingcr, I., Arad, M., & Atsmon, L. (1993). Organophosphates and the heart. *Chest Journal*, 103(2), pp.576-582.

Rush, T., Liu, X.Q., Hjelmhaug, J., & Lobner, D. (2010). Mechanisms of chlorpyrifos and diazinon induced neurotoxicity in cortical culture. *Neuroscience*, 166(3), pp.899-906.

Saadeh, A.M., Farsakh, N.A., & Al-Ali MK. (1997). Cardiac manifestations of acute carbamate and organophosphate poisoning. *Heart*, 77(5), pp.461-464.

Sachana, M., Sidiropoulou, E., Flaskos, J., Harris, W., Robinson, A.J., Woldehiwet, Z. and Hargreaves, A.J. (2014). Diazoxon disrupts the expression and distribution of βIII-tubulin and MAP 1B in differentiating N2a cells. *Basic and Clinical Pharmacology and Toxicology*, 114(6), pp.490-496.

Sachana, M., Flaskos, J., Alexaki, E., Glynn, P., & Hargreaves, A.J. (2001). The toxicity of chlorpyrifos towards differentiating mouse N2a neuroblastoma cells. *Toxicology in Vitro*, 15(4-5), pp.369-372.

Sahoo, S.K., Kim, T., Kang, G.B., Lee, J.G., Eom, S.H., & Kim, D.H. (2009). Characterization of calumenin-SERCA2 interaction in mouse cardiac sarcoplasmic reticulum. *Journal of Biological Chemistry*, 284(45), pp.31109-31121.

Sahoo, S.K., & Kim, D.H. (2010). Characterization of calumenin in mouse heart. *Biochemistry and Molecular Biology Reports*, 43(3), 158-163.

Saleh, M., Vijayasarathy, C., Fernandez-Cabezudo, M., Taleb, M., & Petroianu, G. (2003). Influence of paraoxon (POX) and parathion (PAT) on apoptosis: a possible mechanism for toxicity in low-dose exposure. *Journal of Applied Toxicology*, 23(1), pp.23-29.

Sams, C., Cocker, J., & Lennard, M.S. (2004). Biotransformation of chlorpyrifos and diazinon by human liver microsomes and recombinant human cytochrome P450s (CYP). *Xenobiotica*, 34(10), pp.861-873.

Sardao, V.A., Oliveira, P.J., Holy, J., Oliveira, C.R., & Wallace, K.B. (2007). Vital imaging of H9c2 myoblasts exposed to tert-butylhydroperoxide—Characterization of morphological features of cell death. *Biomed Central Cell Biology*, 8(1), pp.11-27.

Sams, C., Mason, H.J., & Rawbone, R. (2000). Evidence for the activation of organophosphate pesticides by cytochromes P450 3A4 and 2D6 in human liver microsomes. *Toxicology Letters*, 116(3), pp. 217-221.

Sartiani, L., Bettiol, E., Stillitano, F., Mugelli, A., Cerbai, E., & Jaconi, M.E. (2007). Developmental changes in cardiomyocytes differentiated from human embryonic stem cells: A molecular and electrophysiological approach. *Stem Cells*, 25(5), pp.1136-1144.

Saulsbury, M.D., Heyliger, S.O., Wang, K., & Round, D. (2008). Characterization of chlorpyrifos-induced apoptosis in placental cells. *Toxicology*, 244(2-3), pp.98-110.

Savill, J., & Fadok, V. (2000). Corpse clearance defines the meaning of cell death. *Nature*, 407(3), pp.784-788.

Schafer, M., Koppe, F., Stenger, B., Brochhausen, C., Schmidt, A., Steinritz, D., Thiermann, H., Kirkpatrick, C.J. and Pohl, C. (2013). Influence of organophosphate poisoning on human dendritic cells. *Chemico-Biological Interactions*, 206(3), pp.472-478.

Schmuck, G., & Ahr, H.J., (1997). In vitro method for screening organophosphate-induced delayed polyneuropathy. *Toxicology in Vitro*, 11(2), pp.263-270.

Schopfer, L.M., Voelker, T., Bartels, C.F., Thompson, C.M., & Lockridge, O. (2005). Reaction kinetics of biotinylated organophosphorus toxicant, FP-biotin, with human acetylcholinesterase and human butyrylcholinesterase. *Chemical Research in Toxicology*, 18(4), pp.747-754.

Schopfer, L.M., Furlong, C.E., & Lockridge, O. (2010). Development of diagnostics in the search for an explanation of aerotoxic syndrome. *Analytical Biochemistry*, 404(1), pp.64-74.

Schulz, E., Correll, R., Sheikh, H., Lofrano-Alves, M., Engel, P., Newman, G., Wieczorek, D. (2012). Tropomyosin dephosphorylation results in compensated cardiac hypertrophy. *The Journal of Biological Chemistry*, 287(53), pp.44478-44489.

Selmin, O., Thorne, P., Caldwell, P.T., Johnson, P.D., & Runyan, R.B. (2005). Effects of trichloroethylene and its metabolite trichloroacetic acid on the expression of vimentin in the rat H9c2 cell line. *Cell Biology and Toxicology*, 21(2), pp.83-95.

Shah, M.D., & Iqbal, M. (2010). Diazinon induced oxidative stress and renal dysfunction in rats. *Food and Chemical Toxicology*, 48(12), pp.3345-3353.

Shamblott, M., Axelman, J., Wang, S., Bugg, E., Littlefield, J., Donovan, P., Blumenthal, P., Huggins, G., & Gearhart, J. (1999). Derivation of Pleuripotent Stem Cells From Cultured Human Primordial Germ Cells. *Proceedings of the National Academy of Sciences of the United States of America,* 95(3), pp.13726-13731.

Shi, Y., Desponts, C., Do, J., Hahm, H., Scholer, H., & Ding, S. (2008). Induction of Pluripotent stem cells from mouse embryonic Fibroblasts by Oct4 and Klf4 with small-molecule compounds. *Stem Cell*, 3(5), pp.568-574.

Shimizu, K., Kiuchi, Y., Ando, K., Hayakawa, M., & Kikugawa, K. (2004). Coordination of oxidized protein hydrolase and the proteasome in clearance of cytotoxic denatured proteins. *Biochemical and Biophysical Research Communications*, 324(6), pp.140-146.

Shiojima, I. (2005). Disruption of coordinated cardiac hypertrophy and angiogenesis contributes to the transition to heart failure. *Journal of Clinical Investigation*, 115(8), pp.2108-2118.

Shiojima, I., & Walsh, K. (2006). Regulation of cardiac growth and coronary angiogenesis by the Akt/PKB signaling pathway. *Genes and Development*, 20(24), pp.3347-3365.

Sidiropoulou, E., Sachana, M., Flaskos, J., Harris, W., Hargreaves, A.J., & Woldehiwet, Z. (2009). Diazinon oxon affects the differentiation of mouse N2a neuroblastoma cells. *Archives of Toxicology*, 83(4), pp.373-380.

Silveira, C., Eldefrawi, A., & Eldefrawi, M. (1990). Putative M2 muscarinic receptors of rat heart have high affinity for organophosphorus anticholinesterases. *Toxicology and Applied Pharmacology*, 103(3), pp.474-481.

Simard, A., Di Giorgio, L., Amen, M., Westwood, A., Amendt, B.A., & Ryan, A.K. (2009). The Pitx2c N-terminal domain is a critical interaction domain required for asymmetric morphogenesis. *Developmental Dynamics*, 238(10), pp.2459-2470.

Simpson, L., & Parsons, R. (2001). PTEN: Life as a tumor suppressor. *Experimental Cell Research,* 264(1), pp.29-41.

Sjoblom, B., Salmazo, A., & Djinovic-Carugo, K. (2008). α-actinin structure and regulation. *Cellular and Molecular Life Sciences*, 65(17), pp.2688-2701.

Slotkin, T., Seidler, F., & Fumagalli, F. (2007). Exposure to organophosphates reduces the expression of neurotrophic factors in neonatal rat brain regions: similarities and differences in the effects of chlorpyrifos and diazinon on the fibroblast growth factor superfamily. *Environmental Health Perspectives*, 115(6), pp.909-916.

Slotkin, T.A. (2005). Developmental neurotoxicity of organophosphates: a case study of chlorpyrifos. In: Gupta R.C. (ed.) *Toxicity of organophosphate and carbamate pesticides*. San Diego: Elsevier Academic Press, pp.293-314.

Slotkin, T., McKillop, E., Ryde, I., Tate, C., & Seidler, F., (2007). Screening for developmental neurotoxicity using PC12 cells: comparisons of organophosphates with a carbamate, an organochlorine, and divalent nickel. *Environmental Health Perspective*, 115(6), pp.93-101.

Slotkin, T., & Seidler, F. (2012). Developmental neurotoxicity of organophosphates targets cell cycle and apoptosis, revealed by transcriptional profiles in vivo and in vitro. *Neurotoxicology and Teratology,* 34(2), pp.232-241.

Slotkin, T., & Seidler, F. (2007). Comparative developmental neurotoxicity of organophosphates in vivo: transcriptional responses of pathways for brain cell development, cell signaling, cytotoxicity and neurotransmitter systems. *The Brain Research Bulletin*, 72(2), pp.232-274.

Smith, G.S., Walter, G.L. & Walker, R.M. (2013). Clinical pathology in non-clinical toxicology testing. In: *Haschek and Rousseaux's Handbook of Toxicologic Pathology*, Elsevier BV, pp.565-594.

Smith, M.I., & Lillie, R.D. (1931). The histopathology of triorthocresyl phosphate poisoning. *Archives of Neurology and Psychiatry,* 26(2), pp.976-992.

Sogorb, M.A., & Vilanova, E. (2010). Detoxication of anticholinesterase pesticides. In: Satoh, T., Gupta, R.C. (eds.) *Anticholinesterase Pesticides: Metabolism, Neurotoxicity, and Epidemiology*. Wiley, Hoboken, pp.121-132.

Solbu, K., Thorud, S., Hersson, M., Ovreb, S., Ellingsen, D., Lundanes, E., & Molander, P. (2007). Determination of airborne trialkyl and triaryl organophosphates originating from hydraulic fluids by gas chromatography-mass spectrometry. Development of methodology for combined aerosol and vapor sampling. *Journal of Chromatography*, 1161(1-2), pp.275-283.

Somkuti, S.G., & Abou-Donia, M.B. (1990). Disposition, elimination, and metabolism of tri-o-cresyl phosphate following daily oral administration in Fischer 344 male rats*. Archives of Toxicology*, 64(3), pp.572-579.

Song, F., & Xie, K. (2012). Calcium-dependent neutral cysteine protease and organophosphate-induced delayed neuropathy. *Chemico-Biological Interactions*, 200(2-3), pp.114-118.

Song, G., Ouyang, G., & Bao, S. (2005). The activation of Akt/PKB signaling pathway and cell survival. *Journal of Cellular and Molecular Medicine*, 9(1), pp.59-71.

Sorimachi, H., Ishiura S., & Suzuki K. (1997). Structure and physiological function of calpains. *Biochemical Journal*, 328(3), pp.721-732.

Spallarossa, P., Fabbi, P., Manca, V., Garibaldi, S., Ghigliotti, G., Barisione, C., & Barsotti, A. (2005). Doxorubicin-induced expression of LOX-1 in H9c2 cardiac muscle cells and its role in apoptosis. *Biochemical and Biophysical Research Communications*, 335(1), pp.188-196.

Stathopoulou, K., Beis, I., & Gaitanaki, C. (2008). MAPK signaling pathways are needed for survival of H9c2 cardiac myoblasts under extracellular alkalosis. *Heart and Circulatory Physiology*, 295(3), pp.1319-1329.

Stevens, J.C., Hines, R.N., Gu, C., Koukouritaki, S.B., Manro, J.R., Tandler, P.J., & Zaya, M.J. (2003). Developmental expression of the major human hepatic CYP3A enzymes. *Journal of Pharmacology and Experimental Therapeutics,* 307(7), pp.573-582.

Sultatos, L.G. (1994). Mammalian Mammalian toxicity of organophosphorus pesticides*. Journal of Toxicology and Environmental Health*, 43(7), pp.271-289.

Suzuki, H., Swei, A., Zweifach, B.W., & Schmid-Schonbein, W. (1995). In vivo Evidence for Microvascular Oxidative Stress in Spontaneously Hypertensive Rats. *Hypertension*, 25(2), pp.1083-1089.

Swynghedauw, B. (1986). Developmental and functional adaptation of contractile proteins in cardiac and skeletal muscle. *Physiological Reviews*, 66(8), pp.710-771.

Sztrum, A.A., Deramo, J.L., & Herkovits, J. (2011). Nickel toxicity in embryos and larvae of the south American toad: Effects on cell differentiation, morphogenesis, and oxygen consumption. *Environmental Toxicology and Chemistry*, 30(5), pp.1146-1152.

Takahashi, A., Kureishi, Y., Yang, J., Luo, Z., Guo, K., Mukhopadhyay, D., Ivashchenko, Y., Branellec, D., & Walsh, K. (2002). Myogenic Akt signaling regulates blood vessel recruitment during myofiber growth. *Molecular Cell Biology*, 22(3), pp.4803-4814.

Takahashi, K., & Yamanaka, S. (2006). Induction of Pluripotent stem cells from mouse embryonic and adult Fibroblast cultures by defined factors. *Cell*, 126(4), pp.663-676.

Takahashi, K., Tanabe, K., Ohnuki, M., Narita, M., Ichisaka, T., Tomoda, K., & Yamanaka, S. (2007). Induction of Pluripotent stem cells from adult human Fibroblasts by defined factors. *Cell*, 131(5), pp.861-872.

Terai, M. (2005). Immortalization of human fetal cells: The life span of Umbilical cord blood-derived cells can be prolonged without manipulating p16INK4a/RB braking pathway. *Molecular Biology of the Cell,* 16(3), pp.1491-1499.

Terry, A.V. (2003). Repeated Exposures to Subthreshold Doses of Chlorpyrifos in Rats : Hippocampal Damage , Impaired Axonal Transport , and Deficits in Spatial Learning. *Journal of Pharmacology and Experimental Therapeutics*, 305(1), pp.375-384.

Terry, A.V., Gearhart, D.A., Beck, W.D., Truan, J.N., Middlemore, M., Williamson, L.N., Bartlett, M.G., Prendergast, M.A., Sickles, D.W., & Buccafusco, J.J. (2007). Chronic, intermittent exposure to Chlorpyrifos in rats: Protracted effects on Axonal transport, Neurotrophin receptors, Cholinergic markers, and information processing. *Journal of Pharmacology and Experimental Therapeutics, 322(3),* pp.1117-1128.

Thomson, J.A. (1998). Embryonic stem cell lines derived from human Blastocysts. *Science*, 282(5391), pp.1145-1147.

Tirupapuliyar, V., Magdalena, A., Ali, A., & Mohamed, B. (2002). Sarin causes early differential alteration and persistent overexpression in mRNAs coding for glial fibrillary acidic protien (GFAP) and vimentin genes in the central nervoius system of rats. *Neurochemical Research*, 27(5), pp.407-415.

Trapani, J.A., & Smyth, M.J. (2002). Functional significance of the per- forin/granzyme cell death pathway. *Nature Reviews Immunology*, 2(8), pp.735-747.

Trautwein, W., & Hescheler J. (1990). Regulation of cardiac L-type calcium current by phosphorylation and G-proteins. *Annual Review of Physiology*, 52(5), pp.257-274.

Trump, B.F., Berezesky, I.K., Chang, S.H., & Phelps, P.C. (1997). The pathways of cell death: oncosis, apoptosis, and necrosis. *Toxicological Pathology*, 25(9), pp.82-88.

Uehara, T., Bennett, B., Sakata, S.T., Satoh, Y., Bilter, G.K., & Westwick, J.K. (2005). JNK mediates hepaticischemia reperfusion injury. *Journal of Hepatology*, 242(4), pp.850-859.

Ueyama, J., Kamijima, M., Asai, K., Mochizuki, A., Wang, D., & Kondo, T. (2008). Effect of the organophosphorus pesticide diazinon on glucose tolerance in type 2 diabetic rats. *Toxicology Letters*, 182(1-3), pp.42-47.

Umlas, J., Jacobson, M., & Kevy, S.V. (1991). Suitable survival and half-life of red cells after frozen storage in excess of 10 years. *Transfusion*, 31(2), pp.648-649.

Van de Meerakker, J.B.A., Christiaans, I., Barnett, P., Lekanne Deprez, R.H., Ilgun, A., Mook, O.R.F., Mannens, M.M.A.M., Lam, J., Wilde, A.A.M., Moorman, A.F.M. and Postma, A.V. (2013). A novel alpha-tropomyosin mutation associates with dilated and non-compaction cardiomyopathy and diminishes actin binding. *Molecular Cell Research*, 1833(4), pp.833-839.

Van Der Schalie, W.H., Gardner, H.S., Bantle, J.A., Rosa, C.T.D., Finch, R.A., Reif, J.S., Reuter, R.H., Backer, L.C., Burger, J., Folmar, L.C., & Stokes, W.S. (1999). Animals as sentinels of human health hazards of environmental chemicals. *Environmental Health Perspectives*, 107(4), pp.309-315.

Van Tienhoven, M., Atkins, J., Li, Y., & Glynn, P. (2002). Human neuropathy target esterase catalyzes hydrolysis of membrane Lipids. *Journal of Biological Chemistry*, 277(23), pp. 20942-20948.

Vittozzi, L., Fabrizi, L., Consiglio, E. Di, Testai, E., & Elena, V. R. (2001). Mechanistic aspects of organophosphorothionate toxicity in fish and humans. *Environment International*, 26(3), pp.125-129.

Wajant, H. (2002). The Fas signaling pathway: more than a paradigm. *Science*, 296(8), pp.1635-1666.

Wallace, K.B., & Herzberg, U. (1988). Reactivation and aging of phosphorylated brain acetylcholinesterase from fish and rodents. *Toxicology and Applied Pharmacology*, 92(3), pp.307-314.

Wang, H.J., Zhu, Y.C., & Yao, T. (2002). Effects of all-transretinoic acid on angiotensin II-induced myocyte hypertrophy. *Journal of Applied Physiology*, 92(5), pp.2162-2168.

Wang, M., Yang, Y., Yang, D., Luo, F., Liang, W., Guo, S., & Xu, J. (2009). The immunomodulatory activity of human umbilical cord blood-derived mesenchymal stem cells in vitro. *Immunology*, 126(8), pp.220-32.

Wang, M.H., Tseng, C.D., & Bair, S.Y. (1998). Q-T interval prolongation and pleomorphic ventricular tachyarrhythmia ("Torsade de pointes") in organophosphate poisoning: Report of a case. *Human and Experimental Toxicology*, 17(10), pp.587-590.

Wang, Q., Shen, B., Chen, L., Zheng, P., Feng, H., Hao, Q., & Teng, J. (2014). Extracellular calumenin suppresses ERK1/2 signaling and cell migration by protecting fibulin-1 from MMP-13-mediated proteolysis. *Oncogene*, 34(8), pp.1-13.

Wang, W., Watanabe, M., Nakamura, T., Kudo, Y., & Ochi, R. (1999). Properties and expression of Ca2+-activated K+ channels in H9c2 cells derived from rat ventricle. *The American Journal of Physiology*, *276*(5), pp.1559-66.

Washburn, K.S., & Phillips, T.D. (1995). Development of a field-practical assay for water-solvated chlorophenols. *Journal of Hazardous Materials*, 41(2-3), pp.371-381.

Watkins, S.J., Borthwick, G.M., & Arthur, H.M. (2010). The H9C2 cell line and primary neonatal cardiomyocyte cells show similar hypertrophic responses in vitro. *In vitro cellular & developmental biology-Animal*, 47(2), pp.125-131.

Weinberg, R.A., & Weinberg, R. (2013). *The biology of cancer*. New York, Garland Science, pp.175-341.

Watson, F.L., Schmidt, H., Turman, Z.K., Hole, N., Garcia, H., Gregg, J., Tilghman, J., & Fradinger, E.A. (2014). Organophosphate pesticides induce morphological abnormalities and decrease locomotor activity and heart rate in Danio rerio and Xenopus laevis. *Environmental Toxicology and Chemistry*, 33(6), pp. 1337-1345.

Way, M., & Parton, R.G. (1995). M-caveolin, a muscle-specific caveolin-related protein. *Federation of European Biochemical Societies Letters*, 376(1-2), pp.108-112.

Weiss, M.L., & Troyer, D.L. (2006). Stem cells in the umbilical cord. *Stem Cell Reviews*, 2(2), pp.155-162.

Weston, C.R., & Davis, R.J. (2002). The JNK signal transduction pathway. *Current Opinion in Genetics and Development*, 12(1), pp.14-21.

Wettstein, G., Bellaye, P.S., Micheau, O., & Bonniaud, P. (2012). Small heat shock proteins and the cytoskeleton: An essential interplay for cell integrity?. *The International Journal of Biochemistry and Cell Biology*, 44(10), pp.1680-1686.

Wijeyaratne, W., & Pathiratne, A. (2006). Acetylcholinesterase inhibition and gill lesions in Rasbora caverii, an indigenous fish inhabiting rice field associated water bodies in Sri Lanka. *Ecotoxicology*, 15(7), pp.609-619.

Williams, D.G. (1983). Intramolecular group transfer is a characteristic of neurotoxic esterase and is independent of the tissue source of the enzyme. A comparison of the aging behaviour of di-isopropyl phosphorofluoridate-labelled proteins in brain, spinal cord, liver, kidney and spleen from hen and in human placenta. *Biochemical Journal*, 209(3), pp.817-829.

Wilson, B.W. (2001). Cholinesterases. In: Krieger, R.I. (ed.) Handbook of Pesticide Toxicology, 2, San Diego, CA: Academic Press, pp.967-986.

Wilson, P.A. (2006). Characterization of the human patatin-like phospholipase family. *The Journal of Lipid Research*, 47(9), pp.1940-1949.

Winder C., & Balouet J.C., (2000). Aerotoxic syndrome: adverse health effects following exposure to jet oil mist during commercial flights. *Proceeding international congress on Occupational health*, 5, pp.196-199.

Winder, C., & Balouet, J.C., (2001) Aircrew Exposure to Chemicals in Aircraft: Symptoms of Irritation and Toxicity. *Journal of Occupational Health and Safety*, 17(2), pp.471-483.

Winder, C., Fonteyn, P., & Balouet, J.C., (2002). Aerotoxic syndrome: a descriptive epidemiological survey of aircrew exposed to in cabin airborne contaminants. *Journal of Occupatinal Health Safety*. 18(8), pp.321-338.

Wobus, A.M., Kaomei, G., Shan, J., Wellner, M.C., Rohwedel, J., Ji, G., Fleischmann, B., Katus, H.A., Hescheler, J., & Franz, W.M. (1997). Retinoic acid accelerates embryonic stem cell-derived cardiac differ- entiation and enhances development of ventricular cardiomyocytes. *The Journal of Molecular and Cellular Cardiology*, 29(3), pp.1525-1539.

Wolkowicz, I.R., Herkovits, J., & Perez Coll, C.S. (2011). Stage-dependent toxicity of bisphenol a on Rhinella arenarum (anura,bufonidae) embryos and larvae. *Environmental Toxicology*, 29(2), pp.146-154.

Worek, F., & Eyer, P. (2006). The liberation of thiocholine from acetylthiocholine (ASCh) by pralidoxime iodide (2=PAM) and other oximes (obidoxime and diacetylmonoxime). *Toxicology Letters*,167(3), pp.256-262.

Wymann, M.P., Zvelebil, M., & Laffargue, M. (2003). Phosphoinositide 3-kinase signalling – which way to target?. *Trends in Pharmacological Sciences*, 24(7), pp.366-376.

Xia, M., Huang, R., Witt, K.L., Southall, N., Fostel, J., Cho, M.H., Jadhav, A., Smith, C.S., Inglese, J., Portier, C.J., Tice, R.R. and Austin, C.P. (2007). Compound Cytotoxicity profiling using quantitative high-throughput screening. *Environmental Health Perspectives*, 116(3), pp.284-291.

Xia, Z., Dickens, M., Raingeaud, J., Davis, R.J., & Greenberg, M.E., (1995). Opposing effects of ERK and JNK-p38 MAP kinases on apoptosis. *Science*, 270(7), pp.1326-1331.

Xiao, Y., Grieshammer, U., & Rosenthal, N. (1995). *The Journal of Cell Biology*, 129(3), pp.1345-1354.

Xu, C. (2002). Characterization and Enrichment of Cardiomyocytes Derived From Human Embryonic Stem Cells. *Circulation Research*, 91(6), pp.501-508.

Xu, C., Zhang, A., & Liu, W. (2007). Binding of phenthoate to bovine serum albumin and reduced inhibition on acetylcholinesterase. *Pesticide Biochemistry and Physiology*, 88(2), pp.176-180.

Yabe, D., Nakamura, T., Kanazawa, N., Tashiro, K., & Honjo, T. (1997). Calumenin, a ca2+-binding protein retained in the Endoplasmic Reticulum with a novel Carboxyl-terminal sequence, HDEF. *Journal of Biological Chemistry*, 272(29), pp.18232-18239.

Yamanaka, S. (2007). Strategies and new developments in the generation of patient-specific pluripotent stem cells. *Stem Cell*, 1(6), pp.39-49.

Yamada, Y., Yokoyama, S., Fukuda, N., Kidoya, H., Huang, X., Naitoh, H., Satoh, N., & Takakura, N. (2007). A novel approach for myocardial regeneration with educated cord blood cells cocultured with cells from brown adipose tissue. *Biochemical and Biophysical Research Communications*, 353(1), pp.182-188.

Yang, D.D., Kuan, C.Y., Whitmarsh, A.J., Rincon, M., Zheng, T.S., Davis, R.J., Rakic, P., & Flavell, R.A. (1997). Absence of excitotoxicity induced apoptosis in the hippocampus of mice lacking the Jnk3 gene. *Nature,* 389(6), pp.865-870.

Yang, L., Soonpaa, M.H., Adler, E.D., Roepke, T.K., Kattman, S.J., Kennedy, M., Henckaerts, E., Bonham, K., Abbott, G.W., Linden, R.M., Field, L.J., & Keller, G.M. (2008). Human cardiovascular progenitor cells develop from a KDR+ embryonic-stem-cell-derived population. *Nature*, 453(7194), pp.524-528.

Yang, Y., Bauer, C., Strasser, G., Wollman, R., Julien, J.P., & Fuchs, E. (1999). Integrators of the cytoskeleton that stabilize microtubules. *Cell*, 98(8), pp.229-238.

Yarar, D. (2004). A dynamic Actin Cytoskeleton functions at multiple stages of Clathrin-mediated Endocytosis. *Molecular Biology of the Cell*, 16(2), pp.964-975.

Yavuz, Y., Yurumez, Y., Ciftci, I.H., Sahin, O., Saglam, H., & Buyukokuroglu, M. (2008). Effect of diphenhydramine on myocardial injury caused by organophosphate poisoning. *Clinical Toxicology*, 46(1), pp.67-70.

Yu, F., Wang, Z., Ju, B., Wang, Y., Wang, J., & Bai, D. (2008). Apoptotic effect of organophosphorus insecticide chlorpyrifos on mouse retina in vivo via oxidative stress and protection of combination of vitamins C and E. *Experimental and Toxicological Pathology*, 59(9), pp.415-423.

Yu, R., & Ono, S. (2006). Dual roles of tropomyosin as an F-actin stabilizer and a regulator of muscle contraction inCaenorhabditis elegans body wall muscle. *Cell Motility and the Cytoskeleton*, 63(11), pp.659-672.

Yu, X. Y., Chen, H. M., Liang, J.L., Lin, Q.X., Tan, H.H., & Fu, Y.H. (2011). Hyperglycemic myocardial damage is mediated by proinflammatory cytokine: Macrophage migration inhibitory factor. *Plos One*, 6(1), pp.16239.

Zafiropoulos, A., Tsarouhas, K., Tsitsimpikou, C., Fragkiadaki, P., Germanakis, I., Tsardi, M., Maravgakis, G., Goutzourelas, N., Vasilaki, F., Kouretas, D., Hayes, A. & Tsatsakis, A. (2014). Cardiotoxicity in rabbits after a low-level exposure to diazinon, propoxur and chlorpyrifos. *Human and Experimental Toxicology*, 33(12), pp.1241-1252.

Zalizniak, L., & Nugegoda, D. (2006). Effect of sublethal concentrations of chlorpyrifos on three successive generations of Daphnia carinata. *Ecotoxicology and Environmental Safety*, 64(2), pp.207-14.

Zara, S., Monica, G., Valerio, V. Di., & Cataldi, A. (2010). Morphological and molecular events during H9c2 differentiation : role for pPKCδ / SC35 interaction*, Italian Journal of Anatomy and Embryology*, 115(2), pp.179-190.

Zarei, M.H., Soodi, M., Qasemian-Lemraski, M., Jafarzadeh, E., Taha, M.F. (2015). Study of the chlorpyrifos neurotoxicity using neural differentiation of adipose tissue-derived stem cells. *Environmental Toxicology*, 259(6), pp.83-94.

Zeiss, C.J. (2003). The apoptosis-necrosis continuum: insights from genetically altered mice. *Veterinary Pathology*, 40(8), pp.481-495.

Zeng, X., Hunsberger, J.G., Simeonov, A., Malik, N., Pei, Y., & Rao, M. (2014). Concise review: modeling central nervous system diseases using induced pluripotent stem cells. *Stem Cells Translational Medicine*, 3(12), pp.1418-1428.

Zhang, J., Wilson, G.F., Soerens, A.G., Koonce, C.H., Yu, J., Palecek, S.P., Thomson, J.A., & Kamp, T.J. (2009). Functional Cardiomyocytes derived from human induced Pluripotent stem cells. *Circulation Research*, 104(4), pp.30-41.

Zhang, W., Elimban, V., & Nijjar, M. S. (2003). Role of mitogen-activated protein kinase in cardiac hypertrophy and heart failure. *Experimental and Clinical Cardiology*, 8(4), pp.173-183.

Zhang, Y., Hou, Y., Chen, F., Xiao, Z., Zhang, J., & Hu, X. (2011). The degradation of chlorpyrifos and diazinon in aqueous solution by ultrasonic irradiation: effect of parameters and degradation pathway. *Chemosphere*, 82(8), pp.1109-1115.

Zhao, Q., Dourson, M., & Gadagbui, B. (2006). A review of the reference dose for chlorpyrifos. *Regulatory Toxicology and Pharmacology*, 44(2), pp.111-124.

Zhao, X., Zhang, T., Zhang, C., Han, X., Yu, S., Li, S., Cui, N., & Xie, K. (2006). Expression changes of neurofilament subunits in the central nervous system of hens treated with tri-ortho-cresyl phosphate (TOCP). *Toxicology,* 223(1-2), pp.127-135.

Zhou, M.D., Sucov, H.M., Evans, R.M., & Chien, K.R., (1995). Retinoid dependent pathways suppress myocardial cell hypertrophy. *The Proceedings of the National Academy of Sciences in the United States of America,* 92(3), pp.7391-7395.

Zhou, Q., Chu, P.H., Huang, C., Cheng, C.F., Martone, M.E., Knoll, G., Shelton, G.D., Evans, S., & Chen, J. (2001). Ablation of Cypher, a PDZ-LIM domain Z-line protein, causes a severe form of congenital myopathy. *The Journal of Cell Biology*, 155(4), pp.605-612.

Zhu, H. L., Wei, X., Qu, S. L., Zhang, C., Zuo, X. X., & Feng, Y. S. (2011). Ischemic postconditioning protects cardiomyocytes against ischemia/reperfusion injury by inducing MIP2. *Experimental & Molecular Medicine,* 43(4), pp.437-445.

Zhu, H., Lensch, M.W., Cahan, P., Daley, G.Q. (2011). Investigating monogenic and complex diseases with pluripotent stem cells. *Nature Reviews Genetics*,12(4), pp.266-275.

Zoltani, C.K., Thorne, G.D., & Baskin, S.I. (2006). Cardiovascular Toxicity of Cholinesterase Inhibitors. In: *Toxicology of Organophosphate and Carbamate Compound*. pp.381-188.

Zwi, L., Caspi, O., Arbel, G., Huber, I., Gepstein, A., Park, I., & Gepstein, L. (2009). Cardiomyocyte differentiation of human induced Pluripotent stem cells. *Circulation*, 120(15), pp.1513-1523.